THE

LONDON EDINBURGH AND DUBLIN

PHILOSOPHICAL MAGAZINE

AND

JOURNAL OF SCIENCE.

[SEVENTH SERIES.]

MARCH 1930.

XXXIII. *Vibrations damped by Solid Friction.* *By* SYDNEY THOMAS, *M.Sc., Lecturer in Engineering, University College, Cardiff* *.

VIBRATIONS with solid friction as the sole or principal damping agent are of common occurrence, and the solution, when friction is regarded as a force of constant magnitude reversing in direction at each semi-oscillation, presents no difficulty and little, if any, novelty. A variation having a considerable range of application arises, however, when the two bodies between which friction may exist have, on the average, a relative velocity, and its solution differs in certain respects from that of the simpler case; in particular it may be shown, analytically and experimentally, that vibrations, initiated in any manner, tend to persist within a certain maximum amplitude without any impressed disturbing force other than that provided by the relative motion of the bodies. The necessary conditions are frequently met in practice, and it appears possible that the continued vibrations maintained may be responsible, in some measure, for the production of sound by bodies in rubbing contact.

In general, both bodies may vibrate or have local vibrations within them, but for simplicity it will here be assumed that one only may oscillate, the other being regarded as rigid. The conditions are then readily visualized by considering a

* Communicated by Prof. W. Norman Thomas, M.A., D.Phil.

mass M held under elastic control upon a rigid plane which moves at constant velocity V, or, alternatively, they may be found in a brake-shoe pressed upon a stiff revolving wheel of considerable mass or in a turning pair one of the elements of which is relatively inelastic. In that case, of course, moments of inertia, couples, and angular velocities may be substituted as necessary for masses, forces, and linear velocities in what follows.

Solid friction only.

Whilst a relative motion exists between body and plane, the equation of motion is

$$M\ddot{x} = \pm F - Rx, \quad . \quad . \quad . \quad . \quad . \quad . \quad (1)$$

R being the restoring force per unit displacement from the position of zero elastic stresses and F the limiting kinetic frictional resistance. The solution is

$$x = \pm F/R + A\cos(pt+\epsilon), \quad . \quad . \quad . \quad . \quad (2)$$

and

$$\dot{x} = -pA\sin(pt+\epsilon), \quad . \quad . \quad . \quad . \quad . \quad . \quad (3)$$

where $p = \sqrt{R/M}$ and where the sign of F is similar to that of the relative velocity $(V-\dot{x})$ if both V and x are regarded as positive when measured in the same direction.

F is a limiting value, and equation (1) ceases to apply when both $(V-\dot{x})$ is zero and x is not numerically greater than F/R, or, perhaps more accurately, F_s/R, where F_s is the limiting static friction. In those circumstances the frictional resistance called into play is that sufficient to balance the restoring force Rx, the acceleration $\ddot{x}$ is zero, and $\dot{x}$ is equal to V.

The constants in equation (2) depend upon initial conditions, and if it be assumed that the vibrating mass is given an initial maximum positive displacement which ensures that at the outset $\dot{x}$, being zero, is not equal to V, and that the equation therefore applies, then, calling the displacement d_1, and taking zero-time at the instant of release, $\epsilon_1 = 0$, $A_1 = (d_1 - F/R)$, and, until $\dot{x} = V$,

$$x = F/R + A_1\cos pt. \quad . \quad . \quad . \quad . \quad . \quad (4)$$

The motion is harmonic, and the space-time curve may be derived from the projections $(x - F/R)$ of a radius of length A_1 rotating at angular velocity p about a centre C_1 which is distant F/R from the centre of elastic forces O (see fig. 1). Now

$$\dot{x}/p = -A_1\sin pt, \quad . \quad . \quad . \quad . \quad . \quad (5)$$

and if displacements are derived from vertical projections of the rotating radius, as shown in fig. 1, horizontal projections of the same radius lead to values of $-\dot{x}/p$.

A point of discontinuity is reached, and friction undergoes reversal when

$$\dot{x} = \mathrm{V} = -p\mathrm{A}_1 \sin pt,$$

i. e., when $\sin pt = -\mathrm{V}/p\mathrm{A}_1$,

or $pt = -\alpha$ or $\pi + \alpha$,

α being $\sin^{-1} \mathrm{V}/p\mathrm{A}_1$. In the diagram these conditions are

Fig. 1.

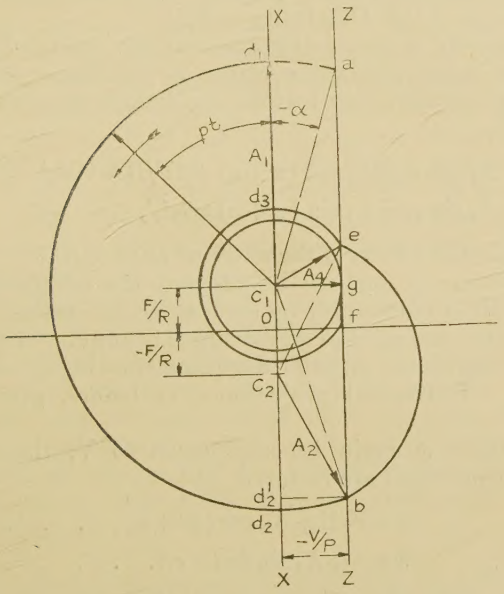

realized at the points a and b at which the circular locus of the extremity of A_1 intersects the vertical ZZ, which is at a distance $-\mathrm{V}/p$ from the centre line XX, and the corresponding displacements are $\mathrm{F/R} \pm \mathrm{A}_1 \cos \alpha$.

For values of pt greater than $(\pi + \alpha)$, and until $\dot{x}$ again becomes equal to V, displacements and velocities are given by

$$x = -\mathrm{F/R} + \mathrm{A}_2 \cos(pt + \epsilon_2), \quad \ldots \quad (6)$$

$$\dot{x} = -p\mathrm{A}_2 \sin(pt + \epsilon_2), \quad \ldots \quad (7)$$

the values of the constants being adjusted to meet the altered conditions. At the instant of friction reversal both sets of equations must be satisfied simultaneously, and if the original time-origin be preserved, so that reversal occurs at $t=(\pi+\alpha)/p$,

$$x=\mathrm{F/R}+\mathrm{A}_1\cos(\pi+\alpha)=-\mathrm{F/R}+\mathrm{A}_2\cos(\pi+\alpha+\epsilon_2),$$

$$\dot{x}=-p\mathrm{A}_1\sin(\pi+\alpha)=-p\mathrm{A}_2\sin(\pi+\alpha+\epsilon_2),$$

whence

$$\mathrm{A}_2\cos(\pi+\alpha+\epsilon_2)=\mathrm{A}_1\cos(\pi+\alpha)+2\mathrm{F/R}=\mathrm{C}_2d_2'\ \text{(fig. 1)},$$

$$\mathrm{A}_2\sin(\pi+\alpha+\epsilon_2)=\mathrm{A}_1\sin(\pi+\alpha)=bd_2'\ \text{(fig. 1)}.$$

Thus $\mathrm{A}_2=\mathrm{C}_2b$ and $(\pi+\alpha+\epsilon_2)=\tan^{-1}bd_2'/\mathrm{C}_2d_2'$, which is the exterior angle $d_1\mathrm{C}_2b$, OC_2 being $-\mathrm{F/R}$.

Alternatively, commencing anew at the point of discontinuity and transferring the origin of the time-space curve to $(\pi+\alpha)/p$, so that now $t=0$ at the instant represented by the point b,

$$\mathrm{A}_2\cos\epsilon_2=\mathrm{A}_1\cos(\pi+\alpha)+2\mathrm{F/R}=\mathrm{C}_2d_2',$$

$$\mathrm{A}_2\sin\epsilon_2=\mathrm{A}_1\sin(\pi+\alpha)=bd_2',$$

whence $\mathrm{A}_2=\mathrm{C}_2b$ and ϵ_2 is the exterior angle $d_1\mathrm{C}_2b$.

Thus, whichever method be adopted, the continuation of the space-time curve may be derived from vertical projections of the radius C_2b revolving at angular velocity p about C_2, additional angular displacements being measured from C_2b. Horizontal projections, as before, give values of $-\dot{x}/p$.

At e, where $\dot{x}$ again becomes equal to V, the original frictional conditions are restored, and

$$x=\mathrm{F/R}+\mathrm{A}_3\cos(pt+\epsilon_3), \quad . \quad . \quad . \quad . \quad (8)$$

$$\dot{x}=-p\mathrm{A}_3\sin(pt+\epsilon_3). \quad . \quad . \quad . \quad . \quad . \quad (9)$$

From equations (6), (7), (8), and (9) it may readily be shown, by methods similar to those used for the determination of A_2, that $\mathrm{A}_3=\mathrm{C}_1e$, and that additional angular displacements should be measured from C_1e.

The construction may thus be continued, the centre of oscillation being transferred from C_1 to C_2 or conversely as points of intersection of the locus of the extremities of the rotating radii with the vertical ZZ are attained. In the figure as given, those portions of the construction which lie to the left of ZZ are drawn with C_1 as centre, those to the right of ZZ are taken about C_2.

The construction ceases to apply when $\dot{x}$ becomes equal to V at a displacement which lies between $\pm$ F/R, *i. e.*, when the projection of a point of intersection with ZZ, such as *f*, lies within the region C_1C_2. As already pointed out, the frictional resistance is then less than its limiting value, and the acceleration is zero ; the vibrating mass accordingly moves awhile in unison with the plane until limiting frictional conditions are restored, when elastic vibrations are resumed, and persist in a manner which is considered later.

It was assumed that the initial displacement was a maximum displacement for which $\dot{x} = 0$, and in those circumstances the diagram begins at a point in the centre line XX such as d_1 in fig. 1. This assumption, of course, is not essential, and should oscillations commence under any other conditions of displacement and velocity, the construction may be commenced from the appropriate point on the circular curve. For example, if the plane, initially at rest, is set in motion at velocity V, the mass is held in contact with it until $x = F_s/R$; at the instant of release $\dot{x} = V$, and the initial conditions are represented by a point on ZZ at a height F_s/R above the horizontal axis OT. Expressions for x and $\dot{x}$ differ from those of equations (4) and (5) only in that $\epsilon_1 = \tan^{-1} - VR/p(F_s - F)$, and the validity of the construction is in no way impaired.

Whilst discontinuities in the expression for x and transfers between the two centres of oscillation are involved, the time-interval between successive maximum displacements is not uniform, and the motion is not truly periodic. A semi-oscillation such as d_1d_2, during which the mass moves in a direction opposed to that of the motion of the plane, occupies an interval of π/p, or half the natural period of oscillation, but the return swing is of longer duration, and requires a time-interval of

$$\frac{1}{p}\,(\text{the sum of the angles } d_2C_1b,\ bC_2e, \text{ and } eC_1d_1).$$

The transfer of the centre of oscillation from C_1 to C_2 has the effect not only of changing the length of the rotating radius in the continuation of the construction but also of advancing its angular displacement, whilst the transfer from C_2 to C_1 retards it. The time-interval which elapses between the successive maximum positive displacements represented by d_1 and d_3 is thus

$$\frac{1}{p}\,(2\pi + \widehat{C_1eC_2} - \widehat{C_1bC_2}),$$

a value which is not independent of the initial displacment, and which is always greater than the natural period of oscillation $2\pi/p$.

Particular cases.—When V is zero, ZZ coincides with XX, the diagram reduces to a series of semicircles about C_1 and C_2 in succession, and the construction is identical with that given by Mr. H. S. Rowell (Phil. Mag., July 1922, p. 284). As pointed out by Mr. C. E. Wright (Phil. Mag., November 1922, p. 1063), this aspect of the problem had also previously been treated analytically by Routh, 'Dynamics of a Particle' (1895 ed.), p. 65.

The time-interval between successive maximum displacements in the same direction is in this case the natural period of oscillation $2\pi/p$; at each change of centre the length of the rotating radius is reduced by 2F/R, each positive or negative extreme displacement is numerically less than the immediately preceding by 2F/R, and the mass finally comes to rest within the stable region when the radius has been decreased to a value equal to or less than 2F/R, or $(F+F_s)/R$ if distinction is drawn between kinetic and static limiting frictions. Mr. Wright has given an expression from which the number of semi-oscillations performed may be estimated when the limiting friction is regarded as constant, or they and the final position of the mass may be determined as follows. If d_1 is the numerical value of an initial position of zero velocity, the radius during the nth semi-oscillation is

$$(d_1-F/R)-(n-1)2F/R=\{d_1-(n-\tfrac{1}{2})2F/R\},$$

and for the final semi-oscillation this $=$ or $<(F+F_s)/R$, whilst the radius for the preceding semi-oscillation $\{d_1-(n-\frac{3}{2})2F/R\} \doteq$ or $<(F+F_s)/R$; thus d_1 cannot exceed $(2Fn/R+F_s/R)$ or be less than $(2Fn/R+F_s/R-2F/R)$, *i.e.*, n is an integer lying between $(d_1R/2F-F_s/2F)$ and $(d_1R/2F-F_s/2F+1)$. When $F_s=F$ these limits become $(d_1R/2F\mp\frac{1}{2})$.

Writing $n=d_1R/2F+k$, the final position is given by

$$d_f=\pm F/R\mp\{d_1-(n-\tfrac{1}{2})2F/R\}=\mp(d_1-2nF/R)$$
$$=\mp(d_1-d_1-2Fk/R)=\pm 2Fk/R,$$

the positive sign applying if the last half-swing is about C_1, the negative if it is about C_2.

When the velocity of the moving plane is such that V/p is not less than (d_1-F/R), the rotating radius does not intersect or is tangential to ZZ, $\dot{x}$ cannot exceed V, friction

is undirectional, and the diagram becomes merely a circle about centre C_1 ; the motion is truly harmonic and, in effect, undamped, the periodic time is that of free vibration, and the sole effect of friction—apart from absorption of energy from the moving system—is to transfer the centre of oscillation from the centre of elastic forces to the position of running equilibrium when vibrations are absent. This case is of interest, for it immediately suggests that, when the bodies concerned have an average relative velocity, solid friction alone is incapable of damping out completely any vibrations which may be set up.

Returning to the more general case, when the vibrating mass attains a velocity V whilst within the region C_1C_2, as already shown, it retains that velocity, and is carried with

Fig. 2.

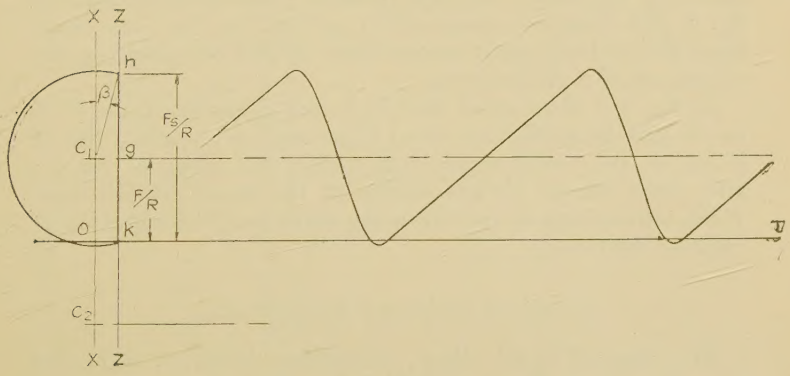

the plane until released at $x = F/R$, *i. e.*, at the point *g* (fig. 1), if F is assumed to be constant. Vibrations of constant amplitude V/p thereafter continue about centre C_1 for reasons which have just been considered. If, as is more likely to occur in practice, the limiting value of static friction exceeds that of kinetic friction, release does not occur until $X = F_s/R$. The "dead" region is thus extended, but since kinetic friction still obtains during the subsequent relative motion between mass and plane, the centre of oscillation remains at C_1 as before.

The graphical construction for such conditions, together with a derived space-time curve, are illustrated in fig. 2; the mass is released at a displacement represented by *h*, performs an oscillatory movement about C_1, acquires again the velocity of the plane at *k*, and thence moves with it to *h*,

where it is once more released. The increase of frictional resistance under static conditions thus provides a stimulus sufficient to maintain vibrations in spite of other damping influences if these are not enough to reduce the rotating radius to a value less than V/p in one oscillation (see also below).

All vibrations now concerned are similar and the motion is truly periodic, though the frequency is not that of the free vibrations. Each complete swing is composed in part of harmonic motion which occupies an interval of $\frac{1}{p}(\pi+2\beta)$, where β is $\cot^{-1}(F_s-F)p/VR$, and in part of uniform motion at velocity V over a displacement $2(F_s-F)/R$, which involves a time-interval of $2(F_s-F)/VR$ or $2\cot\beta/p$. If V is small whilst $p(F_s-F)$ is relatively large, the distortion of the resulting wave-form becomes marked; this is illustrated in fig. 2, and it may be worth while noting that the wave-form there shown bears some resemblance to that representing the vibrations of a violin string.

In fig. 2 it is assumed that F_s is not so far in excess of F as to lead to oscillation about C_2 as well as about C_1, but if it be so, the construction falls within the scope of fig. 1; and since release always occurs at the same displacement F_s/R, movements of the vibrating mass must be repeated at regular intervals.

Combined Solid and Fluid Friction.

Mr. Rowell (Phil. Mag., November 1922, p. 951) has considered the effect of fluid friction, proportional to the velocity, in conjunction with solid friction regarded as a constant force reversing at the end of each semi-oscillation, and Professors Jenkin and Thomas (Phil. Mag., February 1924, p. 303) extended Mr. Rowell's solid friction spiral construction to include that case. The investigation may be made still more general by an extension of the methods which have here been described.

Assuming, as before, that solid friction is provided through the agency of a rigid plane moving at velocity V, and assuming also, to include all cases, that the bulk of the fluid which provides the fluid friction has a velocity v, the equation of motion is

$$M\ddot{x}=\pm F-Rx+c(v-\dot{x}). \quad . \quad . \quad . \quad . \quad (10)$$

Writing $p=\sqrt{R/M}$ and $n=\sqrt{p^2-c^2/4M^2}$, when fluid

damping is not excessive, so that $p^2 > c^2/4M^2$ or $R > c^2/4M$, the solution is

$$x = \pm F/R + cv/R + Ae^{-\frac{ct}{2M}} \cos(nt+\epsilon), \quad . \quad . \quad . \quad (11)$$

and

$$\dot{x} = -Ae^{-\frac{ct}{2M}} \left\{ n \sin(nt+\epsilon) + \frac{c}{2M} \cos(nt+\epsilon) \right\}$$

$$= -pAe^{-\frac{ct}{2M}} \sin(nt+\epsilon+\phi), \quad . \quad . \quad . \quad . \quad . \quad . \quad (12)$$

where $\cos\phi = n/p$ and $\sin\phi = c/2Mp$.

Fig. 3.

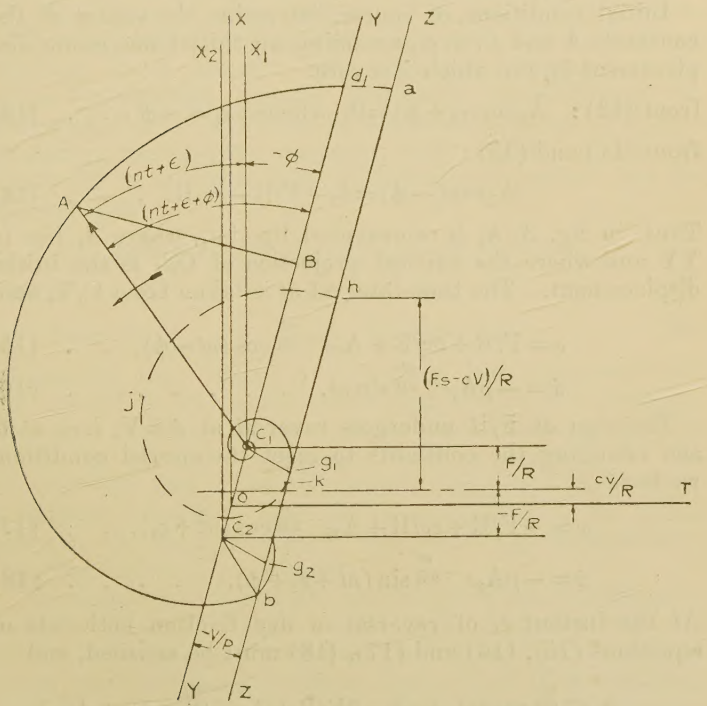

As before, the sign of F is similar to that of $(V - \dot{x})$, and displacements may be derived from vertical projections of $Ae^{-\frac{ct}{2M}}$, which revolves at angular velocity n and the extremity of which performs equiangular spirals about centres C_1 and C_2 in succession, those centres being at heights $(cv \pm F)/R$ above the horizontal axis passing through the position of zero elastic stresses (see fig. 3). Values of $-\dot{x}/p$ are given

by the lengths of perpendicular projectors (such as AB in fig. 3) from the extremity of the rotating arm to the line YY, which is inclined at $-\phi$ to the vertical. When the spiral curve intersects YY the velocity of the vibrating mass is zero, the tangent to the spiral curve is horizontal, and the projections of such points of intersection give extreme displacements of the mass in one direction or the other. In general, the tangent to the curve is inclined at $(\pi/2-\phi)$ to the rotating arm. The centres of oscillation are interchanged at $\dot{x}=\mathrm{V}$, *i. e.*, at points such as *a* and *b*, where the spiral intersects the straight line ZZ parallel to YY and at a distance $-\mathrm{V}/p$ therefrom.

Initial conditions, of course, determine the values of the constants A and ϵ ; *e. g.*, assuming an initial maximum displacement δ_1, for which $\dot{x}$ is zero,

from (12): $\mathrm{A}_1\sin(\epsilon_1+\phi)=0$, whence $\epsilon_1=-\phi$; . . (13)

from (11) and (13) :

$$\mathrm{A}_1\cos(-\phi)=\delta_1-\mathrm{F/R}-cv/\mathrm{R}. \quad . \quad . \quad . \quad (14)$$

Thus, in fig. 3, A_1 is represented by C_1d_1, where d_1 lies in YY and where the vertical projection of $\mathrm{O}d_1$ is the initial displacement. The time-interval *nt* is taken from $\mathrm{C}_1\mathrm{Y}$, and

$$x=\mathrm{F/R}+cv/\mathrm{R}+\mathrm{A}_1e^{-\frac{ct}{2\mathrm{M}}}\cos(nt-\phi), \quad . \quad . \quad (15)$$

$$\dot{x}=-p\mathrm{A}_1e^{-\frac{ct}{2\mathrm{M}}}\sin nt. \quad . \quad . \quad . \quad . \quad . \quad . \quad . \quad (16)$$

The sign of F/R undergoes reversal at $\dot{x}=\mathrm{V}$, *i. e.*, at *b*, and changing the constants to meet the altered conditions we have

$$x=-\mathrm{F/R}+cv/\mathrm{R}+\mathrm{A}_2e^{-\frac{ct}{2\mathrm{M}}}\cos(nt+\epsilon_2). \quad . \quad . \quad (17)$$

$$\dot{x}=-p\mathrm{A}_2e^{-\frac{ct}{2\mathrm{M}}}\sin(nt+\epsilon_2+\phi). \quad . \quad . \quad . \quad . \quad (18)$$

At the instant t_1 of reversal of dry friction both sets of equations (15), (16) and (17), (18) must be satisfied, and

$$\mathrm{A}_2e^{-\frac{ct_1}{2\mathrm{M}}}\cos(nt_1+\epsilon_2)=2\mathrm{F/R}+\mathrm{A}_1e^{-\frac{ct_1}{2\mathrm{M}}}\cos(nt_1+\epsilon_1),$$

$$\mathrm{A}_2e^{-\frac{ct_1}{2\mathrm{M}}}\sin(nt_1+\epsilon_2+\phi)=\mathrm{A}_1e^{-\frac{ct_1}{2\mathrm{M}}}\sin nt_1.$$

These requirements are met if $\mathrm{A}_2e^{-\frac{ct_1}{2\mathrm{M}}}$ is represented by C_2b, $(nt_1+\epsilon_2)$ is the exterior angle $\mathrm{X}_2\mathrm{C}_2b$, and $(\epsilon_2-\epsilon_1)$ is the angle $\mathrm{C}_1b\mathrm{C}_2$.

The construction may thus be continued by a logarithmic spiral about C_2, additional angular displacements being

measured from C_2b. In similar fashion it follows that, if this curve in turn intersects ZZ outside the region g_1g_2, as defined below, the centre of oscillation is retransferred to C_1, and the construction is carried on therefrom as before.

In the equation of motion (10) it has so far been assumed that F is a limiting value of friction and is constant, but whilst $\dot{x}=V$, solid friction may have any value between $\pm F$ provided that x lies between $\pm F/R+c(v-V)/R$. In these circumstances solid friction naturally adjusts itself to balance the elastic force and fluid resistance, and $\ddot{x}$ is zero. If, therefore, the spiral curve intersects ZZ within these values of x, the mass moves in unison with the plane to the limit of the region $\pm F/R+c(v-V)/R$, when, neglecting differences between static and kinetic limiting frictions, it is released; vibrations are resumed and the spiral construction may be continued. Substituting the values of x and $\dot{x}$ at release in equations (11) and (12), and assuming, for present purposes, $t=0$ at that instant, the constants in the equations of subsequent motion may be derived from

$$F/R+c(v-V)/R=F/R+cv/R+A\cos\epsilon,$$

whence
$$A\cos\epsilon=-cV/R, \quad . \quad . \quad . \quad . \quad . \quad (19)$$

and, from (12),
$$V=-pA\sin(\epsilon+\phi). \quad . \quad . \quad (20)$$

Expanding and inserting values of the trigonometrical functions of ϕ, it is readily shown that $A=V/n=(V\sec\phi)/p$, and that $\cos\epsilon=-\sin 2\phi$. These conditions are satisfied if, in fig. 3, A is represented by C_1g_1 inclined to ZZ at $(\pi/2-\phi)$ and ϵ by the angle $X_1C_1g_1=-(\pi/2+2\phi)$; it follows, therefore, that ZZ is tangential to the spiral curve at the point of release, and, since C_2g_2 is parallel to C_1g_1, the region g_1g_2 is defined.

The progressive decrease in the length of the rotating arm makes it impossible that $\dot{x}$ shall again attain the value V; further interchange between centres of oscillation does not occur, and vibrations continue about C_1 (if V is positive) until damped out of existence. Solid friction is now unidirectional, and it serves merely to displace the centre of oscillation and ultimate position of rest to the extent of F/R.

It may be noted that unless the damping fluid moves with the plane, so that $v=V$, g_1g_2 is not symmetrical about the elastic centre O, nor is it defined by horizontals through C_1 and C_2 unless $V=0$. When V is zero the construction reduces to a series of spirals about C_1 and C_2 in succession, each of which commences at the point of intersection of the

preceding curve with YY, and the diagram is complete when a spiral meets YY within the region C_1C_2, when the mass comes to rest, since x then lies between $\pm F/R + cv$ R, Rx lies between $\pm F + cv$, and a value of friction numerically less than the ultimate is sufficient to maintain equilibrium. When V is not zero the mass cannot cease oscillating at any displacement other than those corresponding with C_1 and C_2, according as V is positive or negative. When both v and V are zero the diagram is similar to that given by Professors Jenkin and Thomas.

If no distinction exists between the limiting values of static and kinetic frictions the least degree of fluid damping serves to bring the mass to rest eventually at C_1 or C_2 unless V is zero, but when F_s exceeds F vibration may be continuous. After a period of motion in contact with the plane at velocity V, release is delayed to some such point as h for which $x = \{F_s + c(v - V)\}/R$, and, if the relative values of F_s, F, c, and V are such that a velocity V is again attained during the subsequent vibration, or the spiral meets ZZ (probably within the region g_1g_2), the cycle of uniform motion followed by oscillation is repeated indefinitely. That this may be brought about it is necessary that $C_1h \times e^{-\frac{ct}{2M}}$ shall not be less than C_1g_1 or V/n, t being $\frac{1}{n}$ (the exterior angle hC_1g_1). Small velocity V, small fluid damping coefficient c, and appreciable difference between F_s and F are all favourable to such continued vibrations.

Where fluid damping is heavy and $c^2/4M^2 \geq p$, the motion is non-oscillatory, and the space-time curve is logarithmic and asymptotic to one of the lines $x = cv/R \pm F/R$, according as the initial displacement is positive or negative.

Experimental. Solid friction only.

Observations were made upon the oscillations of a pendulum of relatively small dimensions but appreciable moment of inertia, consisting of a rectangular sectioned steel bar about six inches long, weighted at its lower end. The head of the bar, which was somewhat broader than the body, was bored just large enough to form a "running" fit upon a steel journal one inch diameter. Actually the head of the pendulum was slotted from bore outwards, and fitted with a set screw for the purpose of providing a varying degree of "pinch" of the bearing upon the journal, but the arrangement proved fierce, and was employed only to ensure absence of slack at the bearing. Pressures were thus those due to

the weight of the pendulum alone, apart from small additional pressures arising from centrifugal action. The journal was allowed to remain in the chuck-jaws of the fairly heavy lathe in which it was turned, the pendulum was mounted upon it and records were taken of oscillations with both stationary and rotating unlubricated journal. Movements were recorded by a light scriber mounted on the pendulum, which bore gently upon an endless band of smoked paper stretched between two revolving parallel drums.

Photographic prints of some of these records taken from the originals by direct-contact exposure are here reproduced, and though the oscillations of the pendulum were too large

Fig. 4.

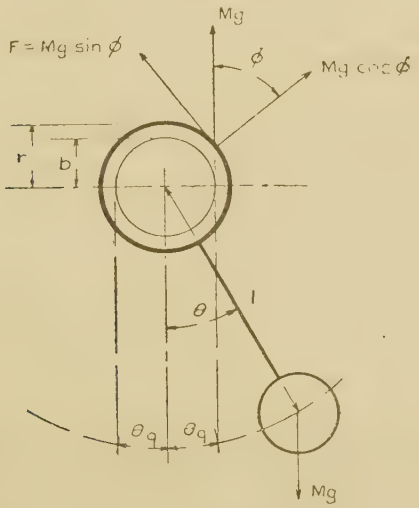

to be considered as "simple harmonic," the principal features of the damped vibrations as already enunciated are not seriously affected, and are well borne out by the numerous records obtained.

The resultant pressures and forces involved whilst motion exists between pendulum and journal are as illustrated in fig. 4, and if $I\ (=Mk^2)$ is the moment of inertia of the pendulum about its centre of oscillation, M its mass, l the distance of its mass-centre from the centre of oscillation, F the ultimate tangential frictional resistance between journal and bearing, and r the radius of the journal, the equation of motion is

$$I\ddot{\theta} = \pm Fr - Mgl\sin\theta, \quad . \quad . \quad . \quad . \quad . \quad (21)$$

whence

$$\dot{\theta}^2 = (2g/k^2)(\pm \mathrm{F}r\theta/\mathrm{M}g + l\cos\theta) + \mathrm{C}$$
$$= a(l\cos\theta \pm b\theta) + \mathrm{C}. \quad . \quad . \quad . \quad . \quad . \quad (22)$$

The sign of F or b is that of $(\Omega - \dot{\theta})$, where Ω is the angular velocity of the journal, and much as in the case of equation (1), equations (21) and (22) cease to apply when $(\Omega - \dot{\theta})$ is zero, and at the same time $\sin\theta$ is not numerically greater than $\mathrm{F}r/\mathrm{M}gl$ or $\mathrm{F}_s r/\mathrm{M}gl$, if static friction is taken into account. $\theta_g = \pm\sin^{-1}\mathrm{F}r/\mathrm{M}gl$ clearly represents the positions of running equilibrium when the pendulum rides, without oscillation, on the rotating journal, and the verticals through the centre of mass are then tangential to the friction circle of radius b or $\mathrm{F}r/\mathrm{M}g$. Generally, whilst F has its limiting value, the line of action of the resultant pressure of the journal upon the bearing is tangential to that circle, as shown in fig. 4; the normal pressure is $\mathrm{M}g\cos\phi$, the tangential force F is $\mathrm{M}g\sin\phi$, and the eccentricity of of the resultant is $b = r\sin\phi = \mathrm{F}r/\mathrm{M}g$. When, as in the experiments performed, the only pressures concerned are those arising from the weight of the pendulum itself, and if small additional pressures due to centrifugal action are ignored, $\mathrm{F} = \mathrm{M}g\sin\phi = \mu\mathrm{M}g\cos\phi$ and $\tan\phi = \mu$.

In applying equation (22) three cases arise as before :—

(1) Rapidly moving journal, Ω positive and always greater than $\dot{\theta}$.

Here friction is uni-directional and, throughout the motion,

$$\dot{\theta}^2 = a(b\theta + l\cos\theta) + \text{const.}$$

Hence, if θ_1 is an initial maximum displacement, subsequent maximum displacements are given by

$$\cos\theta = \frac{b}{l}(\theta_1 - \theta) + \cos\theta_1,$$

i. e., the pendulum eventually returns, after a complete swing, to its initial position θ, and oscillations are continuous (see figs. 5 and 6). During a semi-oscillation from θ_1 to θ_2, the mean position $(\theta_1 + \theta_2)/2$ follows from

$$l(\cos\theta_2 - \cos\theta_1) = b(\theta_1 - \theta_2)$$

or

$$\sin\frac{\theta_1 + \theta_2}{2} = \frac{b}{l}\frac{(\theta_1 - \theta_2)}{2} \Big/ \sin\left(\frac{\theta_1 - \theta_2}{2}\right),$$

and it is thus not coincident with the position of maximum velocity θ_g, but approximates thereto.

(2) Stationary journal, $\Omega=0$.

Friction reverses with reversal of velocity at each semi-oscillation, and for successive maximum positions θ_1, θ_2, θ_3, etc., in either direction,

$$l(\cos\theta_2-\cos\theta_1)=b(\theta_1-\theta_2),$$

$$l(\cos\theta_3-\cos\theta_2)=-b(\theta_2-\theta_3), \text{ etc.},$$

i. e., in the first semi-oscillation the pendulum swings from one extreme to the next, equally placed on the opposite side

Fig. 5.

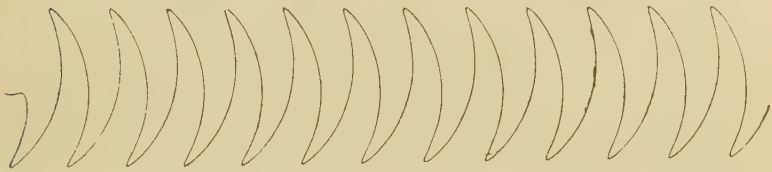

Fig. 6.

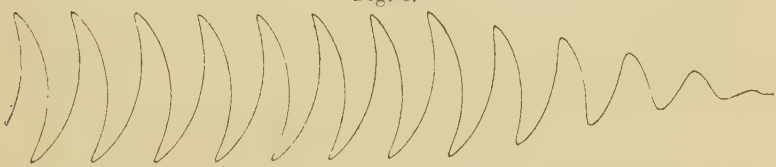

Fig. 7.

of a mean position determined by

$$\sin\left(\frac{\theta_1+\theta_2}{2}\right)=\frac{b}{l}\frac{(\theta_1-\theta_2)}{2}\Big/\sin\left(\frac{\theta_1-\theta_2}{2}\right),$$

whilst on the return swing the mean position is given by

$$\sin\left(\frac{\theta_2+\theta_3}{2}\right)=-\frac{b}{l}\left(\frac{\theta_2-\theta_3}{2}\right)\Big/\sin\left(\frac{\theta_2-\theta_3}{2}\right).$$

The mean position is thus transferred successively from one side of the central vertical position to the other, and amplitudes are diminished until θ becomes zero within the stable region $\pm\theta_q$, when motion ceases (see fig. 7).

(3) Slowly rotating journal, Ω positive but not always greater than $\dot{\theta}$.

From an initial maximum displacement θ_1, F is positive until $\dot{\theta}=\Omega$, when, if θ is numerically greater than θ_q, reversal of sign occurs. The mean position, derived as before from $a(l\cos\theta \pm b\theta)$ a constant, thus changes from one side of the central vertical position to the other, and amplitudes are diminished until eventually $\dot{\theta}$ becomes equal to Ω whilst θ is less than θ_q. The pendulum then turns with the journal until released at $\theta=\theta_q$, if the difference between static and kinetic limiting frictions is negligible, and oscillations continue as in case (1) (see figs. 8 and 9).

Fig. 8.

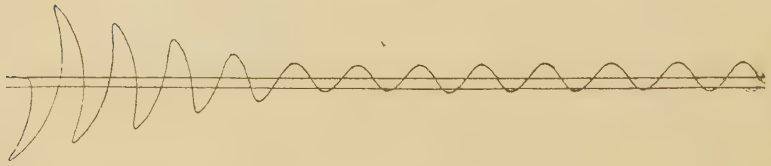

Fig. 9.

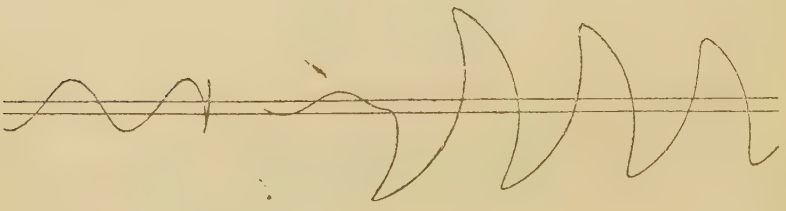

If F_s is appreciably greater than F, release is delayed until a somewhat greater value of θ is attained; subsequent oscillations include each a period of uniform angular velocity, and the effect is continuous.

Of the records here reproduced, figs. 5 and 6 show the beginning and end of a series of oscillations following an initial displacement given to the pendulum when riding upon a rapidly revolving journal (126 rev. per min.), and it will be seen that amplitudes were undiminished until the lathe was stopped, when, as shown at the end of fig. 6, oscillations were rapidly damped out of existence. Fig. 7 is taken from the record of a series of oscillations with stationary journal. The two parallel lines shown in this and in the subsequent figures were recorded with the

pendulum at rest and drawn aside to one or other of its extreme positions of equilibrium, and they define, as nearly as could be obtained, the region of stability. The record illustrates the rapid damping effect of even small values of friction, the approximate equality of angular displacements about the limiting stable positions in succession, and the final cessation of oscillatory motion at different positions within the stable region. Figs. 8 and 9 are portions of records of oscillations performed upon a slowly revolving journal. In the former, the rapid initial damping followed by continuous oscillation when a certain amplitude had been attained is clearly shown, and the latter really portrays the same effect, for the oscillations shown to the left of the record are the continuation of the initial oscillations shown to the right after extending completely around the recording band, a length of about 20 inches.

On each record a circle, not here shown, was described by revolving the pendulum about its centre of rotation with the recording apparatus at rest, and in this fashion the radius and centre of the circular path of the scriber were determined. Using a specially constructed celluloid protractor, on which a circle of similar radius was inscribed, it was possible, by laying the zero line of the protractor along the locus of the centre of oscillation on the record, and noting the angle at which the circle intersected various parts of the oscillatory curve, to determine angular displacements from any chosen datum and to plot the records to rectangular axes. In this manner the double amplitudes of final oscillations in figs. 8 and 9 were determined and compared, and in each of the several records taken it was found that these values were approximately in proportion to the speeds of the journal: *e.g.*, in the records here reproduced the double amplitudes concerned were respectively about 12·5° and 23°, whilst the journal speeds were approximately 8 and 14 rev. per min. The ratio of amplitudes is thus 0·54 and of speeds 0·57.

The means available for driving the recording apparatus did not ensure perfect uniformity of speed during an observation, and the records are probably not quite reliable in respect of time-intervals. For this reason the curves, too, may be slightly distorted from their true forms, but the values of extreme displacements and the general characteristics of the oscillations are not affected. The records fulfil the purpose for which they were intended, that of supporting experimentally the principal deductions previously made analytically, and it is from that standpoint that they are presented.

XXXIV. *On the Free Periods of Resonators.*

By Eric J. Irons, *Ph.D.**

§ 1. Introduction.

In a former paper [1] use was made of the principles of "acoustical impedance" to calculate the free periods of a number of different forms of resonator, and to account for some results obtained by experiments with a Kundt's tube apparatus. In the present note the argument is presented in more detail, and is extended to include resonators having a conical horn as a component part.

Fig. 1.

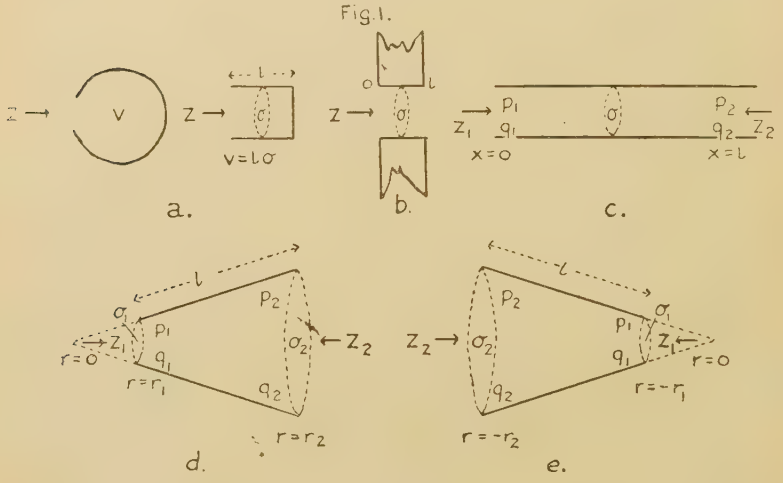

Webster [2] confined his attention to plane waves in horns of narrow cross-section, and wrote

$$-\frac{dq}{dx} = -\frac{1}{\sigma}\frac{d}{dx}(q\sigma),$$

where σ is the area of cross-section and x is a measure of the distance along the horn. It is here shown that with conical horns Webster's differential equation is obtained without restriction as to cross-section if *spherical waves* are postulated †.

* Communicated by the Author.

† Stewart (Phys. Rev. xvi. p. 322, 1920) states that Webster was aware of this result but did not publish it.

Immediate applications of the formulæ to be established are shown to yield more readily results which have been previously obtained by other methods.

In the earlier paper by the present writer [1] the electrical analogy of Stewart [3] was employed, and impedance was defined as $p \Big/ \frac{dX}{dt}$, where p represents excess pressure, and X is volume displacement. In this note Webster's practice of defining impedance by p/X is followed—as the formulæ to be established are thereby simplified—and the whole argument is made more general.

§ 2. Calculation of the Impedances of Various Units.

Let us denote displacement, pressure, elasticity, condensation, frequency, and impedance by η, p, e, s, n, and Z repectively, and define $\omega = 2\pi n$, $k = \omega/a$, and $\beta = \rho a^2 k$, where a is the velocity of sound and ρ is the density of the medium.

The usual assumptions that the fluid in the immediate neighbourhood of an orifice is incompressible, and that the condensation throughout a reservoir is uniform, will be made.

(1) *Reservoir.* (Fig. 1, *a*.)

If an excess pressure p gives rise to a volume displacement X in a reservoir of volume v, then

$$p = e.s = a^2\rho(X/v),$$

and the impedance

$$Z = p/X = a^2\rho/v. \quad . \quad . \quad . \quad . \quad . \quad (1.1)$$

(2) *Orifice.* (Fig. 1, *b*.)

The equation of motion of a mass of fluid m situated in an orifice of length l and area of cross-section σ, when subjected to an alternating pressure p ($= P \exp. i\omega t$), is

$$m\ddot{q} = \sigma P \exp. i\omega t.$$

Integrating twice gives

$$mq = (\sigma P \exp. i\omega t)/(-\omega^2),$$

and, as $m = \rho l\sigma$ and $X = q\sigma$,

$$Z = p/X = -\omega^2\rho/c, \quad . \quad . \quad . \quad . \quad (1\cdot2)$$

where c is the conductance of the orifice.

(3) *Tube.* (Fig. 1, *c*.)

In his paper, Webster [2] gave a general method for determining the impedances of horns (of which the cylindrical tube is a special case); the present note being concerned solely with tubes and conical horns, the required formulæ may be established more directly in the following manner.

Assuming q to vary as exp. $i\omega t$, we may write

$$\dot{q} = i\omega q \quad \text{and} \quad \ddot{q} = -\omega^2 q.$$

Substituting this result in the general equation of motion,

$$\rho \frac{d^2q}{dt^2} + \frac{dp}{dx} = 0,$$

it follows that

$$\omega^2 q = \frac{1}{\rho}\frac{dp}{dx},$$

i. e.,
$$\beta k q = \frac{dp}{dx} \quad \text{or} \quad \beta q = \frac{dp}{d(kx)}. \quad * \quad . \quad . \quad . \quad (2)$$

For plane waves in a cylindrical tube

$$a^2 \frac{d^2q}{dx^2} = \frac{d^2q}{dt^2} = -\omega^2 q \quad \text{or} \quad a^2 \frac{d^2}{dx^2}\left(\frac{dq}{dx}\right) = -\omega^2\left(\frac{aq}{dx}\right),$$

which, since

$$p = e\left(-\frac{dq}{dx}\right),$$

leads to

$$\frac{d^2p}{dx^2} + k^2 p = 0. \quad . \quad . \quad . \quad . \quad . \quad (2.1)$$

the solution of this equation is

$$p = \mathrm{A}\cos kx + \mathrm{B}\sin kx, \quad . \quad . \quad . \quad . \quad (2.2)$$

and, using the result of (2), we may write

$$\beta q = -\mathrm{A}\sin kx + \mathrm{B}\cos kx. \quad . \quad . \quad . \quad (2.3)$$

Denoting values at the two ends of the tube at $x=0$ and $x=l$ by the subscripts 1 and 2 respectively, and writing σ for the cross-sectional area of the tube, we have

$$p_1 = \mathrm{A}, \qquad \beta q_1 = \mathrm{B},$$
$$p_2 = \mathrm{A}\cos kl + \mathrm{B}\sin kl, \quad \beta q_2 = -\mathrm{A}\sin kl + \mathrm{B}\cos kl,$$

* This assumes that the excess pressure p is so small that ρ may be taken as constant.

whence

$$Z_2 = p_2/X_2 = \frac{\beta}{\sigma} \cdot \frac{p_2}{\beta q_2} = \frac{\beta}{\sigma} \cdot \frac{(p_1/\sigma q_1)\cos kl + (\beta/\sigma)\sin kl}{(-p_1/\sigma q_1)\sin kl + (\beta/\sigma)\cos kl}$$

$$= \frac{\beta}{\sigma} \cdot \frac{Z_1 \cos kl + (\beta/\sigma)\sin kl}{-Z_1 \sin kl + (\beta/\sigma)\cos kl}. \quad (3.1)$$

Similarly,

$$Z_1 = \frac{\beta}{\sigma} \cdot \frac{Z_2 \cos kl - (\beta/\sigma)\sin kl}{Z_2 \sin kl + (\beta/\sigma)\cos kl}. \quad . \quad . \quad (3.2)$$

These results correspond to equation (28) of Webster's paper [2].

(4) *Conical Horn.* (Fig. 1, *d*.)

For spherical waves we have [4]

$$\frac{d^2(r.s)}{dt^2} = a^2 \frac{d^2(r.s)}{dr^2} \quad . \quad . \quad . \quad . \quad . \quad (4)$$

(the symbols having their usual significance), and, since $p = e.s$,

$$r\frac{d^2p}{dt^2} = a^2 \frac{d^2(r.p)}{dr^2}.$$

Further, if p varies as $\exp. i\omega t$, then

$$\ddot{p} = -\omega^2 p,$$

so that finally

$$\frac{d^2p}{dr^2} + \frac{2}{r}\frac{dp}{dr} + k^2 p = 0. \quad . \quad . \quad . \quad . \quad (4.1)$$

The solution of this equation is

$$p = \frac{A\cos kr}{kr} + \frac{B\sin kr}{kr}. \quad . \quad . \quad . \quad . \quad (4.2)$$

Differentiating with respect to kr, we have, by virtue of (2),

$$\beta q = A\left\{-\frac{\sin kr}{kr} - \frac{\cos kr}{k^2r^2}\right\} + B\left\{\frac{\cos kr}{kr} - \frac{\sin kr}{k^2r^2}\right\}.$$

$$. \quad . \quad . \quad (4.3)$$

Considering the propagation of spherical waves in a conical horn, the smaller and larger ends of which are situated at distances $r = r_1$, and $r = r_2$ from the vertex of the cone at $r = 0$, and again denoting the values of p, σ, and X at these ends by the subscripts 1 and 2 respectively, equations for p_1, p_2, βq_1, and βq_2 may be written down. Solving for A and B between the equations for p_1 and βq_1, and substituting the values obtained in the equations for p_2 and βq_2, gives p

and βq_2 respectively in terms of p_1 and βq_1. After some reduction, we have

$$Z_2 = p_2/X_2 = \frac{p_2}{\beta q_2} \cdot \frac{\beta}{\sigma_2}$$

$$= -\frac{\beta}{\sigma_2} \cdot \frac{Z_1 \sin k(l+\epsilon_1)/\sin k\epsilon_1 + (\beta/\sigma_1)\sin kl}{Z_1 \sin k(l+\epsilon_1-\epsilon_2)/\sin k\epsilon_1 . \sin k\epsilon_2 + (\beta/\sigma_1)\sin k(l-\epsilon_2)/\sin k\epsilon_2}, \quad \ldots \quad (5.1)$$

where $l=(r_2-r_1)$ and ϵ_1 and ϵ_2 are defined by $\tan k\epsilon_1 = kr_1$ and $\tan k\epsilon_2 = kr_2$.

In a similar manner it may be shown that

$$Z_1 = -\frac{\beta}{\sigma_1} \cdot \frac{Z_2 \sin k(l-\epsilon_2)/\sin k\epsilon_2 + (\beta/\sigma_2)\sin kl}{Z_2 \sin k(l+\epsilon_1-\epsilon_2)/\sin k\epsilon_1 . \sin k\epsilon_2 + (\beta/\sigma_2)\sin k(l+\epsilon_1)/\sin k\epsilon_1} \quad (5.2)$$

These results correspond to equation (32) of Webster's paper [2].

§ 3. Notes on the Formulæ.

Throughout the paper the "length" of a pipe or cone with a *completely open* end is to be interpreted as the sum of its geometrical length and the appropriate end-correction, and the quantities involved are as shown on the respective diagrams. Terms involving friction are neglected as small compared with the terms retained, so that for resonance in any system the total impedance may be equated to zero.

The formulæ so far obtained yield immediately the following well-known results for:—

(1) *Resonance in Tubes* (using equation (3.2)).

a. Tube open at both ends. $Z_1 = Z_2 = 0$.

$$\therefore \quad -(\beta/\sigma).\tan kl = 0 ;$$

$$\therefore \quad kl = m\pi \quad \text{and} \quad l = m\lambda/2,$$

where m is any integer and λ is a wave-length.

b. Tube closed at one end. $Z_1 = 0$, $Z_2 = \infty$.

$$\therefore \quad (\beta/\sigma)\cot kl = 0 \quad \text{and} \quad l = [(2m+1)/2].[\lambda/2].$$

c. Tube closed at both ends. $Z_1 = Z_2 = \infty$.

$$\therefore \quad (\sigma/\beta)\tan kl = 0 \quad \text{and} \quad l = m\lambda/2.$$

Similar results are obtained using equation (3.1).

(2) *Resonance in Cones* (using equations (5.1) and (5.2)).

a. Cone open at both ends. $Z_1 = Z_2 = 0$.

By (5.1),

$$(-\beta/\sigma_2)\sin kl.\sin k\epsilon_2/\sin k(l-\epsilon_2) = 0,$$

and by (5.2),

$$(-\beta/\sigma_1)\sin kl.\sin k\epsilon_1/\sin k(l+\epsilon_1) = 0.$$

The only reasonable solution of both these equations is

$$\sin kl = 0 \quad \text{leading to} \quad m\lambda/2 = (r_2 - r_1),$$

with the usual notation (*cf.* Rayleigh [5]).

b. Cone closed at

(i.) Smaller end. $Z_1 = \infty$, $Z_2 = 0$.

By (5.1),

$$(-\beta/\sigma_2)\sin k(l+\epsilon_1).\sin k\epsilon_2/\sin k(l+\epsilon_1-\epsilon_2) = 0,$$

and by (5.2),

$$(-\beta/\sigma_1)\sin kl.\sin k\epsilon_1/\sin k(l+\epsilon_1) = \infty.$$

Hence in both instances

$$\sin k(l+\epsilon_1) = 0 \quad \text{or} \quad \tan kl + kr_1 = 0,$$

(*cf.* Paris [6], eqn. 44).

(ii.) Larger end. $Z_1 = 0$, $Z_2 = \infty$.

By (5.1),

$$(-\beta/\sigma_2)\sin kl.\sin k\epsilon_2/\sin k(l-\epsilon_2) = \infty,$$

and by (5.2),

$$(-\beta/\sigma_1)\sin k(l-\epsilon_2)\sin k\epsilon_1/\sin k(l+\epsilon_1-\epsilon_2) = 0.$$

Hence in both instances

$$\sin k(l-\epsilon_2) = 0 \quad \text{or} \quad \tan kl = kr_2$$

(*cf.* Aldis [7]). Further, if the cone be continued to the vertex,

$$l = r_2 \quad \text{and} \quad \tan kl = k$$

(*cf.* Rayleigh, *loc. cit.*).

c. Cone closed at both ends. $Z_1 = Z_2 = \infty$.

By (5.1),

$$(-\beta/\sigma_2)\sin k(l+\epsilon_1)\sin k\epsilon_2/\sin k(l+\epsilon_1-\epsilon_2) = \infty,$$

and by (5.2),

$$(-\beta/\sigma_1)\sin k(l-\epsilon_2)\sin k\epsilon_1/\sin k(l+\epsilon_1-\epsilon_2) = \infty.$$

Hence in both instances

$$\sin k(l+\epsilon_1-\epsilon_2) = 0 \quad \text{or} \quad \tan^{-1} kr_1 - kr_1 = \tan^{-1} kr_2 - kr_2$$

(*cf.* Rayleigh, *loc. cit.*). If the cone be continued to the vertex so that $r_1=0$ and $r_2=l$, then, as in the last paragraph,

$$\tan kl = kl.$$

When dealing with a system of resonators, distances will, for consistency, be measured in the direction of x positive, and the impedances of the systems to sound incident in the same direction will be calculated. This will necessitate an alteration in the formula for the impedance at the larger end of a cone. Putting r_1, r_2, and l negative, so that $-l=-(r_2-r_1)$ (fig. 1, *e*), and substituting in (5.1), leads to

$$Z_2 = -\frac{\beta}{\sigma_2}\,\frac{Z_1 \sin k(l+\epsilon_1)/\sin k\epsilon_1 - (\beta/\sigma_1)\sin kl}{-Z_1 \sin k(l+\epsilon_1-\epsilon_2)/\sin k\epsilon_1 . \sin k\epsilon_2 + (\beta/\sigma_1)\sin k(l-\epsilon_2)/\sin k\epsilon_2} \quad . \quad (5.3)$$

It may be noted that if $-l$ be substituted for l in (3.1), then the formulæ (3.1) and (3.2) for a tube become identical.

Moreover, if we make $r_1 \to \infty$ and $r_2 \to \infty$ in such a manner that (r_2-r_1) remains finite and equal to l, then the cone becomes equivalent to a tube with $\sigma_1=\sigma_2=\sigma$ (the cross-sectional area of the tube) and the values of both Z_1 given by (5.2) and Z_2 given by (5.3) become identical with that of Z_1 for a tube (3.2).

Further, if the tube be short (so that kl may be substituted for $\tan kl$) and closed ($Z_2=\infty$), then the formula for Z_1 (3.2) reduces to $a^2\rho/v$ (*cf.* fig. 1, *a*), which is the value for a reservoir. Similarly, if the tube be short and open ($Z_2=0$), then the formula for Z_1 becomes $-\omega^2\rho/c$, which is the value for an orifice.

It may also be noted that the formula for Z_2 for a cone given in (5.1) reduces to that for Z_2 for a tube given in (3.1) under the appropriate conditions.

§ 4. Application of Formulæ to some Compound Systems.

As a preliminary it may be noted that the impedance of a component part consisting of an orifice leading to a reservoir is, by virtue of (1.1) and (1.2), given by

$$-\omega^2\rho/c + a^2\rho/v.$$

For resonance this quantity must be equated to zero and, if n_1 represents the natural frequency of such a resonator, then

$$n_1 = a/2\pi . \surd (c/v),$$

the well-known formula for a Helmholtz resonator. The impedance of the system to a note of frequency n may therefore be written as

$$-(2\pi n)^2 . \rho/c + (2\pi n_1)^2 . \rho/c \quad \text{or} \quad -(4\pi^2 \rho n n_1/c) . \left(\frac{n}{n_1} - \frac{n_1}{n}\right) \quad . \quad . \quad . \quad (1.3)$$

by substituting for a^2/v in terms of n_1.

All the formulæ to obtain results previously given by Paris (*loc. cit.*), Aldis (*loc. cit.*), Rayleigh (*loc. cit.*), and by Lees [8] have now been established. Some of these results have, subject to an implied but unnecessary assumption, already been obtained on impedance principles [1] but are included here for the sake of completeness.

(1) *Stopped Pipe with Helmholtz Resonator at the End. (Boys' Resonator.)* (Fig. 2.)

For resonance, Z_1, as determined by (3.2), must be zero, *i. e.*,

$$Z_2 \cos k\mathrm{L} - (\beta/\sigma) \sin k\mathrm{L} = 0,$$

where Z_2 has the value given by (1.3). It follows that

$$\tan k\mathrm{L} = -\frac{2\pi\sigma n_1}{ac_1}\left(\frac{n}{n_1} - \frac{n_1}{n}\right), \quad . \quad . \quad . \quad . \quad (6)$$

which is the same as the result of Paris (Ref. 6, eqn. 1).

(2) *Stopped Pipe with Helmholtz Resonator on the Side.* (Fig. 3.)

The impedance at $x = l$ of the closed tube of length $(\mathrm{L} - l)$ is $(\beta/\sigma) . \cot k(\mathrm{L} - l)$. When a displacement passing from $x = 0$ to $x = l$ reaches $x = l$, it may be propagated either through the orifice into the reservoir or into the tube of length $(\mathrm{L} - l)$; the impedances of these components must therefore be considered in parallel, so that

$$1/Z_2 = 1/(\beta/\sigma) \cot k(\mathrm{L} - l) - 1/(4\pi^2 \rho n n_1/c_1) . (n/n_1 - n_1/n),$$

Z_1 having the value given by (3.2), for resonance,

$$Z_2 \cos kl - (\beta/\sigma) \sin kl = 0,$$

whence

$$\frac{1}{\cot kl - \tan k(\mathrm{L}-l)} = -\frac{2\pi\sigma n_1}{ac_1}\left(\frac{n}{n_1}-\frac{n_1}{n}\right) \quad . \quad . \quad (7)$$

(*cf.* Ref. 6, eqn. 10).

(3) *Stopped Pipe with Two Helmholtz Resonators on the Side.* (Fig. 4.)

The impedance at $x=l_1+\delta$ (where δ is small) is, by application of the formulæ and principles evoked in the last example, equal to

$$\frac{\beta}{\sigma}\cdot\frac{\mathrm{Z}_0\cos k(l_2-l_1)-(\beta/\sigma)\sin k(l_2-l_1)}{\mathrm{Z}_0\sin b(l_2-l_1)+(\beta/\sigma)\cos k(l_2-l_1)},$$

where

$$1/\mathrm{Z}_0 = 1/(\beta/\sigma)\cot k(\mathrm{L}-l_2) - 1/(4\pi\rho n n_2/c_2)\,.\,(n/n_2-n_2/n).$$

The impedance at $x=l_1-\delta$, Z_2, is equal to the sum in parallel of this quantity and $-(4\pi\rho n n_1/c_1)\,.\,(n/n_1-n_1/n)$. Finally, for resonance, the impedance at $x=0$, Z_1, is zero, so that

$$\mathrm{Z}_2\cos kl_1-(\beta/\sigma)\sin kl_1 = 0.$$

After some reduction this gives

$$\frac{\cot kl_2+\mathrm{T}_2\cot k(\mathrm{L}-l_2)}{1-\mathrm{S}_2\cot k(\mathrm{L}-l_2)} = \frac{1+\mathrm{S}_1\cot kl_1}{\mathrm{S}_1-\cot kl_1}, \quad . \quad . \quad (8)$$

where, following Paris (Ref. 6, eqns. 12, 27, and 28), we write

$$\mathrm{S}_1 = \cot kl_1+\cot k\gamma_1, \qquad \mathrm{T}_2 = 1-\cot k\gamma_2\,.\cot kl_2,$$
$$\mathrm{S}_2 = \cot kl_2+\cot k\gamma_2, \quad \tan k\gamma_s = (2\pi\sigma n_s/ac_s)\,.\,(n/n_s-n_s/n).$$

(4) *Conical Horn fitted with Helmholtz Resonator at the Smaller End.* (Fig. 5.)

Substituting the value of Z_1 from (1.3) in the formula (5.3) for Z_2, and equating to zero for resonance, gives

$$-(4\pi\rho n n_1/c_1)\,.\,(n/n_1-n_1/n)\,[\sin k(\mathrm{L}+\epsilon_1)/\sin k\epsilon_1] - (\beta/\sigma_1)\sin k\mathrm{L} = 0\,;$$

whence, writing $\Omega\mathrm{R}_0^2$ for σ_1, where Ω is the solid angle of the cone, and remembering that $\cot k\epsilon_1 = 1/k\mathrm{R}_0$, we have

$$\frac{1}{(a/2\pi n\mathrm{R}_0)+\cot(2\pi n\mathrm{L}/a)} = \frac{-2\pi\Omega\mathrm{R}_0^2 n_1}{ac_1}\left(\frac{n}{n_1}-\frac{n_1}{n}\right), \quad (9)$$

which is the result obtained by Paris (Ref. 6, eqn. 43).

(5) *Cone Closed at Smaller End with Helmholtz Resonator on the Side.* (Fig. 6.)

At the closed end of the cone $Z_0 = \infty$, so that the impedance due to this unit at the large end of the cone R_0R_1

Fig. 2.

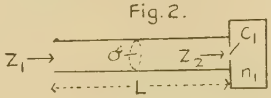

Fig. 3.

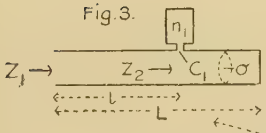

Fig. 4.

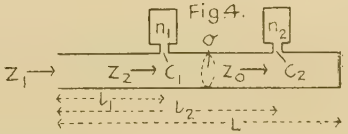

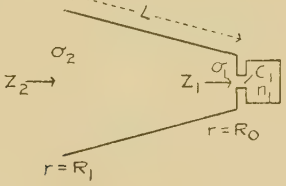

Fig. 5.

Fig. 6.

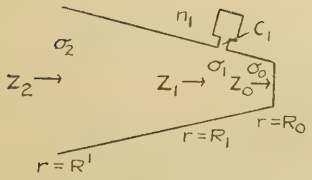

Fig. 7.

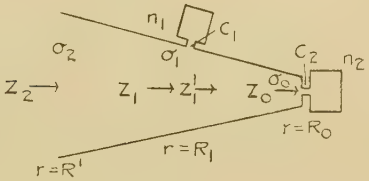

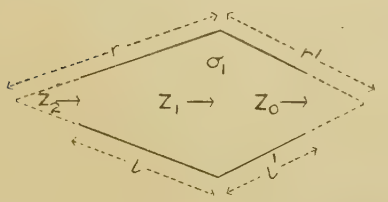

Fig. 8.

$\tan k\epsilon_1 = kr$; $\tan k\epsilon_1' = kr'$

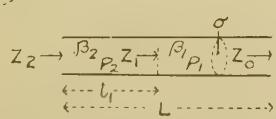

Fig. 9.

is, by substitution of the relevant quantities in (5.3), equal to

$$(\beta/\sigma_1).[\sin k(R_1 - R_0 + \epsilon_0).\sin k\epsilon_1/\sin k(R_1 - R_0 + \epsilon_0 - \epsilon_1)] = Z_1' \quad \text{(say)}.$$

The effective impedance at R_1, Z_1, is found by adding in parallel the impedance of the cone R_0R_1 and the orifice and reservoir—thus

$$1/Z_1 = 1/Z_1' - 1/(4\pi^2\rho n n_2/c_1).(n/n_1 - n_2/n).$$

Finally, equating the value of Z_2 given by (5.3) to zero,

$$Z_1 \sin k(R' - R_1 + \epsilon_2)/\sin k\epsilon_1 - (\beta/\sigma_1)\sin k(R' - R_1) = 0,$$

and substituting the value of Z_1 leads to

$$\frac{1}{\cot k(R - R_1 - \epsilon_2) - \tan k(R_1 - R_0 - \epsilon_1)} = \frac{-2\pi\Omega R_1^2 n_1}{} \left(\frac{n}{n_1} - \frac{n_1}{n}\right). \quad \ldots \quad (10)$$

where, as in Paris's notation, ρ_0 is defined by

$$\cot k\rho_0 = k R_0$$

(*cf.* Ref. 6, eqn. 30).

(b) *Cone with one End Open: Resonance at the Smaller End and Antinode on the Side.* (Fig. 7.)

At the smaller end of the cone

$$Z_0 = -(4\pi^2\rho n n_2/c_2).(n/n_2 - n_2/n).$$

The impedance at R_1 ($= Z_1'$, say) of the system R_0R_1 is given by

$$Z_1' = -\frac{\beta}{\sigma_1}.\frac{Z_0 \sin k(R_1 - R_0 + \epsilon_0)/\sin k\epsilon_0 - (\beta/\sigma_0)\sin k(R_1 - R_0)}{-Z_0 \sin k(R_1 - R_0 + \epsilon_1 - \epsilon_2)/\sin k\epsilon_2 . \sin k\epsilon_1 + (\beta/\sigma_0)\sin k(R_1 - R_0 - \epsilon_1)/\sin k\epsilon_1},$$

so that the total impedance at R_1, Z_1, is such that

$$1/Z_1 = 1/Z_1' - 1/(4\pi^2\rho n n_1 c_1).(n/n_1 - n_1/n).$$

Finally, equating the impedance at $R' = Z_2$ to zero for resonance, we obtain

$$Z_1 \sin k(R - R_1 + \epsilon_2)/\sin k\epsilon_2 = (\beta/\sigma_1)\sin k(R - R_1).$$

Following Paris [6], and defining

$$\cot k\gamma = \frac{c_2}{1 - (n_2^2/n^2)} \cdot \frac{1}{k\Omega R_0^2}$$

and

$$\cot kK = \frac{kR_0(\cot kR_0 - \cot k\gamma) - 1}{kR_0 + \cot kR_0 + kR_0 . \cot kR_0 . \cot k\gamma} *$$

* There is a mistake in sign in the revised form of Paris's eqn. 35.

we obtain his result,

$$\frac{1}{\cot k(\mathrm{R}'-\mathrm{R}_1)}-\tan k(\mathrm{R}_1-\mathrm{K}) = \frac{-2\pi\Omega\,\mathrm{R}_1{}^2 n_1}{ac_1}\left(\frac{n}{n_1}-\frac{n_1}{n}\right),$$

for the resonant tones. . . . (11)

(7) *Two Open Cones joined at their Larger Ends.* (Fig. 8.)

As $Z_0=0$, then

$$Z_1 = (\beta/\sigma_1)\sin kl'.\sin k\epsilon_1'/\sin k(l'-\epsilon_1')$$

by (5.3). For resonance $Z_2=0$, *i. e.*,

$$-(\beta/\sigma_2)\left[Z_1\sin k(l-\epsilon_1)/\sin k\epsilon_1+(\beta/\sigma_1)\sin kl\right]=0$$

by (5.2), or

$$\sin kl'.\sin k(l-\epsilon_1).\sin k\epsilon_1' = -\sin kl.\sin k(l'-\epsilon_1').\sin k\epsilon_1,$$

or

$$\sin kl.\sin kl'(1/r+1/r') = k\sin k(l+l'), \quad . \quad . \quad . \quad (12)$$

which is the result given by Aldis (*loc. cit.*).

(8) *A Composite Column of Gas.* (Fig. 9.)

Prof. Lees[8] has recently derived equations giving the free periods of a composite column consisting of two gases: his results may be obtained by impedance methods and, as an example, the formula for the instance in which both ends of the column are antinodes is derived below.

As $Z_0=0$, the impedance at $x=l_1$ of the column of length $(\mathrm{L}-l_1)$ containing the first gas to a note of frequency n is

$$Z_1 = -(\beta_1/\sigma)\tan k_1(\mathrm{L}-l_1),$$

where $\beta_1=\rho_1 a_1{}^2 k$ and $k_1=2\pi n/a_1$, and the subscripts refer to the constants of the first gas. Again, as $Z_2=0$, then by (3.2),

$$Z_1\cos k_2 l_1-(\beta_2/\sigma)\sin k_2 l_1 = 0,$$

where $\beta_2=\rho_2 a_2{}^2 k_2$ and $k_2=2\pi n/a_2$. Now if the period of the column when filled with the first constituent is n_1, then

$$2\mathrm{L}n_1 = a_1 = \surd(\mathrm{F}_1/\rho_1), \qquad k_1=(\pi/\mathrm{L})(n/n_1),$$

and

$$\beta_1 = \mathrm{F}_1(\pi/\mathrm{L})(n/n_1),$$

where F_1 is the modulus of adiabatic elasticity of this constituent. By writing down the equations which hold when

the second constituent fills the column similar values for k_2 and β_2 are obtained, so that finally

$$(n_2/\mathrm{F}_2)\cot\frac{\pi}{\mathrm{L}}\cdot\frac{n}{n_2}\cdot l_1 = -(n_1/\mathrm{F}_1)\cot\frac{\pi}{\mathrm{L}}\cdot\frac{n}{n_1}(\mathrm{L}-l_1), \quad (13)$$

which is Lees' equation (7.3).

Fig 10.

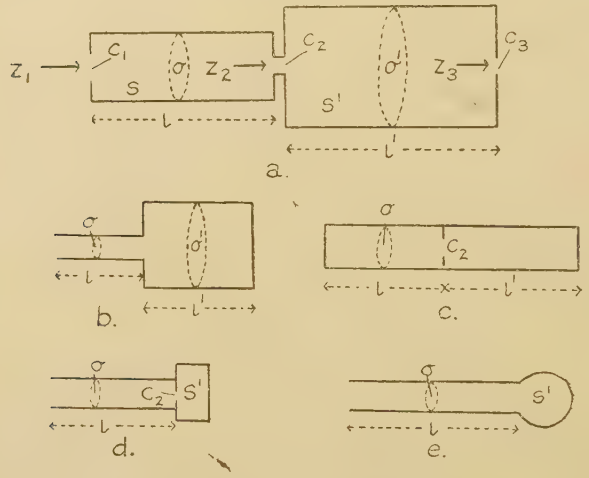

(9) *Two Coaxial Tubes with Orifices communicating with the Outer Atmosphere and with each other.*

As a final example, the resonant frequencies of the system shown in fig. 10, *a* will be calculated.

From equations (1.2) and (3.2) we have :—

$$\mathrm{Z}_3 = -\omega^2\rho/c_3,$$

$$\mathrm{Z}_2 = \frac{\beta}{\sigma'}\left[\frac{(-\omega^2\rho/c_3)\cos kl' - (\beta/\sigma')\sin kl'}{(-\omega^2\rho/c_3)\sin kl' + (\beta/\sigma')\cos kl'}\right] - \omega^2\rho/c_2$$

$$\mathrm{Z}_1 = \frac{\beta}{\sigma}\left[\frac{\mathrm{Z}_2\cos kl - (\beta/\sigma)\sin kl}{\mathrm{Z}_2\sin kl + (\beta/\sigma)\cos kl}\right] - \omega^2\rho/c_1 = 0,$$

for resonance. Whence, substituting for Z_2 and β,

$$\left[\frac{\omega^2/c_3 + (a\omega/\sigma')\tan kl'}{1 - (\sigma'\omega/ac_3)\tan kl'}\right] + \left[\frac{\omega^2/c_1 + (a\omega/\sigma)\tan kl}{1 - (\sigma\omega/ac_1)\tan kl}\right] + \frac{\omega^2}{c_2} = 0. \quad (14)$$

This may be regarded as the general equation for resonance

in a "series" system, and from it the following results are obtained on substituting the appropriate conditions :—

a. "Bottle-Pipe" Resonator. (Fig. 10, *b*.)

$$c_3 = 0, \quad c_1 = c_2 = \infty, \quad \text{and} \quad \tan kl \,.\, \tan kl' = \sigma/\sigma', \qquad . \quad . \quad . \quad (14.1)$$

where l has now to be interpreted as the length of the pipe, together with the end correction as ordinarily understood (*cf.* Ref. 7).

b. Tube Closed at Both Ends and fitted with a Coaxial Diaphragm. (Fig. 10, *c*.)

$$\sigma' = \sigma, \quad c_1 = c_3 = 0, \quad \text{and} \quad \cot kl' + \cot kl = \omega\sigma/ac_2 \qquad . \quad . \quad . \quad (14.2)$$

(*cf.* Ref. 1, eqn. 6, and Part II. for experimental verification.)

c. Boys Resonator. (Fig. 10, *d*.)

If l' is small—which is tantamount to assuming that the condensation within the volume S′ is sensibly uniform—$\tan kl'$ may be replaced by kl', and the "pipe" becomes a reservoir. With the additional conditions $c_1 = \infty$, $c_3 = 0$, and remembering $l'\sigma' = \mathrm{S}'$, and that l now includes the end correction, it follows that

$$\tan kl = \frac{-2\pi\sigma n_1}{ac_2}\left(\frac{n}{n_1} - \frac{n_1}{n}\right), \qquad . \quad . \quad . \quad (14.3)$$

where n_1 has its former significance (*cf.* equation (6)).

d. Pipe near its Closed End expanding into a Bulb of Small Capacity. (Fig. 10, *e*.)

As in the previous example, $\tan kl'$ will be replaced by kl', and, as the shape of the bulb is immaterial, it will be considered that $\mathrm{S}' = \sigma' l'$: in addition, $c_1 = c_2 = \infty$ and $c_3 = 0$. Substituting in (14) yields

$$\tan kl = \sigma/k\mathrm{S} \qquad . \quad . \quad . \quad . \quad . \quad (14.4)$$

(*cf.* Ref. 5, p. 209).

e. Rayleigh Double Resonator.

In this resonator the pipes of fig. 10, *a* are replaced by reservoirs, and, as before, we shall write kl and kl' for $\tan kl$ and $\tan kl'$ respectively in (14), so that

$$\left[\frac{1/c_3 + l'/\sigma'}{1 - \omega^2\mathrm{S}'/a^2c_3}\right] + \left[\frac{1/c_1 + l/\sigma}{1 - \omega^2\mathrm{S}/a^2c_1}\right] + \frac{1}{c_2} = 0,$$

taking the volumes of the reservoirs S and S′ to be σl and $\sigma' l'$ respectively. It is to be noted that the expression $1/c_3 + l'/\sigma'$ represents the "resistance" of the orifice, together with the "resistance" of the short tube or reservoir. If, following Rayleigh, we neglect the effect of inertia in the interior of the reservoir, and assume that the l/σ terms are small compared with the $1/c$ terms, then

$$\omega^4 - \omega^2 a^2 \left[\frac{c_1 + c_2}{S} + \frac{c_3 + c_2}{S'}\right] + \frac{a^4}{SS'}\left[c_1 c_3 + c_2(c_1 + c_3)\right] = 0, \quad . \quad . \quad . \quad (14.5)$$

which is the result obtained by Rayleigh (Ref. 5, p. 190). Equation (14) would yield information concerning the overtones of this system, assuming the reservoirs to be of the form shown in fig. 10, *a*.

For a general discussion of the results obtained in this paragraph the reader is referred to the sources cited.

§ 5. Conclusion.

Examples of resonator problems to which the methods of this paper afford an easy solution could be multiplied, but it is hoped that the above will serve both to illustrate the principles involved and to show their general applicability. It should be noted that the method will also yield solutions to other elastic problems in which the counterparts of the general equations of § 2 obtain.

The application of the method to the theory of certain "wind" instruments is reserved for a further paper.

The author has pleasure in recording his appreciation of the kindly interest Professor Lees and Dr. E. T. Paris have shown in the present work.

References.

(1) Irons, Phil. Mag. vii. p. 873 (1929).
(2) Webster, Proc. Nat. Acad. Sci. v. p. 275 (1919).
(3) Stewart, Phys. Rev. xx. p. 528 (1922) *et seq.*
(4) See, *e. g.*, Barton, 'Text-Book of Sound,' p. 220. (Macmillan & Co.)
(5) Rayleigh, 'Theory of Sound,' ii. p. 114. (Macmillan & Co.)
(6) Paris, Phil. Mag. xlviii. p. 769 (1924).
(7) Aldis, 'Nature,' cxiv. p. 309 (1924).
(8) Lees, Proc. Phys. Soc. xli. p. 204 (1929).

XXXV. *The Paramagnetic Rotatory Dispersion of Aqueous Solutions of Cobalt Sulphate in the Visible and Ultra-Violet Regions of The Spectrum.* By R. W. Roberts, *M.Sc., The University, Liverpool* *.

I. *Introduction.*

In two previous investigations † on the magnetic rotatory dispersion of certain cobalt salts in aqueous solution it was found that the magneto-optical dispersions of these solutions do not follow the laws holding for diamagnetic substances. Also it was found that the Co^{++} ion, like the ions Fe^{++} and Fe^{+++}, is capable of exerting a negative rotation of the plane of polarization. This negative rotation of the Co^{++} ion was found in solutions of the sulphate, chlorate, acetate, nitrate, and ammonium sulphate. In the case of solutions of cobalt chloride and cobalt bromide the negative rotation of the Co^{++} ion was found to be overpowered by the diamagnetic rotation due to the chlorine and bromine ions respectively. In view of these results, and others which were mentioned in the introduction to paper II., it was pointed out that the study of the Faraday effect in paramagnetic substances is capable of yielding information which cannot be obtained from ordinary dispersion data. Since the appearance of these papers Ladenburg ‡, in an outstanding work, has shown, contrary to what was usually supposed, that there are two types of magnetic rotation of the plane of polarization, the usual diamagnetic rotation found in all transparent substances, and the paramagnetic rotation which arises from paramagnetic atoms. Ladenburg has deduced a formula for this paramagnetic rotation, and also from quantum considerations given a rule governing the occurrence of negative rotations, which could not in any way be explained on classical grounds.

Recently the Ladenburg formula has been brilliantly verified by Becquerel and de Haas § for the paramagnetic

* Communicated by Prof. L. R. Wilberforce, M.A.

† R. W. Roberts, J. H. Smith, and S. S. Richardson, Phil. Mag. xliv. p. 917 (1922); R. W. Roberts, Phil. Mag. xlix. p. 397 (1925). (Referred to as Papers I. and II. respectively.)

‡ *ZS. f. Phys.* xxxiv. p. 898 (1925).

§ *Journ. de Phys.* x. p. 283 (1925).

rotatory dispersion of the rare earth crystals tysonite and parisite at very low temperatures.

In view of these advances in our knowledge of paramagnetic rotation, it was thought that a further study of the magnetic rotatory dispersion of cobalt solutions would be of experimental and theoretical interest.

Cobalt sulphate solutions were chosen as suitable, because the diamagnetic effect due to the SO_4^{--} ion is small compared with that due to most anions.

A graph exhibiting the rotatory dispersion of a solution of $CoSO_4$ in water has already been given in paper I.

II. *The Solutions.*

Measurements of the natural and magnetic rotatory dispersions have been made on five solutions denoted by

Table I.

Solution.	W.	d_4^{20}.	d_4^{25}.
A	4·33	1·04249	1·04112
B	6·45	1·06524	1·06362
C	10·23	1·10664	1·10500
D	19·14	1·21308	1·21101
E	22·26	1·25525	1·25313
F	25·09	—	1·29465

A, B, C, D, and E. The solutions were prepared from a reagent quality of cobalt sulphate, stated to be nickel and iron free, and distilled water. The cobalt sulphate was recrystallized from distilled water several times before use. The strengths, expressed in Table I. as W grams of $CoSO_4$ in 100 grams of solution, have been determined from the weights of the components on the assumption that the crystals had the composition $CoSO_4 7H_2O$. The strength of E (W_E), owing to error, had to be corrected by setting up, using the data for solutions B, C, D, and F (an extra solution made up for this purpose), an interpolation formula expressing W as a function of $d_s^{25} - d_w^{25}$. d_s^{25} and d_w^{25} denoting the densities at 25° C. of the solutions and water respectively. Inserting the density of E in this formula, W_E was found to be equal to 22·28. Another determination, using the interpolation formula for a solution obtained

by diluting E. gave $W_E = 22{\cdot}24$. The mean value 22·26 has been taken throughout the work as the strength of E. The densities were determined at temperatures in the neighbourhood of 20° C. and 25° C., and reduced to 20°C. and 25° C. by linear interpolation. Owing to the small capacity of the pycknometer, the values of the densities are uncertain to about four units in the fifth decimal place.

TABLE II.

d_4^{25}.	W—Manchot.	W—Interpolation.
1·1131	10·98	10·96
1·2218	20·00	19·98

Manchot, Zahrstorfer, and Zepter * give the densities and strengths of two cobalt sulphate solutions at 25° C. For the sake of comparison their strengths and the strengths calculated by using the interpolation formula are given in Table II. It will be seen that the agreement between the two values is quite satisfactory.

III. *Magnetic Rotation Measurements.*

PART 1. *Measurements in the Visual Spectrum (with A. Weale).*—As the apparatus used in the present investigation is different from that employed in the earlier work a brief description of it will be given.

The electromagnet was a large Du Bois model which was water-cooled. The gap between the pole-pieces was kept fixed throughout the work at a distance of about 1·5 cm. Preliminary investigations by Dr. A. V. Moses and one of us (R. W. R.) with a search-coil and flux-meter showed that the field in the gap was not uniform, there being, owing to the existence of the borings, two maxima, symmetrically placed with respect to the centre of the gap. Lack of uniformity of the field is of no disadvantage in the present investigation so long as the cell holding the solution under test is always replaced in the same position. The cell was placed almost symmetrically between the pole-pieces. This adjustment need not be rigorously exact, owing to the symmetrical nature of the field.

* *Zs. Anorg. Ch.* 141. p. 50 (1924).

The magnet was excited with a current of 10·50 amperes taken from the city mains. The current was kept constant by pressure control of a carbon resistance in series with an open wire resistance. When no loads were being taken from the mains the current was kept constant to about ±·01 ampere.

The cell containing the solution under test was made from a piece of plate glass whose approximate dimensions were 6·7 cm. by 11·2 cm. by 1·2 cm. A cylindrical boring A (fig. 1) 1·5 cm. in diameter was made through the plate glass perpendicular to the largest pair of faces, the axis of the boring being 1·7 cm. from the upper face of the plate. This boring was closed by cementing two plates B, about $\frac{1}{4}$ mm. thick, of left-handed and right quartz cut perpendicular to the optic axis.

Fig. 1.

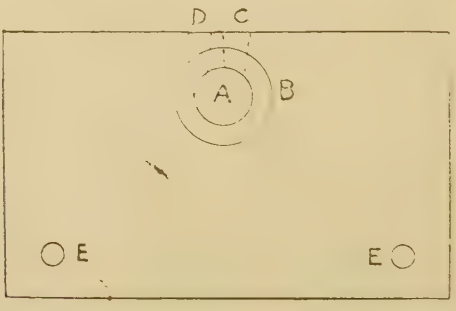

A conical boring C provided with a ground stopper served for filling purposes. A second conical boring D was fitted with a ground stopper containing a thermo-junction of copper-constantan. The base of this stopper was ground very thin and projected slightly into A. To prevent any evaporation of the solution during the observations the ground stoppers fitting C and D were waxed at the top of the conical holes.

The cell was fixed to a holder screwed into the base of the magnet by means of two screws passing through the clearance holes E drilled into the glass plate. The holder could be rotated about horizontal and vertical axes, for the purpose of setting the cell normal to the axis of the electromagnet.

The second thermo-junction was kept inside a transparent Dewar vessel containing water, stirrer, and thermometer. The thermo-junctions were in series with a moving coil galvanometer, which could be read by the observer watching the ammeter at a considerable distance away from the electromagnet.

The polarizer and analyser were mounted in bronze tubes fitting into the conical borings of the Du Bois electromagnet. This arrangement is of great convenience in securing a fixed alignment of the optical parts. The polarizer was a two-part Lippich with variable half shadow angle. The horizontal dividing line of the Lippich was very fine, and practically vanished when the setting for equal intensities in the two parts of the polarizer field was made. The polarizer tube also carried a condensing lens, by means of which an image of the source of light could be focussed centrally on the analyser diaphragm.

The analyser was a Thompson Glan glycerine-cemented prism with an opening of 10 mm. This analyser was also used for the ultra-violet work described later. Both the polarizer and analyser were provided with suitable diaphragms, so that the correct polarimetric conditions for the path of the light rays were obtained. The analyser rotated with a graduated circle provided with two opposite fixed verniers reading to ·01°.

The axis of rotation of the circle was set parallel to the axis of the electromagnet. The dividing line of the polarizer was focussed on the slit of a constant deviation spectroscope by means of an achromatic lens of about 20 cm. focal length. This was mounted on the analysing circle, and rotated with it.

Two sources of light were mainly used—a quartz mercury vapour lamp and a carbon arc. The chief advantages of the mercury vapour lamp arise from its great and steady intensity, which is only slightly influenced by the reversal of the current through the electromagnet. The carbon arc, although capable of giving great intensity, is not easy to maintain constant and centred, particularly when it is fed with metallic salts.

The rotations for each line have been deduced from the mean of at least ten settings of the analyser (in many cases from much more than ten), the current being reversed after every five settings. As the intensities of the lines for which readings were taken differ widely, partly

Table III.—Observed Rotations.

Upper line : rotations in degrees. Lower line : temperature in ° C.

λ in A.U.	H_2O.	A.	B.	C.	D.	E.
6908	.....	5·01 ± ·030 18·8	.....	5·07 ± ·020 18·8	4·86 ± ·011 15·5	
6708	5·537 ± ·0089 18·7	5·46 ± ·011 19·0	5·447 ± ·0083 16·7	5·410 ± ·0096 16·9	5·25 ± ·023 18·9	5·29 ± ·012 19·2
6104	6·760 ± ·0046 18·7	6·736 ± ·0057 19·0	6·698 ± ·0073 16·7	6·70 ± ·012 16·6	6·57 ± ·011 17·0	6·48 ± ·012 19·2
5893	7·265 ± ·0027 18·7	7·289 ± ·0045 18·5	7·252 ± ·0086 16·7	7·208 ± ·0076 16·8	7·27 ± ·010 15·1	7·281 ± ·0082 19·3
5780	7·519 ± ·0047	7·548 ± ·0035 16·9	7·658 ± ·0057 16·7	7·610 ± ·0037 17·2	7·746 ± ·0052 15·5	7·739 ± ·0052 19·3
5461	8·464 ± ·0013	8·594 ± ·0050 17·9	8·748 ± ·0045 16·7	8·75 ± ·012 19·8	9·13 ± ·058	absorption.
4916	10·669 ± ·0058	10·18 ± ·068 19·5	10·09 ± ·023*			
6234	.....	.....	.....	.....	6·24 ± ·022 17·0	
5682	.....	.....	.....	7·94 ± ·013 16·9		
5230	.....	9·36 ± ·013				
5194	.....	.....	9·40 ± ·022			
5167	.....	9·515 ± ·031				
4958	.....	10·04 ± ·087				
4529	.....	12·24 ± ·040	12·02 ± ·02†			
4384	.....	.....	13·05 ± ·033			

* λ 4910. † λ 4527.

on account of the differences in the intensities of the lines emitted by the source, and partly on account of the unequal absorption of the lines by the solutions, I have recorded in Table III. with each rotation the mean probable error. In order to follow the course of the dispersion of the

Fig. 2.

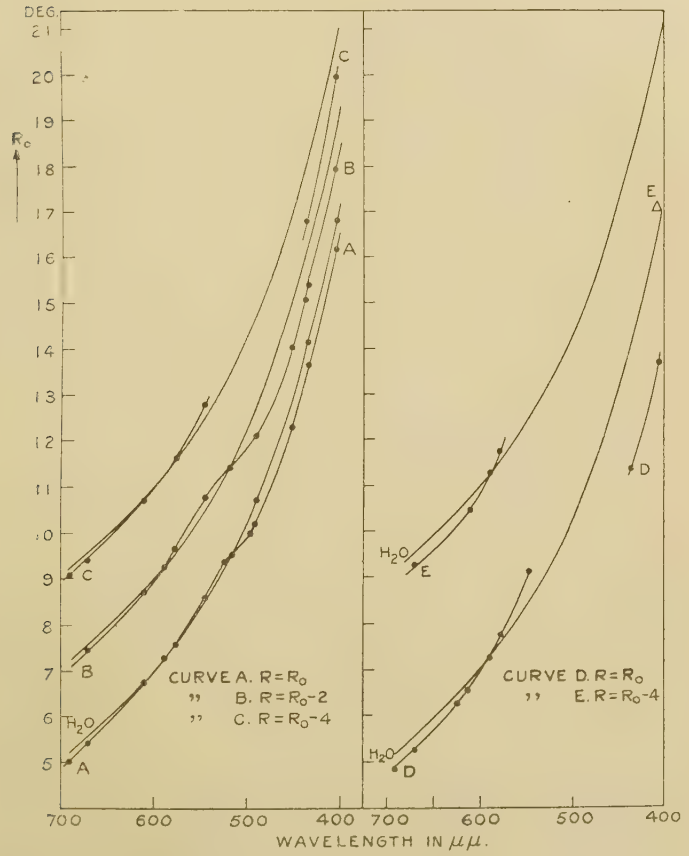

rotation on the graph shown in fig. 2 the radii of the open circles representing the rotations have been taken equal to ·04°.

For the sake of clearness the rotation graphs for each solution have been drawn displaced with reference to the ordinate axis. The necessary correction in order to

obtain the observed rotation from the scale reading is indicated for each curve.

The readings in the red region of the spectrum were found to be rather trying, owing to the low intensities of the available sources, the low sensitivity of the eye in the red, and the disturbing influence due to the light scattered from the surfaces of the spectroscope lenses and prism. For the denser solutions this scattered light was considerably cut down, owing to the presence of the strong absorption band in the green.

The half-shadow angle was varied to suit the intensity of the particular line under observation. It varied from 15° in the red to $1\frac{1}{2}$° for the bright lines.

TABLE IV.

Verdet's Constants.

λ in A.U.	H_2O.	A.	B.	C.	D.	
6908	...	·00955	...	·00961	·00875	
6708	·00998	·00983	·00981	·00989	·00975	·00979
6104	·01218	·01213	·01206	·01206	·01191	·01165
5893	·01309	·01313	·01306	·01298	·01309	·01312
5780	·01355	·01360	·01381	·01372	·01398	·01396
5461	·01534	·01549	·01577	·01578	·01649	absorpn.
4916	·01934	·01830	·01813*	...	...	
6234	...	...	...	...	·01124	
5682	...	...	...	·01432		
5230	...	·01685				
5194	...	...	·01692			
5167	...	·01723				
4958	...	·01830				
4529	...	·02201	·02163†			
4384	...	...	·02345			

* λ 4910. † λ 4527.

The observed values of the rotation, corrected for the rotation due to the end-plates (determined directly), have been reduced to give Verdet constants, which are recorded in Table IV. To this end the rotation due to the cell, filled with water, was determined for the Na line 5893 at 18·7° C. from forty settings of the analyser. Using the formula given by Rodger and Watson* for Verdet's constant V_t for water at t° C. (D line),

$$V_t = 0{\cdot}01311' \,(1 - 0{\cdot}0_4305\, t - 0{\cdot}0_5305\, t^2).\quad 3 < t < 98.$$

* Phil. Trans. A, clxxxvi. p. 621 (1895).

the change of magnetic potential on reversal of the field with a current of 10·50 amperes was found to be 31.953 cm. gauss.

No corrections have been made for the rotation due to more than one passage of the light through the solutions, as the reflected light, owing to the want of parallelism of the plates, did not enter the slit of the spectroscope. The cell was adjusted by an autocollimation method using the analysing lens, so that the plane bisecting the angle between the faces was perpendicular to the axis of the apparatus.

From fig. 2 it will be seen that the rotations of all the solutions are less than that of water in the red, and become greater than the rotations of water on approaching the 5100 A.U. band *. On the violet side of this band the rotation curves for the solutions are again below the water curve. An attempt was made to obtain more values of the rotation in the neighbourhood of the absorption band, using the continuous radiation from a carbon arc passing a current of about 17 amperes. The curves obtained by plotting the simultaneous readings of the drum of the constant deviation spectroscope, giving the wave-length for which matching of intensity occurred, against the readings of the analyser circle showed a similar course to those in fig. 2, both for a magnetizing current of 10·5 and 14·5 amperes.

The negative rotation due to cobalt sulphate has been previously noticed. Ingersoll † finds that, for an aqueous solution of cobalt sulphate of density 1·322 at 23° C., the rotation for $\lambda = \cdot 8\mu$ is less than that of water by 5 parts in 70. At the Na line 5893 Wachsmuth ‡ finds that the rotation for a solution of density 1·1378 is less than that of water by 7 parts in 10,000.

Part 2. *Measurements in the Violet and Ultra-Violet.*—As visual observations in the violet region of the spectrum could not be made with ease and certainty, the rotations for the lines Hg 4358 and Hg 4047 A.U. were obtained photographically.

* "Absorption Measurements according to Houstoun," Proc. Roy. Soc. Edinb. xxi. pp. 521, 530, 547 (1911).

† J. O. S. A. vi. p. 663 (1922).

‡ Wied. *Ann.* xliv. p. 377 (1891).

For the ultra-violet beyond 3300 A.U. the polarizer was replaced by a modified Jellett prism of fixed half-shadow angle equal to about $5\frac{1}{2}^{\circ}$. The glass condensing lens used for the visual work was replaced by a quartz-fluorite achromatic combination of 32 cm. focal length. The quartz-mercury vapour lamp, suitably housed and screened, was placed at the focus of this achromat, as with the Jellett polarizer it is necessary to use parallel light. The glass achromat mounted on the divided circle was also replaced by a second quartz-fluorite achromatic lens of about 32 cm. focal length. This lens formed an image of the horizontal dividing line of the Jellett prism on the slit of a small quartz spectrograph.

A large number of plates were taken (in conjunction with Mr. A. Weale) for each solution, using the iron arc as source. The method of burning the arc recommended by Lowry * was adopted, and was found to give remarkable steadiness. In spite of this, some of the plates gave rather erratic values for the rotation, which indicated that the arc could not always have been symmetrically placed with respect to the axis of the apparatus. The arc was kept on the axis by hand control, so that its image, cast by a lens placed on the side of the arc remote from the apparatus, always fell on a small area marked out on the room-wall. The centre of the lens and the centre of the area were arranged to be on the axis of the apparatus.

The method adopted, when using the iron arc, was to determine the wave-length of the spectral line for which a match in intensity in its upper and lower halves was attained for a known analyser setting. Owing to the varying intensities of the lines in the iron arc spectrum, it was difficult in some cases to fix the wave-length of the match-point within narrow limits.

On account of these disadvantages in using the iron arc for magneto-optical polarimetry it was replaced by a quartz-mercury vapour lamp. This lamp was mounted geometrically on the plan of the hole, slot, and plane device. With this lamp the rotations were determined by finding the setting on the analyser circle which gave equal intensity in the upper and lower parts of the spectral line. As emphasized by Landau† and Darmois‡, for success in this

* Phil. Trans. A, ccxxvi. p. 391 (1927).
† *Phys. Zeit.* ix. p. 417 (1908).
‡ *Ann. de Chim. et Phys.* xxii. (8) p. 247 (1911).

method it is necessary to obtain the correct time of exposure for each line.

Settings were made for the nine lines

Hg 4358, 4047, 3663, 3341, 3131, 2805, 2655, 2537, 2482 A.U.

TABLE V.

1st line. Difference of analyser readings in degrees.
2nd „ Sum „ „ „
3rd „ Temp. in ° C.

λ.	H_2O.	A.	B.	C.	D.	E.	Z.
4358	14·13	13·67	13·40	12·79	absorpn.	absorpn.	210·50
	210·53	210·57	210·45	210·45			
	18·4	15·9	17·8	18·8			
4047	16·80	16·19	15·95	15·35	13·72	13·02	
	210·55	210·45	210·45	210·39	210·48	210·42	210·46
	18·4	15·9	17·8	16·9	17·3	18·3	
3665	21·20	20·70	20·20	19·58	17·86	17·00	
	210·30	210·40	210·40	210·36	210·40	210·40	210·38
	20·5	16·3	17·8	17·2	17·5	17·2	
	26·53	25·80	25·49	24·75	22·70	21·75	
3341	210·23	210·24	210·25	210·33	210·24	210·15	210·24
	18·2	17·3	17·6	17·5	17·3	17·3	
	31·28	30·48	30·04	29·25	26·92	25·90	
3131	210·22	210·02	209·90	210·09	210·12	210·00	210·08
	19·6	18·4	17·9	16·6	18·0	16·8	
	42·00	41·13	40·62	39·57	36·80	35·67	
2805	209·90	209·97	209·84	209·85	209·84	209·93	209·91
	18·8	17·7	18·1	18·0	17·0	18·4	
	49·45	48·33	47·62	46·60	43·60	42·40	
2655	209·65	209·93	209·82	209·74	209·66	209·60	209·70
	19·1	18·2	17·6	19·0	18·3	18·4	
	56·50	55·37	54·86	53·56	50·34	48·96	
2537	209·60	209·53	209·50	209·50	209·60	209·60	209·55
	19·5	18·8	18·3	15·9	18·6	19·2	
	60·35	59·02	58·72	57·29	53·92	52·30	
2482	209·55	209·45	209·28	209·36	209·58	209·40	209·44
	18·3	19·5	19·2	17·4	19·0	18·9	
Av. Temp.	19·6	18·0	18·6	18·1	18·4	18·6	

for each of the five solutions (with the exception of 4358 for solutions D and E). In most cases the settings of the analyser were made at intervals of ·1°. For the lines 4358, 4047, and 3663, settings were made at intervals of ·05°. On each plate usually thirty exposures were made, the time of exposure varying from 1 second to 1½ minutes

(for 2482). The magnetizing current was reversed after every five exposures. It was arranged, at the expense of some repetition, that a reversal of the intensities in the upper and lower halves of a spectral line occurred for both senses of the magnetizing current, so that the rotation for

Fig. 3.

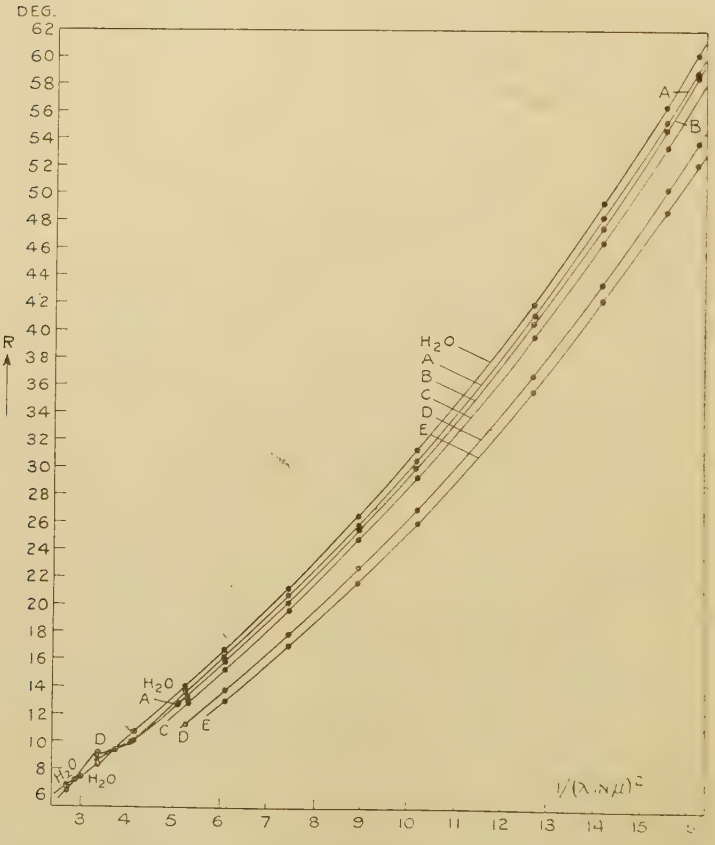

the line in question could be obtained from the one plate. As the field of the polarizer is not normal, it is necessary to match for equality of intensity just in the neighbourhood of the dividing line.

To facilitate the timing of the exposure an electromagnetically-operated steel ball was bifilarly suspended

in front of the slit of the spectroscope. This was controlled by the observer reading the ammeter.

Only settings in one region of the divided circle have been carried out, as it was found that rotation of the circle through 180° did not give any change in the rotation of water for λ 3131 A.U. within the limits of experimental error. Interpolation between the settings of the analyser has been used to the extent of one-third of the interval 1°.

In Table V. will be found recorded with each wave-length, the difference between the analyser match-point settings for the passage of the current in both senses through the magnet, the sum of these settings, and the mean temperature of the solution during the taking of the photograph.

TABLE VI.

Verdet's Constants (min. per. cm. Gauss).

λ in A.U.	H_2O.	A.	B.	C.	D.	E.
4358	·0252	·0245	·0240	·0229	·0202	absorpn.
4047	·0301	·0292	·0286	·0275	·0244	·0231
3665	·0382	·0372	·0363	·0352	·0319	·0303
3341	·0477	·0464	·0458	·0444	·0405	·0388
3131	·0565	·0548	·0540	·0525	·0481	·0461
2805	·0756	·0739	·0730	·0710	·0658	·0637
2655	·0890	·0869	·0855	·0836	·0780	·0757
2537	·1017	·0996	·0986	·0960	·0901	·0876
2482	·1086	·1061	·1056	·1029	·0965	·0935
Av. Temp. in ° C.	19·6	18·0	18·6	18·1	18·4	18·6

The sum of the analyser settings should be constant for a given wave-length for all the solutions, provided the zero of the apparatus does not alter. The constant values vary with the wave-length, owing to the natural rotation of the end-plates not being quite compensated. This variation with the wave-length can be readily obtained by plotting the average value of the sum of the readings (last column of Table V.) against the wave-length. The rotations due to the end-plates have been determined directly.

The observed rotations are plotted against the inverse square of the wave-length in fig. 3.

Table VI. gives the Verdet constants for the violet and

ultra-violet lines. These constants have been calculated in the same way as described for the visual work.

Fig. 4

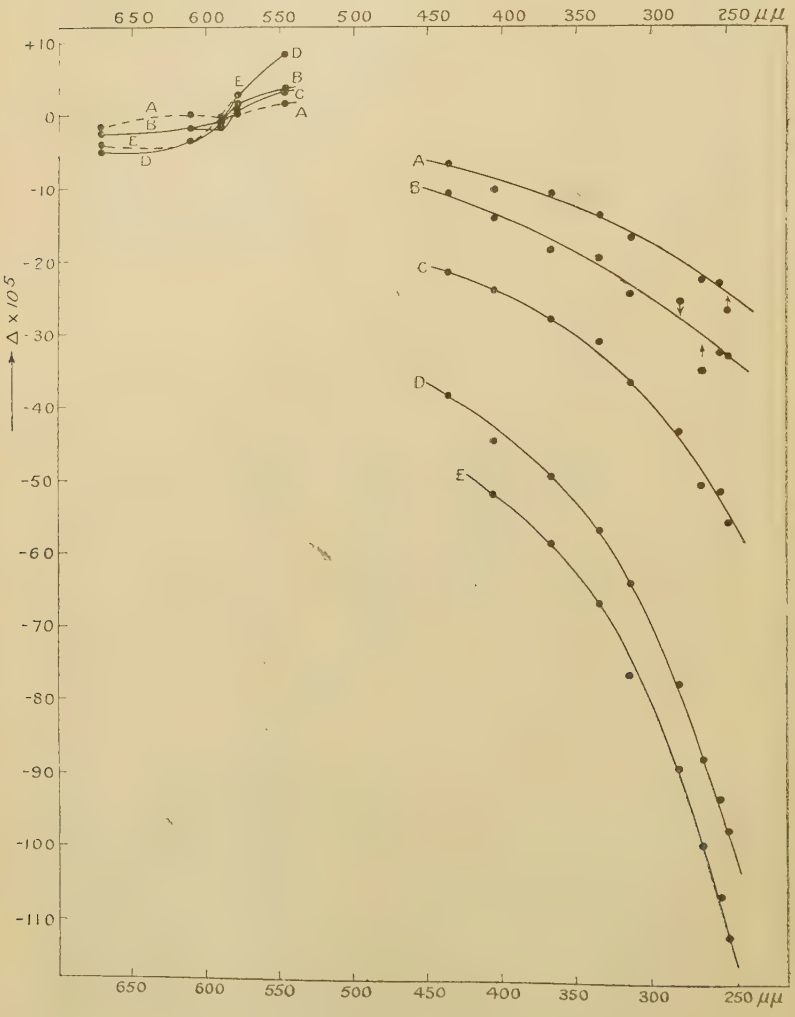

IV. *Natural Dispersion Measurements.*

In order to apply Ladenburg's formula to the foregoing observations, the refractive indices of the solutions and water must be determined. For the purpose of obtaining

the rotation due to the salt $CoSO_4$ in solution, a knowledge of the refractive indices to three places of decimals for a number of wave-lengths throughout the spectrum suffices. When it is desired, however, to make estimations of the frequencies of vibration of the electrons controlling the dispersion and refraction of the solutions, the refractive indices must be determined with an exactness amounting to several units in the fifth decimal place. As far as I am aware the only measurements of the ultra-violet dispersion of solutions which have been made are those of Heydweiller * and his co-workers. In their work they used a method similar to that of Hallwachs, and obtained the differences between the refractive indices of water and the solutions directly. Their apparatus necessitated calibration by other methods.

It was thought, at first, that the method of normal incidence used by Simon † for measurements of the ultra-violet dispersion of liquids would be very convenient and of sufficient accuracy for the present work. This method, however, was found not suitable, because the two quartz-fluorite combinations used with the spectrometer were not sufficiently achromatic to permit of autocollimation adjustments with the visible light to be of value in the ultra-violet.

Also, as the axis of rotation of the telescope did not coincide with the axis of rotation of the spectrometer table, the method of setting for perpendicular incidence described by Feussner ‡ could not be adopted. After some further trials Martens' § method was used. This method, although time consuming, possesses the advantage that all the necessary measurements, with the exception of those relating to the angle of the prism, can be obtained from the photographic plate. The spectrometer, which was kindly lent to me by Prof. Baly, had a divided circle 10 inches in diameter, which could be read to 1 second of an arc by means of two microscopes provided with micrometer eyepieces.

The glass lenses provided with the instrument were replaced by the two quartz-fluorite achromatic combinations used for the magnetic dispersion work. Instead of

* *Phys. Zeit.* xxvi. p. 526 (1925) (Summary).
† *Ann. der Phys.* liii. p. 542 (1894).
‡ *ZS. f. Phys.* xlv. p. 689 (1927).
§ *Ann. der Phys.* vi. p. 603 (1901).

the eyepiece a light aluminium frame was screwed to the telescope tube. This frame supported a metal plate-holder carrying plates 6 cm. by 4·5 cm. This holder could be raised or lowered by means of two friction rollers without any appreciable strain on the telescope mounting.

The spectrometer adjustments were carried out in the usual way. For the setting of the axis of the telescope and collimator perpendicular to the axis of rotation of the telescope Lebedeff's method * was found very convenient.

Three positions of the draw-tube carrying the slit were used at intervals of 2 mm. in order to obtain light sufficiently parallel to cover the region 7068-2378 A.U. These positions, together with the corresponding positions of the draw-tube supporting the plate-holder, were found by Cornu's method †.

In order to deduce the angular deviation of the spectral lines on the plate, three direct slit images were recorded on each plate, with the telescope set in the direct position, and at azimuths $\pm 1^\circ$ (sometimes 45′) with respect to this position. The angle of incidence was obtained by taking two exposures of the slit images reflected from the first prism face, with the telescope in such an azimuth that the reflected slit images were recorded on the plate in suitable positions. The mean angle of the incidence obtained by means of these two reflected images was adopted.

As all the angular deviations were small, these deviations were obtained by linear interpolations from the screw readings.

Most of the plates have been read four times, following the procedure given by Cornu ‡. This was necessary in order to eliminate errors arising from imperfections of the screw of the measuring instrument, and errors of reading arising from the lack of sharpness of the lines due to the presence of spherical aberration.

As it was necessary to remove the prism table (to which the prism was rigidly attached) from the spectrometer in order to photograph the direct slit image, the setting of the prism table had to be controlled. This was done by autocollimation with the aid of a telescope fitted with a Gauss eyepiece. To this end a mirror was attached to the side of the prism opposite the refracting edge.

* Journ. Scient. Instr. iv. p. 100 (1926).
† *Journ. de Phys.* v. p. 341 (1886).
‡ *Loc. cit.*

The solutions were contained in a 30° hollow prism, which was closed by means of two plane parallel quartz plates (7·5 mm. thick) cut parallel to the optic axis. These plates were cemented to the prism. The prism was provided with a filling-hole into which fitted a thermometer graduated in tenths of a degree, so that estimations to hundredths of a degree could be made. The thermometer, which was the same as used in the density determinations, was calibrated against a standard thermometer provided with a recent certificate.

Most of the plates have been taken at temperatures in the neighbourhood of 21° C. In order to reduce the observations to a standard temperature taken to be 20° C., it is necessary to know the temperature coefficients of the refractive indices. In the case of water Flatow's values * for $\frac{dn}{dt}$ have been used. For the solutions the values of $\frac{dn}{dt}$ have been obtained by finding the shift of the spectral lines on gradually heating the room through about 5° C. Exposures were made before heating and during the heating when the temperature became sufficiently steady. In order to distinguish between the lines of the two spectra obtained, the first spectrum was taken with a long slit and the second with a short slit.

Table VII. gives a summary of the work.

The omissions arise partly through the obscuring of some of the lines by the superposition on the spectrum of either the direct slit images or the reflected slit images and partly through absorption. No attempt has been made to follow the course of the dispersion through the absorption band, as this would require an entirely different experimental method.

In the literature † there appear considerable discrepancies among the values of the refractive indices of water in the ultra-violet. I find, on correcting for temperature and wave-length differences, that the tabulated results for water lie nearer to Gifford's † results than to those of other observers.

Table VIII. gives the values of the molecular refraction R of $CoSO_4$ at 20° C. which have been deduced from the

* *Ann. der Phys.* xii. p. 85 (1903).
† See Duclaux and Jeantet, *Journ. de Phys.* v. p. 92 (1924).
‡ Proc. Roy. Soc. A, lxxviii. p. 406 (1907).

TABLE VII.

Refractive Indices at 20° C.

λ in A.U.	H_2O.	A.	B.	C.	D.	E.
7065 He	1·33003	1·33796	...	...	1·36708	1·37400
6678 ,,	1·33087	1·33882	1·34284	1·35016	1·36802	1·37498
6563 H_α	1·33115	1·33913	1·34312	...	1·36834	
5876 He	1·33305	1·34106	1·34509	1·35241	1·37044	1·37743
5461 Hg	1·33440	1·34254	1·34666	1·35382		
4471 He	1·33945	1·34762	1·35173			
4358 Hg	1·34027	1·34845	1·35258	...	1·37841	
4047 ,,	1·34284	1·35108	1·35518	1·36254	1·38128	1·38839
3886 He	1·34432	1·35263	1·35678	1·36422	1·38291	1·39013
3341 Hg	1·35165	1·36015	1·36436	1·37193	1·39106	1·39834
3187 He	...	1·36317	1·36745	...	1·39426	1·40169
3131 Hg	1·35567	1·36435	1·36860	1·37632	1·39556	1·40293
2893 ,,	1·36168	1·37050	1·37478	1·38254	1·40220	1·40968
2805 ,,	1·36442	1·37334	1·37779	1·38543	...	...
2576 ,,	1·37338	1·38247	1·38698	1·39482	1·41506	1·42276
2482 ,,	1·37809	1·38732	...	1·39977	...	1·42803
2378 ,,	1·38434	1·39366	1·39827	1·40627	1·42705	1·43496

refractive indices of Table VII. by means of the well-known formula

$$\frac{1}{d_4^{20}}\frac{n^2-1}{n^2+2} = \frac{1}{d_w^{20}}\left(1-\frac{W}{100}\right)\frac{n_w^2-1}{n_w^2+2} + \frac{W\,R}{100\,M}, \quad . \quad (1)$$

where n_w = refractive index of water at 20° C.,

n = ,, ,, ,, solution at 20° C.,

R = molecular refraction of $CoSO_4$,

M = molecular weight of $CoSO_4$ (155·1).

The extrapolations given under W = 0 for zero concentration have been obtained from the molecular refractivities of the five solutions by using the method of Least Squares. It was assumed with Fontell * :

(1) that the molecular refraction is a linear function of the concentration,

(2) that the error in the molecular refraction arising from the observations is inversely porportional to the concentration.

* Soc. Scient. Fenn., Comm Phys.-Math. iv. no. 8 (1927).

On determining the linear function it appears that the molecular refraction increases with increasing concentration —that is, in the opposite direction to the behaviour of the majority of salts. This indicates that in $CoSO_4$ the molecular refractivity in the crystalline state (100 per cent. solution) is greater than in the ionic state at infinite dilution. It is noteworthy that certain fluorides, in which F^-, like SO_4^{--}, has only a small dispersive effect, behave in a similar way.

Table VIII.

Molecular Refraction of $CoSO_4$ at 20° C. (M=155·1).

W / λ	0.	4·33.	6·45.	10·23.	19·14.	22·26.	Mean (obs.).
7065	...	15·86	...	...	16·09	16·05	16·00
6678	16·00	15·90	15·90	16·09	16·12	$16·08^5$	16·02
6563	...	15·96	15·90	...	16·14	...	16·00
5876	16·07	16·02	15·98	16·14	16·21	16·17	16·10
5461	...	$16·23^5$	16·23	16·17	...	...	16·21
4471	...	16·25	16·22	...	...	...	16·24
4358	...	16·26	16·25	...	16·46	...	16·32
4047	16·42	16·27	16·26	$16·32^5$	16·56	$16·49^5$	16·38
3886	16·43	16·47	16·40	$16·46^5$	16·62	16·56	16·50
3341	16·72	16·76	16·65	16·70	16·92	16·81	16·77
3131	16·98	17·06	16·89	16·95	17·04	$16·96^5$	16·98
2893	17·10	17·27	17·04	17·07	17·27	17·17	17·16
2576	17·60	17·66	17·54	$17·55^5$	17·61	17·55	17·58
2482	17·63	17·82	...	17·55	17·74	17·68	17·70
2378	17·77	17·98	17·82	17·69	17·93	17·85	17·85

Calculation of the Characteristic Frequencies of the Electrons in $CoSO_4$.

Heydweiller * has shown how one can calculate, on the basis of Drude's theory of dispersion, the characteristic frequencies of the electrons responsible for the refraction and dispersion of electrolytes. He points out that the effect on the dispersion due to the kation is small, and that the dispersion is mainly governed by the comparatively loosely bound valency electrons associated with the anion. The remaining electrons in the molecule are assumed to have a common frequency which is very much greater than that of the valency electrons.

* *Loc. cit.*

Let ν_1 = the frequency of the valency electrons in 10^{-15} sec.,

ν_2 = ,, ,, ,, remaining electrons in 10^{-15} sec.,

p_1 = the number of valency electrons in 1 molecule,

p_2 = ,, ,, electrons in 1 molecule less p_1.

Then, according to Heydweiller, the molecular refraction $R\nu^0$ at infinite dilution for light of frequency ν is given by the formula

$$R_\nu{}^0 = 16{\cdot}28_0 C_\nu,$$

$$\text{where } C_\nu = \frac{p_1}{\nu_1{}^2 - \nu^2} + \frac{p_2}{\nu_2{}^2 - \nu^2} \quad . \quad . \quad . \quad . \quad (2)$$

The values of $\nu_1{}^2$, $\nu_2{}^2$ can therefore be determined from the values of C_ν for two different frequencies.

TABLE IX.

λ (vac.).	$R_\nu{}^0$ calc.—$R_\nu{}^0$ obs. $\nu_1{}^2 = 6{\cdot}198$, $\nu_2{}^2 = 112{\cdot}6$.	$R_\nu{}^0$ calc. $R_\nu{}^0$ obs. $\nu_1{}^2 = 6{\cdot}140$, $\nu_2{}^2 = 112{\cdot}6$.
6680	0	+5
5877	−1	+5
4048	−6	+1
3890	−1	+5
3342	−5	+2
3133	−18	−11
2894	−9	−2
2577	−8	−11
2483	−4	+4
2379	0	+9

Applying this formula to the values $R_\nu{}^0$ of $CoSO_4$ for the lines 6678 and 2738 A.U., we find, taking $p_1 = 2$, $p_2 = 73$, that $\nu_1{}^2 = 6{\cdot}20$, and $\nu_2{}^2 = 112{\cdot}6$. On forming the difference between the values of R_ν calculated by means of (2) using these values of $\nu_1{}^2$ and $\nu_2{}^2$ and the observed values, it will be seen from the second column of Table IX. that the deviations (in units of the second decimal place) are large and lie in the same direction. A slightly better distribution of these differences is obtained by taking as $\nu_1{}^2$ the mean of the values $\nu_1{}^2$ obtained from the value of $R_\nu{}^0$ for each line, keeping $\nu_2{}^2$ ($= 112{\cdot}6$) constant. This process gives a mean value of $\nu_1{}^2 = 6{\cdot}14$. The differences between the values of $R_\nu{}^0$ calculated by using $\nu_1{}^2 = 6{\cdot}14$ and $\nu_2{}^2 = 112{\cdot}5$ in equation (2) and the observed values are given in the third column of Table IX. The

maximum deviation does not exceed 7 per 1000. In the formula we have neglected the effect of the absorption band at 5100 A.U., as the effect on the dispersion due to this band is very small.

The value $\nu_1^2 = 6{\cdot}14$ agrees well with Heydweiller's * value $\nu_1^2 = 6{\cdot}15$ for SO_4^- in Li_2SO_4. The method of extrapolating for zero concentration employed by Heydweiller is, however, entirely different from the one used here. For Li_2SO_4 Heydweiller obtains $\nu_2^2 = 100{\cdot}4$. The higher value $\nu_2^2 = 112{\cdot}6$ for $CoSO_4$ may arise through the more rigid binding of the electrons in $CoSO_4$ than in Li_2SO_4, owing to the higher nuclear change in the former salt.

V. *The Application of Ladenburg's Magnetic Dispersion Formula to the Magnetic Observations.*

Ladenburg † gives thefollowing formula for the magnetic rotation of a paramagnetic substance :

$$\chi = \sum_i \left[\frac{(n^2+2)\omega}{3(\omega_i^2-\omega^2)} \right]^2 \frac{\rho_i l o_L}{cn} \left\{ 1 \pm \frac{\mu_i H}{3kT} \frac{\omega_i^2-\omega^2}{\omega_i o_L} \right\}, \quad (3)$$

where l is the length of path traversed; $c = 3 \cdot 10^{10}$, $\omega = 2\pi c/\lambda$, ω_i the characteristic frequency of the electrons giving rise to the ith band, $o_L = -eH/2mc$, $\rho_i = 4\pi N_i e^2/m$, N_i being the number of classical dispersion electrons of type i per unit volume, μ_i their magnetic moment, k the Boltzmann constant, and T the absolute temperature.

In order to apply this formula to a dissolved salt it is necessary to correct for the rotation due to the solvent. It is clear from the formula that it is not χ which is additive, but the quantity $\frac{n}{(n^2+2)^2}\frac{\chi}{d}$, d being the density of the substance.

To facilitate reference to the experimental results, we shall consider the Verdet constant V instead of χ, χ/Hl being equal to $\pi V/60 \times 180$. By analogous considerations to those employed in the deduction of formula (1) we may regard the difference

$$\Delta \equiv \frac{n}{(n^2+2)^2}\frac{V_s}{d_s} - \frac{n_w}{(n_w^2+2)}\frac{100-W}{100}\frac{V_w}{d_w}$$

as a quantity characteristic of the rotation of the dissolved

* *Loc. cit.*

† *ZS. f. Phys.* xlvi. p. 168 (1927). See also C. G. Darwin and W. R. Watson, Proc. Roy. Soc. A, cxiv. p. 474 (1927).

salt, V and V' being the Verdet constants for the solution and water respectively.

Table X. gives the values of Δ and Δ/W, and fig. 4 a graphical representation of the values of Δ. The paramagnetic character of the rotation due to $CoSO_4$ is clearly

TABLE X.

Upper line : $\Delta \times 10^5$.
Lower „ : $\Delta/W \times 10^5$.

λ.	A.	B.	C.	D.	E.	Weighted Mean.
6708	— 1·51	— 2·48	...	— 4·99	— 4·10	
	— ·37	— ·38	...	— ·26	— ·18	— ·25
6104	— ·02	— 1·75	— 1·87	— 3·52	— 3·79	
	— ·00⁵	— ·27	— ·18	— ·18	— ·17	— ·17⁵
5893	— ·46	— ·94	— 1·79	— ·92	— ·36	
	— ·11	— ·15	— ·18	— ·05	— ·02	— ·07
5780	— ·11	— 1·60	— ·64	+ 2·71	— 2·84	
	+ ·02⁵	+ ·25	+ ·06	— ·14	+ ·13	+ ·13
5461	+ 1·50	— 3·60	+ 3·05	+ 8·32	absorpn.	
	+ ·35	+ ·56	+ ·30	+ ·43⁵	...	+ ·41
4358	— 6·7	—10·7	—21·4	—38·2		
	— 1·55	— 1·66	— 2·09	— 2·00	absorpn.	—1·92
4047	—10·2	—14·1	—23·9	—44·4	— 51·7	
	— 2·36	— 2·18	— 2·33	— 2·32	— 2·32	—2·33
3665	—10·7	—18·5	—27·8	—49·2	— 58·4	
	— 2·47	— 2·87	— 2·72	— 2·57	— 2·62	—2·64
3341	—13·6	—19·6	—31·0	— 56·6	— 66·6	
	— 3·15	— 3·04	— 3·03	— 2·96	— 2·99	—3·01
3131	—16·8	—24·4	—36·4	—63·8	— 76·3	
	— 3·92	— 3·78	— 3·56	— 3·34	— 3·43	—3·50
2805	—18·2	—25·4	—43·1	—77·5	— 88·8	
	— 4·20	— 3·94	— 4·21	— 4·08	— 3·99	—4·06
2655	—22·4	—34·8	—50·5	—87·7	— 99·3	
	— 5·18	— 5·39	— 4·93	— 4·58	— 4·46	—4·73
2537	—22·9	—32·4	—51·2	—93·0	—106·2	
	— 5·29	— 5·02	— 5·00	— 4·86	— 4·77	—4·91
2482	—26·8	—32·9	—55·3	—97·0	—113·8	
	— 6·19	— 5·10	— 5·40	— 5·08	— 5·11	—5·23

put in evidence, as we have an asymmetrical behaviour with respect to the two sides of the 5100 A.U. band, and a negative rotation, which increases with decreasing wavelength.

On evaluating the diamagnetic and paramagnetic parts of formula (3) we find,

$$\Delta \equiv \frac{\pi}{180}\frac{\Delta}{60}\frac{100}{W}f = \sum_i p_i(D_i \pm P), \quad . \quad . \quad . \quad (4)$$

where

$$f \equiv \frac{2\pi e^3}{9m^2c^2}\frac{1}{M m_H},$$

m_{H} being the mass of the hydrogen atom,

$$\left.\begin{aligned} D_i &\equiv \frac{\omega^2}{\omega_i^2-\omega^2} = 2{\cdot}815\,.\,10^{-33}\,\frac{\lambda^{12}}{(\lambda_i'^2\lambda_i^2-1)^2} \\ P_i &\equiv \frac{\mu_i \mathrm{H}}{3kT}\,\frac{\omega^2}{\omega_i^2-\omega^2}\,\frac{1}{\varpi_i \rho_{\mathrm{L}}} = x_i\,4{\cdot}478\,.\,10^{-31}\,\frac{\lambda_i'}{(\lambda^2/\lambda_i^2-1)} \end{aligned}\right\}, \quad (5)$$

where $\lambda' = 10^5\lambda$, λ being in cm., x_i is the number of Bohr magnetons associated with the ith paramagnetic band, and p_i is the number of electrons associated with the ith band. T has been taken equal to 291.

In order to obtain the frequency of the absorption band giving rise to the negative rotation, we must eliminate the diamagnetic rotation due to the bands which account for the natural dispersion of $CoSO_4$. The wave-lengths of these bands are

$$\lambda_1 = 1{\cdot}217\,.\,10^{-5} (\nu_1^2 = 6{\cdot}14),\ \lambda_2 = {\cdot}283\,.\,10^{-5} (\nu_2^2 = 112{\cdot}6),$$

and $\lambda_0 = 5{\cdot}100\,.\,10^5$.

The relative contribution due to these bands to the value Δ' may be obtained by inspection of Table XI., which gives the D and P terms for a few wave-lengths. For the P terms x has been taken equal to unity for convenience. Table XII. gives the values of Δ' for solutions D and E. Also in the second column of this Table is given the weighted mean value of Δ' for all the solutions, the weight being taken proportional to W.

Taking, as before, $p_1 = 2$ and $p_2 = 73$, we see that the valency electrons will give rise to a large diamagnetic rotation, whereas the high frequency electrons will only give rise to a comparatively small rotation. The valency electrons cannot be paramagnetically active, as the P values for $\lambda_1 = 1{\cdot}217\,.\,10^{-5}$ are 100 times (approx.) the D values, which are of the same order of magnitude as the observed Δ' values. We can also exclude the possibility of a paramagnetic effect due to the valency electrons on another ground. For in the case of $CoCl_2$ and $CoBr_2$, where the frequencies of the valency electrons are not so high as in $CoSO_4$, the diamagnetic rotation overpowers the paramagnetic rotation giving rise to a positive rotation in the ultra-violet.

The 5100 A.U. band will also contribute to the diamagnetic rotation, but at present we do not know the corresponding value p_0. As more observations have been

Table XI.

D and P Values.

	$\lambda_0 = 5{\cdot}100 \times 10^{-5}$.		$\lambda_1 = 1{\cdot}217 \times 10^{-5}$.		$\lambda_2 = {\cdot}283 \times 10^{-5}$.	
λ in A.U.	D_0.	P_0.	D_1.	P_1.	D_2.	P_2.
6708	$+ 2{\cdot}38 \times 10^{-31}$	$+ 3{\cdot}13 \times 10^{-30}$	$+ 1{\cdot}44 \times 10^{-34}$	$\pm 1{\cdot}83 \times 10^{-32}$	$+ 4{\cdot}01 \times 10^{-37}$	$\pm 2{\cdot}25 \times 10^{-34}$
5780	+11·54 ,,	+ 8·25 ,,	+ 1·98 ,,	± 2·49 ,,	+ 5·40 ,,	± 3·04 ,,
4358	+ 7·34 ,,	8·73 ,,	+ 3·74 ,,	± 4·53 ,,	9·54 ,,	5·35 ,,
2805	+ ·46 ,,	− 3·38 ,,	+11·61 ,,	±12·41 ,,	+23·22 ,,	±12·99 ,,
2482	+ ·30 ,,	− 3·08 ,,	+ 16·90 ,,	±16·93 ,,	+29·95 ,,	±16·71 ,,

carried out on solution D than on solution E, we shall confine the working to this solution, and compare the calculated results with the observed results recorded in Table XII.

On subtracting $2D_1+73D_2$ from the values of Δ' for solution D, we obtain the joint contribution due to the paramagnetic and diamagnetic terms of the 5100 band and the ultra-violet paramagnetic bands. The results are given in the last column of Table XII.

To eliminate the effect due to the 5100 band we observe that for wave-lengths less than 3341 A.U. P_0+D_0 is approximately constant, the variation occurring in the second decimal place. We may therefore, as a first approximation, take the effect of this band as constant ($=C_0$) for these wave-lengths. Assuming that there is only one effective paramagnetic band in the ultra-violet, we have for the three wave-lengths 3341, 2805, and 2482 A.U.,

$$-3{\cdot}68^5\,.\,10^{-33}=\frac{a_-}{11{\cdot}16\,.\,10^{-10}-\lambda_-}+C_0,$$

$$-5{\cdot}41\,.\,10^{-33}=\frac{a_-}{7{\cdot}87\,.\,10^{-10}-\lambda_-}+C_0,$$

$$-7{\cdot}25\,.\,10^{-33}=\frac{a_-}{6{\cdot}16\,.\,10^{-10}\lambda_-^2}+C_0,$$

λ_- being the wave-length of the active band giving rise to the negative rotation, and a_- a constant.
The equations give

$$C_0={\cdot}351\,.\,10^{-33},$$
$$a_-=32{\cdot}23\,.\,10^{-43},$$
$$\lambda_-=1{\cdot}221\,.\,10^{-2}.$$

Having obtained an approximate value for a_- and λ_-, we can obtain the effect of the 5100 band by evaluating $\frac{a_-}{\lambda^2-\lambda_-^2}$ for all the wave-lengths, and subtracting these values from the last column of Table XII. If we represent the effect due to the 5100 band by $p_0(D_0+x_0P_0)$, we find for the pair of wave-lengths 5780 and 4358

$$+{\cdot}68\,.\,10^{-33}=1{\cdot}15\,.\,10^{-30}p_0+8{\cdot}25\,.\,10^{-30}p_0x_0$$
$$-{\cdot}40\,.\,10^{-33}={\cdot}73\,.\,10^{-30}p_0-8{\cdot}73\,.\,10^{-30}p_0x_0,$$

which give

$$p_0=1{\cdot}62\,.\,10^{-4},$$
$$p_0x_0={\cdot}60\,.\,10^{-4}.$$

Table XII.

Values of Δ', etc.

λ in A.U.	Weighted Mean.	E.	D.	Δ' calc. λ_1 1187.	Δ' calc. λ_1 1046.	$\Delta' - 2D_1 - 73D_2$ λ' 1187.
6708	$-\cdot18\times10^{-33}$	$-\cdot13\times10^{-33}$	$-\cdot19\times10^{-33}$	$-\cdot22\times10^{-33}$	$-\cdot24\times10^{-33}$	$-\cdot50\times10^{-33}$
6104	$-\cdot13$,,	$-\cdot12$,,	$-\cdot13$,,	$-\cdot12$,,	$-\cdot14$,,	$-\cdot52$,,
5893	$-\cdot05$,,	$-\cdot01$,,	$-\cdot04$,,	$-\cdot005$,,	$+\cdot01$,,	$-\cdot45$,,
5780	$+\cdot09$,,	$+\cdot09$,,	$+\cdot10$,,	...	...	$-\cdot33$,,
5461	$+\cdot30$,,	absorpn.	$+\cdot31$,,	$+1\cdot07$,,	$+1\cdot06$,,	$-\cdot18$,,
4358	$-1\cdot39$,,	,,	$1\cdot44$,,	...	...	$2\cdot26$,,
4047	$-1\cdot68$,,	$-1\cdot67\times10^{-33}$	$-1\cdot67$,,	$-1\cdot57$,,	$-1\cdot68$,,	$-2\cdot64$,,
3665	$-1\cdot90$,,	$-1\cdot89$,,	$-1\cdot85$,,	$-1\cdot81$,,	$-1\cdot82$,,	$-3\cdot08$,,
3341	$-2\cdot17$,,	$-2\cdot15$,,	$-2\cdot13$,,	$-2\cdot07$,,	$-2\cdot11$,,	$-3\cdot68^5$,,
3131	$-2\cdot52$,,	$-2\cdot47$,,	$-2\cdot46$,,	$-2\cdot37$,,	$-2\cdot38$,,	$-4\cdot30^5$,,
2805	$-2\cdot92$,,	$-2\cdot87$,,	$-2\cdot91$,,	$-2\cdot90$,,	$-2\cdot89$,,	$-5\cdot11$,,
2655	$-3\cdot40$,,	$-3\cdot21$,,	$-3\cdot30$,,	$-3\cdot24$,,	$-3\cdot20$,,	$-6\cdot20$,,
2537	$-3\cdot53$,,	$-3\cdot43$,,	$-3\cdot50$,,	$-3\cdot50$,,	$-3\cdot50$,,	$-6\cdot86$,,
2482	$-3\cdot76$,,	$-3\cdot68$,,	$-3\cdot65$,,	$-3\cdot64$,,	$-3\cdot65$,,	$-7\cdot25$

From these values we can calculate the contribution to Δ' due to the 5100 band, and thence obtain a better value for a_- and λ_-.

These were found to be $a_- = 33{\cdot}76 \cdot 10^{-43}$, and $\lambda_- = 1{\cdot}187 \cdot 10^{-5}$. With these improved values for a_- and λ_- we can obtain improved values for p_0 and $p_0 x_0$. On carrying out the calculation, we find

$$p_0 = 2{\cdot}18 \cdot 10^{-4}, \quad p_0 x_0 = {\cdot}57 \cdot 10^{-4}.$$

Using these constants, the values of Δ' have been calculated, and are given in the fifth column of Table XII. The agreement between the observed and calculated values of Δ for the different lines is as good as one can expect, with the exception of λ 5461.

Formula (4), for solution D, thus becomes

$$\Delta' = 2D_1 + 73D_2 + p_0(D_0 + x_0 P_0) + \frac{a_-}{\lambda^2 - \lambda_-^2},$$

where

$$p_0 = 2{\cdot}18 \cdot 10^{-4},$$
$$p_0 x_0 = {\cdot}57 \cdot 10^{-4},$$
$$a_- = -33{\cdot}76 \cdot 10^{-43},$$
$$\lambda_- = 1{\cdot}187 \cdot 10^{-5},$$

and P and D are defined by (5).

The number of Bohr magnetons associated with the 5100 A.U. band is $x_0 = {\cdot}27$.

In the above calculations we have assumed that the values of the frequencies of the diamagnetic bands obtained from dispersion measurements will serve for the purpose of magnetic calculations. In the case of diamagnetic salts with highly dispersive anions there appears, according to Heydweiller, good agreement between the values of the characteristic frequencies of the electrons calculated from dispersion and magnetic measurements. Also the values of these frequencies depend very little on the kation. For the more rigidly bound valency electrons such as occur in SO_4 there is a much larger difference between the frequencies calculated from dispersion and magnetic observations.

According to Heydweiller the value of ν_1^2 for Li_2SO_4 is about 6·9 from magnetic measurements, whereas from dispersion data the value ν_1^2 6·15 is obtained. Let us assume that this value of ν_1^2 6·9 is the value to be used for the purpose of calculating the diamagnetic rotation

in $CoSO_4$ due to the valency electrons, on the grounds that the dispersion frequencies of $CoSO_4$ and Li_2SO_4 are nearly the same.

I have carried out a similar method to that described above, using the value $\nu_1^2 = 6{\cdot}90$ instead of $\nu_1^2 = 6{\cdot}14$ as above. In this case the new constants are found to be

$$p_0 = 2{\cdot}16 \,.\, 10^{-4},$$
$$p_0 a'_0 = {\cdot}57 \,.\, 10^{-4},$$
$$a_- = -31{\cdot}36 \,.\, 10^{-43},$$
$$\lambda_- = 1{\cdot}046 \,.\, 10^{-5},$$

and the number of Bohr magnetons for the 5100 band is ·26. The values of Δ' calculated by means of these constants are given in the sixth column of Table XII.

The question naturally arises, what physical significance have these constants ?

The value p_0 is proportional to the strength of 5100 band. From absorption data Houstoun * calculates that the number of electrons per molecule causing the 5100 band in cobalt salts is $1{\cdot}2 \,.\, 10^{-4}$.

From the magnetic data we have found $p_0 = 2{\cdot}2 \,.\, 10^{-4}$. It must be borne in mind that this value has been obtained by applying equation (3), which has been obtained by neglecting damping. This neglect of damping is shown in the small observed value for λ 5461 A.U. in comparison with the calculated value for this wave-length.

From the value of a_- we can calculate the product of the magnetic moment of the paramagnetic band and number of electrons per molecule responsible for this band. We find from equation (5)

$$a_- = 4{\cdot}478 \,.\, 10^{-31} \lambda'_- \lambda_-^2 (p_- x_-),$$

giving for $\lambda_- = 1{\cdot}187 \,.\, 10^{-5}$, $p_- x_- = {\cdot}046$,

and for $\lambda_- = 1{\cdot}046 \,.\, 10^{-5}$, $p_- x_- = {\cdot}061$.

In the case of tysonite Becquerel and de Haas † find that there is exactly one Bohr magneton associated with the active band, in spite of the much larger magneton value of the magnetic susceptibility of the crystal. If we assume that in the case of $CoSO_4$ the moment of the active band is 1 magneton, then the number of electrons per molecule is ·046 for $\lambda = 1{\cdot}187 \,.\, 10^{-5}$ and ·061 for $\lambda = 1{\cdot}046 \,.\, 10^{-5}$.

We know, however, from susceptibility measurements that in solution the salts of cobalt possess ionic carriers of

* Proc. Roy. Soc. Edinb. xxxi. p. 547 (1911). † *Loc. cit.*

moment equal to about four Bohr magnetons. If we suppose, which is very probable, that the magnetic moment determining the main paramagnetic rotation has the same value as that of the ionic carriers, then the strength of the ultra-violet paramagnetic band will be equal to about ·01.

We have neglected the diamagnetic rotation arising from the paramagnetic band in all the calculations. For a strength equal to ·01, the maximum diamagnetic contribution to Δ' will not exceed 2 units in the second decimal place for the wave-lengths investigated. Neglecting the term for the diamagnetic rotation of the paramagnetic band will therefore not affect the results materially.

The 5100 A.U. band has been treated throughout as paramagnetic. It may be thought that the increase in the rotation on approaching this band from the red side can be accounted for by means of a single diamagnetic term in the dispersion formula. This would require, however, a much greater strength of the absorption band than is actually found from absorption measurements. Further, unless we treat this band as paramagnetic we do not obtain consistent values of λ_- from the ultra-violet observations.

The conclusion that the 5100 A.U. band is paramagnetic is in agreement with Ladenburg's * considerations concerning paramagnetism and colour, as it is to the presence of this band that cobalt solutions owe their red colour.

Further experiments, particularly at low temperatures, are necessary in order to fix more definitely the magnetic moment determining the paramagnetic rotation of cobalt salts. In this connexion one must point out that the use of low temperatures for the investigation of paramagnetic rotation phenomena has long ago been introduced by J. Becquerel. Experiments on the magnetic circular dichroism of the 5100 A.U. band are also required in order to fix more definitely the dispersion constants and magnetic moment of this band. Experiments on these lines are contemplated.

Summary.

(1) The magnetic rotations of five solutions of cobalt sulphate in water have been investigated in the visible and ultra-violet regions at room-temperatures.

* *ZS. f. Elektrochem.* xxvi. p. 270 (1920).

(2) The results indicate that the rotation of $CoSO_4$ is negative in the red and ultra-violet regions, becoming positive on approaching the 5100 A.U. band.

(3) The refractive indices of the same solutions have been determined in the same spectral regions.

(4) The molecular refractivities of $CoSO_4$ for different wave-lengths have been calculated.

(5) The characteristic frequencies of the electrons controlling the dispersion of $CoSO_4$ in water have been calculated.

(6) Ladenburg's rotatory dispersion formula has been used to obtain

(i.) the frequency of the ultra-violet paramagnetic band,

(ii.) the number of electrons per molecule causing the 5100 A.U. band and the moment of this band.

I wish to express my best thanks to Prof. Wilberforce for the interest he has taken in the work, and for the facilities and the apparatus placed at my disposal; to Prof. E. C. C. Baly for his kindness in lending me the spectrometer and accessories; to Mr. A. Weale, for his collaboration during the Session 1927-28; to Mr. W. Band for his assistance during the magnetic measurements in the ultra-violet; and to Dr. A. V. Moses for his assistance in some preliminary work.

The George Holt Physics Laboratory,
The University, Liverpool,
Dec. 19th, 1929.

XXXVI. *Luminosity in Gaseous Combustion.* *By* W. T. David, *Sc.D.*, *M.Inst.C.E.*, *and* W. Davies, *B.Sc.**

[Plates V.–VIII.]

FOR some time past we have been taking continuous photographic records of the ultra-violet and luminous radiation emitted during the explosion and subsequent cooling of inflammable gaseous mixtures contained in closed vessels, and correlating them with continuous records of pressure variation. A typical experiment was described

* Communicated by the Authors.

in a communication to Section G of the British Association in 1927 *. Since then we have carried out similar experiments on a gas-engine designed to give the well-known Clerk zigzag diagram.

We had hoped, among other things, to be able to infer from these experiments when combustion became complete in a gaseous explosion and in a gas-engine, but serious difficulties arose when we attempted to interpret our results on the hypothesis that luminosity results from chemical combination. We found that the intensity of the luminous radiation at any instant was dominated by the temperature of the gaseous medium (as inferred from its pressure), and that it appeared to be hardly influenced at all by the amount of chemical combination taking place at that instant. Indeed, luminosity was manifest long after chemical union was generally supposed to have been complete, and convincing confirmation of this was afforded by the gas-engine experiments.

It was not possible, however, to explain the results on a purely thermal basis, for the more permanent gases remain dark when heated to higher temperatures than those sufficient to produce luminosity in our experiments, and we are therefore led to believe that chemical combination results in the formation of molecules (probably of CO_2 and H_2O) which are in an abnormal condition, and that in this condition the vibrations which give rise to luminous radiation are excited by much softer collisions than would be required to produce the same effect in normal CO_2 and H_2O molecules.

A hypothesis of this kind serves to explain our results only if we assume that the abnormal condition of the molecules can persist for many seconds when combination takes place in the gaeous phase.

We discuss this in some detail later in this paper, and suggest that the overall process of combustion may be analysed broadly into two stages :—(i.) chemical combination resulting in the formation of abnormal molecules, and (ii.) the change from the abnormal to the normal molecular state.

The second stage we believe to be a long drawn out process (except in the case of surface combustion), and in a subsequent paper we shall describe experiments which

* 'Engineering,' Aug. 1927.

suggest that it involves an appreciable amount of energy, and is therefore of practical importance.

Description of Apparatus and Experimental Procedure.

Two explosion vessels cylindrical in shape were employed in these experiments. One of these was of dimensions 12 inches in diameter by 12 inches in length, and the other 6 inches by 6 inches. The pressure indicators used were generally of the piston type, but in some experiments a diaphragm indicator was employed. They were fitted with moving mirror systems for optical recording on a revolving photographic film. The indicators were calibrated in position by admitting air under pressure into the explosion vessels and balancing the pressures against a column of mercury in a compound gauge on which readings were taken to half a millimetre.

The light emitted during the explosion, after passing through a small quartz window in the end cover, illuminated a narrow slit which was focussed on the film with its length perpendicular to the direction of motion of the film and in alignment with the reflected beam of light from the indicator mirror, so that a pressure-time curve and a simultaneous photographic record of the luminosity were obtained.

The gaseous mixtures were prepared by exhausting the explosion vessel and refilling several times with one of the constituents of the mixture to be used until all traces of the products of combustion from the previous experiment had been eliminated, and then admitting the gases from storage cylinders in the required proportion. The whole mixture was then thoroughly mixed by means of a fan mounted on a spindle passing through a gland in the end-cover. This fan was also used to produce turbulence during explosion in certain experiments which are described in the paper.

The explosions were initiated by an electric spark at the centre of the vessel from an induction coil, the primary circuit of which was closed at the proper time by a travelling contact on the revolving spindle carrying the film-drum.

The films used were Eastman Super Speed, H & D 500. Great care was exercised in developing them equally under conditions which were kept as uniform as possible.

Results of Experiments.

A typical record from an explosion of 30 per cent. carbon monoxide and air in the 6 in. cylinder is shown in fig. 1 (Pl. V.). In this experiment the initial pressure, represented by the zero-line of the indicator diagram, was 1 atmosphere, and the rise of pressure at any time during the explosion is shown by the height of the diagram above this line *. The horizontal band immediately below the pressure-curve is a continuous record of the luminous radiation emitted by the gaseous mixture after ignition at the centre of the vessel by the electric spark, which was recorded on the film at the point A. During the interval between the passage of the spark and the beginning of the rise of pressure the luminosity was comparatively small, but it increased rapidly with rise of pressure to a maximum value in the neighbourhood of the maximum pressure, and afterwards decreased slowly as the products of combustion cooled. An examination of this record shows that during the actual explosion period the luminous radiation emitted was of no greater intensity than that emitted immediately after the moment of maximum pressure, although, of course, the bulk of chemical combination took place during that period. As the gases cooled the luminosity gradually decreased, but remained sufficiently intense to mark the film for a considerable time after maximum pressure. Indeed, even after this we noticed in all our experiments that the products remained incandescent for some seconds, and therefore long after the cessation of all chemical combination of the original gases as well as of any dissociated molecules.

These facts appear to be at variance with the theory that luminous emission during gaseous explosion results solely and directly from chemical combination. The record rather suggests that the intensity of the luminosity during the actual period of explosion, as well as afterwards, is entirely dependent upon the temperature of the gaseous medium as inferred from its pressure. Subsequent experiments which are now to be described definitely confirm these conclusions.

Figs. 2 to 5 (Pl. V.) show how the intensity and amount of luminous radiation emitted during explosion increased

* The scale against the pressure-curve gives the mean gas temperature as inferred from the pressure.

as the maximum temperature was raised by substituting diluent gases of lower specific heats in mixtures containing the same amount and proportion of combustible gases. Figs. 2 and 3 (Pl. V.) were obtained with 20 per cent. H_2—10 per cent. O_2—70 per cent. N_2, and 20 per cent. H_2—10 per cent. O_2—70 per cent. Ar mixtures respectively. The chemical energy was therefore the same in both cases, but, on account of the lower heat capacity of the argon mixture, the maximum temperature developed was about 500° C. higher than in the nitrogen mixture, and, as will be seen, the luminous radiation was much more intense. The substitution of nitrogen for carbon dioxide as a diluent in a given mixture of carbon monoxide and oxygen also produced a similar result. This is shown in figs. 4 and 5 (Pl. V.), which were obtained with 26 per cent. CO—30 per cent. O_2—44 per cent. CO_2, and 26 per cent. CO—30 per cent. O_2—44 per cent. N_2 mixtures respectively, with the fan running at 1500 r.p.m. In the former the maximum temperature reached was about 400° C. less than in the latter.

It is a well-established experimental fact that the ratio of the maximum pressure to the initial pressure, and hence the maximum temperature attained in the explosion of an inflammable gaseous mixture of any given composition, increases with the density of the mixture. This is due in the main to more effective combustion in a medium of high density. If radiation was emitted in virtue of chemiluminescence alone it would therefore be expected that the duration of emission after maximum pressure would become less as the density increased. This, however, is far from being the case, as is shown by the records in figs. 6, 7, 8 and 9 (Pl. VI.), which were obtained in experiments in the 6 in. vessel with a mixture of 28 per cent. CO and air at initial pressures varying from $\frac{3}{4}$ to 3 atmospheres*. Indeed, as will be noted, the duration of emission after the moment of maximum pressure in these experiments increased with the density, and this seems to be wholly due to the fact that cooling proceeded more slowly in the denser mixtures, for the temperature at which the luminosity ceased to be recorded by the films was the same at all densities. Further proof of this is given by the photometric

* In these records the pressure-scales are different because stronger springs had to be used in the indicator at the higher pressures.

measurements recorded in fig. 10 *. These relate to two mixtures, the one $2CO+O_2+4N_2$ at atmospheric density, and the other $2CO+O_2+4O_2$ at five atmospheres density. It will be noted that, in spite of the much slower cooling in the denser mixture, the relationship between the luminosity and the temperature is much the same in the two mixtures. We hope to investigate this relationship in a subsequent paper.

Similar experiments were carried out with mixtures of composition $2CO+O_2+4CO$, in which dissociation would be largely suppressed. The results were in every way similar to those obtained with CO-air mixtures.

Fig. 10.

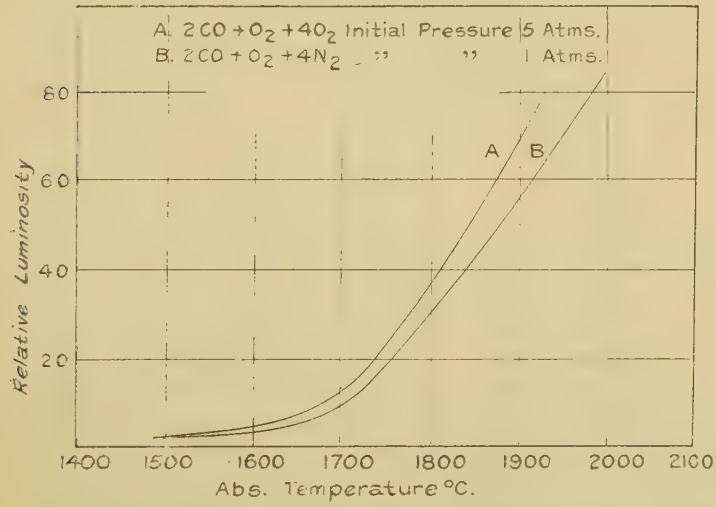

We have also made two series of experiments in the large vessel with the mixtures $2CO+O_2+nCO$ at atmospheric density in which n was varied from 2 to 7. In the first series the mixtures were fired in the stagnant condition, and in the second they were put in turbulent motion by means of a fan. They can, perhaps, best be summarized in the manner shown in the Table on p. 396. It will be noted that the temperature at which luminosity reached a certain intensity, namely, that at which it became just

* We wish to express our indebtedness to the late Mr. S. R. Pyke and to Mr. J. Tylor, who very kindly made the photometric measurements for us in Professor Whiddington's laboratory.

too weak to mark the film, was practically the same (about 1150° C.) in all cases, although the time taken after explosion to reach this temperature varied greatly (from ·26 sec. to ·64 sec.), and consequently the chemical condition of the gaseous mixture varied considerably.

Although the luminosity at a temperature of 1150° C. was on the point of becoming too weak to mark the photographic film, luminosity visible to the eye continued to be manifest for some seconds afterwards, until, indeed, the temperature had fallen to 300° C. as nearly as we could judge.

Gaseous mixture.	Condition during explosion.	Time to max. press. (secs.)	Max. gas temp. ° C.	Duration of luminous record on film after max. press. (secs.).	Gas temp. at termination of luminous record. ° C.
$2CO+O_2+2CO$	Fan at work	·07	3080	·64	1150
3CO		·08	2780	·55	1190
4CO		·095	2570	·52	1170
5CO		·12	2200	·47	1180
6CO		·155	2030	·44	1170
7CO		·28	1710	·34	1160
$2CO+O_2+2CO$	Fan running	·03	3110	·47	1140
3CO		·04	2860	·41	1170
4CO		·045	2680	·35	1160
5CO		·055	2340	·33	1150
6CO		·065	2140	·29	1160
7CO		·08	1930	·26	1130

These results make it clear that the amount of radiation emitted in any given explosion depends entirely on the time integral of some function of the temperature during the explosion and the cooling period, and further confirmation of this may be obtained from an examination of the records given in figs. 11, 12, and 13 (Pl. VII.). In these figures are shown the effects of a more rapid explosion and an increased rate of cooling when this is caused by turbulence produced by a fan in the explosion vessel. Similar results are shown in figs. 14 and 15 (Pl. VII.), in which the explosion period and cooling-rate were varied by the addition of water vapour to CO-air mixtures.

Gas-Engine Experiments.

For these experiments the engine was designed to give the Clerk "zigzag" indicator diagram, which is obtained

by closing the valves automatically at the end of a suction-stroke, so that after the explosion has taken place the products of combustion are retained in the cylinder and are subjected to alternate compression and expansion, while the engine continues to run under its own momentum. From the moment of the tripping of the valves a continuous indicator diagram was recorded on a revolving photographic film by means of an optical indicator which had previously been calibrated in its working position against a standard gauge tester. The film was carried by a drum which was driven from the crank-shaft of the engine, so that the indicator diagram was recorded on a base representing angular displacements of the crank.

The results confirmed those obtained in the closed vessel, and they also show that when the products of combustion are re-heated by adiabatic compression immediately after cooling they again become highly luminous.

A typical record is shown in fig. 16 (Pl. VIII.). At the point A the piston was at the commencement of the compression-stroke with a fresh charge in the cylinder, and the valves disengaged from their cams; towards the end of compression at B ignition took place, and soon afterwards the pressure increased almost instantaneously to a maximum value at C. Immediately above the indicator diagram is the record of the luminous radiation emitted during the explosion and the expansion-stroke. The products of combustion cooled more rapidly in this case than in the closed vessel experiments on account of expansion, and they reached the temperature at which the luminosity ceased to mark the film about the middle of the stroke. At the end of the explosion-expansion stroke it is generally believed that combination is complete, for the analysis of the exhaust gas from gas-engines in normal running invariably indicates complete combination; but nevertheless the heating of the products of combustion during the subsequent compression-stroke caused them to become vividly luminous again, as shown in the record at E. The temperature reached at the end of this stroke was about 1550° C.

Owing to the continual loss of heat from the gas to the piston and the cylinder-walls the temperature reached at the end of successive compressions gradually became less, and during the next compression-stroke the temperature did not rise high enough to produce luminosity of sufficient

intensity to mark the film; but it was clearly visible to the eye at this point, and even at the end of three or four compressions afterwards, at which time the temperature was of the order of 300° C.

The record shown in fig. 17 (Pl. VIII.) was obtained by retarding the ignition until the piston had moved forward some distance on the expansion-stroke, with the result that the gases were raised to a higher temperature at the end of the first compression than was obtained during the actual explosion, and the record shows that the luminosity at this point was actually greater than during the period of chemical combination. The temperature reached at the end of the second compression in this case, viz., 1180° C., was also just high enough to give rise to a luminosity just sufficiently powerful to produce a faint impression on the film, as shown at G.

Discussion.

The photographic method is now extensively employed in this and other countries in investigating combustion phenomena in gaseous mixtures. The basic idea underlying this work is that luminosity results from chemical activity, and therefore that the existence of luminosity at any instant is an indication that such activity is proceeding at that instant. Pringsheim, who had made many unsuccessful attempts to make the more permanent gases luminous by direct heating to the highest temperatures he could command, was also of this opinion, but he believed that, as long as chemical activity was proceeding, the temperature of the medium in which it was taking place had a great influence upon the intensity of the luminosity. Many recent workers, however, do not appear to attach much importance to the temperature factor *.

Our experiments appear to put beyond doubt the overwhelming influence of temperature upon the intensity of the luminous emission. The only question that arises is the part played by chemical activity †. The experiments

* See, for example, 'Gaseous Combustion at High Pressures,' by Bone, Neuitt, & Townend. (Longmans, Green & Co., 1929, p. 202.)

† Ionization seems to have little influence on the luminous emission. Garner (Trans. Faraday Soc. vol. xxii. Oct. 1926, p. 334) has shown that the addition of a small quantity of lead tetra-ethyl suppressed ionization during explosion to a large extent, but the addition of lead tetra-ethyl to our gaseous mixture did not affect the luminosity to any measurable extent.

at once show that the intensity of luminosity at any moment is little influenced by the volume of *chemical combination* taking place at that instant, and, indeed, luminosity is manifest in our exploded gases long after the moment when chemical combination appears to have been completed. In proof of this may be urged the fact that luminosity is manifest for some time (suitably measured in seconds) after explosion, during the greater part of which time chemical analysis fails to suggest the presence of uncombined gas. Furthermore, in our gas-engine experiments it will be remembered that a series of rapid compressions of the working fluid subsequent to the explosion-expansion stroke reproduced luminosity, although, as has been frequently shown, chemical analysis of the exhaust gases of a gas-engine in normal running always suggests that combination is practically complete at the end of the explosion-expansion stroke. We think, too, that it is a safe inference from our experiments that, had we used a larger explosion vessel so that cooling took place more slowly, luminosity would have been manifest for a longer time than we observed in our vessel *. Similarly, had our gas-engine been larger so that cooling would have been slower, re-illumination in the working fluid would have been observable over a large number of compressions.

It seems safe, therefore, to assume that luminosity may be manifest in exploded gaseous mixtures long after combination is complete ; and in view of the fact that the more permanent gases cannot be rendered luminous by direct heating to temperatures at which luminosity is manifest in our experiments, it is reasonable to suggest that chemical combination results in the formation of abnormal molecules which persist for some time and only slowly pass into normal molecules †.

In a subsequent paper we describe experiments which seem to indicate that a considerable amount of energy is associated with these abnormal molecules, *i. e.*, that the energy they contain is in excess of that which would be

* This has since been confirmed. During the explosion of a 30 per cent. CO-air mixture at three atmospheres density in an 18-inch silver-plated spherical vessel, luminosity was manifest for at least 14 seconds after maximum pressure.

† This applies only to combustion in the gaseous phase. The process seems to be enormously speeded up in contact with a hot body. This we will deal with in our next paper. (See p. 402.)

possessed by normal molecules of CO_2 and H_2O constituting a gas of the same temperature. At first sight the theory that in the act of combination the heat of combustion first passes, either wholly or in part, into the form of rotational and vibratory energy of the newly formed molecules might be accepted as affording a satisfactory explanation. But the long life-history possessed by these abnormal molecules (in the absence of a disturbing cause, such as contact with a hot surface) introduces a very real difficulty, for partitioning would doubtless be effected very rapidly at explosion temperatures, and proof of this seems to be furnished by the fact that the energy in the vibrations corresponding to luminous radiation, as well as that in the vibrations corresponding to infra-red radiation*, is always in equilibrium with the temperature (translational energy). Another explanation that might be offered is that complex molecules are formed during combination. This seems possible as a stage in the combination process, but again unlikely that they could possess a long life-history, for disintegration at explosion temperatures would probably be rapid.

We think that a possible explanation may be found in the suggestion that combination results in the formation of molecules of abnormal molecular *structure*, and that these molecules pass gradually into molecules possessing the normal structure, the process being an exothermic one. The overall process of combustion would thus be analysed broadly into two stages :—

(i.) chemical combination resulting in the formation of molecules of abnormal molecular structure, and

(ii.) the passage (requiring time when combustion takes place in the gaseous phase) of these molecules into molecules possessing normal structure.

Our experiments, of course, offer no information as to the type of structure possessed by the abnormal molecules, but it is interesting to speculate as to possible types. Let us confine the attention to carbon-monoxide-oxygen combination. It is conceivable that the abnormal CO_2 first resulting from this combination may consist of an atom of oxygen with its distinctive electron atmosphere attached as a whole to a more or less normal CO molecule.

* David, Phil. Trans. A, vol. ccxi. p. 386.

which we will suppose consists of two atomic nuclei surrounded by a more or less common electron atmosphere. The passage to the normal type of CO_2 may then be represented by the assimilation of the oxygen atom into the system producing a molecule consisting of three nuclei surrounded by a common electron atmosphere. It may be that the very considerable stability which we have to postulate for the abnormal type of molecule in order to account for our results is apparent rather than real, and that the apparent stability is due to continual dissociation and recombination brought about by collision or by continual interchange of partners with neighbouring molecules.

Summarizing, we suggest that the first stage in the overall process of combustion may be represented thus :—

$$\overline{A}\,|+|\underline{B} \rightarrow |\underline{A}\,|\underline{B}| + (H - x), \quad . \quad . \quad . \quad (1)$$

where H is the heat of combustion, and that the second stage is indicated by

$$\overline{A}\,|\,\overline{B} \rightarrow \overline{A\,B} + x. \quad . \quad . \quad . \quad . \quad . \quad (2)$$

It has always been our view that the process of combination (the first stage indicated above) in any given thin layer of gas is by no means an instantaneous process, and although our present experiments offer no information on this point we are still of this opinion in view of some earlier experiments by one of us*. We feel, however, that they do show that the second stage is a very long drawn out process in the gaseous phase, and in our next paper we describe experiments which suggest that the energy released in this stage, viz., x, is an appreciable fraction of the heat of combustion.

We think that our experiments show that flame photographs, while they give invaluable information in regard to flame propagation in inflammable mixtures, yield no information as to the chemical condition of the gases behind the flame-front, but merely indicate their temperature.

We wish to express our indebtedness to Mr. S. G. Richardson, who made the experiments on the gas-engine and gave us great assistance in the earlier stages of the closed-vessel experiments.

* Proc. Roy. Soc. A, vol. xcviii. p. 313 (1920).

XXXVII. *Temperature Measurements in Gaseous Combustion.* *By* W. T. David, *Sc.D.*, *M.Inst.C.E.*, *and* W. Davies, *B.Sc.**

[Plate IX.]

IN this paper experiments are described in which the temperatures of thin platinum-rhodium wires immersed in inflammable gaseous mixtures during their explosion and subsequent cooling in closed vessels were recorded continuously and compared with the gas temperatures as inferred from the pressures.

Our results differ markedly from those of other investigators who have made similar experiments, and consequently, in order to ensure the correctness of our work, we made a large number of experiments under as widely different conditions as possible.

Briefly, they indicate that, in whatever position the wire is placed within the explosion vessel, its temperature is several hundred degrees (often 500° C. or more) higher than that of the gas (as inferred from its pressure), not only during the explosion, but also for some seconds afterwards. We found this to be the case, even when the gaseous mixtures were fired in a state of violent turbulence so that the temperature distribution subsequent to the explosion was reasonably uniform.

Similar experiments were also made in the cylinder of a gas-engine designed to give the Clerk "zigzag" indicator diagram, and the results fully confirmed those obtained in the closed vessels.

We believe that these experiments lend support to the views put forward in a previous paper on the emission of luminous radiation by gaseous mixtures during and after explosion, and they further indicate that considerable energy is associated with the abnormal molecules which are formed as a result of chemical combination in the gaseous phase.

Experimental Procedure.

The experiments were carried out in the explosion vessels and in the cylinder of the gas-engine described in the previous paper, and the general arrangement of the

* Communicated by the Authors.

apparatus for recording the temperature of the wire is shown in fig. 1.

The platinum-rhodium wire P was ·001 inch in diameter * and $\frac{3}{4}$ inch long and was connected to one arm of a slide-wire bridge by thick copper leads which passed into the explosion chamber through a sealed metal tube T. This tube could be adjusted to bring the wire into any desired position within the explosion chamber.

Callendar's method of compensating for the change of resistance in the leads and for their cooling effect at the junctions of the wire was adopted by connecting a short length of the same wire through a similar pair of leads to the opposite arm of the bridge and adding sufficient

Fig. 1.

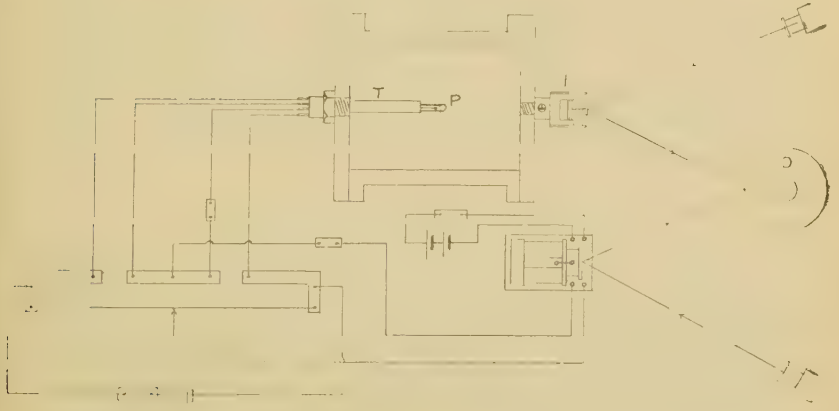

external resistance to bring the point of balance to the middle of the slide wire at room temperature.

The galvanometer used in the experiments was of the Torsion String type with a natural period of 1/50 of a second, so that it recorded very acutely the rapid change

* We made several experiments with wires of different diameters ranging from ·003 to ·0005 inch, and found that a wire of ·001 inch diameter followed the most rapid temperature changes without an appreciable lag, and this size was used in all the experiments described in the paper.

As a further check on our work we made a number of experiments in which the temperatures were measured by thermocouples consisting of platinum-rhodium and platinum-iridium wires of ·001 inch diameter, the results of which were found to be in complete agreement with those obtained by the resistance method.

of temperatures in the wire during an explosion. Its deflexions were recorded on a photographic film mounted on a revolving drum D, and at the time time a continuous record of the pressure was obtained on the same film by means of the optical indicator I. The calibration of the temperature scale for the wire was obtained directly by recording the deflexions of the galvanometer when the wire was placed in an electric furnace at different temperatures up to a maximum of 1100° C. This calibration was made for every new wire used in the experiments, and the extrapolation of the calibration curve to higher temperatures was verified by recording the deflexions of the galvanometer when the wire was placed in a Bunsen flame, and finally, after the completion of a series of experiments, when the wire reached its fusing point in an explosion of a strong gaseous mixture. The relationship between the temperature of the wire and the galvanometer deflexion above 800° C. was practically linear, and therefore intermediate points between the maximum furnace temperature and the melting-point of platinum rhodium could be determined with a fair degree of accuracy.

Result of Closed Vessel Experiments.

A typical record is shown in fig. 2 (Pl. IX.), in which G is the pressure record and W the curve traced by the galvanometer. The spark passed at the point A, and the temperature of the wire increased very rapidly as soon as the flame passed over it before any appreciable rise of pressure had taken place. A further and slower rise of temperature occurred in the wire after this, due to the adiabatic compression of the inflamed gases at the centre of the vessel while combustion was proceeding in the outer layers, and the wire reached its maximum temperature at the moment of maximum pressure. But after this it will be noted that the wire did not cool at the same rate as the gas.

This record was obtained with a mixture of 19 per cent. CO and air in the 6-inch vessel when the wire was placed on the axis of the cylinder at a distance of one inch from the centre. The mean gas temperature (curve G) calculated from the pressure curve and the corresponding temperature of the wire (curve W) for a period of one second after ignition are shown in fig. 3.

It will be seen that the temperature of the wire was some hundreds of degrees above that of the mean gas temperature (as inferred from the pressure), both during explosion and for more than a second afterwards. It is well known that in a stagnant mixture fired centrally the temperature of the mixture in the centre is well above the mean gas temperature; but this could hardly be to the extent shown by this experiment, and no explanation in terms of temperature variation in the gaseous mixture during the cooling period could possibly be adequate to account for the very large difference between the wire and gas temperature (of the order of 500° C. or more) during this period.

Fig. 3.

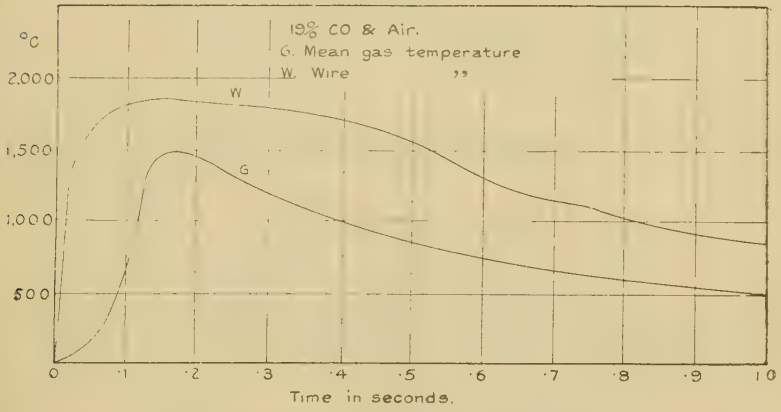

This view is confirmed by the results shown in fig. 4. These were obtained with a mixture of 17 per cent. hydrogen and air, first when the fan was at rest and then when it was running at a speed of 1500 revolutions per minute. The violent turbulence produced under these conditions practically eliminated any temperature differences in the gas, but nevertheless, as will be seen, the large temperature difference between wire and gas was maintained throughout explosion and subsequent cooling.

Moreover, we found that the temperature of the wire in any given explosion differed very little when it was placed in different positions within the 6-inch vessel. The results shown in fig. 5 were obtained with a mixture of 6·5 per cent. methane and air, first when the wire was

placed near the centre and then when it was placed near the end cover of the vessel. In the latter position it will be seen that a small increase of temperature (about 80° C. in this case) occurred in the wire before the flame reached it, due to the adiabatic compression of the unburnt gases

Fig. 4.

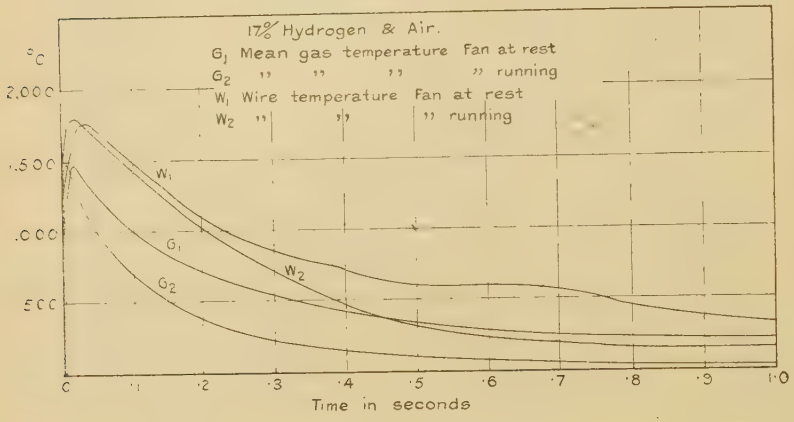

Fig. 5.

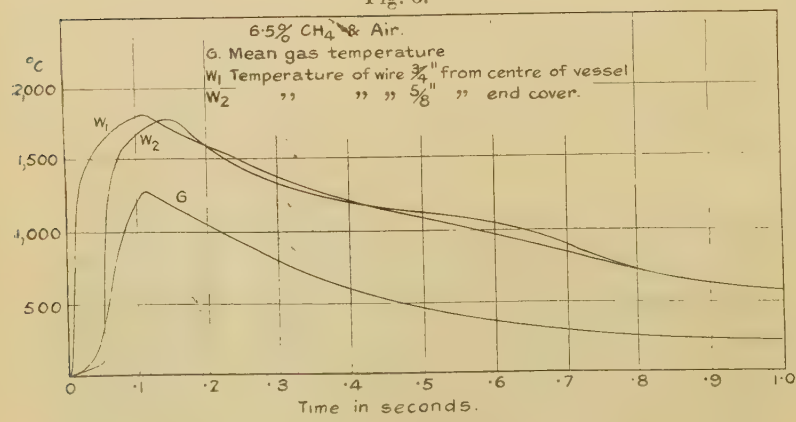

while the flame was moving outwards from the centre. We found that this initial rise of temperature in the wire agreed very closely with the calculated temperature of the unburnt gases, assuming true adiabatic compression before ignition. At the moment of maximum pressure the temperature reached by the wire in the two positions was

practically the same and about 500° C. higher than the maximum mean gas temperature. The subsequent rate of cooling was also very nearly the same in both cases. When, however, the wire was placed in the bottom corner of the cylinder about half an inch away from the walls and the end cover, its temperature, while well maintained above the mean gas temperature for a considerable portion of the cooling period, fell eventually below the mean gas temperature. This is clearly shown on fig. 6, which was obtained with a mixture of 16·5 per cent. hydrogen and air when the wire was in this position. But it is very probable that even here the temperature of the wire was at all times

Fig. 6.

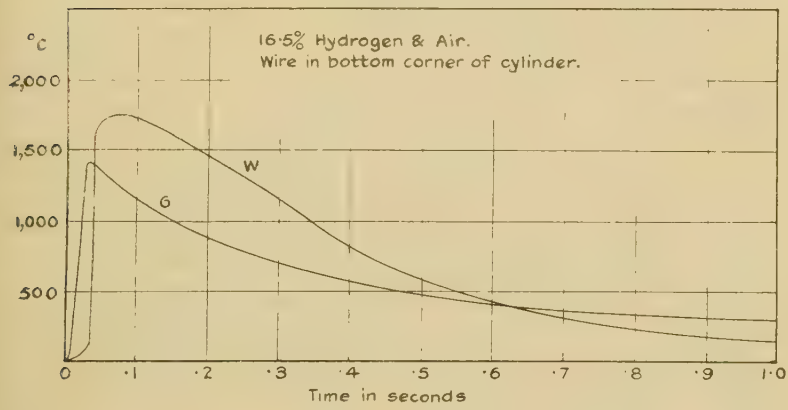

far above that of the gas actually in contact with it, because, owing to very rapid cooling in the corner of the vessel, the temperature of the gas there was well below the mean gas temperature; and this view is supported by the fact that with turbulence the temperature of the wire in the same position did not at any time fall below the mean gas temperature.

The rate of explosion and the maximum gas temperature developed in a given mixture may be varied very considerably without producing any appreciable change in the rate of heating of the wire or in the maximum temperature reached by it: thus, when the explosion of dry mixtures of carbon monoxide and oxygen is accelerated by the addition of a small amount of hydrogen, the maximum mean gas temperature is considerably increased, but the

results given in fig. 7 show that, even when the gas temperature is raised by nearly 400° C. in this way, no appreciable change is produced in the rate of heating of the wire or in the maximum temperature attained by it. A similar

Fig. 7.

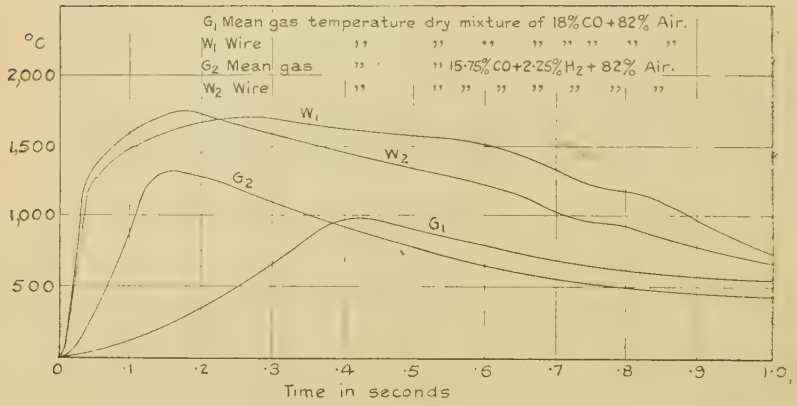

Fig. 8.

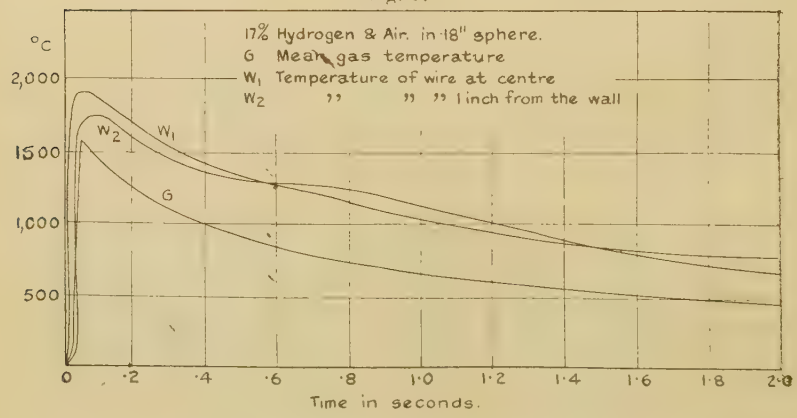

result was also obtained when water-vapour was added to the same mixture instead of hydrogen.

Similar experiments were made in a larger vessel—an 18-inch sphere. Typical results are shown in fig. 8. They relate to a mixture of 17 per cent. hydrogen and air centrally fired, and show the wire temperature in two positions—the one central and the other near the walls

—for a period of 2 seconds after ignition. They appear to confirm in every way our experiments with the smaller vessel, except that there is a rather greater difference in the maximum wire temperatures in the two positions in the larger vessel.

In all the experiments to which reference has been made, the wire was completely exposed to the gas throughout the period of explosion, and therefore only comparatively weak mixtures which would not cause the wire to fuse could be used. In order to investigate the conditions in stronger mixtures, the apparatus shown diagramatically in fig. 9 was designed to shield the wire until it could be safely exposed at some instant during the cooling period.

Fig. 9.

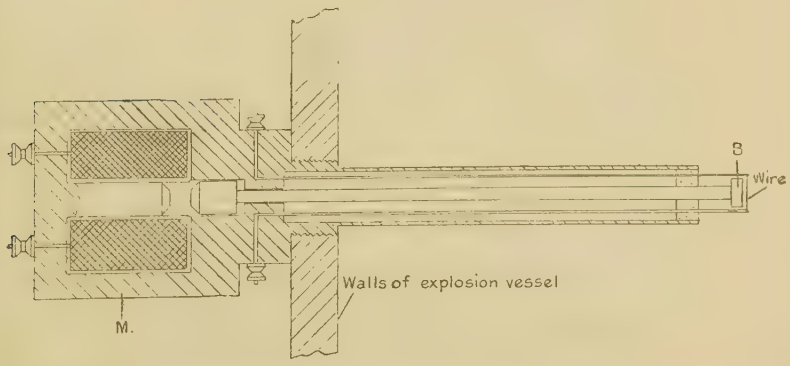

Its action depended on the shielding effect of the mass of metal B due to its proximity to the wire until, at the proper moment, it was pulled away from the wire by the electromagnet M when the circuit of the solenoid was closed by a switch automatically operated by a cam on the spindle of the film-drum. The result of an experiment with a mixture of 30 per cent. hydrogen and air in the smaller vessel is shown in fig. 10. The wire was exposed when the gases had cooled to about 700° C., as inferred from the pressure, and its temperature was immediately raised to about 1400 C°. From this point the wire remained fully exposed while the products of combustion cooled down to the temperature of the room. By exposing the wire at different times during the cooling period

in the explosion of any particular mixture, we found that its subsequent cooling curve was the same whether it was exposed early or late, so that the wire always reached the same temperature relative to that of the gas at any given instant after maximum pressure, whether it approached this temperature from above or from below.

In a later form of the apparatus the wire was completely shielded from contact with the gas until the proper time for exposure, but this modification of the apparatus did not produce any change in the results, provided no obstruction was offered to the free circulation of the gas in the vertical plane of the wire. In its original form the

Fig. 10.

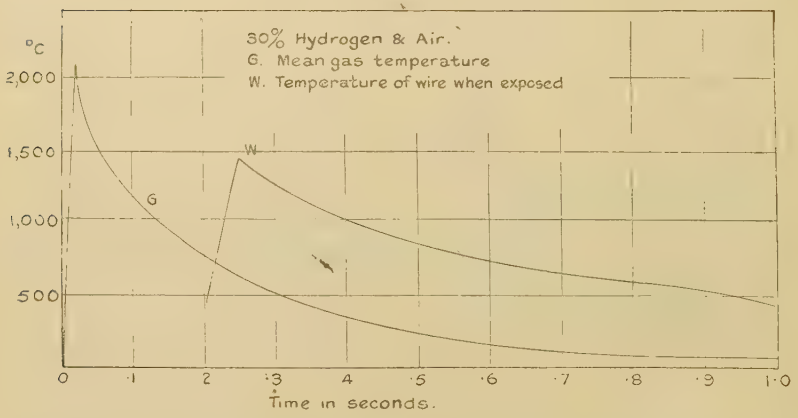

modified shield consisted of a cylinder of $\frac{1}{8}$ inch external diameter divided along its axis into two halves which fitted closely over the wire, and when released by the magnet the two parts moved upwards and downwards respectively a total distance of about 1 inch from the wire. With the shield in this position the wire recorded a temperature of about 300° C. to 400° C. less than when fully exposed, but when the shield was made to open horizontally through an equal distance from the wire, its presence had no measurable effect upon the temperature of the wire. This fact is of considerable interest in that it shows the existence of vertical currents of hot gases at the centre of the vessel, even when the fan is running during the explosion.

Gas-engine Experiments.

The wire was fixed on the ends of thick brass terminals projecting into the combustion chamber as shown in fig. 11, and the recording of its temperature was carried out in the same manner as in the closed vessel experiments. At the end of the suction stroke its temperature was about 60° C., and its rise of temperature during the compression stroke agreed very closely with the gas temperature inferred from the indicator diagram; but after ignition and during the greater part of the expansion stroke its temperature exceeded that of the gas by about 500° C., as in the closed vessel experiments.

Fig. 11.

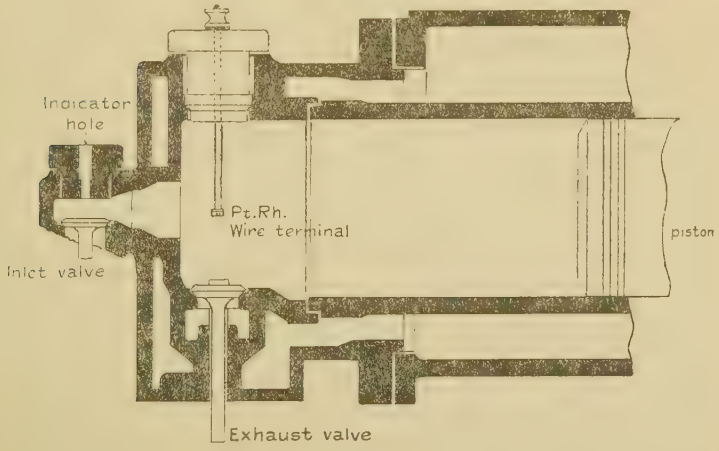

NOTE.—The platinum-rhodium wire was ·001 inch diameter and $\frac{3}{4}$ inch long, mounted with its length perpendicular to the axis of the cylinder.

The results shown in fig. 12 were obtained during three revolutions of the crank after an explosion had taken place and the valves had been tripped so that the products of combustion were retained in the cylinder and alternately expanded and compressed while the engine was running under its own momentum. The temperature cycles of the wire are shown by the upper curve, and the corresponding gas temperatures as inferred from the indicator diagram are shown by the lower curve. Owing to its position in the cylinder, the wire was exposed to the

relatively small amount of cold gas emerging from the valve pocket towards the end of the expansion stroke, and after the first expansion it was cooled below the mean gas temperature during this part of the cycle. It is very probable, however, that even at this time the wire was much hotter than the gas actually in contact with it, and this is strongly suggested by the fact that it was very quickly heated above the mean gas temperature again during the early part of the next compression stroke before the hottest part of the gas came into contact with it. The extreme range of temperature variation in the wire was thus greater in this experiment than would have been the case had it not been influenced by the small quantity of

Fig 12.

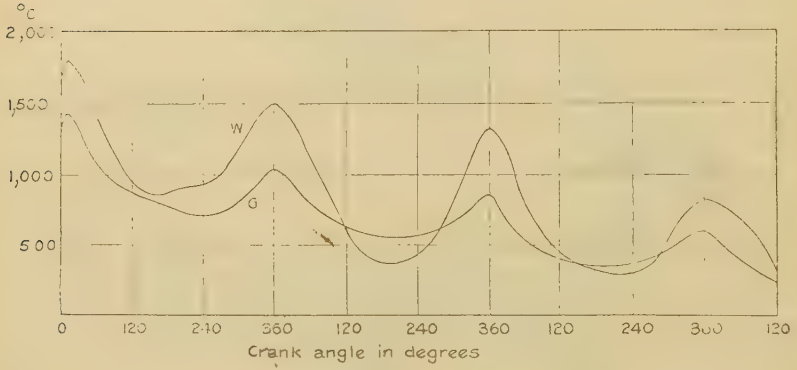

cold pocket gas, as, for example, had it been moving with the piston so that it was always in the general body of the gas in the cylinder. There seems little doubt that in that case the wire would always have remained at a much higher temperature than the gas throughout the period of the experiment.

Just before tripping the valves in this experiment the engine was running at a speed of 230 r.p.m., which remained sensibly constant during the following three revolutions, so that the total time taken to perform the three cycles shown was about 0·8 second.

We take pleasure in thanking our research mechanic, Mr. H. Marvel, for assistance in the design of our apparatus and for making suggestions of value from time to time.

Discussion.

Our experiments are in agreement with those of Hopkinson* in showing that the temperature of the wire as the flame passes over it almost instantaneously rises to its maximum value (apart from a small subsequent rise resulting from the adiabatic compression of the gas surrounding the wire). Harrison and Baxter †. on the other hand. found that the rise of wire temperature takes an interval of time which for any given mixture was of the order of the time of explosion of that mixture in their vessel. We are unable to reconcile their results with our own or with those of Hopkinson. though a possible explanation is that they may have had a mass of metal somewhere near the wire which may have affected the gas in its neighbourhood ; and in this connexion we draw attention to the difficulties we experienced in designing our apparatus so as to secure consistent results (see p. 410).

Hopkinson inferred from his experiments that combustion was completed in any given thin layer of gas almost instantaneously after inflammation. This view did not accord with that deduced from calorimetric measurements made by one of us ‡, and it was suggested that the rapid rise of temperature of the wire was in a large measure due to combustion on the surface of the hot wire §. Our present experiments appear to confirm that suggestion.

In one important respect our work differs entirely from Hopkinson's. We found that at the moment of maximum pressure the temperature of the wires did not vary much with their position in the explosion vessel and that their temperature was always many hundreds of degrees above that of the mean gas temperature as inferred from the pressure. Hopkinson, however, found that his wires showed a wide temperature variation in the exploded gases at this moment which seemed to be rational in the light of an examination of the explosion process. He found, for example, that the temperature of the hot core of a centrally-fired mixture was at this moment much above that of the mean gas temperature as inferred from the pressure, but that as the wire was moved outwards towards the walls of the explosion vessel the temperature

* Proc. Roy. Soc. A, lxxvii. pp. 389 & 399 (1906).
† Phil. Mag. pp. 37–41, Jan. 1927.
‡ Proc. Roy. Soc. A, xcviii. p. 310 (1920).
§ Trans. Faraday Soc. xxii. p. 343 (Oct. 1926).

fell away and became much less than the mean gas temperature *. The wire temperature averaged over a large number of positions would thus, according to Hopkinson, be equal to the mean gas temperature (translational energy). We think that a large error must have crept into the calibration of his wire temperature recording system for wires other than the central wire, which had a separate recording system; and, indeed, Hopkinson himself does not claim great accuracy for the former recording system †.

Our experiments further show that the large difference which exists between the wire temperature and the gas temperature (translational energy) at maximum pressure continues for some seconds afterwards, and therefore long after chemical combination has been completed. The gas-engine experiments also lead to the same conclusion. We believe that the explanation is the same as that offered to account for the luminosity experiments ‡, namely, that combination in the gaseous phase results in the formation of long-lived abnormal molucules, and that considerable energy is associated with these molecules which can be unloaded upon the surface of a hot wire when they come in contact with it.

Reference may be made to the discussion in our previous paper for a fuller account of our views. We should add that in interpreting the results in the present paper it is convenient to regard the temperature of the wire as being equal to the temperature of the gas (translational energy) *plus* an amount corresponding to the excess internal energy unloaded upon it by the abnormal molecules.

We hope to be able to obtain an estimate of the magnitude of the energy associated with the abnormal molecules by calorimetric methods both in closed vessel explosions and also in a gas-engine.

Many of the curious results obtained by workers who have used platinum wires to measure the cyclical changes of temperature of the working fluid of internal-combustion engines and the temperature of the exhaust gases become understandable in the light of these experiments. A discussion of them is reserved for another paper.

* *Loc. cit.* p. 390. † *Loc. cit.* pp. 397–8.

‡ Ionization seems to have no influence upon the temperature of our wires as inferred from their resistance, for the addition of lead tetraethyl to our gaseous mixtures made no difference to the wire temperatures (see footnote, p. 398).

XXXVIII. *Some Experiments with Carbon Line Resistances.*

By J. B. Seth, *M.A.* (*Cambridge*), *Professor of Physics, Government College, Lahore*, Chetan Anand, *M.A.*, *and* Girdhari Lal Puri, *M.Sc.* (*Punjab*)*.

In a paper † from this laboratory it has already been announced how the resistance of carbon (pencil) lines drawn on ebonite or waxed ground-glass surface, when subjected to moist air of different humidities, changes in a regular manner with the relative humidity to which it is exposed; and a suggestion was made that this behaviour of carbon lines may be utilized for hygrometric purposes. The experiments described in the present paper were undertaken to study the properties of such resistances in greater detail before arriving at any suitable form of hygrometer or hygrometry based on these principles. The pencil lines for the present work were mainly those drawn on ebonite, although a number of experiments were also performed on lines on ground-glass plates, the free surface having been waxed. Lines drawn on other insulators such as sulphur and sealing-wax (blocks of which were obtained by pouring the molten materials in a wooden mould and allowing it to solidify) have also been tried, and these were found to behave in a manner similar to those drawn on ebonite. The lines which were to be subjected to humid atmospheres were drawn rather broad, several millimetres wide, in order to have a fairly large exposed surface. Their resistances were usually of the order of a tenth of a megohm.

The present experiments can be divided into two main classes, namely: (1) observing the behaviour of a line enclosed in a tube containing (*a*) air at low pressures, (*b*) nitrogen; and (2) subjecting the line to humid air in a variety of ways. The line was exposed to the humid air either by passing a continuous current of moist air over it or by placing it in a chamber containing air of a definite humidity. We may call the former the dynamical and the latter the statical method of exposure.

* Communicated by the Authors.

† "The Effect of Moist Air on the Resistance of Pencil Lines," by J. B. Seth, Chetan Anand, and Gian Chand. Proc. Phys. Soc. Lond. xli. pp. 29–35 (Dec. 15, 1928).

For the dynamical mode of the experiment a current of ordinary air from the room was, to begin with, dried by making it first pass through calcium-chloride tubes and then bubble through concentrated sulphuric acid. It then passed through a pair of wash-bottles containing a solution of sulphuric acid and water of suitable strength, where it took up the desired humidity. There were a number of such pairs of wash-bottles arranged in parallel, different pairs containing solutions of different strengths, so that the dry air could be made to pass through any one of these pairs by merely turning off and on suitable stopcocks. A current of air of the definite humidity so acquired was then passed over the pencil line, an aspirator being used to draw the air-current, and a couple of calcium-chloride tubes and a wash-bottle containing concentrated sulphuric acid having been placed between the aspirator and the glass tube containing the line. Or the air could be first stored in large bottles under pressure and then forced through the whole arrangement just described.

To obtain the static conditions the line was placed in a fairly large rectangular glass trough, which contained a dish in which sulphuric acid-water mixture of the required strength could be placed. The chamber also contained a tiny fan worked by a small motor to circulate air-currents throughout the chamber in order to make the humidity of the air inside the trough everywhere uniform. The chamber could be covered by a wooden lid, and the whole arrangement could be made air-tight by suitable means *.

The results of various experiments are given below —

1. A line drawn on ebonite was placed in a suitably wide glass tube connected on one side to an exhaust-pump and on the other to a closed-end mercury manometer. The electrical connexions with the ends of the line were made through side-tubes with platinum wires sealed in. The only sources of leak were thus a few necessary connecting glass stopcocks, and there was only a very small leak through these: but by occasional working of the pump the exhaustion was maintained for fairly long periods. The line was thus exposed to rarefied air at a pressure of a few

* For details of this method of getting the so-called static state, see Proc. Phys. Soc. xxxiv. "Discussion on Hygrometry," p. 11.

millimetres. The resistance was found at first to decrease when the tube was first exhausted; but afterwards a slow increase set in, the rate of increase being greater in the beginning. Thus it was 7 in 1000 during the first week and only 2 in 1000 during the third week.

2. Another line, also on ebonite, was kept in an atmosphere of nitrogen for a period of about four weeks. Here also there was an abrupt fall of resistance during the first 24 hours, after which there was a gradual increase, the rate of increase being much greater than in the previous case. It was of the order of 1 in 14 during the first 5 days and 1 in 24 during the last 5 days.

The nitrogen was prepared by gently heating a mixture of solutions of potassium dichromate, sodium nitrite, and ammonium chloride, and was purified by being passed through potash bulbs, wash-bottles containing strong sulphuric acid, and calcium-chloride tubes containing plugs of glass-wool. It was introduced into the chamber containing the line by alternate exhaustion and filling, the process being carried out several times.

In both these experiments, *i. e.* the pencil line in vacuum and in nitrogen, the resistance fell during the night and rose during the day. This is apparently a temperature effect.

3. A previously dried (by means of a current of dry air) pencil line, on ebonite as well as on waxed ground-glass, was subjected to a current of moist air of a definite known humidity and afterwards to a current of dry air. Values of the resistance were found every few minutes. In these as well as in the experiments described below the relative humidities of the moist air to which the lines were exposed were 10, 25, 35, 50, 65, 75, and 90 per cent. The curves between resistance and time for different humidities, plotted from these observations, were of the same type as those given in the previous paper. Generally the increase of resistance with time increased with the relative humidity. In the case of 90 per cent. humidity, however, the changes in resistance were rather erratic. Sometimes the final resistance, after passing 90 per cent. humid air for, say, 15 minutes, was greater than that for 75 per cent. humidity, and sometimes it was even less than that for still lower humidities. Also, in the case of 10 per cent. humidity,

the resistance did not increase uniformly with time. Quite often, on passing moist air of this humidity, there was a fall of resistance after an initial increase, and sometimes even this initial increase was absent. Now and again, however, it increased, slowly but uniformly, throughout the period that the air of this humidity was being passed over the line.

It must also be mentioned that the changes in resistance with any particular humidity were not always the same when the same line was subjected to this humidity again

Fig. 1.

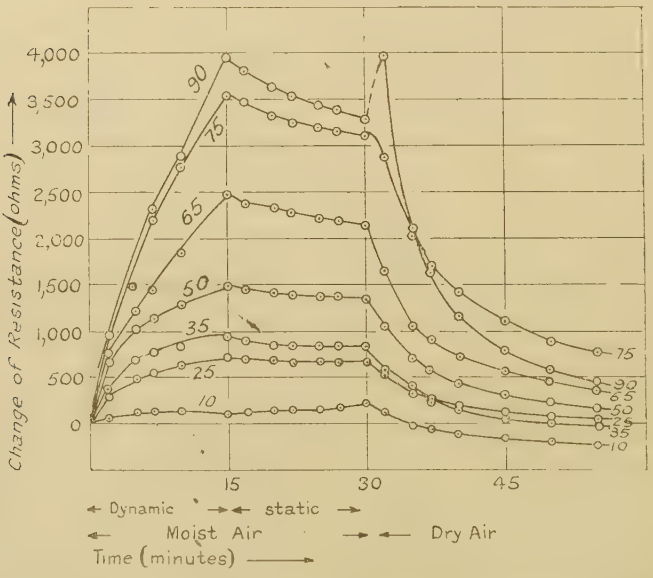

and again for the same length of time. This would seem to preclude the use of carbon lines for hygrometric purposes; but from later experiments it became evident that the changes depended not only on the relative humidity of the moist air, but also on the rate at which the current of the moist air passed over the line. More details about this matter are given later in section 7 below.

4. If, after subjecting a previously dried line to the current of moist air, say, for 15 minutes, and before passing the current of dry air over it, the moist air current is

stopped and the line allowed to remain in this humid atmosphere (giving a static state of affairs, as it were), the resistance does not remain quite steady, but changes slightly, generally increasing for lower humidities, but decreasing for the higher humidities, the decrease being more marked with increasing humidities. This is illustrated in fig. 1, where the numbers given against each curve represent the relative humidity of the moist air.

5. If a cycle of operations is performed on a previously dried line, that is to say, a current of air of 10 per cent. relative humidity passed over the line for, say, 20 minutes, then a current of higher humidity for the same length of time, and so on, till we get up to the 90 per cent. humidity, and after this air-currents of decreasing humidities are passed, coming back to the 10 per cent. humidity, then the resistance gradually increases (except that in the case of the 10 per cent. at the beginning of the cycle, there is first a slight fall of resistance), reaches a maximum, and then decreases, more or less following the cycle of humidities. In the case of the line on waxed ground glass the resistance, in our experiments, reached its maximum at the maximum humidity, but the final resistance after one complete cycle was considerably less than what it was at the beginning. For the line on ebonite the resistance attained its maximum value *after* the maximum humidity had been passed, namely at about 75 per cent. relative humidity on the descending half of the humidity cycle; but the final resistance after the complete cycle was nearly the same as, or only very slightly less than, that in the beginning.

In all cases mentioned in 3, 4, and 5 the changes are most marked in the first few minutes, the rate of change decreasing with time.

6. When experiments of the types 3, 4, and 5 are performed on lines with humidity conditions being static, the changes in resistance are not at all as regular as in the dynamic state. With the line on waxed ground-glass the changes in resistance were very erratic, and the various types of experiments were therefore confined to the line on ebonite. But here also the curves between resistance and time for different humidities were not at all regular and were more or less jumbled up.

7. If we study the drying part of the curves obtained in the dynamic experiments, some rather interesting conclusions follow. For this purpose we replot the drying parts of the curves for various humidities by shifting the initial resistance (namely the resistance which the line had when the current of dry air was commenced after the line had been exposed to the moist air) to the same origin. We now find in the first place that these curves vary in much more regular manner than the curves obtained for the condition when the moist air was being passed. The anomalous behaviour for 10 and 90 per cent. humidities, previously mentioned, disappears for these curves. Thus in fig. 1, although the curves for 75 and 90 per cent. cross each other and so do those for 25 and 35 per cent., when the drying parts are drawn by shifting the initial resistance to the same origin, the curves fall in a regular manner. Secondly, it appeared as though these drying curves were parabolic, the change in resistance after a certain time (and after the line had been previously subjected to the certain humidity) being proportional to the square root of the time.

It was while studying these curves that it appeared that their size depended upon the rate at which the dry air was being passed over the pencil line. Special experiments were therefore performed to find the change in resistance with time when a previously dried line, after being exposed to currents of air of different humidities, was subjected to a current of dry air, keeping the rate at which this current was passed fixed and determinable. The rate of passage of the air was measured in terms of the fall in the level of water in the aspirator in a given time, or by collecting the air forced over the resistance in a cylinder over water. From this study it was found (1) that for a fixed humidity, H, and a fixed rate of flow of the dry air, F, the curves between the change in resistance, R, and the square root of time, t, were straight lines passing through the origin; and (2) that for a fixed humidity and a constant time the curves between R and F were also straight lines passing through the origin. Thus $R^2 = kF^2t$, where k is a constant, would give the equations of the drying curves: that is to say, they are parabolic. The constant k depends on the relative humidity and seems to be rather a complicated function of H. The relation between R and H appears to be nearly but not quite an exponential one. Further

experiments are needed to determine the exact relationship between these two variables, *i. e.* to find the value of the constant k in terms of the relative humidity.

The values of this constant for 10, 50, and 75 per cent. humidities turned out to be $(5{\cdot}6)^2$, $(11{\cdot}0)^2$, and $(30{\cdot}8)^2$ respectively, as determined from the curves giving the results of the present experiments. In fig. 2 are given the drying curves, between change in resistance and time, for 10, 50, and 75 per cent. humidities, the rate of flow having been respectively 12·1, 11·2, and 12·5 cm. of fall of water

Fig. 2.

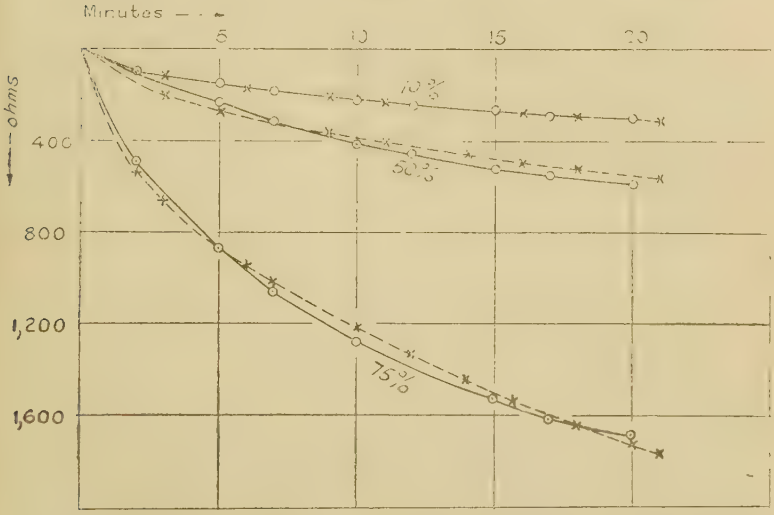

column in 20 minutes in the cylinder in which the issuing air was collected. The circles represent points experimentally determined, and the full lines the curves passing through these. The broken lines are parabolas with the values of parameters as given above, the crosses representing the points calculated for these parabolas. It will be seen that the fit between the experimental and calculated curves is so close for 10 per cent. humidity that the two are indistinguishable from each other on the scale of the figure. The fit for the 50 and 75 per cent. curves is not so good. But it is expected that this will become closer by improving the method of maintaining a constant rate of flow.

Presumably, the increase in the resistance when a dried line is exposed to a current of moist air would also depend on the rate at which the current of the moist air is passed over it. This would account for the behaviour of the lines remarked at the end of section 3. From the fact, however, that the drying curves are more regular and vary in a more uniform manner with the humidities to which the lines have been subjected previous to the drying process than the "wetting" curves, it would appear that if a pencil line is to be used for hygrometric purposes, it would be more profitable to study the drying curves for the line and utilize this for the purpose of measuring humidities. Moreover, from the nature of things, one may not always be able to regulate the rate of the "wetting" of a carbon line when exposed to an atmosphere of which the relative humidity is to be determined: but one can easily regulate the drying process, and from the fall of resistance during a certain time one may compute the required humidity.

XXXIX. *The Effect of a Permanent Electrical Dipole on the Internal Latent Heat of Vaporization of a Liquid.* *By* A. R. Martin, *Ph.D.**

IN the light of modern views of the electrical structure of matter the internal latent heat of vaporization of a liquid can be regarded as the work required to separate the molecules of the liquid to an infinite distance from each other against the attractive forces due to the electric field surrounding each molecule. The work of vaporizing a single molecule is, therefore, neglecting electrical saturation effects, the change in the energy in the medium resulting from the transfer of the molecule to a vacuum from a medium of dielectric constant equal to that of the liquid. In so far as the molecule may be regarded entirely as a permanent electrical dipole, this energy change is given by the expression deduced previously †,

$$\frac{\mu^2}{3a^3}\left(1-\frac{1}{D}\right),$$

* Communicated by Prof. J. C. Philip, F.R.S.

† Martin, Phil. Mag. viii. p. 547 (1929).

where μ = the moment of the dipole,
a = the radius of the molecule,
D = the dielectric constant of the liquid.

This expression should therefore give the effect of a permanent electrical dipole on the internal latent heat of vaporization of a liquid. It can be expected to yield good results only when the molecule can with a fair degree of truth be treated as a single permanent dipole at the centre of a sphere.

In applying this idea, that part of the latent heat which is not due to the dipole (but which nevertheless is probably of electrical origin) has been allowed for in organic compounds by subtracting from the total latent heat values for the alkyl and phenyl groups derived from the latent heats of the parent hydrocarbons. Thus the value of the methyl group has been taken as one-half that of ethane, of the ethyl group five-sixths that of ethane, of the propyl group seven-eighths that of propane, of the butyl group nine-tenths that of butane, of the iso-amyl group eleven-twelfths that of iso-pentane, and of the phenyl group five-sixths that of benzene. This treatment is only approximate, especially as the data for the hydrocarbons are usually not for the same temperature as those for their derivatives. And further, it may not be justifiable to treat the external field of a weakly dipolar bond as entirely due to the dipole.

The values of a required to give the observed effect of a dipole on the internal latent heats of vaporization of twenty-one liquids are tabulated below. The latent heats have been taken from 'International Critical Tables,' vol. v., the dielectric constants at the boiling points from Grimm and Patrick *, and at other temperatures from Landolt-Börnstein's 'Tabellen,' and the dipole moments from the table given by Hφjendahl †, with the exception of the dipole moment of acetonitrile, which was taken from Werner ‡. The internal latent heats are given in joules per mole and are denoted by λ_i, and that portion of them due to the dipole by $\Delta\lambda_i$.

The values of the molecular radii are of the correct order of magnitude. They are smaller than those calculated from gaseous viscosities, the values obtained by this method for water, sulphur dioxide, and ammonia being respectively

* Grimm and Patrick, J. Amer. Chem. Soc. xlv. p. 2794 (1923).
† Højendahl, 'Thesis,' Copenhagen (1928).
‡ Werner (O.), *Z. physikal. Chem.* iv. p. 382 (1929).

1·25 *, 1·73 †, and 1·43 ‡ Å.U. The radius of gyration of the ammonia molecule found by Robertson and Fox § from its infra-red absorption spectrum is 0·82 Å.U.

Liquid.	Temp. °C.	D.	$\mu \times 10^{18}$.	λ_∞.	$\Delta\lambda_\infty$.	a, Å.U.
Water	25	78	1·8	41330	—	1·16
Sulphur dioxide	20	14	1·75	20090	—	1·42
Ammonia	−33	22	1·49	21290	—	1·26
Ethane	0	—	—	7150	—	—
Methyl iodide	42	6·48	1·66	24690	21115	1·30
Methyl alcohol	20	31·2	1·64	35020	31445	1·19
Acetaldehyde	21	14·8	2·72	22660	19085	1·94
Acetone	56	17·68	2·76	27470	20320	1·93
Acetonitrile	80	26·2	3·11	26870	23295	2·00
Nitromethane	100	27·75	3·42	31380	27805	2·01
Ethyl bromide	38	8·81	1·97	24775	18815	1·55
Ethyl alcohol	78	17·30	1·33	36440	30480	1·22
Ethyl ether	35	4·11	1·22	23420	11500	1·26
Ethylamine	15	6·2	1·33	25110	19150	1·16
n-Propane	20	—	—	12920	—	—
n-Propyl alcohol	97	11·83	1·65	38210	26910	1·23
n-Butane	20	—	—	18795	—	—
n-Butyl alcohol	117	8·19	1·65	40510	23600	1·27
Iso-pentane	13	—	—	24332	—	—
Iso-amyl alcohol	130	5·82	1·80	40750	18450	1·43
Benzene	80	—	—	27880	—	—
Chlorbenzene	131	4·20	1·59	33230	10030	1·57
Nitrobenzene	210	15·61	3·85	36740	13540	2·75
Aniline	183	4·54	1·51	36560	13360	1·39
Toluene	110	2·17	0·44	30120	3345	0·86
Pyridine	114	9·38	2·11	32250	9050	2·07

For substances in which the dipole is at one end of a large molecule the values of a are too small. The reason is that in such cases the medium approaches closely to one of the poles,

* Smith, Proc. Roy. Soc. A, cvi. p. 83 (1924).
† Smith, Phil. Mag. xliv. p. 508 (1922).
‡ Rankine and Smith, Phil. Mag. xlii. p. 601 (1921).
§ Robertson and Fox, Proc. Roy. Soc. A, cxx. p. 206 (1928).

where the field is strong, and hence the filling of space at a fairly great distance from the other pole, where the field is much weaker, has comparatively little effect. Thus in the homologous series of alcohols a does not increase as rapidly as might be expected. However, the increment is larger than usual in passing from *n*-butyl to iso-amyl alcohol, where the paraffin chain is branched and the molecule less unsymmetrical about the dipole than it would be in *n*-amyl alcohol. For benzene derivatives a probably corresponds rather to the volume of the substituent than to that of the whole molecule, and might therefore be a measure of the steric hindrance effects exerted by the substituent. The order $NO_2 > Cl > CH_3$ is the same as that given by the work of Victor Meyer and his followers* on steric hindrance effects in the catalytic esterification of carboxylic acids.

Since the expression

$$\frac{\mu^2}{3a^3}\left(\frac{1}{D_1}-\frac{1}{D_2}\right)$$

does not consider the thermal energy and is for a hypothetical absolute zero, it gives the change in both free energy and the heat content in transferring the dipole from a medium of dielectric constant D_1 to one of dielectric constant D_2. It might therefore be possible to calculate partition coefficients in the same way in which Bjerrum and Larsson † used Born's expression,

$$\frac{z^2e^2}{2r}\left(\frac{1}{D_1}-\frac{1}{D_2}\right),$$

to calculate ionic partition coefficients. However, the calculation leads in many cases to absurd results, and even to negative radii. The disturbing factor is probably dipole association. Dipole association, which is a form of electrical saturation, does not affect the calculation of the latent heat of vaporization, because a dipole which is about to be vaporized is already a simple molecule, and in its interaction with the rest of the liquid the polarization is at least approximately proportional to the field-strength.

34 Sandy Lane,
Teddington, Middlesex.
9th November, 1929.

* Werner (A.), 'Lehrbuch d. Stereochemie,' p. 385 *et seq.* (1904).
† Bjerrum and Larsson, *Z. physikal. Chem.* cxxvii. p. 358 (1927).

XL. *Problems of determining Initial and Maximum Stresses in Ties and Struts under Elastic or Rigid End Constraints.*—Part II. *By* W. H. Brooks, *B.Sc., Ph.D.(Eng.)Lond.**

IN the foregoing cases † the results are largely dependent upon the degrees of flexing constraints imposed by the terminal conditions. Equations obtained by the following methods will be seen to be less dependent upon terminal conditions, and practically independent of them when nL > about 3.

Method 2 A :—

In this method, instead of applying a central load W independently, a flexing bridge EFD is applied centrally to the pin-jointed tie, as shown in fig. 8, by means of which

Fig. 8.

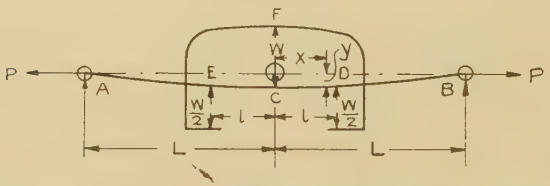

W is applied at C by hydraulic or mechanical means, and the resulting change in total deflexion at C *or*, alternatively, the slope at D is measured.

Taking an origin as shown, and remembering that y is of negative sign, in accordance with the mathematical convention of signs adopted, and that M_x is discontinuous at D, equations for the deflexion δ at C and the slope θ at D are established thus :—

Between C and D.

$$M_x = W(l-x)/2 + P.y = EId^2y/dx^2. \quad . \quad . \quad (20)$$

$$\therefore \quad d^2y/dx^2 - n^2y = Wl/2EI - Wx/2EI \quad . \quad . \quad (21)$$

where $n^2 = P/EI$.

The general solution to equation (21) is

$$y = A\cosh nx + B\sinh nx + Wx/2P - Wl/2P, \quad (22)$$

where A and B are constants.

* Communicated by the Author.

† See Part I., Phil. Mag. (7) viii. p. 943 (1929).

Between D and B.

$$M_x = P \cdot y - EI d^2y/dx^2 ; \quad . \quad . \quad . \quad . \quad (23)$$

$$\therefore \quad d^2y/dx^2 - n^2y = 0. \quad . \quad . \quad . \quad . \quad . \quad (24)$$

The general solution to equation (24) is

$$y = C \cosh nx + D \sinh nx, \quad . \quad . \quad . \quad (25)$$

where C and D are other constants to be found.

Now it follows from equations (22) and (25) that

$$y = Wx/2P - WL/2P + (W/2Pn) \cdot \cosh nx \cdot K - (W/2Pn) \cdot \sinh nx, \quad (26)$$

where $K = \sinh nl - \cosh nl \cdot \tanh nL + \tanh nL$.

Equation (26) gives the deflexion from the axis of P at all points between C and D. When $x = 0$, *i. e.*, at C,

$$y_0 = -Wl/2P + (W/2Pn) \cdot K. \quad . \quad . \quad . \quad (27)$$

i. e.,

$$\delta \text{ or } -y_0 = Wl/2P - W. K/2Pn = W(l - K/n)/2P. \quad (28)$$

Thus

$$\delta/W = [l - \{\sinh nl - \tanh nL(\cosh nl - 1\}]/2n^2EI, \quad (29)$$
$$= (\textit{Tie equation } G_\theta)$$

When $nL >$ about 3,

$$\delta/W \doteqdot \{l - (\sinh nl - \cosh nl + 1)/n\}/2n^2EI, \quad . \quad (30)$$

i. e.,

$$2n^2EIa \doteqdot \{l - \frac{1}{n_a}(\sinh n_a l - \cosh n_a l + 1)\}, \quad . \quad (31)$$

where "a" = the initial value of $\delta/W = 0/0$, as described in the General Procedure.

Graphical solutions to equation (29) are given by typical "G" curves in Chart III. for an instrument constant $l = 10$ units. For values of $L > 20$ units the dotted curve plotted from equation (31) obtains. To use this Chart, the curves plotted from generating equation G (equation (29)) are used. Having first determined the initial W. δ derivative $= a$, the value of EI . a is next located up the ordinate along which polar values of EI . a are plotted, and a polar ray drawn to the origin. The intersection of this ray with the appropriate "G" curve of L (L is the half-length of the pin-jointed tie) locates a point vertically above the solution to n^2 on the abscissa.

Thus P sought $= n^2EI$.

Method 2 A. *Alternatively* :—

It follows from the foregoing equations that the slope θ at D

$$= W(\cosh nl - 1)(\cosh nl - \sinh nl \,.\, \tanh nL)/2P, \qquad (32)$$

and $= (1 - \operatorname{sech} nL)/2P$ when $l = L$, as in Method 1. Initially, therefore, this Method gives

$$\text{“}a\text{”} = (\cosh n_a l - 1)(\cosh n_a l - \sinh n_a l \,.\, \tanh n_a L_a)/2n_a^2 EI. \qquad (33)$$

$$= (\textit{Tie equation } G_\theta)$$

CHART III.

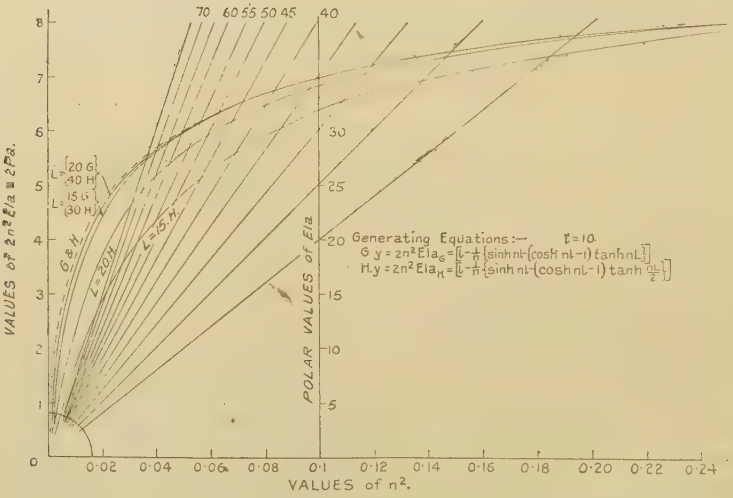

Stress Chart for Ties G and H by deflexion.

Here “a” = the W.θ derivative, and when $n_a L_a >$ about 4,

$$\text{“}a\text{”} = (\cosh n_a l - 1)(\cosh n_a l - \sinh n_a l)/2n_a^2 EI, \qquad (34)$$

which may be used as a first approximation in the absence of a Stress Chart.

Graphical solutions to equation (33) may be obtained from the typical “G” curves for low values of L and instrument constant = 10 units on Chart IV. For values of L > about 25 units the dotted curve obtains, and yields solutions to equation (34).

To obtain a solution from Chart IV., the polar value of $10EIa$ is first interpolated up the ordinate lined in where

$100n^2 = 10$, or interpolated up an intermediate ordinate for values of $10EIa > 25$ and a polar ray drawn. The vertical projection of the point of intersection of this ray with the correct "L" curve yields solutions to $100n^2$, and hence to the value of $P = n^2EI$.

CHART IV.

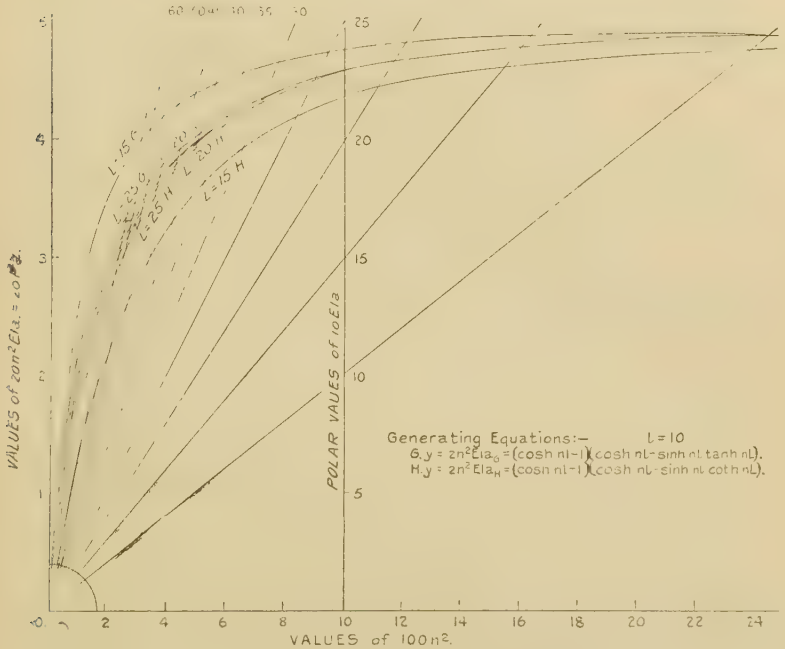

Stress Chart for Ties G and H by slope.

Fig. 9.

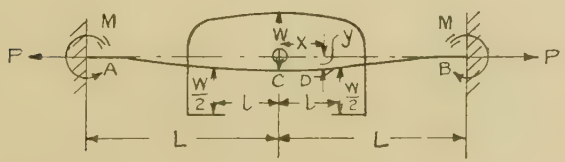

Method 2 B :—

This method is similar to Method 2 A, but is applicable to a tie having fixed ends, *i.e.*, the conditions are as in Method 2 A, but the ends of the tie are constrained in the line of action of P by reaction couples M at A and B, as shown in fig. 9.

Between C and D.

$$M_x = W(l-x)/2 + P \,.\, y - M = EId^2y/dx^2, \quad . \quad (35)$$

or $$d^2y/dx^2 - n^2y = Wl/2EI - Wx/2EI - M/EI. \quad . \quad (36)$$

The general solution to equation (36), giving the deflexion at all points between C and D, is

$$y = A \cosh nx + B \sinh nx + Wx/2P - Wl/2P + M/P. \quad (37)$$

Between D and B.

$$M_x = P \,.\, y - M = EId^2y/dx^2, \quad . \quad . \quad . \quad (38)$$

i. e., $$d^2y/dx^2 - n^2y = -M/EI, \quad . \quad . \quad . \quad (39)$$

of which the general solution, giving the deflexion at all points between D and B, is

$$y = C \cosh nx + D \sinh nx + M/P. \quad . \quad (40)$$

From the foregoing equations it follows that the conditions are satisfied when

$$M = W(\cosh nl - 1)/2n \,.\, \sinh nL.$$

Also when $x = 0$ at C, the deflexion numerically $= \delta$, say

$$= W[l - \{\sinh nl - \tanh nL/2 \,.\, (\cosh nl - 1)\}/n]/2P. \quad (41)$$

$$= (\textit{Tie equation } H_\delta)$$

In this case

$$\delta/W = \text{“}a\text{”} \quad \text{when} \quad n = n_a.$$

The result given in equation (41) may be checked by making the substitution $l = L$ of Method 1 B. Thus, making this substitution, and simplifying,

$$\delta W = (L - 2/n \,.\, \tanh nL/2)/2P, \text{ as in Method 1 B.}$$

Comparing equation (41) with the corresponding equation (29) of Method 2 A, it is seen that the only difference lies in the occurrence of $\tanh nL/2$ in the former in place of $\tanh nL$ in the latter, so that when $nL/2 >$ about 4—a quite probable value for a long slight tie under a moderate stress—the equations become practically identical and initially equal to equation (31) given in Method 2 A. This is clearly shown in Chart III., in which the typical H curves plotted yield solutions to equation (41) for an instrument span = 20 units.

The procedure to be followed in using Chart III. here is similar to that described under Method 2 A, but using curves such as those marked H instead of using curves marked G.

The merging of the G and H curves on Chart III. into the one common dotted curve plotted from equation (31), which is independent of L, the half-length of the tie, clearly shows the negligible effect of the end constraints on the value of "a," except for low values of nL. This being so, the further deduction follows, and is fully analytically investigated in the complete Thesis, that for the higher values of nL which usually obtain in practice, it is immaterial whether the flexing bridge used in testing is applied centrally or non-centrally to the tie, or whether the tie be jointed or unjointed at any point of its length.

Method 2 B. *Alternatively by measurement of the slope* θ *at* D :—

From the foregoing equations it follows that

$$\theta = W(\cosh nl - 1)(\cosh nl - \sinh nl \,.\, \coth nL)/2P. \quad (42)$$

Typical graphical solutions to this equation are given by the H curves of Chart IV., the use of which is described under Method 2 A. Alternatively.

Fig. 10.

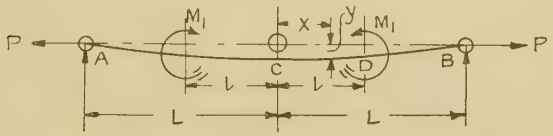

Comparing equations (42) and (32), it is seen that they will become identical when $\coth nL = \tanh nL$, and this is practically so when $nL >$ about 3. An inspection of Chart IV. also clearly shows that for $l = 10$ units, coincidence practically obtains when $L > 25$ units. Thus variations in end conditions or in the length of a member above a minimum length of about 25 units do not greatly affect the difference of deflexion at C or of the slope at D, as given by the use of a flexing bridge, the slope being the least affected in all cases, but practically unaffected by terminal conditions when

$$L(P/EI)^{\frac{1}{2}} > 4, \quad i.e., \text{ when } L/K \,.\, (f_d/E)^{\frac{1}{2}} > 4.$$

Tie. Method 3 A :—

In this method a tie AB of length 2L, having assumed frictionless pin-joints at A and B, is flexed by the application of equal and opposite couples M_1 and M_1, applied by mechanical or hydraulic means, with axis distance $= 2l$ apart, as shown in fig. 10.

Between C and D.

$$M_x = M_1 + P.y = EI \cdot d^2y/dx^2 ;$$

$$\therefore \quad d^2y/dx^2 - n^2y = M_1/EI. \quad . \quad . \quad . \quad . \quad (43)$$

The general solution to equation (43) is

$$y = A\cosh nx + B\sinh nx - M_1/P, \quad . \quad . \quad (44)$$

where A and B are constants to be found, and giving the deflexion at all points between C and D.

Between D and B.

$$M_x = P \cdot y = EId^2y/dx^2 ;$$

$$\therefore \quad d^2y/dx^2 - n^2y = 0,$$

and $$y = C\cosh nx + D\sinh nx,$$

where C and D are other constants to be determined.

Now it follows from the above equations that the constant A in equation (44) $= M_1(\cosh nl - \sinh nl \tanh nL)/P$ and the constant $B = 0$, in conformity with terminal conditions. Substituting these constant values in equation (44) yields, when $x = 0$,

$$y_0 = M_1(\cosh nl - \sinh nl \tanh nL - 1)/P, \quad . \quad . \quad (46)$$

i. e., the numerical value of the deflexion at C

$$= \delta, \quad \text{say} \quad = -y_0 = M_1(1 - \cosh nl + \sinh nl \tanh nL)/P,$$

$$. \quad . \quad . \quad (47)$$

$$\text{or} \quad \delta/M_1 = (1 - \cosh nl + \sinh nl \tanh nL)/P, \quad . \quad (48)$$

and $$\doteqdot (1 - \cosh nl + \sinh nl)/P,$$

for values of $nL >$ about 4.

When $l = L$,

$$\delta/M_1 = (1 - \operatorname{sech} nL)/P. \quad . \quad . \quad . \quad . \quad (49)$$

Initially, when both δ and $M_1 = 0$, equation (48) becomes

$$n_a^2 EIa = 1 - \cosh n_a l + \sinh n_a l \tanh n_a L_a, \quad . \quad (50)$$

(*Tie equation* Iδ)

which $$\doteqdot 1 - \cosh n_a l + \sinh n_a l, \quad . \quad . \quad . \quad . \quad (51)$$

and equation (49) becomes

$$n_a^2 EIa = 1 - \operatorname{sech} n_a L_a, \quad . \quad . \quad . \quad . \quad (52)$$

where "a" here = the $M_1\delta$ derivative, and is determined as described in the General Procedure, substituting δ for Y and M_1 for X.

When nL > about 6, equation (49) becomes

$$"a" \doteq 1/P_a, \quad . \quad . \quad . \quad . \quad . \quad . \quad (53)$$

since sech nL then becomes a very small fraction,

i. e., $P_a = 1/a$ = reciprocal of initial $d\delta/dM_1$.

Chart V.

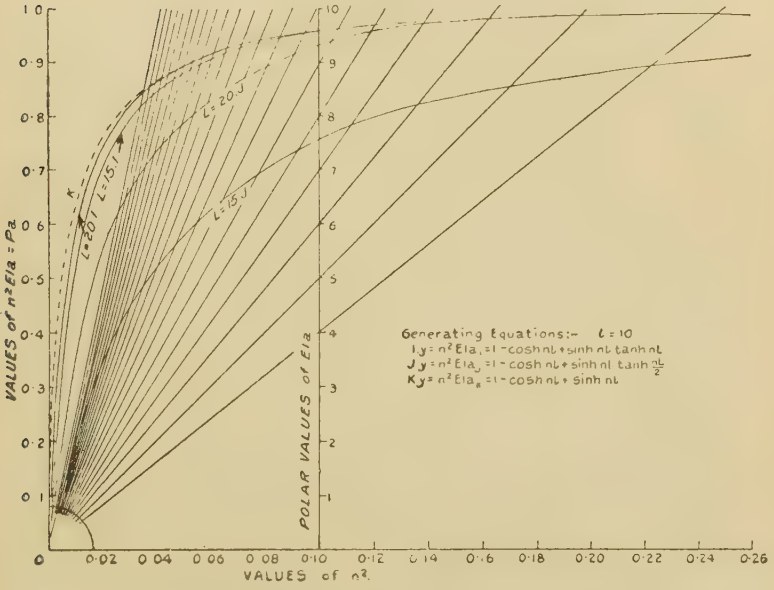

Stress Chart for Ties I, J, and K by deflexion.

In the general case of l < L, equation (51) could be used as a first approximation in solving for n_a, and equation (50) applied when $n_a L_a$ is found to be < about 4.

The right-hand sides of the expressions (50) and (51) are the generating equations used in plotting the full-line curves I and the dotted curve K respectively, of Chart V. (*q.v.*), from which n_a^2 may be found by interpolation for an instrument constant l = 10 units. This Chart also clearly shows the degree of approximation introduced by using equation (51) instead of equation (50).

To obtain a solution from this Chart, the product EIa is first determined, and the corresponding polar ray drawn (by the aid of the scale and rays shown) through the origin. The intersection of this ray with the appropriate I or K curve is then interpolated and projected on to the abscissa which gives the value of n_a^2, and hence the solution to $P_a = n_a^2 EI$ sought. (Herein the suffix "a" is suppressed for simplicity.)

Tie. Method 3 A. *Alternatively by measurement of the slope* θ *at* D:—

From the foregoing equations it follows that

$$\theta/M_1 = n \sinh nl(\cosh nl - \sinh nl . \tanh nL)/P, \quad (54)$$

(*Tie equation* I_θ)

and for values of $nL >$ about 4 may be written

$$\theta/M_1 = n \sinh nl\,(\cosh nl - \sinh nl)/P\,;$$

i. e., $$\theta/M_1 = \sinh nl\,(\cosh nl - \sinh nl)/n . EI, \quad . \quad (55)$$

which, in the absence of a Stress Chart, may be used for a first approximation to indicate the probable value of n and hence of nL. If nL is seen to be > about 4, no further approximation will be necessary, since $\tanh nL$ is then very nearly equal to unity and equation (55) practically = equation (54). When $nL <$ about 4, the exact expression (54) should be used.

In any case, the initial value of "a," which is here the $M_1\theta$ derivative, may be found by substituting M_1 for X and θ for Y, as shown in the General Procedure.

When "a" is known, equation (54) may be written

$$an_a . EI = \sinh n_a l\,(\cosh n_a l - \sinh n_a l \tanh n_a L_a), \quad (56)$$

and equation (55) may be written

$$an_a . EI = \sinh n_a l(\cosh n_a l - \sinh n_a l). \quad . \quad . \quad (57)$$

The right-hand side of expression (56) is the expression used in plotting the I curves of Chart VI., in which also the dotted curve K is obtained by plotting the right-hand side of expression (57). This Chart shows clearly how the former expression approximates to the latter as L increases.

Having measured "a" by the above method, and computed the value of $a . EI$, a solution to P_a is obtained from Chart VI., by locating the point of intersection of the corresponding polar ray with the appropriate I or K curve. Projecting

from the point so found on to the abscissa determines n_a, and hence $P_a = n_a^2 . EI$.

CHART VI.

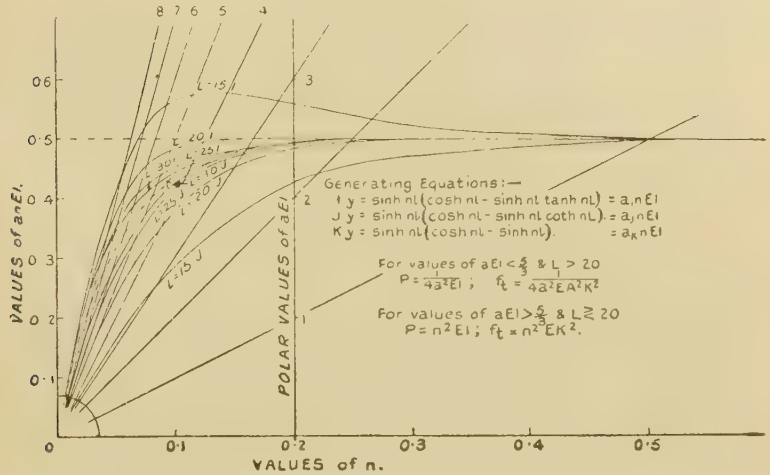

Stress Chart for Ties I, J, and K by slope.
$l = 10$ units.
Distance between couples = 20 units.

Tie. Method 3 B :—

Here a tie AB of length 2L, having its ends constrained in the direction of AB by fixing couples M and M, as shown in fig. 11, is flexed as in Method 3 A.

Fig. 11.

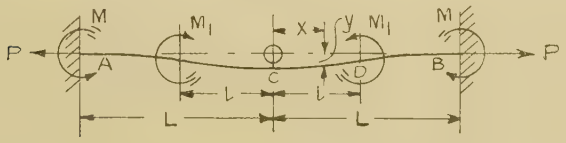

Between C and D.

$$M_x = M_1 + P.y - M = EI.d^2y/dx^2;$$

$$\therefore \quad d^2y/dx^2 - P.y/EI = (M_1 - M)/EI = d^2y/dx^2 - n^2y. \quad (58)$$

The general solution to equation (58) is

$$y = A \cosh nx + B \sinh nx - (M_1 - M)/P, \quad . \quad (59)$$

where A and B are constants to be determined.

Between D and B.

$$M_x = P.y - M = EI.d^2y/dx^2;$$

$$\therefore \quad d^2y/dx^2 - n^2y = -M/EI. \quad . \quad . \quad . \quad . \quad (60)$$

The solution to equation (60) is

$$y = C\cosh nx + D\sinh nx + M/P, \quad . \quad . \quad (61)$$

where C and D are constants to be determined.

On evaluating the constants in the above equations, substituting and reducing, it is seen that

$$M = M_1 \sinh nl/\sinh nL.$$

It also follows that

$$y = M_1 \sinh nl\,(\sinh nL\coth nl - \cosh nL)\cosh nx/P\sinh nL - M_1(1-\sinh nl/\sinh nL)/P,$$

and when $x = 0$, the numerical value of the deflexion y_0 at C

$$= \delta, \text{ say } = M_1(1-\cosh nl + \sinh nl\tanh(nL/2))/P, \quad (62)$$

or the deflexion per unit couple

$$= \delta/M_1 = \left(1-\cosh nl + \sinh nl.\tanh\frac{nL}{2}\right)\Big/P \quad (63)$$

(*Tie equation* J_δ)

= the $M_1\delta$ derivative when $P = P_a$. (See General Procedure.)

When $nL >$ about 8, equation (63) becomes

$$\text{“}a\text{”} = (1-\cosh n_a l + \sinh n_a l)/n_a{}^2EI, \quad . \quad . \quad (64)$$

which is the same as equation (51) in Method 3 A.

Graphical solutions to equation (63) may be rapidly obtained by interpolation from curves such as those lettered J in Chart V., which curves approximate to the dotted curve K for higher values of L, as was also seen in Method 3 A.

Tie. Method 3 B. *Alternatively by measurement of the slope* θ *at* D :—

It follows from the foregoing equations that

$$\theta/M_1 = \sinh nl(\cosh nl - \sinh nl.\coth nL)/n.EI, \quad (65)$$

or initially, when $P = P_a$,

$$\text{“}a\text{”} = \sinh n_a l\,(\cosh n_a l - \sinh n_a l.\coth n_a L_a)/n_a.EI, \quad (66)$$

(*Tie equation* J_θ)

and when $n_a L_a$ > about 4, coth $n_a L_a$ practically = unity, and equation (66) may then be written

$$a \cdot n_a \cdot EI = \sinh n_a l \,(\cosh n_a l - \sinh n_a l), \quad . \quad (67)$$

which is the same expression as obtains for the same tie with assumed frictionless hinges, as may be seen by comparing this equation with equation (57) of Method 3 A.

Graphical solutions to equations (66) and (67) may be readily obtained by the aid of Chart VI., which also clearly indicates the approximation of the former expression to the latter expression as L_a or $n_a L_a$ increases.

While it is experimentally possible in practice to secure the frictionless hinged results (see paragraph under Method 1 A), it is very improbable that constraints, however rigid they may appear, will provide the exact conditions assumed in the foregoing case, and, in general, it should be assumed that the actual cases arising in practice will fall somewhere between these two ideal conditions. In other words, when a tie is pin-jointed at the ends through elastic constraints, friction couples will be set up at the ends directly flexing is attempted, of the same order as but smaller in magnitude than those set up by yielding clamps which allow the extremities of the tie to take up a slight unknown slope. This combination of conditions is discussed fully in the Thesis under "Case K," in which unknown couples, M and M, are assumed to constrain the ends of the tie at an unknown slope varying with M.

In the Thesis it is theoretically established that under these latter conditions the equation which obtains is

$$\theta/M_1 = \frac{n}{P} \cdot \sinh nl\{(\cosh nl - \sinh nl \cdot \tanh nL) - M \cdot \operatorname{sech} nL/M_1\}, \quad . \quad . \quad . \quad (68)$$

which agrees with equation (54) when M = 0.

Now when nL in equation (68) > about 4, which would generally be the case for a tie of fair length under a moderate stress, tanh nL and coth nL approach very nearly to unity. For example, in a tie rod 1 in. diameter and 20 feet long under an initial axial stress (f_t) of only 5000 lb. per square inch, and $E = 30 \times 10^6$ lb. per in.^{2} nL, *i.e.*, $\frac{L}{K} \cdot \sqrt{f_t/E}$ (where K is the radius of gyration of the cross-section about a diameter at right angles to the plane of bending $= d/4$), $= 120/\frac{1}{4} \cdot (5000/30 \times 10^6)^{\frac{1}{2}} = 6{\cdot}2$, and tanh nL = coth nL = 1.

(Here and in the following, the suffix "a" is suppressed for clarity.) For a tie of the same dimensions as the above, under half the above stress,

$$nL = 480/100 . (2{\cdot}5/3)^{\frac{1}{2}} = 4{\cdot}380,$$

$$\tanh nL = 0{\cdot}99969, \quad \text{and} \quad \coth nL = 1{\cdot}0003.$$

Hence, in expression (68), $\tanh nL$ may be taken $= 1$.

Again, for the 1-in. diameter tie-rod taken above, when $f_t = 5000$ lb. per sq. in., $\operatorname{sech} nL = 1/201{\cdot}7156$, and when $f_t = 2500$ lb. per sq. in., $\operatorname{sech} nL = 1/39{\cdot}9253$. Consider, therefore, the term $M . \operatorname{sech} nL/M_1$ in equation (68). M will have its greatest value when the ends of the tie are rigidly clamped, and then $= M_1 . \sinh nl/\sinh nL$, which, substituted in the term under consideration, reduces it to $\sinh nl . \operatorname{sech} nL/\sinh nL$, which when $f_t = 5000$ lb. per sq. in. $= \sinh nl/201{\cdot}7156 \times 201{\cdot}713$, a negligible fraction of $\sinh nl$.

When $f_t = 2500$ lb. per sq. in. only, the term reduces to $\sinh nl/39{\cdot}9253 \times 39{\cdot}9128$, again a negligible fraction of $\sinh nl$.

Hence a very near approximation to equation (68) is

$$\theta/M_1 = n \sinh nl(\cosh nl - \sinh nl)/P,$$

or initially, when $P = P_a$, for $\theta = 0$ and $M_1 = 0$,

$$"a" = \sinh nl(\cosh nl - \sinh nl)/n . EI, \quad . \quad . \quad (69)$$

where "a" is the $M_1\theta$ derivative. (See General Procedure.)

Graphical solutions to this general expression may be quickly obtained by using the dotted curve K in Chart VI.

It therefore appears that the slope of the tie at the axis of the couple M_1 applied at D is practically independent of the manner in which the tie has its ends constrained, and the expression (69) is general for values of nL greater than about 4. Experimental verification of this deduction is given fully in the Thesis.

When $nL <$ about 4, it is instructive to investigate what percentage error will be introduced by using the approximate expression (69) instead of the exact expression (68), or by using the equivalent expression (66), to which expression (68) reduces when the greatest value of $M = M_1 . \sinh nl/\sinh nL$ is substituted therein. Taking this latter approximation, the difference consists in using $(\cosh nl - \sinh nl)$ instead of the exact quantity

$$(\cosh nl - \sinh nl . \coth nL).$$

Considering again, therefore, the tie-rod in which L = 120 in., l = 20 in., diameter = 1 in., E = 30×10^6 lb. per sq. inch, and assuming that the direct tensile stress has been lowered to only 500 lb. per sq. inch from various causes unforeseen when designing the member,

$$nL = L/K \cdot (f/E)^{\frac{1}{2}} = 120/\tfrac{1}{4} \cdot (500/30 \times 10^6)^{\frac{1}{2}} = 1{\cdot}96,$$

$$nl = l/K \cdot (f/E)^{\frac{1}{2}} = 0{\cdot}3264,$$

$\sinh nl = 0{\cdot}33181$: $\cosh nl = 1{\cdot}05361$; and $\coth nL = 1{\cdot}04050$

$$\therefore \quad \cosh nl - \sinh nl = 0{\cdot}72180,$$

and

$$\cosh nl - \sinh nl \cdot \coth nL = 1{\cdot}05361 - 0{\cdot}34500 = 0{\cdot}70861.$$

The error, therefore, is 0·01319 in 0·70861, or only 1·862 per cent. for this very low stress, and will clearly become less as $\coth nL$ approaches unity with increase of stress in the same member.

Hence the expression

$$\text{“}a\text{”} = \sinh nl \cdot (\cosh nl - \sinh nl)/n \cdot EI$$

may be applied to all but perhaps very short and stout tie-rods flexed as discussed in Methods 3 A and 3 B, when the ends are constrained in any manner and the length is unknown. Thus, having found “a” experimentally, the above equation may be solved for n by the aid of Chart VI. Then initially, P (really P_a) = $n^2 \cdot EI$, and the direct stress in the tie when the readings were taken to determine “a”

$$= f_a = n^2 E K^2,$$

where K is the radius of gyration of the uniform cross-section of the tie about an axis at right angles to the plane of flexing.

When discussing Methods 2 A and 2 B applicable to ties, further theoretical investigations were made in the Thesis to ascertain whether the equations which were obtained in the centrally loaded cases held for non-central loading also. The conclusions were there found to be affirmative. Similar further investigations into Methods 3 A and 3 B were also made, and the conclusions obtained were likewise found to be affirmative, and were experimentally verified.

(To be continued.)

XLI. *Thermionic Emission and Electrical Conductivity of Oxide Cathodes.* *By* A. L. Reimann *and* R. Murgoci *. (Communication from the Staff of the Research Laboratories of the General Electric Co., Ltd., Wembley.)

Abstract.

The following observations were made :—

(1) The electrical conductivity, c, of a "formed" alkaline earth oxide varies with the temperature, T, according to a law of the form

$$c = \alpha\epsilon^{-\frac{\beta}{T}},$$

where α and β are constants.

(2) During the process of forming, both the thermionic emission and the conductivity grow similarly, and after its completion both are "poisoned" similarly by exposure of the oxide to

(*a*) oxygen,
(*b*) a discharge in carbon monoxide, and
(*c*) a discharge in hydrogen.

Complete recovery of the formed condition by re-forming is possible only a few times in succession after poisonings by (*a*) and (*b*), but any number of times after poisoning by (*c*).

(3) At current densities comparable with those in the coatings of oxide cathodes from which saturated thermionic space current is being taken, the current conducted through an oxide powder between two electrodes, embedded therein, also saturates.

On the basis of these observations, together with the results of related work by other investigators, we have formulated the following theory of the action of oxide cathodes :—

(1) The coating conducts the space current, which, of necessity, passes through it, electrolytically. Practically only the metallic ions are mobile, the oxygen ions playing no active part in the electrolysis.

Communicated by C. C. Paterson, Director.

(2) The whole surface of each crystal of oxide of a formed cathode is covered with a mobile monatomic layer of alkaline earth metal. The passage of space current is accompanied by a continual circulation of this metal, which diffuses outward along the surfaces of the crystals and inward through the crystals in the form of electrolytic ions.

(3) At the usual operating temperatures of oxide cathodes the average life of alkaline earth metal particles on the emitting surface is of the order of 10^{-3} second, and the rate of flow of this metal over the surface of an idealized independent unit of barium circulation in the form of a cube of side l would be of the order of $300\,l$ per second.

(4) The coating is probably in very imperfect contact with the core metal, so that the space current passes from core metal to coating mainly in the form of thermionically emitted electrons. Sufficiently copious electron emission of the core metal at the low temperatures of operation of these cathodes would be made possible by a contamination of its surface with adsorbed barium or with barium and oxygen.

Explanations are suggested for

(1) the eventual "life-failure" of oxide cathodes,

(2) the observed phenomena relating to poisoning,

(3) the considerable variation in the published values of the thermionic constants of oxide cathodes.

Introduction.

IT is well known that before an alkaline earth oxide cathode will give its characteristically high thermionic emission it has to be "activated" or "formed." The forming process may consist in merely heating the cathode to bright redness in a good vacuum [1, 2] but activation is much more rapid and a higher final emission is generally obtained if, whilst the cathode is being heated, electrons are drawn from it [3, 4]. In the latter case, the growth of emission is accompanied by a considerable evolution of gas [3, 4], which has been shown to be oxygen [5]. The electron emission is increased some thousandfold by the forming operation, but it is at once destroyed, or "poisoned," if the cathode is exposed to certain electro-

negative gases, such as oxygen [1, 3, 4, 6]. Considerable de-activation also results from prolonged heating of the cathode at a high temperature, which is, however, insufficient to bring about appreciable loss of coating by evaporation [1, 2, 3, 4].

The study of these phenomena has led to the formulation of the theory that the high electron emissivity of a formed cathode is due to the presence of free alkaline earth metal at the emitting surface. If the cathode is activated by the first method the free metal is supposed to be formed from the oxide by thermal dissociation, if by the second mainly by the electrolytic action of the space current on the oxide through which it passes [1, 2, 3, 4]. To overcome the difficulty arising from the fact that at the usual operating temperatures of these cathodes ($\sim$1000° K.) the vapour pressures of the alkaline earth metals are of the order of some centimetres of mercury, Schottky and Rothe [7] have suggested that the metal forms an adsorbed film at the surface of the oxide only a single atom in thickness, and so has a vapour pressure of a much lower order than that characteristic of the metal in bulk, as in the case of an adsorbed monatomic film of thorium [8] or of cæsium [9, 10, 11, 12] on tungsten.

Now the theory that the passage of the space current through the coating electrolyses it, although apparently demanded by the experimental facts [3, 4, 5], involves certain difficulties. It may readily be calculated what quantity of electricity, passing electrolytically through a coating of known weight, will completely break it up into its chemical constituents. On the assumption that the products of electrolysis escape from the cathode as they are liberated from the coating, we may thus determine for how long any given space current may be passed before all the coating will have disappeared. It is found, however, that normally the "life" of an oxide cathode, *i. e.*, the time during which it retains its high electron emissivity, is of the order of 10^5 or 10^6 times as long as it could possibly be if the above assumptions (electrolytic conduction, escape without recombination of electrolysed material) were correct, and that at the end of life there is no important diminution in the quantity of coating present. Also it is not clear why, if the evolution of gas which accompanies forming is due to electrolysis, it does not continue to be evolved after activation is complete.

In the hope of finding a solution of these difficulties we have carried out an investigation of the electrical conductivity of the coatings of oxide cathodes. There have been two previous investigations of the conductivity of alkaline earth oxides, by Horton [13] and by Spanner [14], both of whom found that the conductivity, c, varies with temperature according to an exponential law of the form

$$c = \alpha\epsilon^{-\frac{\beta}{T}} \quad . \quad . \quad . \quad . \quad . \quad . \quad . \quad . \quad . \quad (1)$$

Their measurements were not, however, made under electron-emitting conditions, but with the oxides exposed to air. They could not therefore hope to discover any changes in conductivity accompanying thermionic activation, the observation of which might throw some light on the cessation of the evolution of gas upon the completion of activation and on the problem of the long life of oxide cathodes.

Experimental Arrangements.

All our measurements were made with diode valves, whose cathodes consisted of two filaments, each of length 1·5 cm. and diameter 0·04 mm., which, after having been provided with a coating of oxide, made adherent by sintering at a red heat, had 0·5 cm. of their central portions twisted together. Another coating of oxide was then applied to the twisted portion of the cathode, in order to provide a substantial bridge of oxide between the wires. Finally the free ends were de-coated by being immersed in weak nitric acid. With this arrangement it was found that when the cathode was heated in vacuo by passing a current through the wires, the central coated portion had a very uniform temperature distribution.

The coating consisted of equal proportions by weight of barium and strontium oxides. The core-wires were usually of nickel, but in some cases they were of Pt-10 per cent. Rh alloy. The central, twisted portion of the cathode formed the axis of a cylindrical anode of nickel, of length 0·3 cm. and diameter 1·0 cm. One or more small "getter" disks of previously out-gassed nickel, carrying small pieces of magnesium, were also provided. The whole was mounted on a pinch and sealed into a small glass bulb provided with a length of glass tubing for attachment to the pump.

For heating the cathode and measuring the current conducted between the two filaments through the oxide a specially designed motor-driven commutator was utilized, capable of being run at either 50 or 100 revolutions per second. Connexion to the cathode-heating and conductivity-measuring circuits could be made in such a way that when the commutator was run these circuits were completed during alternate equal periods of time, separated from one another by short intervals to provide against accidental overlapping. The contacts, which were of tungsten, were of the "make and break" type, each controlled by an adjustable spring, and actuated by an eccentric cam (stroke 1/50 in.) and lever. During the cathode-heating phase the heating current was passed through the two filaments in series. This current was measured by a milliammeter, the conduction current by a microammeter with universal shunt, and the potential across the coating by a voltmeter. In calculating the conductivity from the readings of the two last-named instruments, the resistance of the microammeter and shunt was allowed for. The factor by which the readings of the instruments had to be multiplied to give the true intermittent values of the quantities they were designed to measure was readily calculated from the "make and break factor" of the commutator. It was found that when the cathode had the dimensions given the resistance of the hot nickel filament-wires involved in the conductivity-measuring circuit was negligible in comparison with that of the oxide.

The procedure up to the point of sealing off a valve from the pump was as follows :—

After having baked the valve on the pump at 400° C., the cathode was heated to bright redness and the anode raised to a red heat by high-frequency induction. Finally, magnesium getter was dispersed from one of the disks, also by induction heating, whereupon the valve was sealed off.

Experimental Results.

1. *Forming.*

During the process of thermionic forming the conductivity of the oxide increases about a thousandfold. The conductivity may also be made to grow to its maximum

value by passing a current through the oxide between the two filaments instead of between both filaments together and the anode. It is then necessary, in order for complete "conductivity forming" to take place, that about the same quantity of electricity should be passed through the oxide, and this at about the same temperature as in the case of thermionic forming. "Conductivity forming" is accompanied by thermionic activation in the same way as thermionic forming is accompanied by growth in conductivity. This is, perhaps, not surprising, for so far as the oxide itself is concerned the only thing that physically differentiates the two kinds of forming from one another is the path taken by the forming current. The maximum values attained by the emission and the conductivity sometimes, however, differ slightly according to the direction in which the forming current is passed. The value of either quantity is then up to 20 per cent. greater when this direction is that in which the current passes in the measurement of the quantity in question than when it is not. Also, if one quantity has been formed to its maximum value by passing the current in the more favourable direction, its value may be decreased by anything up to about 20 per cent. upon thereafter passing the current in the less favourable direction. In these cases the formed condition is thus slightly directional.

2. *Poisoning.*

Not only are conductivity and thermionic emission formed together, they are also poisoned together.

Our first experiments on poisoning were made with oxygen, obtained by heating a small grain of potassium permanganate contained in a glass tube attached to the valve. After the coating of the cathode had been formed a little oxygen was introduced into the valve, which was thereupon immediately re-gettered from another disk in order to make sure of the removal of any trace of oxygen not absorbed by the first deposit of getter. The short exposure of the cold cathode to oxygen was found to poison completely both the emission and the conductivity. A certain degree of recovery of both occurs on re-forming, *i. e.*, heating the cathode to a suitable temperature whilst a current is passed through the oxide. This recovery is, however, not often complete, and invariably takes place

very slowly. The extent to which recovery is possible becomes progressively less after successive oxygen poisonings.

Oxide cathodes may also be poisoned by exposure to an electric discharge in carbon monoxide. A bulb containing a nickel spiral was attached to the valve. The nickel spiral, when heated by a current, gave off a mixture of carbon monoxide and hydrogen. The hydrogen could readily be diffused out through an attached palladium tube heated in the extreme oxidizing tip of a blowpipe-flame. By this means the whole system, consisting of valve, bulb containing nickel spiral, palladium tube, and Pirani gauge, could be filled several successive times with CO to a pressure of the order of 1/100 mm.

When a discharge is passed between cathode and anode the carbon monoxide is cleaned up on to the getter. In the course of this clean-up both the emission and the conductivity of the oxide become partially poisoned, being reduced to about one-tenth and one-quarter respectively of their initial values. Re-forming at first completely restores the initial values, but after CO has been cleaned up a few times in succession recovery by re-forming is no longer possible or occurs only to a very slight extent.

In other experiments hydrogen was admitted through a palladium tube and cleaned up on to the magnesium getter by passing a discharge. Poisoning was observed qualitatively similar to that brought about by a discharge in CO, but quantitatively it was much less, and after each poisoning it was found possible to recover completely by re-forming both the emission and the conductivity.

3. *Temperature-Dependence of Conductivity.*

No means were provided in the construction of these valves for accurate temperature measurement. Nevertheless from the known law of variation of thermionic emission with temperature, and the measured relationship between conductivity and thermionic emission at different (unknown but reproducible) temperatures, we have been able to confirm the result of Horton [13] and Spanner [14] that the conductivity varies with temperature according to an exponential law of the form

$$\sigma = \alpha \epsilon^{-\frac{\beta}{T}} \quad . \quad . \quad . \quad . \quad . \quad . \quad . \quad . \quad . \quad (1)$$

Although, strictly speaking, the law of variation of emission with temperature is of the form

$$i = aT^2\epsilon^{-\frac{b}{T}}, \quad . \quad . \quad . \quad . \quad . \quad . \quad . \quad (2)$$

over a restricted range of temperatures a practically equally good empirical formula is

$$i = A\epsilon^{-\frac{B}{T}}, \quad . \quad . \quad . \quad . \quad . \quad . \quad . \quad (3)$$

in which

$$A = aT_m^2, \quad B = b + 2T_m\text{*}. \quad . \quad . \quad . \quad (4)$$

where T_m represents the mean temperature of the range in question. The test for the validity of formula (3) is the rectilinearity of the curve connecting $\log i$ with $\frac{1}{T}$.

In order for the departure from strict rectilinearity of this curve to be detected when the temperatures at which readings are taken extend over a range of only a few hundreds of degrees, it would be necessary for temperatures in the region in question (here of the order of 1000° K.) to be measurable with a possible error not exceeding a small fraction of a degree. For all practical purposes, then, we may take formula (3) as representing sufficiently accurately the dependence of emission on temperature.

Eliminating T between formulæ (1) and (3), we have

$$B(\log c - \log \alpha) = \beta(\log i - \log A). \quad . \quad . \quad . \quad (5)$$

Therefore, by plotting $\log c$ against $\log i$ we should, if formula (1) is a true representation of the temperature dependence of conductivity, obtain a straight line, whose slope is β/B. From fig. 1, in which a few typical plots of $\log c$ against $\log i$ are shown, it is seen that the relationship between the two quantities is indeed linear. We may therefore conclude that formula (1) represents the law of temperature dependence of conductivity to the same order of accuracy as formula (3) represents that of emission.

In the case of a few valves the rate of increase of conductivity with temperature was apparently abnormally low at relatively low temperatures (shown dotted in two

* The relationships between the constants in (2) and (3) are best obtained by equating the expressions for $\log i$ in the two formulæ and differentiating with respect to T.

of the curves of fig. 1). We cannot suggest any plausible explanation for this.

The slopes of the straight lines connecting $\log c$ with $\log i$ vary about a mean value of approximately 45°. The mean of sixteen measurements of β/B is 0·99, and the

Fig. 1.

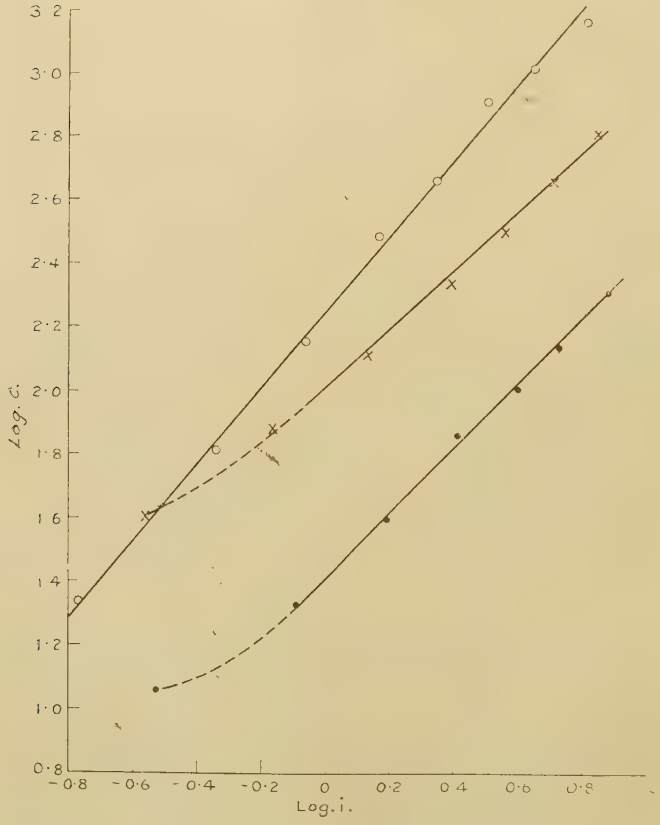

Relationship between $\log c$ and $\log i$.

spread is from 0·83 to 1·20. The variations are too great to be due to experimental error and must be attributed to real differences in the condition of the oxides. No special theoretical significance is therefore to be attached to the fact that the mean of several determinations happens to come out to almost exactly 1.

It is interesting to compare these results with those obtained by Horton [13] and Spanner [14] in the case of single oxides under conditions different from those obtaining in our experiments. The value of β obtained from Horton's measurements on CaO is $2{\cdot}16\times10^4$ deg. The value of B for CaO, according to the recent very careful measurements of Espe [4], is $2{\cdot}3\times10^4$ deg. From these two determinations we obtain for β/B the value 0·94. From Spanner's measurements the following values are obtained :—

	β.	B.	β/B.
CaO	$1{\cdot}68\times10^4$	$2{\cdot}85\times10^4$	0·59
SrO	$1{\cdot}53\times10^4$	$2{\cdot}55\times10^4$	0·60
BaO	$1{\cdot}29\times10^4$	$2{\cdot}20\times10^4$	0·59

In view of our observations on the effects of oxygen poisoning, it may seem surprising that the values of β obtained from the measurements of Horton and Spanner, whose specimens of oxide were exposed to air, are of the same order as those obtained by us when the conductivity was measured in a good vacuum. It must be remembered, however, that we have not made any measurements of the *temperature dependence* of the conductivity of a poisoned oxide coating, and therefore know nothing of the effects of poisoning on β.

4. *Saturation of Conduction Current.*

In the foregoing the conductivity was measured by the slope of the straight line which connects the conduction current with the voltage between the two wires when both of these quantities are small. At current densities comparable with those existing when saturated thermionic space current is being taken the current-voltage relationship ceases to be linear, showing incipient current-saturation. Examples of such curves, two of which have been taken far enough to show the effect, are given in fig. 2.

5. *Polarization.*

The conduction current-voltage curves to which we have just referred generally, but not always, pass through the origin. In those cases where they do not, the intercept on the voltage axis may be taken to be a measure of the back E.M.F. due to polarization.

Another method by which we attempted to measure polarization was, by means of a change-over switch, suddenly to substitute a galvanometer or a microammeter for the conductivity-measuring circuit in the non-heating phase of the commutator. A deflexion was then observed on the instrument which corresponded in sign with the

Fig. 2.

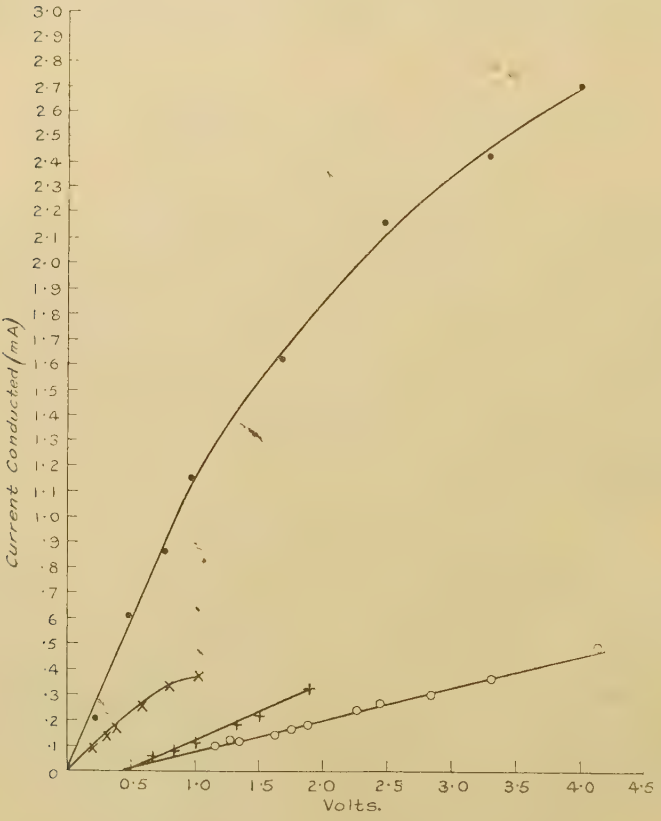

Relationship between Conduction Current and Voltage.

intercept of the current-voltage curve on the voltage axis. From the magnitude of this deflexion and the known resistance of the coating and galvanometer the polarization E.M.F. could then be calculated.

The results given by the two methods agree in order of magnitude, but that is all that can be said. Relatively

few valves showed polarization at all. When a back E.M.F. was observed it was usually of the order of $\frac{1}{2}$ volt. Two valves, with which polarization was at first observed, failed to show any polarization later. They had in the meantime been used for other experiments.

We have not been able to discover any general law which determines under what conditions polarization is to be observed. We were prevented from pursuing our work on polarization by the fact that the time which one of us (R. M.) was able to devote to the investigation was limited. Further work is now in progress in these Laboratories.

Discussion.

1. *Preliminary Remarks.*

The similarity of the phenomena exhibited by the conduction current and the thermionic current as regards forming, poisoning, and saturation is very striking, and might lead one to suspect that what has been measured as conductivity is, perhaps, merely some manifestation of the thermionic properties of the oxide, bearing little or no relationship to the true electrical conductivity of the oxide crystals.

The following considerations, however, make this view untenable. Conductivities were always measured by the slopes of the rectilinear lower portions of the conduction current-voltage curves. Now, if these were essentially thermionic space-current curves, and the fall of potential in the oxide powder were located mainly in the spaces separating adjacent crystals from one another, the lower infra-saturation parts of the current-voltage curves would be the same, or almost the same, at all temperatures. As we have seen, however, the rate of change of current with voltage in this region increases with temperature according to the exponential law (1). The falls of potential across the spaces between the crystals must therefore, in this infra-saturation region, be small in comparison with those across the crystals themselves. The slopes of the lower portions of the current-voltage curves are therefore a measure of the true conductivity of the crystals. On the other hand, the saturation of the conduction current at high current densities is probably a thermionic phenomenon. We shall discuss this in Section 6.

2. *Nature of the Conductivity.*

The fact that the oxides are dielectrics and that the law connecting conductivity with temperature is of the form (1) is, as we shall see, strong evidence pointing to the conclusion that the oxides conduct electrolytically, and not, as Horton [13] and Spanner [14] supposed, electronically.

The only cases of which we are aware in which electronic conduction in dielectric crystals has been observed are those in which an enhanced conductivity has been induced by photoelectric means. Such photoelectrically induced conductivity has been studied by Röntgen, Joffé [15, 16], and others, and Lukirsky [17] has been able to show conclusively that the carriers of the enhanced current are electrons. Where, as in the case of rock-salt, observations have been made of the temperature coefficient of this electronic conductivity, it has been found to be negligibly small [18].

On the other hand, Tubandt and Lorenz [19], Lukirsky, Shukareff, and Trapesnikoff [20], and Joffé [21], in investigations of the normal (*i. e.*, not photoelectrically induced) conductivity of a large number of transparent dielectric crystals, have shown that, without exception, the conductivity is electrolytic, accurately obeying Faraday's law. Joffé and Kirpitchewa [22] and others have furthermore found that the conductivity of such crystals increases with temperature according to an exponential law of precisely the form (1) which Horton [13], Spanner [14], and we have found to apply in the case of alkaline earth oxides.

The behaviour of oxide cathodes during the early stages of "forming" also favours the view that their coatings conduct electrolytically, at least initially. Horton [13] has actually found that the rate of evolution of gas in the initial stages of forming is within 8 per cent. of that required by Faraday's law. The fact that gas is no longer evolved by a completely formed cathode means either:

(1) that some new material has appeared in the coating through which the current is now conducted electronically instead of through the electrolytically conducting oxide; or

(2) that the change which accompanies forming is of such a nature as thereafter to prevent the escape of the products of electrolysis, and to make possible their recombination.

The objection to the former of these alternatives is that the temperature dependence of the conductivity of formed

coatings is that characteristic of electrolytes. The latter alternative requires that either one or both of the products of electrolysis shall be capable of diffusing through the coating in the direction opposite to that in which the corresponding ions move in electrolysis, and that this diffusion shall not be accompanied by any appreciable evaporation. Espe[4] has already suggested that the barium* liberated electrolytically at the boundary between coating and core-metal diffuses outward to the emitting surface.

3. *Barium Circulation.*

Now it has been shown by Tubandt and Lorenz ([19]) and by Lukirsky, Shukareff, and Trapesnikoff ([20]) that generally, in the electrolysis of solid dielectrics, practically only one kind of ion (usually the positive one) is mobile. Let us suppose that the alkaline earth oxides are no exception to this general rule, and that the Ba^{++} ions are mobile, the O^{--} practically immobile. In the coating of an oxide cathode, then, a given atom of barium must be capable of functioning as an ion in electrolysis at least 10^5-10^6 times. In the steady state there can be no progressive change in the number of ions inside a crystal. Therefore, corresponding to every ion arriving and being neutralized at the electrolytic cathode, there must on the average be one ion separated from a surface layer at the electrolytic anode. We thus see that the electrolytic theory of the conductivity of oxide coatings, together with the assumption that, as in most solid dielectrics, practically only the positive ion is mobile, leads necessarily to the conclusion that there must be uncombined barium at the thermionically emitting anode side of the coating. This conclusion is in striking agreement with the "free barium" theory of the thermionic emission of oxide cathodes [1, 2, 3, 4]. The question as to the precise condition of this surface barium may be left open for the present.

The diffusion of barium in a direction opposite to that of the drift of the electrolytic ions may take place in either of two ways—through the bodies of the crystals or along their surfaces. In either case, of course, the mechanism of the diffusion is one of thermal agitation, and the rate of transport of barium by it must equal that associated

* We shall, for the sake of brevity, write barium where we mean barium and/or strontium and/or calcium.

with the ionic drift taking place under the directional action of the field. The mobility (using the word now in its wider meaning) of atoms inside the crystals must be considerably less than that of the ions, on account of the greater size of the former, and in the case of a " volume " diffusion the relative sluggishness of their motion could only be compensated for if their concentration greatly exceeded that of the ions. On the basis of this picture it is difficult to imagine why mere exposure of the cold formed oxide to oxygen, affecting as it does only the surfaces of the crystals, should so completely poison the conductivity. If, on the other hand, it is supposed that the barium diffuses along the surfaces of the crystals, such poisoning becomes quite understandable, for the surface barium, being oxidized, is no longer available for the formation of fresh barium ions to take the place of those being removed by electrolysis. Such surface diffusion would be analogous to the case of thoriated tungsten, in which, as Clausing [23] has conclusively shown, the thorium diffuses to the surface of the cathode during the process of thermionic activation along the tungsten grain boundaries, and not through the actual crystals. Thus we may conclude that the diffusing barium almost certainly constitutes a mobile adsorbed layer of atomic thickness, or a quasi-two-dimensional gas, on the surfaces of the crystals.

It is interesting to consider some of the quantitative requirements of the theory of barium circulation. The emission obtainable from a well-formed oxide cathode at its normal operating temperature is usually of the order of $\frac{1}{3}$ ampere per cm.^{2}, or 2×10^{18} electrons per cm.^{2} per sec. Assuming that the electrolytic ions are doubly charged, we see that 10^{18} ions will be formed from surface barium per second from each square centimetre of emitting crystal surface. In a closely packed barium layer there will be roughly 10^{15} atoms per square centimetre. Therefore the average life of an adsorbed particle (atom, or ion associated with two electrons) of barium on the emitting surface must be of the order of 10^{-3} second. This result is in excellent agreement with the value (also 10^{-3} second) calculated by Schottky [24] from Johnson's [25] measurements of the " flicker " effect of oxide cathodes. Incidentally it is plain that Schottky's result, when considered in conjunction with the great length of life of oxide cathodes, constitutes independent evidence in support of an

essential part of our theory, viz., the repeated appearance of the same particles of barium at the emitting crystal surfaces.

The rate at which barium must diffuse along the surface of the oxide in an independent unit of barium circulation in order to maintain the supply of electrolytic ions at its anode depends, of course, both upon the size of the unit and upon the current passing through it. Let us imagine an idealized independent unit of barium circulation in the form of a cube of side l. If the temperature is such that the emission density has the above value of $\frac{1}{3}$ ampere per cm.^{2}, then, roughly, each thousandth of a second it is necessary for the barium particles on the emitting face to be replaced by fresh ones diffusing over the four adjacent faces. The average distance over which the latter will have to move in order to take the place of those which have disappeared from the emitting face is roughly $0{\cdot}3\ l$. The rate of flow of the two-dimensional barium gas will therefore be of the order of $300\ l$ per second. The approximately independent units of barium circulation will not have linear dimensions of a greater order than the thickness of the coating, but, as we shall see later, they may be much less. Thus, in the case of a coating of thickness 1/100 mm., the rate of barium diffusion during the passage of saturated space current would certainly not have to be greater than about 3 mm. per second.

4. *Thermionic Emission from Adsorbed Barium.*

The two-dimensional gas adsorbed on the surfaces of the crystals is the source from which are drawn not only the electrolytic Ba^{++} ions, but also the thermionically emitted electrons. Now, if the surface layer consisted of ordinary barium atoms the work-function of an oxide cathode, as measured by the temperature-dependence of the emission, would be of the same order of magnitude as the second ionization potential of the metallic constituent of its coating, for each atom would have to part with both its valence electrons in becoming converted into an electrolytic ion. These second ionization potentials are 9·95, 11·0, and 11·8 volts respectively for Ba, Sr, and Ca. However, the thermionic work-functions of the corresponding oxides, according to the more recent published data, range only from about 1 to about 2 volts. It follows therefore that in the two-dimensional gas the barium

must be at least very nearly in the ionized condition, owing, no doubt, to the electrical forces exerted on it by the underlying oxide. We have thus to regard the surface layer as consisting of a mixture of Ba^{++} ions and electrons in some kind of loose association with one another, and together forming an electrically neutral system—a partial two-dimensional analogue of an ordinary three-dimensional mass of metal containing its "free" electrons *.

It should be pointed out here that the thermionic emission from such a two-dimensional gas adsorbed on the surface of an insulator differs in several important respects from that of a metal whose surface is covered by a monatomic layer of foreign atoms or ions, such as thoriated or cæsiated tungsten. In the latter case the emitted electrons originate from underneath the electrical double layer due to the adsorbed film, and must pass through it on their way out. It has been shown that if the effects of the forces exerted laterally on one another by the adsorbed particles (atoms or ions) on the double layer may be neglected the work-function varies linearly with the concentration of the adsorbed particles [8, 26]. In the case we are considering, however, the electrons do not pass through the double layer, but originate from its outer portion. There does not therefore appear to be any reason why the work-function should vary linearly with the concentration of the two-dimensional gas.

In the case of metallic cathodes an appreciable fraction of the work function is due to the forces of attraction exerted on the escaping electrons by their electrical images in the conductor [27, 28]. In the case of oxide cathodes, however, the image force contribution to the work-function must be considerably smaller, owing to the fact that the electrons are ejected from the surface of a dielectric instead of from that of a metal.

Finally, whereas in the case of metallic cathodes with adsorbed films, the latter are not affected in any way by the electrons which pass through them, the taking of space current from an oxide cathode involves a continuous removal of the constituents of the adsorbed film, one barium ion passing into an oxide crystal for every two electrons escaping. The concentration of the film

* We are indebted to Mr. R. H. Fowler for this picture of the surface layer.

is therefore determined, in any given case, by the requirement of statistical equilibrium between the rate of removal of the two-dimensional gas from the emitting surface (determined by the magnitude of the space current) and the rate of its replenishment by diffusion.

5. *Forming and Poisoning.*

On the basis of the theory of barium circulation it is easy to explain the forming and poisoning of the conductivity under conditions in which the thermionic emission is also formed or poisoned, as the case may be. If barium has not yet appeared at the anode surfaces of the units of barium circulation, or if it has been removed or combined with, fresh barium ions are not available to take the place of those being removed by electrolysis, the concentration of the barium ions inside the crystals falls below its surface barium conditioned value, *i. e.*, below that of the immobile oxygen ions, and the conductivity, which at a given temperature is proportional to the concentration of the mobile ions, also falls. Conductivity and emission are formed and poisoned together, simply because they both depend on the same thing, viz., the presence of uncombined barium at the surfaces of the crystals.

In the process of forming or recovery from poisoning (which is essentially the same thing) the movement under the action of the field of the barium ions which are constantly being formed by temperature dissociation, and their recapture by immobile oxygen ions at positions in the crystal lattices nearer the cathode than the points of their birth by dissociation, results in the gradual appearance of oxygen at the electrolytic anode, whence it evaporates. This oxygen is then removed, either by the pump or by the getter. After a time the barium in the system is in excess of the oxygen by a sufficient amount to cover the surface of each crystal of oxide with a monatomic layer. Evolution of oxygen then ceases, and the forming is complete.

6. *Condition of the Surface of the Core-Metal and of the Coating. Effects of Ageing and Poisoning.*

The appearance of saturation of the conduction current at about the same current density as corresponds to the

passage of saturated thermionic space current suggests that there is some thermionic limitation to the conduction current. Such limitation may occur either at the boundary between core-metal and coating or within the coating itself. Wherever the limitation exists there must be imperfection of contacts, so that the current passes from core-metal to coating, or from one crystal of oxide to the next, as the case may be, mainly in the form of electrons, emitted by the one and collected by the other. On the whole, perhaps, such imperfection of contacts may be expected to occur rather at the boundary between the dissimilar core-metal and coating than between the crystals of the oxide. It is, of course, possible that the contacts are imperfect in both cases. Whatever may be the condition of the coating, however, it is probable that the electrons pass from the core-metal to the coating thermionically. It is obviously impossible that they should do this if the surface of the core-metal remained clean. It is, however, not to be expected that the core-metal should remain uncontaminated during the process of forming. We have already supposed that in this process the crystals of oxide become covered with a mobile monatomic layer of barium. Extending slightly the theory of activation already developed, we may suppose that the barium covering the crystals of oxide adjacent to the core-metal is able to flow across such contacts as exist between oxide crystals and metal, and to spread over the surface of the latter. Oxygen may also reach the core-metal during the forming process, when, as we have seen, it is evolved from the oxide. Now it has been observed that if oxygen and barium are supplied to hot tungsten two monatomic layers are, in general, formed on its surface, the inner one being of oxygen and the outer one of barium. This will be so, irrespectively of the order in which the oxygen and barium are supplied to the hot tungsten, since barium on oxygen on tungsten is more stable than oxygen on barium on tungsten. There is evidence that the same thing is true when other metals take the place of tungsten. Now the thermionic properties of monatomic layers of barium on tungsten and of barium and oxygen on tungsten have been very exhaustively studied by Ryde and Harris * in these Laboratories, who have found that

* A series of papers on this work is in course of preparation.

the emission obtainable from them is of the same order as that given by ordinary oxide-coated cathodes at the same temperature. Thus it appears entirely plausible that the thermionic activation of oxide cathodes is accompanied by the contamination of the surface of the core-metal by a monatomic layer of barium or by a double atomic layer of barium and oxygen, and that, in either case, the core-metal thereby acquires an extraordinarily high electron emissivity. If, as we have supposed, the core-metal and coating are only imperfectly in contact with one another, these electrons must be collected by the coating and re-emitted from its outer surface. If, in addition, the crystals of coating are in poor contact with one another, each crystal must be supposed to collect electrons on its inner surface and re-emit them from its outer. If this is the case, the linear dimensions of the independent units of barium circulation may be of a much lower order than the thickness of the coating.

Assuming that, as we have supposed, electrons pass from the core-metal to the coating mainly thermionically, it is seen that it is *à priori* by no means certain whether the Richardson straight line represents the thermionic properties of the contaminated core-metal or those of the coating. Either the core-metal emits electrons at a greater rate than the coating can re-emit them, in which case a fraction of the electrons emitted by the core-metal returns to it, or else the coating emits more electrons than it receives from the core-metal, so that it re-absorbs a fraction of them. In other words, the thermionic emission of the cathode as a whole is limited either by the coating or by the core-metal, whichever of the two systems in series has the lesser thermionic emissivity.

It appears that, at least in certain cases, it is the contaminated core-metal, and not the coating, by which the emission is limited. Since, according to our assumption, the coating receives as many electrons from the space that separates it from the core-metal as it permanently loses, by re-emission, from its outer surface, there can be no net heat loss from the coating, and the only cooling that the cathode will suffer by its electron emission will be that due to the evaporation of electrons from the contaminated core-metal. The work-function of the cathode, calculated from the latent heat of evaporation of electrons, will therefore in any case be that of the contaminated core-metal.

Occasional comparisons have been made, *e.g.*, by Davisson and Germer[29], between the work-function measured in this way and that determined from the slope of the Richardson straight line, and the two determinations have been found to be in good agreement. But we have already seen that the slope of the Richardson straight line corresponds to the work-function of whichever of the two systems (core-metal or coating) has the lesser emissivity. Thus in those cases where there is agreement between the work-functions determined by the two methods we may conclude that, if the coating is indeed in poor contact with the core-metal, it is the core-metal which limits the emission. This conclusion accords well with the fact of experience that the nature of the core-metal has a considerable influence on the thermionic properties of coated cathodes.

On the other hand, however, it would appear that if only the units of barium circulation in the coating could be made large enough, the emission of the cathode should no longer be limited by the core-metal, but by the coating. The rate of disappearance of barium from the thermionically emitting surface of such a unit is proportional to the space current, and in the steady state the rate of replenishment by surface diffusion must be equal to the rate of disappearance. The rate of flow of the two-dimensional barium gas must be proportional to the surface concentration gradient. There is an upper limit to the concentration of the monatomic layer of barium (which concentration will be greatest at the cathode end of the unit), determined by the underlying oxide crystal lattice. Thus it is seen that, with a given space current, the greater the linear dimensions of the units of barium circulation, the less will be the concentration of barium at their thermionically emitting anode surfaces. Now the electron emissivity of the oxide must certainly diminish with decreasing concentration of the barium adsorbed on its surface, so that we may say that the larger the units of barium circulation the smaller will be the electron emissivity of the oxide.

The gradual formation of large units in which barium has to circulate, *e.g.*, by crystal growth, may possibly be responsible for the deterioration in the emissive properties of coated cathodes that occurs in life. The initial emission of a cathode that has deteriorated in this way cannot be restored by any thermal or electrical treatment (such as

re-forming) or by any improvement in the vacuum. It would appear, then, that the loss in thermionic activity is due to some change in the coating. It is difficult to imagine any such change other than one of size or mutual relationship of the crystals.

The permanence of the poisoned condition of a filament which has been exposed, when formed, to oxygen, may perhaps be explained in a similar manner. An unformed cathode suffers no harm when it is exposed, cold, to oxygen. The only thing that differentiates a formed from an unformed crystal is the presence on the surface of the former of a monatomic layer of adsorbed barium. On exposure of such a formed crystal to oxygen the adsorbed barium will be oxidized and the crystal will increase in size by one layer of oxide molecules. Whatever may be the condition of the coating, such a growth of its component crystals will tend to increase the size of the barium circulation units. If, as a result of re-crystallization having occurred when the cathode was first heated, the coating is in the form of a compact mass, with crystals in good contact with each other, the barium must be supposed to diffuse to the outer surface of the coating along the grain boundaries. These, however, would in time be filled up by the oxidation of their contained barium. On the other hand, if the crystals are originally in poor contact with one another, each must be regarded as an almost independent barium circulation unit. The crystals will, however, not be entirely independent units, for there must be some contacts between adjacent crystals. It is quite conceivable that the growth of each crystal by a molecular thickness will increase the areas of contact many times, and thus, by reducing the degree of independence of the separate crystals, increase the effective sizes of the units of barium circulation.

Exposure of a formed oxide cathode to a discharge in CO also results in progressive poisoning, which presently becomes permanent. It has been shown by Hogness and Harkness[30] that oxygen is one of the products of the disintegration of CO molecules by an electric discharge. The effect of exposing an oxide cathode to such a discharge is therefore probably the same as that of exposure to oxygen.

If a formed oxide is made the cathode of a discharge in hydrogen presumably the only possible effect of the

discharge on the coating is the removal of the adsorbed barium. There is then nothing to prevent the adsorbed layers from being re-formed on the crystals in the same manner as they were formed originally. Mere removal of barium cannot increase the areas of contact between the crystals. Hydrogen poisoning is therefore not permanent.

7. *Variability of Emission from Oxide Cathodes.*

Published values of the thermionic constants of oxide cathodes are much less in agreement with one another than

Fig. 3.

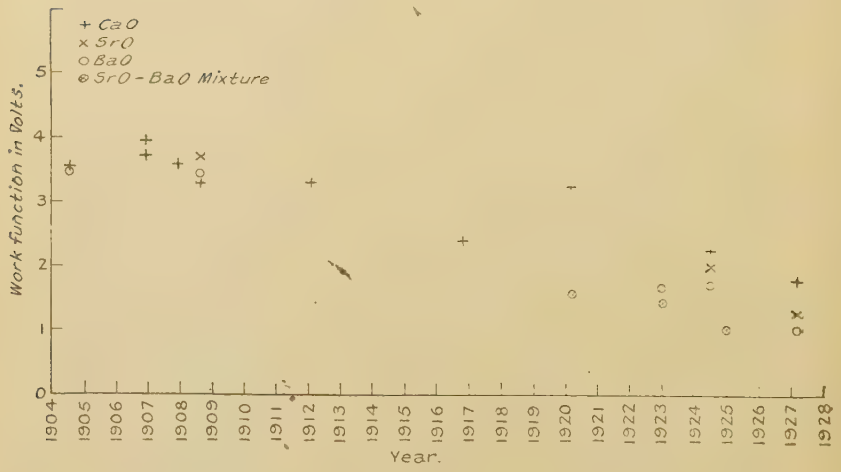

Published Values of Work-functions of Oxide Cathodes.

are those of any other kind of thermionic emitter. A good idea of the poorness of the agreement may be formed by plotting the values of one of these constants (*e. g.*. the work-functions) against the times of their publication. This has been done in fig. 3*. Uncertainty of temperature measurement, although probably a contributory cause, seems alone to be hardly adequate to account for the whole

* The papers from which these values have been taken are Nos. 2, 6, 8, 12, 15, and 17 of Arnold's [6] Bibliography, and Nos. 1, 3, 4, 6, 14, and 19 of our own.

of this variation. We must therefore look for other causes.

Let us first consider the case where the condition of the coating is so unfavourable that it is the coating, and not the contaminated core-metal, by which the emission is limited. We do not know in what manner the thermionic constants of a formed oxide depend upon the surface concentration of adsorbed barium. Probably all that it is safe to say is that the concentration and the emission increase and decrease together. We have already seen that at each temperature the surface concentration of barium is determined by the condition that there must be equilibrium between the removal of barium by its conversion into electrolytic ions and the arrival of fresh barium by diffusion. The coefficient of diffusion may itself vary violently with the temperature, in the same kind of way as does the emission. This will, for example, be the case if, in diffusing, the particles of barium move in "jumps" between neighbouring positions of equilibrium in relation to the underlying crystal lattice. Thus the temperature variation of the emission may not be a measure of the true work function at all, the surface concentration of barium being different at each temperature. The relative importance of this falsification of the work-function measurements will depend upon the size of the units of barium circulation.

If, on the other hand, the units of barium circulation in the coating are so small that it is the core-metal which limits the emission, certain variations in thermionic properties may still occur. That different contaminated core-metals should have different thermionic properties is, of course, quite natural. But even when the core-metal is not changed, some variation in these properties may still occur as a result of gas contaminations. Such variation is more particularly to be expected in the case of metals which are only with difficulty out-gassed, such as, for example, platinum. The thermionic behaviour even of uncoated platinum is notoriously erratic. Unfortunately platinum is the metal which has generally been used hitherto as the core-material of coated cathodes.

Further work on oxide cathodes is in progress in these Laboratories, by means of which it is hoped that more precise information may be obtained concerning several points with regard to which uncertainty still exists.

References.

(1) L. R. Koller, Phys. Rev. xxv. p. 671 (1925).
(2) M. S. Glass, Phys. Rev. xxviii. p. 521 (1926).
(3) H. Rothe, *ZS. f. Phys.* xxxvi. p. 737 (1926).
(4) W. Espe, *Wiss. Veröff. d. Siem. Konz.* v. pp. 29, 46 (1927).
(5) F. Detels, *Jahrb. d. drahtl. Telegr.* xxx. pp. 10, 52 (1927).
(6) H. D. Arnold, Phys. Rev. xvi. p. 70 (1920).
(7) W. Schottky and H. Rothe, *Handb. d. Experimentalphysik*, vol. xiii. pt. ii. p. 221.
(8) I. Langmuir, Phys. Rev. xxii. p. 357 (1923).
(9) I. Langmuir and K. H. Kingdon, 'Science,' pp. 57, 58 (1923).
(10) K. H. Kingdon, Phys. Rev. xxiv. p. 510 (1924).
(11) I. Langmuir and K. H. Kingdon, Proc. Roy. Soc. cvii. A, p. 61 (1925).
(12) J. A. Becker, Phys. Rev. xxviii. p. 341 (1926).
(13) F. Horton, Phil. Mag. xi. p. 505 (1906).
(14) H. J. Spanner, *Ann. d. Phys.* lxxv. p. 609 (1924).
(15) W. C. Röntgen and A. Joffé, *Ann. d. Phys.* xli. p. 449 (1913).
(16) W. C. Röntgen and A. Joffé, *Ann. d. Phys.* lxiv. p. 1 (1921).
(17) P. Lukirsky, Journ. Russ. Phys. Chem. Soc. (1916). A. Joffé, 'The Physics of Crystals,' p. 129.
(18) P. Lukirsky, Rep. Phys. Tech. Inst. p. 174 (1926). A. Joffé, 'The Physics of Crystals,' p. 129.
(19) C. Tubandt and F. Lorenz, *ZS. f. Phys. Chem.* lxxxvii. pp. 513, 543 (1914).
(20) P. Lukirsky, S. Shukareff, and O. Trapesnikoff, *ZS. f. Phys.* xxxi. p. 524 (1925).
(21) A. Joffé, 'The Physics of Crystals,' p. 92.
(22) A. Joffé and M. Kirpitchewa, Journ. Russ. Phys. Chem. Soc. xlviii. (1916). A. Joffé, 'The Physics of Crystals,' p. 87.
(23) P. Clausing, 'Physica,' vii. p. 193 (1927).
(24) W. Schottky, Phys. Rev. xxviii. p. 74 (1926).
(25) J. B. Johnson, Phys. Rev. xxvi. p. 71 (1925).
(26) W. Schottky and H. Rothe, *Handb. d. Experimentalphysik*, vol. xiii. pt. ii. p. 163.
(27) P. Debye, *Ann. d. Phys.* xxxiii. p. 441 (1910).
(28) W. Schottky, *ZS. f. Phys.* xiv. p. 63 (1923).
29) C. Davisson and L. H. Germer, Phys. Rev. xxi. p. 208 (1923); and xxiv. p. 666 (1924).
(30) T. R. Hogness and R. W. Harkness, Phys. Rev. xxxii. p. 936 (1928).

XLII. *Effect of Occluded Gases and Moisture on the Resistance of Air Condensers at Radio Frequencies.* By Hazel M. Fletcher, *Instructor in Physics, Wellesley College, Wellesley, Mass.**

Introduction.

In some work done in this laboratory, Department of Physics, Indiana University, on the resistance of air

* Communicated by Prof. R. R. Ramsey, Ph.D.

condensers. Mr. B. D. Morris * thought that he had discovered evidence that the radio-frequency current was pulling out gas from the plates of the condenser. This was given as the explanation of the fact that the two bulbs of the differential thermometer used in the experiment cooled at different rates. To avoid the effect that this liberation of gas might have on the equilibrium pressure, Morris substituted a thermojunction method in which a number of junctions were connected so that a galvanometer in the circuit registered a deflexion which was proportional to the difference of temperature of the two bulbs. The final equilibrium temperature was then independent of

Fig. 1.

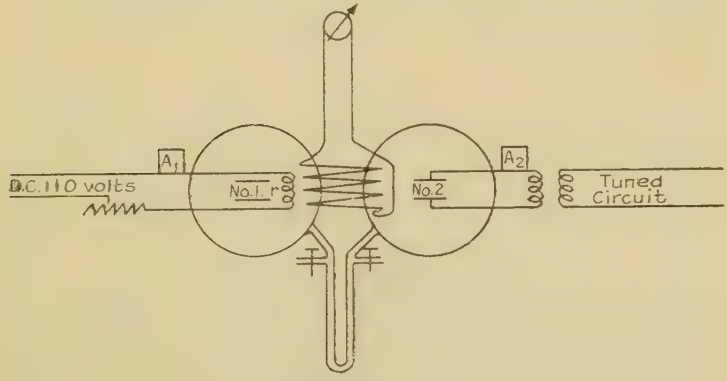

Diagram of apparatus.

liberation of gas, which was not true if a U-tube filled with water were used.

To investigate this supposed gas effect was the primary purpose of this investigation.

Apparatus and Method of taking Data.

The apparatus used in this experiment was similar to that used by Ramsey and Morris. However, in this experiment both a water manometer and thermocouple were used.

The diagram of the apparatus is shown in fig. 1. Two air-tight bulbs were formed by sealing with beeswax two 1·5 litre pyrex-glass beakers on to photographic glass plates. In each bulb was placed a radio-frequency condenser of the same size and kind. Condenser No. 2

* Phys. Rev. xxxiii. p. 1076 (1929).

was connected with a variable inductance which was coupled to a vacuum-tube oscillator circuit; condenser No. 1 was placed in the other bulb in order to maintain the same thermal capacity. The resistance wire r was connected in series with a variable resistance and the 110-volt mains. The water manometer measured the differential pressure in the two bulbs, and the difference in temperature was indicated by the D'Arsonval galvanometer in the thermocouple circuit, which consisted of eight iron advance-junctions in opposition series.

Three sets of condensers were used in this experiment, and three separate sets of apparatus were assembled. Readings were taken on a brass condenser of capacity ·000265 M.F., an aluminium condenser, No. 1, of capacity ·0002678 M.F., and another aluminium condenser, No. 2, of capacity ·0002 M.F.

Suppose i is the direct current in the resistance wire registered by the D.C. milliammeter (A_1), I is the radio-frequency current in condenser No. 2 registered by the hot-wire ammeter (A_2), r is the resistance of the resistance wire, and R is the resistance of condenser No. 2. Now, if the heating effects are balanced, $I^2R = i^2r$. All quantities in this equation are known except R.

Before taking measurements the bulbs must be at the same temperature, which will be shown if there is no deflexion of the galvanometer. The screw stopcocks were opened to make sure that the bulbs were at atmospheric pressure, and then closed. Tests were made before and after runs to make sure that there were no leaks. The primary circuit was closed, and the capacity of the variable condenser in the primary or oscillator circuit and the inductance in the secondary circuit were varied until the desired current and wave-length were obtained. The direct current was then varied until the heating effect of the resistance wire was balanced by the heating effect of condenser No. 2. The equilibrium was shown when the galvanometer showed no deflexion and the pressures as shown by the manometer were the same.

Results and Discussion on Occluded Gas.

The fact that the condenser heated by the radio-frequency current always was slower in heating and cooling led Morris to think that gas was being driven out. Fig. 2

is a typical curve showing the heating and cooling of the condensers. In preliminary experiments with the aluminium condensers a direct current of ·5 ampere was found to balance a radio-frequency current of 2 amperes. These currents were turned on at the same time, and readings were taken of time in minutes, temperature in centimetres of deflexion of the galvanometer, and differential pressure in centimetres of water. After the currents had been running for 65 minutes the bulbs were at thermal equilibrium, and the circuits were opened and readings taken while the condensers cooled. During the time of heating it was thought that the radio-frequency current was pulling out occluded gas from the plates of the condenser. Part of the heat energy would be used, and

Fig. 2.

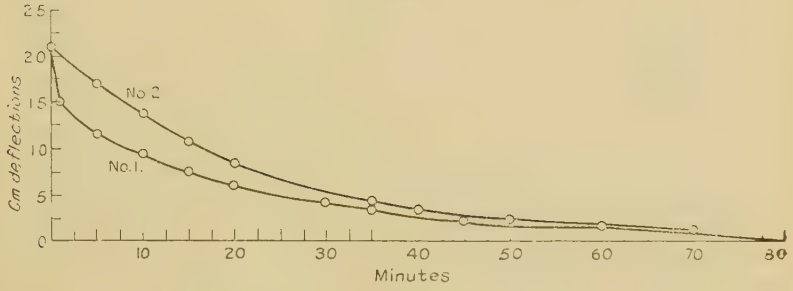

Cooling curves for brass condensers.

Direct current ·335 ampere.
Radio-frequency current 2·1 amperes.
Wave-length 170 m.
No. 1, cooling curve for brass condenser heated with direct current.
No. 2, cooling curve for brass condenser heated with radio-frequency current.

this would cause a slower rate of heating for condenser No. 2. During the cooling period it was thought that the gas was readsorbed on the plates, and the heat of adsorption was given out which would cause slower cooling of condenser No. 2.

If occluded gas were driven out, the pressure in bulb No. 2 would be greater than in No. 1 when the galvanometer indicated thermal equilibrium. In many runs the final pressures were often the same: but usually the final pressure in bulb No. 1 was slightly greater than in

No. 2, and there were a few runs in which the final pressure in No. 2 was the greater.

Calculations were made from cooling curves to see if the volume of gas could be determined. Fig. 3 shows the cooling curves for the brass condensers. In preliminary experiments it had been found that the heating effect of a direct current of ·335 ampere just balanced that of a radio-frequency current of 2·1 amperes. Curve No. 1 was obtained by heating condenser No. 1 with ·335 ampere without any radio-frequency current flowing. After an hour and a quarter the current was turned off, and readings

Fig. 3.

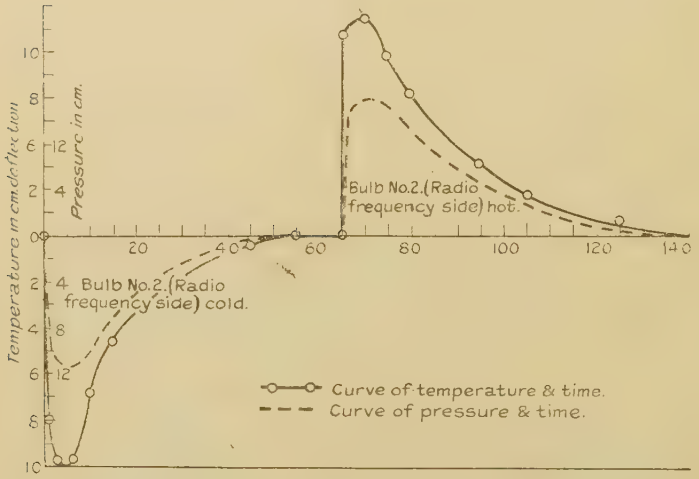

Differential heating and cooling curves for aluminium condenser No. 1.

Radio-frequency current 2 amperes.
D.C. current ·5 ampere.
Wave-length 120 metres.
Current turned off at 65 min.

were taken of the time and deflexions. Curve No. 2 is the cooling curve of the brass condenser heated with the radio-frequency current.

Let θ be the excess of the temperature of the bulbs above the temperature of the room. T the time in seconds, and R the radiation constant of the two condensers, assuming Newton's law of cooling. At thermal equilibrium both condensers are radiating heat as fast as they

are being supplied, and $R\theta = \frac{i^2 r}{4 \cdot 2}$. The heat given out by either condenser can be calculated by the relation $H = \theta RT$. Then the difference in the amount of heat given out by the two condensers is $\Delta H = \int R\theta dT$. But $\int \theta dT = A$ is proportional to the area between the two curves. Therefore $\Delta H = RA$. Now, if this difference in the amount of heat given out is due to the heat of adsorption of gas, ΔH must be equal to the heat of adsorption of the occluded gas. Let C represent the number of calories of heat given out when 1 c.c. of gas is adsorbed and V the volume of occluded gas driven out. Then $CV = RA$. Data from the cooling curves gave a result of 47 calories. Heat of adsorption tables showed that a value of 1 to $\frac{1}{2}$ calorie per 1 c.c. of adsorbed gas would be reasonable to assume for C. Then V would equal from 50 to 100 c.c. of gas. Larger results were calculated from the cooling curves of the aluminium condenser. These results are unreasonable when the difference of pressure as measured by the U-tube is considered.

This gas effect was also tested by placing the condenser in an exhausted air-chamber and noting the change of pressure when radio-frequency current flowed in the condenser. There was no noticeable change in pressure.

These different rates of heating and cooling cannot be due to occluded gases, but are due to an unequal heat distribution in the two bulbs. Between the 55- and 65-minute interval on the curve in fig. 2 the condensers are radiating heat at the same rate as they are receiving heat. The source of heat in bulb No. 2 is inside the condenser, while the source of heat in bulb No. 1 is a small wire outside the condenser. Even though the thermojunctions in both bulbs are at the same temperature, condenser No. 2 is at a higher average temperature than No. 1, since the heat must be conducted from the inside to the outside of condenser No. 2.

Resistance of Condensers.

It was soon noticed that the measured resistance varied from time to time, and it was suspected that this might be due to moisture. At first measurements were taken without any attempt being made to vary the amount of

moisture. Later the air was saturated and measurements were repeated. Then the bulbs were opened, the condensers dried out by heating, and some P_2O_5 put in the bulbs to take up any moisture. It was difficult to check these resistances with those found before when saturated vapour was in the bulbs. It was thought that there might be moisture in the bulbs from the water in the U-tube. The water in the manometer was then

TABLE I.

Brass Condenser, capacity ·000265 M.F.

		Wave-length.	R_0.	R_s.	Ratios of R_0.
(1) ...	Air not	70 m.	·076 ohm.	·044 ohm.	(2)÷(1)=2·34
(2) ...	saturated.	170	·178	·043	
(3) ...	Air	70	·173	·101	(4)÷(3)= 2·31
(4) ...	saturated.	170	·400	·096	
(5) ...	P_2O_5 in	70	·125	·073	(6)÷(5)=2·04
(6) ...	jars.	170	·255	·061	
(7) ...	P_2O_5 in jars,	70	·070	·040	(8)÷(7)=2·06
(8) ...	cymene in	170	·144	·035	(9)÷(8)=2·28
(9) ...	manometer.	350	·329	·038	

Ratios of resistances (R_0) when air is saturated and when not saturated:

70 m.	170 m.
(3)÷(1)=2·28	(4)÷(2)=2·25
(3)÷(5)=1·38	(4)÷(6)=1·57
(3)÷(7)=2·47	(4)÷(8)=2·78

replaced by cymene, which has a specific gravity of 0·856 and boils at 175° C

The results are given in the column marked R_0 in Tables I., II., and III. Morris has found that the resistance of a condenser can be reduced to "standard values" by the empirical formula,

$$R_s = R_0(300/\lambda_0)\ (C_0/\cdot001)^{3/2}.$$

The brass condenser obeys the law,

$$R_s = R_0 \left(\frac{\lambda_s}{\lambda_0}\right)\left(\frac{C_0}{C_s}\right)^{3/2},$$

and both the aluminium condensers obey the law,

$$R_s = R_0 \left(\frac{\lambda_s}{\lambda_0}\right)^{1\cdot2} \left(\frac{C_0}{C_s}\right)^{3/2},$$

TABLE II.

Aluminium Condenser No. 1, capacity ·0002678 M.F.

		Wave-length.	R_0.	R_s.	Ratios of R_0.
(1) ...	Air not	70 m.	·226 ohm.	·064 ohm.	(2)÷(1)=1·05
(2) ...	saturated.	170	·237	·043	
(3) ...	Air	70	·274	·077	(4)÷(3)=1·19
(4) ...	saturated.	170	·326	·059	
(5) ...	P_2O_5 in	70	·171	·048	(6) ÷ (5) = 1·04
(6) ...	jars.	170	·178	·032	
(7) ...	P_2O_5 in jars,	70	·205	·058	(8) ÷ (7) = 1·25
(8) ...	cymene in	170	·256	·046	(9) ÷(8)=1·27
(9) ...	manometer.	350	·325	·041	

Ratios of resistance (R_0) when air is saturated and when not saturated :

70 m.	170 m.
(3)÷(1)=1·21	(4)÷(2)=1·37
(3)÷(5)=1·60	(4)÷(6)=1·83
(3)÷(7)=1·33	(4)÷(8)=1·27

rather closely. R, λ_s, and C are standard resistance, wave-length, and capacity : and R_0 λ_0, and C_0 are the measured values. Since the resistance of a condenser consists of metallic resistance and dielectric resistance, the relative amounts of which vary with the condenser, it cannot be expected that the same formula will apply to all condensers. Tables I., II., and III. give the average results of the three condensers with various amounts of

moisture. R_s is the calculated value using the empirical formula,

$$R_s = R_0\left(\frac{300}{\lambda_0}\right)\left(\frac{C_0}{\cdot 001}\right)^{3/2}$$

for the brass condenser, and

$$R_s = R_0\left(\frac{300}{\lambda_0}\right)^{1/2}\left(\frac{C_0}{\cdot 001}\right)^{3/2}$$

for the aluminium condensers.

Table III.

Aluminium Condenser No. 2, capacity ·0002 M.F.

		Wave-length.	R_0.	R_s.	Ratios of R_0.
(1) ...	Air not	70 m.	·058 ohm.	·010 ohm.	(2)÷(1)=1·15
(2) ...	saturated.	170	·064	·007	
(3) ...	Air	70	·100	·018	(4) : (3) =1·67
(4) ...	saturated.	170	·167	·019	
(5) ...	P_2O_5 in	70	·034	·006	(6)÷(5)=1·23
(6) ...	jars.	170	·042	·005	
(7) ...	P_2O_5 in jars,	70	·030	·005	(8)÷(7)=1·03
(8) ...	cymene in	170	·031	·003	(9)÷(8)=1·32
(9) ...	manometer.	350	·041	·003	

Ratios of resistances (R_0) when air is saturated and when not saturated:

70 m.	170 m.
(3)÷(1)=1·72	(4)÷(2)=2·60
(3)÷(5)=2·94	(4)÷(6)=3·98
(3)÷(7)=3·34	(4)÷(8)=5·38

The resistance of each condenser increases with the amount of moisture present. The ratios of R_0 when the air is saturated and when not saturated, except one (ratios 1·33 and 1·27 for aluminium condenser No. 1), increase with wave-length. These ratios show that the dielectric losses are larger than the metallic losses in aluminum condenser No. 2, and that the dielectric losses are relatively smaller in aluminium condenser No. 1.

The ratios of the resistance (R_0) given in the last columns of the tables show that the resistance increases with wave-length. Since the metallic resistance decreases and the dielectric losses increase with wave-length, these ratios show that the dielectric losses are greater than the metallic resistance. The metallic resistance of the brass condenser is greater than that of the two aluminium condensers, for the ratios for the aluminium condensers are approximately 1·1, and for the brass 2·2. The resistance of aluminium No. 1 and the brass condenser are comparable, but the resistance of aluminium condenser No. 2 is much lower. An appreciable amount of the resistance of the first two must be due to metallic resistance since the plates of aluminium condenser No. 2 were larger in area and much thicker.

In conclusion, radio-frequency currents do not pull out an appreciable amount of adsorbed gas from the metal plates of condensers. The resistance of condensers varies with the amount of moisture present. These variations are considerable, and probably this accounts for the fact that the results obtained by different experimenters for resistance of condensers do not check very closely. The dielectric losses and the metallic resistance vary with wave-length, and the ratio of these resistances is not the same in all condensers. The dielectric losses of the three condensers tested in this experiment were greater than the metallic resistance.

This investigation was made under the direction of Dr. R. R. Ramsey, Professor of Physics of Indiana University. The writer is indebted to him for whatever merits this paper may possess.

Bibliography.

Bureau of Standards, Circular No. 74.
C. N. Weyl and S. Harris, Institute of Radio Engineers, xiii. p. 109, Feb. 1925.
E. Offerman, *Zeit. für Hochfreqy.* xxvi. p. 152 (1925).
C. D. Callis, Phil. Mag. i. p. 428 (1926).
R. R. Ramsey, Phil. Mag. ii. p. 1213 (1926).
S. L. Brown, C. F. Weibusch, and M. Y. Colby, Phys. Rev. xxix. p. 887 (1927).
D. W. Dye, Proc. Phys. Soc. xl. p. 285 (1928).
R. W. Wilmotte, Journ. Sci. Instruments, xii. p. 369 (1928).
C. W. Sutton, Proc. Phys. Soc. xli. p. 126 (1929).

XLIII. *On an Anomalous After-Effect of Dielectrics for their Apparent Resistivity.* *By* Prof. H. Saegusa *and* S. Shimizu, *Physical Institute of Tohoku Imperial University, Sendai* *.

§ I. *Introduction.*

THAT the electrical conductivity of quartz is greatly affected by a previously applied potential is discussed in A. F. Joffé's book†. This is an interesting and important phenomenon from the point of studying the electrical conduction in dielectrics. For the past several years the conductivity of dielectrics has been studied in our institute as one of the main topics for dielectrics, and during the course of studying we found independently the fact that the electrical conductivity of quartz is greatly affected by a previously applied potential, and that there is an anomalous after-effect with respect to its recovery time duration.

The present investigation was undertaken for the purpose of studying systematically the anomalous after-effect of dielectrics, and the results for quartz plate cut perpendicular to its optical axis are given in this paper.

§ II. *Apparatus and some Precautions for the Experiment.*

The main part of the present apparatus is shown in fig. 1. The constancy of temperature of the interior part of the metallic box which contains the main part of the apparatus is ensured by means of the following devices.

Both sides of the metallic box are covered with asbestos paper, and this box is covered with a wooden box the outside of which is also covered with a thick felt. The electric heaters, made of nichrome wire, are fixed on the upper and the bottom sides of the inside of the wooden box. The copper-constantan thermo-junction is placed near the specimen in the interior of the metallic box for measuring the temperature of the specimen, this thermo-junction

* Communicated by the Authors. An abstract of this paper was published in 'Nature,' vol. cxxiii. p. 713 (1929), under the title "Anomalous After-effect with Quartz," and was read before the annual meeting of the Math. Phys. Soc. Japan, July 24 (1929).

† A. F. Joffé, 'The Physics of Crystals' (1928).

being made by connecting copper and costantan wires, fifteen each in series ; and an ordinary thermometer is also put in the interior of the metallic box. By adjusting the heating current, the temperature of the interior of the metallic box is kept constant within $\frac{1}{10}^\circ$ during 2 hours at least near the room-temperature.

The interior of the metallic box is maintained in as dry a state as possible, using P_2O_5 and circulating perfectly dried air through the box ; thus, the humidity in the interior of the box is kept always below 5 per cent. of the relative humidity at the temperature 10° C.

The leakage-rate of electricity through the apparatus is taken before the beginning of the experiment, and the

Fig. 1.

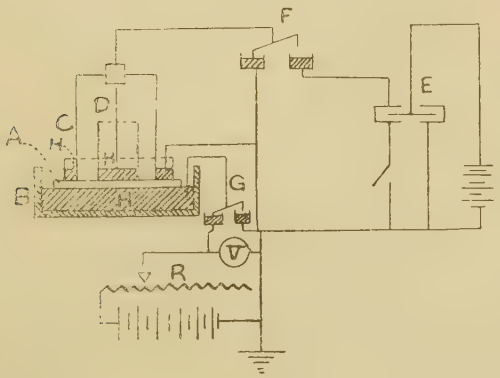

The symbols in the figure are as follows:—

A. Specimen, thin circular plate which is floating on the surface of mercury H.
B. Circular vessel made of ebonite.
C. Concentric cylinder made of iron, and the mercury between the outside walls is earthed.
D. Open circular cylinder made of iron which is situated at the centre of the specimen.
E. Dolezalek's quadrant electrometer.
F. Mercury locker for connecting the inside part of D to one pair of quadrants of the electrometer or to the earth.
G. Mercury locker for connecting the mercury between A and B to the potential source or to the earth.
H. Mercury.
R. Reducing resistance.
V. Precision voltmeter for measuring the applied voltage.

correction for it is made in the results of the experiment if necessary.

The specimen used in the present experiment is well-polished quartz circular plate cut perpendicular to its optical axis and 0·85 mm. thick.

§ III. *Method of Experiment.*

We put a known potential to the mercury on which the specimen floats during a certain constant time (always 10 minutes in the present experiment, except in some special

Fig. 2.

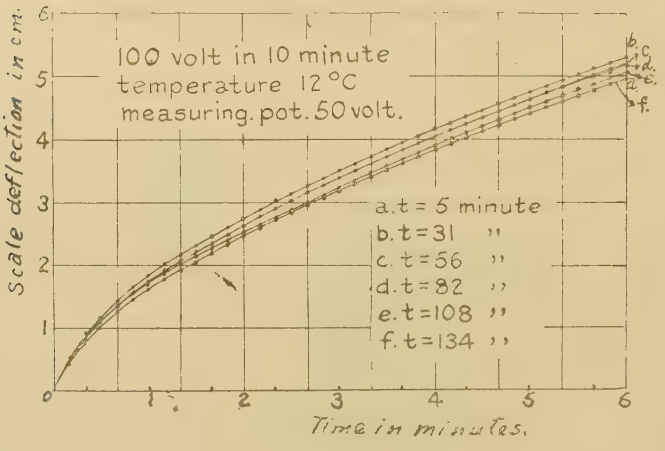

cases); during this time interval the opposite side of the specimen is kept in connexion with the earth; thus, the electricity is conducted freely to the earth through the specimen, and we call this previously applied potential "A potential" for convenience. Then the other side of the specimen is also connected to the earth during a known time, and it is then disconnected from the earth and connected to the potential source of a constant potential. The opposite side of it, *i. e.*, the mercury inside cylinder D, is also disconnected from the earth and connected to the electrometer, the deflexion of which is observed with time up to several minutes (always 6 minutes, except in some special cases). Next, both sides of the specimen are earthed until the residual charge and the time effect due to

the latter measuring potential have almost disappeared, and then the observation, as before, is made under the same external condition as above during the same time interval, and then both sides of the specimen are again earthed. These processes of the observation are repeated till the rate of accumulation of the electric charge becomes almost the same as in the neutral state of the specimen, *i. e.*, till the effect of A potential on the apparent resistivity of the specimen has completely disappeared.

Fig. 3.

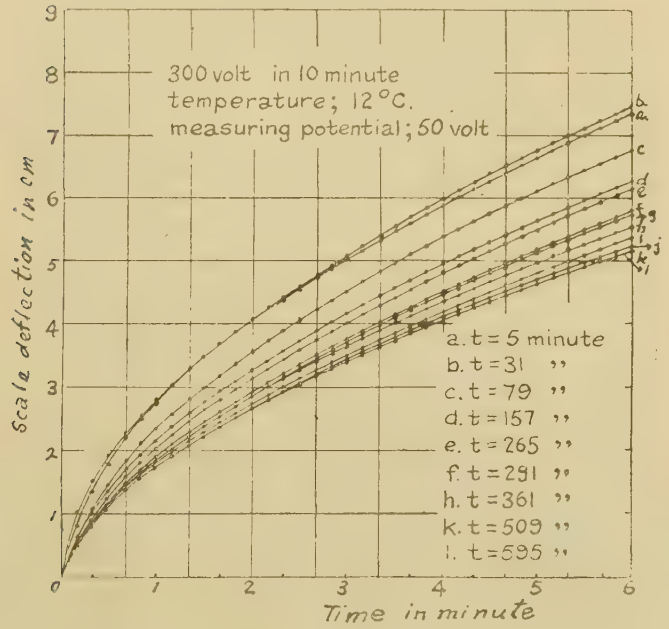

The correction of the residual charge due to A potential is made for the observed value.

The apparent resistivities for every earthing time from the initial are calculated from the ratio of the measuring potential (always 50 volts, except in some special cases) to the initial tangent of every accumulating curve as

$$R = \frac{V}{\frac{dQ}{dt}}, \quad . \quad . \quad . \quad . \quad . \quad . \quad . \quad (1)$$

This is the same expression as equation (16) in the former paper * by one of the writers. And it gives correctly the apparent resistivity at given time from initial, and here we state that Curtis's equation

$$V = Ri + \frac{1}{c}\int_0^t i\,dt$$

Fig. 4.

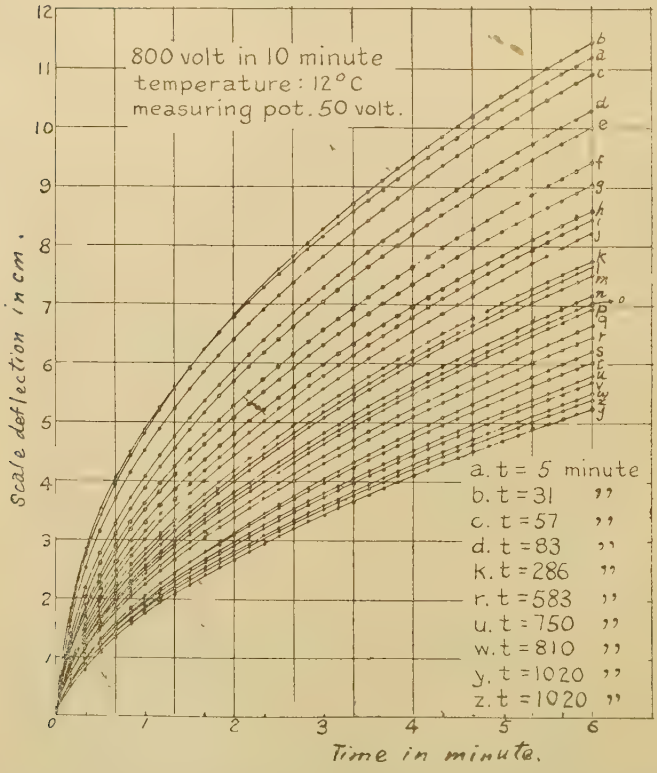

though used in the former paper above referred to, is not generally applicable to the calculation of the apparent resistivity at any time. Thus, equations (14), (15) in the same former paper give also nothing accurate as to apparent resistivity, but equation (16) gives the accurate value at $t=0$ as above stated.

* H. Saegusa and K. Saeki, Sci. Rep. Tohoku, xviii. p. 231 (1929).

§ IV. *Anomalous After-Effect with Quartz.*

(1) *The relation between A potential and the recovery time.*—Some experimental results of the accumulating curves for various A potentials and for various earthing times as graphically given in figs. 2–4 and fig. 5 show the

Fig. 5.

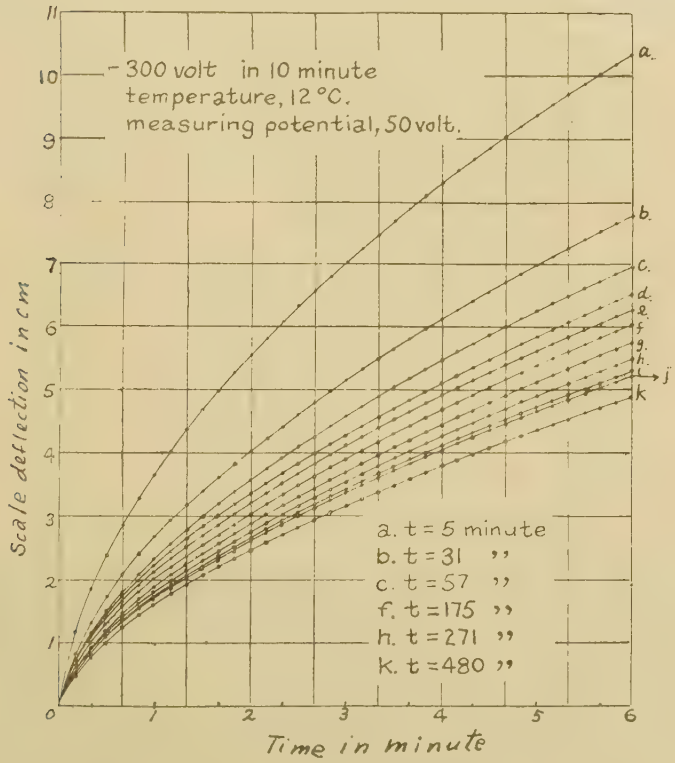

typical one of the experimental results for negative A potential. The letters *a*, *b*, *c*. . . . . in these curves show that *a* is the curve at 5 minutes' earthing (the first earthing) from the instant A potential is earthed, *b* the curve at 20 minutes after the observation of a curve is finished (the observation of *a* curve continues 6 minutes and then the side which is connected to the electrometer is earthed till the beginning of the observation of *b* curve). *i. e.*, at

31 minutes from the initial, and so also in the same way the curves $c, d, \ldots$ (the time intervals for these curves are written in these figures). But for the cases when A potential is comparatively large, the time interval of earthing between each two successive observations is made longer and longer as the accumulation curve approaches the neutral state.

As seen from these curves, the initial inclination is much larger than that of the neutral state, and it becomes smaller

Fig. 6.

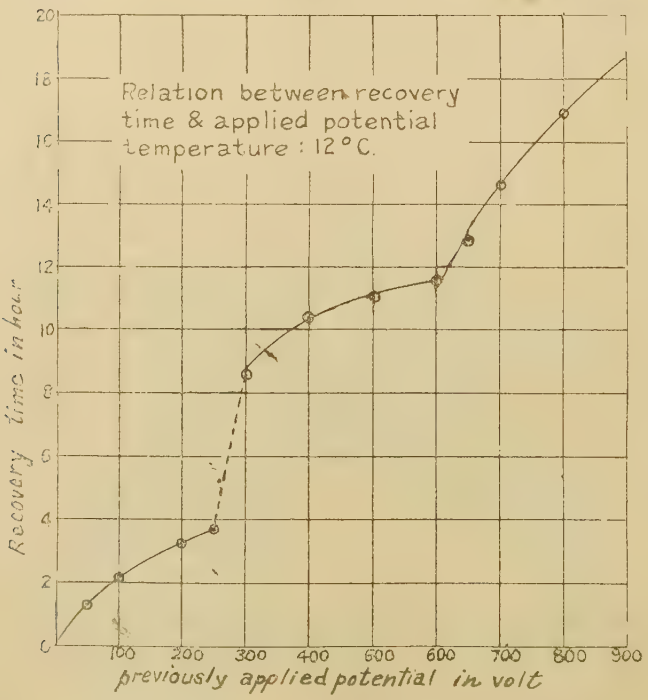

as the earthing time increases and gradually tends to that of the neutral state. Thus from equation (1) the apparent resistivity will be much smaller than that of the neutral state, and it gradually becomes equal to the latter.

Fig. 6 and Table I. show the relation between A potential and the recovery time of the after-effect, *i. e.*, the time interval between the instant of the first earthing and the

final state ; during this time interval the after-effect of A potential continues. As seen from fig. 6, the recovery time of the after-effect is considerably long, and it becomes gradually longer as A potential increases, and at the potential between 250-300 volts (about 300–350 volts per mm. thick) it discontinuously becomes long, and again the increase rises slowly up to 600 volts (700 volts per mm. thick), and after that the time interval increases rapidly with the potential and tends gradually to a saturation value. It is a noticeable fact that the variation of the recovery time with A potential is exactly the same for both cases whether A potential is positive or negative.

In a paper* by one of the writers it was concluded that the limit potential is most important for several dielectric

Table I.

A potential in volts.	Recovery time in minutes.	A potential in volts.	Recovery time in minutes.
50	70	500	663
100	134	500	695
200	200	650	770
250	223	700	882
300	509	800	1020
400	620		

phenomena—for example, the so-called stationary dielectric hysteresis appears for larger applied potential than the limit potential, and an anomaly for the residual charge is also observed at this potential. And the limit potential for quartz plate cut perpendicular to its optical axis is equal to 324 volts per mm. thickness as the mean value from the residual charge and the time effect.

Hence the discontinuous increase of the recovery time occurs at about the limit potential ; thus, we should like to call this discontinuous change of the after-effect "the anomalous after-effect for resistivity of dielectrics," and we conclude that it appears at the limit potential of dielectrics.

It seems to be a noticeable fact that the increase of the recovery time from 600 volts is due also to the same cause

* H. Saegusa, Sci. Rep. vol. x. p. 101 (1921).

to which the increase of the stationary values of the residual charge and the time effect with respect to the applied potential from about 600 volts is due, as shown in the paper above referred to.

(2) *Variation of the apparent resistivity.*—The relation between the ratio of the apparent resistivity at 5 minutes

Fig. 7.

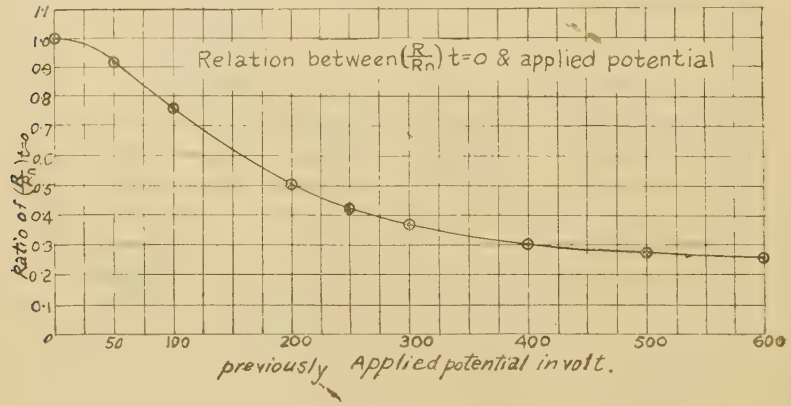

TABLE II.

A potential in volts.	$\frac{R}{Rn}$.	A potential in volts.	$\frac{R}{Rn}$.
0	1·000	300	0·371
50	0·910	400	0·301
100	0·773	500	0·280
200	0·503	600	0·260
250	0·418		

after the beginning of the first earthing (calculated from initial tangent of a curve using equation (1)) to that of the neutral state and A potential is shown in fig. 7 and Table II. As seen from this figure the apparent resistivity decreases rapidly as A potential increases, and from about 300 volts of A potential the decrease of the resistivity gradually becomes small and the resistivity tends to a stationary value. These features are quite

similar for both cases where A potential is either positive or negative.

Figs. 8–11 show that the ratio of the apparent resistivity at neutral state to that of every earthing time (they are calculated from every initial tangent of a, b, c, ... curves using equation (1)) decreases as the time interval from the beginning of the first earthing increases and gradually tends to unity. This variation shows that the apparent resistivity recovers gradually as the time elapses,

Fig. 8.

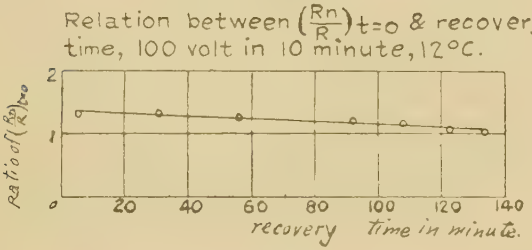

Fig. 9.

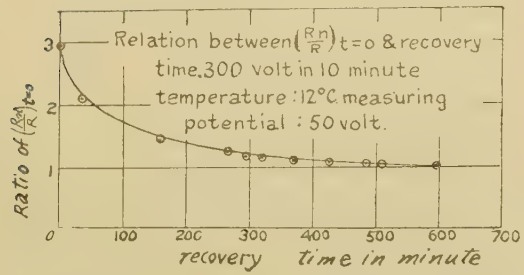

and tends to that of the neutral state. The recovery of the apparent resistivity is also quite similar for both cases, namely, when A potential is either positive or negative.

The correction of the residual charge of A potential is mainly made for the point from a curves in figs. 2–5. When A potential is small the points near the origin in figs. 8–11 are not so affected by the residual charge of A potential as in the cases when A potential becomes large. Thus, as A potential becomes large several points near the

origin except the initial point from a curve are omitted to avoid much effort for the correction of the residual charge. These points are not very necessary to show the general feature of the recovery of the apparent resistivity.

Fig. 10.

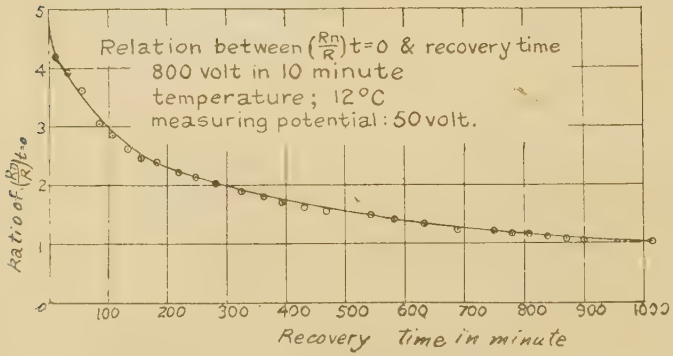

Fig. 11.

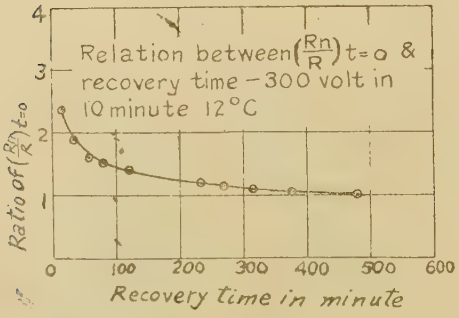

§ V. *Various Experiments for the After-Effect.*

For the purpose of studying thoroughly the nature of the after-effect for the apparent resistivity, the following experiments were made :—

(1) The case when A potential is smaller than the measuring potential:

The boundary conditions for the experiment are the same as in § IV., but in this case A potential is constant and

equal to 300 volts, and we take the measuring potentials 400, 500, and 600 volts, and every observing time, 1 minute.

Figs. 12–14 show the results of the experiment. In this case the ratio of the apparent resistivity at the neutral

Fig. 12.

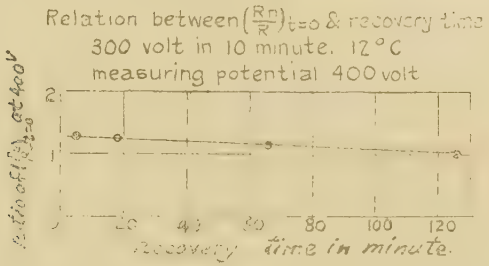

Fig. 13.

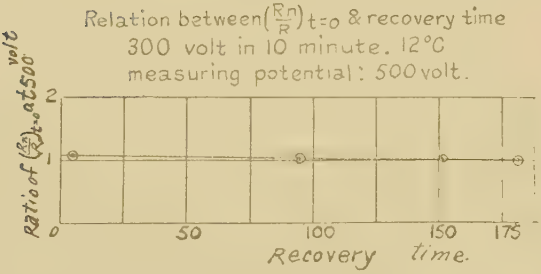

Fig. 14.

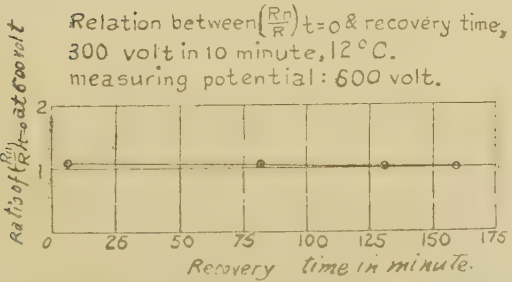

state to that at various times from the beginning of the first earthing is much smaller than that of the case when A potential is larger than the measuring potential, and the recovery time duration is also much less. This variation

becomes small as the measuring potential increases. Thus, the after-effect due to A potential, which is smaller than the measuring potential, is small, and there appears no after-effect where A potential is negligible with respect to the measuring potential.

(2) The case when the applied time interval of A potential is much longer than the case in § IV. :

Fig 15 shows the decrease of the ratio of the apparent resistivity at the neutral state to that at various observing

Fig. 15.

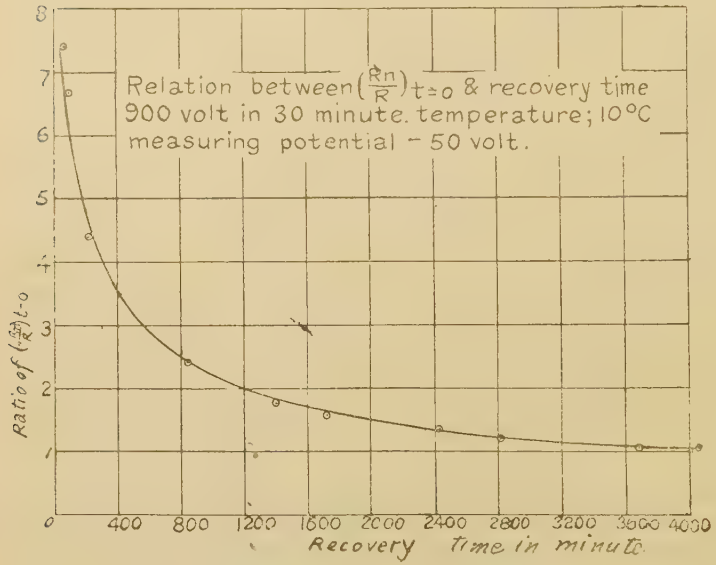

times with respect to the recovery time. In this case A potential is 900 volts, and its applied time interval 30 minutes, and the measuring potential −50 volts. The after-effect becomes large in comparison with that in § IV.

Fig. 16 shows a similar relation when the measuring potential is +50 volts. In this case, however, the recovery time is smaller than in the case when the measuring potential is negative.

Fig. 17 shows a similar relation to the above, but in this case as A potential 900 volts is first applied during 30 minutes, and after 3 minutes −900 volts is then applied

during 30 minutes, and then the observation is made as in the cases in § IV. In this case the ratio of the apparent resisitivity at the neutral state to that at various times up to the neutral state varies similarly with the above case, but the recovery time is nearly equal to the case when fig. 15 is obtained.

Fig. 16.

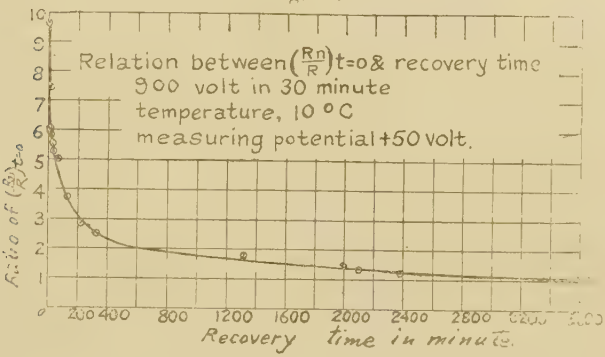

Fig. 17.

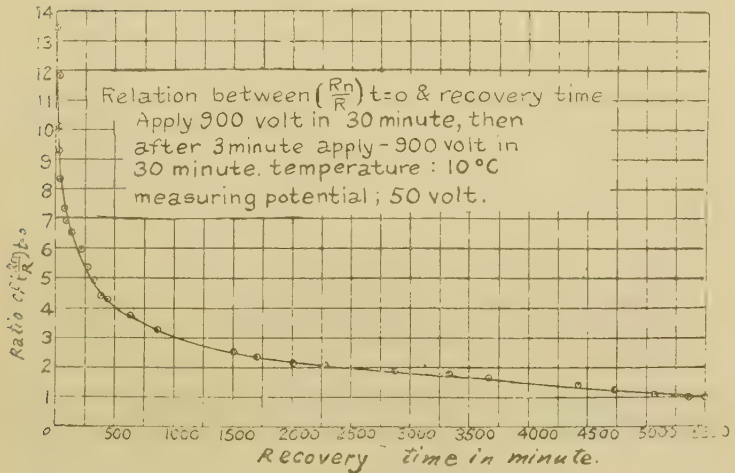

No result is shown in this paper, but a cyclic application of A potential between positive and negative was made. And from these results we may state here that the after-effect due to the cyclic application of A potential becomes larger and larger as the number of applications increases,

and gradually tends to a saturated state. And we state here that the after-effect becomes large with applied time interval of A potential, and gradually tends to a saturated state.

§ VI. *Concluding Remarks.*

The anomalous after-effect for the apparent resistivity is one of the interesting and important characteristics of dielectrics for the problem of electrical conduction in dielectrics, and it is a new characteristic of non-metallic crystals.

It is a remarkable fact the the anomalous after-effect appears at the limit potential. Thus, it seems to us that there will be a close connexion among the after-effect, the residual charge, and other dielectric phenomena, such as dielectric hysteresis, etc.

As shown in the present experiment, the recovery time of the after-effect is as long as several hours or more ; hence the apparent resistivity of a dielectric is not so easily determined except in the case when the dielectric is in its neutral state. Thus, the apparent resistivity must be defined not only by the charging time, as shown in the former paper, but also by its history of charging.

The anomalous after-effect for the apparent resistivity is exactly the same for both cases when the previously applied potential is either positive or negative ; hence the after-effect depends simply on the absolute value of the applied potential, so that it is likely to be due to some nature of the atomic lattice of crystalline dielectrics.

It seems that the after-effect increases rapidly with the time interval of the previously applied potential, and then gradually tends to a stationary value. And by cyclic application of the previously applied potential between positive and negative it also increases and tends to a stationary value.

The after-effect due to a previously applied potential which is smaller than the measuring one is comparatively small, and it becomes smaller and smaller as the former potential becomes smaller and smaller than the latter potential.

In conclusion, we are sincerely thankful to the Saito Gratitude Foundation in Sendai for the financial aid given us for these experiments.

XLIV. *On the Vortex System in the Wake of a Cylinder in a Fluid.* *By* Prof. H. Levy *and* S. G. Hooker, *A.R.C.S., B.Sc.* *

IN an investigation of the stability of two parallel rows of rectilinear vortex filaments as they would be originated in the wake of a cylindrical obstacle in unbounded fluid, Karman has found theoretically † that, if h = distance between the parallel rows, and a = distance between consecutive vortices of the same row, then the spacing of the stable system, in alternate arrangement, is such that

$$\frac{h}{a} = 0{\cdot}281.$$

From momentum considerations, moreover, he deduced that the resistance D of the body giving rise to the system is

$$D = \rho V(2{\cdot}828 - 1{\cdot}12\,U_0)U_0 h,$$

where ρ = density of the fluid,

V = velocity of the body,

and U_0 = velocity of the vortex system relative to the obstacle.

In its application to real liquids the assumption was made, of course, that while the fluid was viscous enough to enable the vortices to be generated, it was not so viscous that their strength would decay appreciably during the time taken to establish a fairly long street.

In this formula for resistance the ratios $\frac{U_0}{V}$ and $\frac{h}{b}$ (b being a characteristic linear dimension of the body) were not found by analysis, but required to be determined experimentally. This arose from the fact that Karman's theory did not connect up the established vortex street with the conditions at the obstacle which gave rise to it.

In an extension of the theory, Heisenberg ‡ sought to evaluate these two ratios for the case of a flat plate, from the two following assumptions :—

(*a*) A discontinuous surface springs from the edge of the obstacle, and all the vorticity so produced passes down the wake as individual vortices.

* Communicated by the Authors.

† Karman and Rubach, *Phys. Zeit.* xiii. (1912).

‡ *Phys. Zeit.* xxiii. (1922).

(*b*) The amount of fluid swept forward by the plate in its forward motion is equal in volume to the amount of fluid streaming back between the parallel rows.

These lead to the values

$$\frac{U_0}{V}=0{\cdot}2295, \qquad \frac{h}{b}=1{\cdot}54,$$

and therefore

$$k_D=\frac{D}{b\rho V^2}=0{\cdot}909.$$

These compare with Karman's experimentally determined values of

$$\frac{U_0}{V}=0{\cdot}20, \qquad \frac{h}{b}=1{\cdot}545, \qquad k_D=0{\cdot}805.$$

It is important to notice that Heisenberg's assumptions lead to a rate of generation of vorticity $R=\frac{1}{2}V^2$ at the edge of the plate.

In its experimental application to a wind-channel the effect of the walls on the state of motion and on the resistance has to be considered. This has been dealt with by Glauert * on the following assumptions:—

(1) In any practical application the breadth h of the vortex street will not exceed one-sixth of the breadth H of the channel.

(2) The increase of the suction in the dead-water region behind the body, due to the constraint of the channel walls, is equal to the drop in pressure outside the vortex street far behind the body.

(3) The values of K, $\surd$R, $\surd$S, which are proportional to V in an unlimited fluid, are assumed to be proportional to a certain effective velocity in the channel, which is the arithmetic mean of the velocities far in front of and far behind the body.

Broadly speaking, the main justification that Glauert advances for the validity of these assumptions is that they are not essentially unreasonable and that they lead to values of D' and k_D' which are verified experimentally. He then obtains the following formulæ:

$$\frac{U_0'}{U_0}=1-\frac{2\surd 2\dfrac{U_0}{V}}{1-\dfrac{2U_0}{V}}\cdot\left(\frac{U_0 h}{V b}\right)\cdot\frac{b}{H}, \quad \ldots \quad (1)$$

* Proc. Roy. Soc. A, vol. cxx. p. 34 (1928).

$$\frac{K'}{K} = 1 + \sqrt{2} \cdot \left(\frac{U_0 h}{V b}\right) \cdot \frac{b}{H}, \quad . \quad . \quad . \quad . \quad . \quad (2)$$

$$\frac{h'}{h} = \frac{a'}{a} = 1 + \frac{\sqrt{2}}{1 - \frac{2U_0}{V}} \left(\frac{U_0 h}{V b}\right) \frac{b}{H}, \quad . \quad . \quad (3)$$

$$k_D' = k_D + 16 \left(\frac{U_0 h}{V b}\right)^2 \cdot \frac{b}{H}, \quad . \quad . \quad . \quad (4)$$

where b = breadth of plate,

H = breadth of channel;

the accented letters denote values in the channel, and unaccented ones values in the infinite fluid.

Apart from the difficulty of perceiving adequate physical reasons why precisely these assumptions, and these only, should lead to experimentally verified results, there are one or two criticisms that might legitimately be raised.

Glauert's assumptions lead to the conclusion that R, the rate of discharge of vorticity at the edge of the obstacle, is given by $R = V^2$. In checking his formulæ (1), (2), (3), (4) against experiment, however, he has made use of Heisenberg's values for $\frac{U_0}{V}$, $\frac{h}{b}$, and k_D, which themselves have been derived on the basis that $R = \frac{1}{2}V^2$. This, however, while it throws doubt on the effectiveness of his check, does not in itself affect the validity of the argument leading to the above formulæ.

In actual fact it can easily be shown * that Heisenberg's assumption (3) applied to Glauert's case would lead directly to $K = K'$, a result quite inconsistent with equation (2). It is clear that the two treatments, Heisenberg's and Glauert's, cannot possibly be consistently combined.

Moreover, even if Heisenberg's final results are taken to check Glauert's conclusions, the values obtained from direct experiment by Fage and Johansen for certain other quantities not used by Glauert in illustration, do not provide such happy agreement, as the following table shows:—

* $\frac{Kh}{a} = V_0 b$, and $\frac{K'h'}{a'} = V_0 b$. $\therefore \quad \frac{Kh}{a} = \frac{K'h'}{a'}$.

If $h'/a' = h/a$, then $K = K'$.

Quantity.	Fage and Johansen.	Glauert.
$\frac{h'}{a'}$	$\left\{\begin{array}{c}(x/b=5{\cdot}0,\ 10{\cdot}0,\ 20{\cdot}0)\\ 0{\cdot}248,\ 0{\cdot}381,\ 0{\cdot}525\end{array}\right\}$	0·281
$\frac{K'}{a'V}$	0·74	0·628
$\frac{W-U_0'}{V}$	0·767	0·847
$\frac{a'}{b}$ †	5·25	5·84
$\frac{R^1}{V^2}$ †	1·10	1·07
$\frac{k'}{D}$ †	1·065	1·052
$\frac{b}{a'}\frac{W-U_0'}{V}$ †	0·146	0·146

† Shown by Glauert in illustration.

The above experimental values were obtained by Fage and Johansen from their experiments on a flat plate in a wind-channel, fourteen times the width of the plate. While these values in the cases checked by Glauert appear to provide good agreement, serious divergencies occur in other cases, notably in such fundamental values as the spacing of the vortices and the strength of the vorticity.

Before drawing any hard and fast conclusions therefrom, it is necessary to consider more closely the possible accuracy of some of the experimental values. A detailed examination of the work of Fage and Johansen makes it certain that their values of the drag coefficient k_D', f the frequency of the vortices, and therefore the longitudinal spacing, are accurate. Difficulties however arise, as the experimenters themselves indicated, in connexion with the lateral spacing h' of the two rows, for this involves the specification of the centre of each moving vortex. For this purpose the experimenters determined the positions of maximum and minimum velocity outside and inside the street respectively, taking a point midway between these positions as the centre. While the position of the maximum was very definite, the same could not be said for the position of the minimum, where a fair margin of error might result. This means that quantities in the above table, depending for their value directly on the lateral spacing, are subject to possible inaccuracy. One vital point, however, appears to be certain—that Fage and Johansen *, working over a range of twenty diameters in the wake of the obstacle, find that the

* Roy. Soc. Proc. A, cxvi. p. 170 (1927).

Karman ratio $\frac{h}{a}$ specifying the spacing is, with one exception, much greater than 0·281 ; the difference is too great for this to be accounted for by an error in the measurement of h. Moreover, it cannot be traced to the image effect of the channel walls, for L. Rosenhead *, who has given a complete investigation of the stability of the double row in the channel, finds that the stability ratio h/a is given by

$$\frac{h}{a} = 0{\cdot}281 - 0{\cdot}090\ (a/\mathrm{H})^6,$$

where 2H is the breadth of the channel, and in the presence of walls is therefore always less than 0·281. As long as the values of h/a stand, viz. 0·248, 0·381, 0·525 at distances of 5, 10, and 20 diameters respectively behind the body, deductions as regards resistance drawn from an assumed constant arrangement specified by 0·281 can hardly be reliable. *Between 5 and 20 diameters the spacing ratio increases by over* 100 *per cent.*

These experimental results then, if they are to be accepted, seem to suggest that the vortex street does not in fact behave stably in the wake of a body in a channel, in spite of the mathematical theory.

It becomes of some interest therefore to examine whether the assumptions made in establishing the stability of the vortex street in these circumstances are sufficiently valid for the purposes in hand. These assumptions are comparatively simple, and may be detailed as follows :—

(1) The viscosity of the fluid is presumed to be sufficient to allow of the origin of the vortex street, but not sufficient to effect any appreciable decay.

(2) The vortices are presumed concentrated throughout the whole process as filaments, so that no spread under viscous action takes place.

(3) The distribution of basic velocity, *i.e.*, the flow upon which the vortex effect is superposed, is presumed constant across the channel.

The experimental work of Fage and Johansen, and their efforts to determine the centres of the vortices by measuring their radii, are sufficient to show that the assumptions (1) and (2) are not realized in practice. Whether this is sufficient to invalidate the theory is a matter for examination.

* Phil. Trans. A, ccxxviii. pp. 275–329.

Assumption (3), on the other hand, may be seen almost from the beginning to involve a possible serious error. In a uniform channel in which there is no obstacle there is no doubt that over a wide portion of the section the mean velocity distribution is fairly constant, although it drops to zero at the walls ; but it is not at all clear that when an obstacle is inserted the full distribution of velocity can everywhere in the wake be completely analysed into two simple constituents, viz. :—

(*a*) A uniform distribution throughout,

(*b*) That due to the idealized vortex street.

The point has, apparently, not been dealt with by any of the writers on this subject. In a very wide channel, where the *body* is in motion along the axis, there appears no reason to suspect the contrary, and, in fact, Karman and others appear to have found his arrangement verified *. In the normal case of a wind-tunnel test, on the other hand, where the *fluid* moves past the stationary body at a speed corresponding to a Reynolds' number well above the critical value for the channel, conditions are very different. Along the walls it is known that there develops a boundary layer whose depth increases down wind, and, if turbulent, may spread well into the centre of the channel. Although the walls, regarded as completely replaced by images, may have little direct influence on the arrangement of the vortices shed behind a body in such a channel, as Glauert and Rosenhead have shown, the vortices themselves may have a considerable effect on the spreading boundary layer by drawing out the vorticity in that layer until it intermingles with that concentrated in the individual eddies that have sprung from the edge of the body. Thus the eddies of positive sign shed from one edge of the body may be expected to be swept along in a milieu of negative vorticity drawn from the boundary layer, and the negative eddies from the opposite edge in one of positive vorticity. Such a state of affairs may make a considerable difference to the conclusion as regards stability, since the vortices would be in motion in a field in which a velocity gradient existed. From the experimental work of Fage and Johansen † it is, in fact, quite simple to examine whether such a basic velocity gradient actually exists.

* It is to be expected nevertheless that the Karman spacing would be a function of Reynolds's number, but this does not appear to have been examined experimentally.

† Fage and Johansen, p. 194.

In fig. 1, Curve I.* is the mean velocity at various points across a section of the channel in the rear of a flat plate at a down-stream distance of ten breadths of the plate. Curve II., obtained from Curve I. by graphical differentiation, and verified by integration back to it, gives the mean vorticity across the same section. It will be seen that the

Fig. 1.

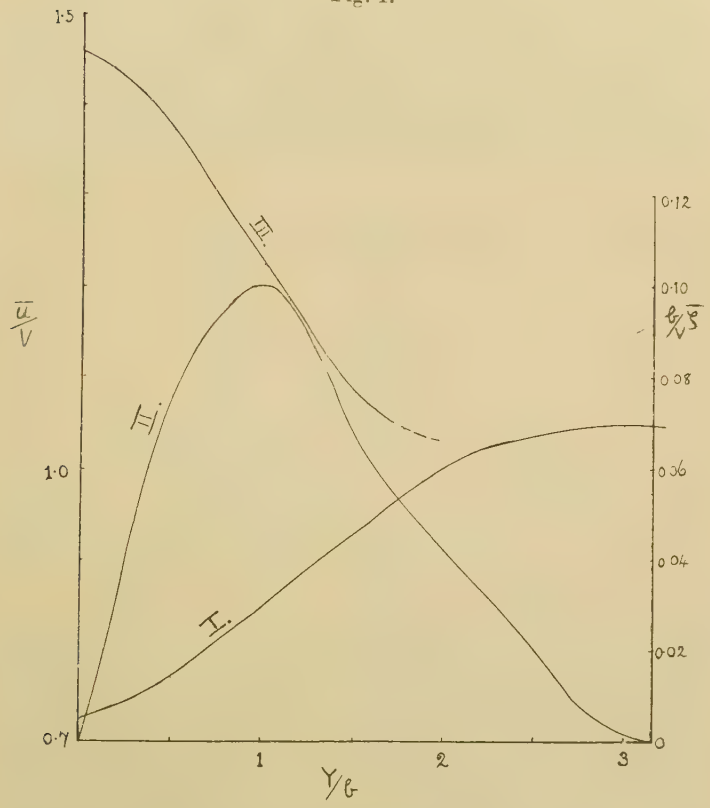

general shape is similar to that of a skew frequency curve. According to Fage and Johansen the centre of the vortex is situated at $Y/b = 1{\cdot}0$, and its inner and outer boundaries lie at $Y/b = 0$ and $Y/b = 2{\cdot}0$.

The validity of the assumption that the whole vortex may be regarded as concentrated at one position ($Y/b = 1{\cdot}0$)

* *Loc. cit.* p. 188.

becomes doubtful if the spread and asymmetry of this curve are noted. This distribution of vorticity and the corresponding distribution on the other half of the channel will correspond to an equivalent gradient in velocity. We have to examine whether this can be wholly accounted for by the individually concentrated vortices assumed in the simplified analysis. It may be remarked that the total vorticity as determined from this curve amounts to 0·32, whereas the strength adopted for the concentrated vortices was 0·74, indicating a strong basic field of negative vorticity.

Since it is the mean velocity which is measured experimentally at points in a wind-channel, let us seek in the first place the mean distribution, across the channel, of the

Fig. 2.

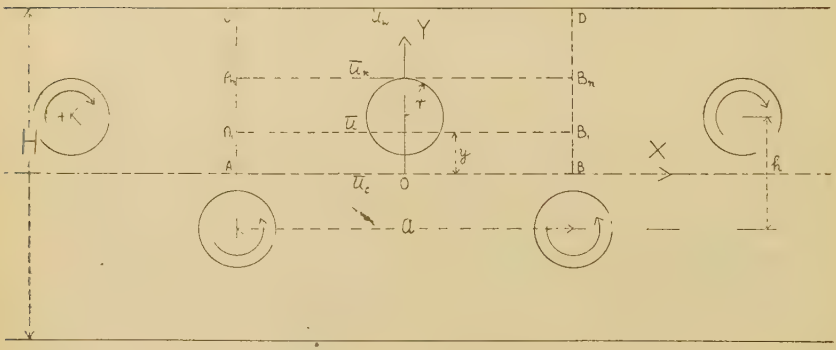

velocity due to a street of eddies of finite circular areas with constant vorticity ω. Fage and Johansen have found that the diameter of these eddies is approximately equal to the width of the street. At a distance of ten diameters down-stream neighbouring vortices appear to be at least three diameters apart ; but it is clear that since the diameter (as seen in fig. 1, Curve II.) is not very clearly defined, the effect of neighbouring vortices on each other's sectional shape will not be as pronounced as if they were entirely confined to the circular regions here assumed. At any rate, we shall assume as a rough approximation that they can move forward as a system without change of shape.

In fig. 2, CD represents a period lengthwise along the channel. From symmetry the flow across AC and BD is everywhere at right angles to these lines. If A_nB_n does

not intersect an eddy, then, taking the circulation round $A_nB_nDCA_n$, we have

$$I(A_nB_nDCA_n) = 0,$$

i.e.,
$$\int_{A_nB_n} u\,dx = \int_{CD} u\,dx,$$

or
$$\bar{u}_n = u_\omega,$$

where $\bar{u}_n$ and u_ω are respectively the mean velocities along A_nB_n and the sides of the channel.

Thus the mean horizontal velocity at all points outside the street due to the vortex system is constant, and equal to that at the channel wall. We shall see in a moment that, in fact, this is zero.

Again,
$$I(ABDCA) = -K = -\pi r^2\omega$$

where K is the total vorticity in the eddy,

$$\int_{AB} u\,dx - \int_{CD} u\,dx = -K,$$

i.e.,
$$u_c - \bar{u}_\omega = -K/a,$$

where $\bar{u}_c$ is the mean velocity along the centre of the channel.

Now it is easily demonstrated that the mean back flow along the centre of the channel is K/a, *i.e.*,

$$\bar{u}_c = -K/a.$$

Hence also
$$\bar{u}_n = \bar{u}_\omega = 0.$$

Thus the mean effect on the fluid outside the street is zero, while between the rows the vortices continue to pump the fluid back towards the obstacle. We note incidentally that the mean slip due to the vortices of the fluid at the boundary is zero.

Considering a circuit such as $(A_1B_1DCA_1)$ we find immediately

$$ua = -(\text{Area of circle enclosed in the circuit}) \times \omega$$

$$= -\omega\left\{\pi r^2 - r^2\cos^{-1}\left(\frac{h/2 - y}{r}\right) + \left(\frac{h}{2} - y\right)\sqrt{r^2 - \left(\frac{h}{2} - y\right)^2}\right\}.$$

At points removed from the street the circular vortices are equivalent to line vortices of strength K where

$$K = \omega \pi r^2,$$

$$u = -\frac{K}{\pi a}\left\{\pi - \cos^{-1}\left(\frac{h-2y}{2r}\right) + \left(\frac{h-2y}{2r}\right)\sqrt{1-\left(\frac{h-2y}{2r}\right)^2}\right\}.$$

This is the expression for the mean down-stream velocity due to the street, and holds for positive values of y between $\frac{h}{2} - r$ and h. Fage and Johansen found experimentally that the diameter of the vortices was approximately equal to the distance between the rows, *i. e.*,

$$r = \frac{h}{2}.$$

In this case, if $Y = y/h$,

$$\bar{u} = -\frac{K}{\pi a}\{\pi - \cos^{-1}(1-2Y) + (1-2Y)\sqrt{1-(1-2Y)^2}\},$$

when $0 < Y < 1$,

and $\bar{u} = 0$, when $1 < Y < \frac{H}{2h}$.

At a distance of ten breadths behind the plate the following experimental values were obtained:

$$\frac{K}{aV} = 0{\cdot}74, \qquad \frac{h}{b} = 2{\cdot}0,$$

where b = breadth of the plate, and

V = undisturbed velocity at a distance in front of the plate.

Substituting these values in the above formulæ for the mean velocity distribution, this can be plotted across the channel. Subtracting this from the experimentally determined mean velocity distribution, we obtain the basic flow which is given by fig. 1, Curve III. This curve indicates that there is a distinct gradient of velocity over the region where the vortex trail exists, and this must be assumed to arise from that vorticity which exists in the fluid and has not been accounted for in the concentrated vortices of the Karman street. Where the centres of the vortex exist this basic velocity (fig. 1, Curve III.) would appear to have a gradient of approximately $-0{\cdot}3$.

The stability analysis must therefore be considered *de novo* without the assumption made by Glauert and others that there is a uniform distribution of velocity across a section. It will, in point of fact, be seen that with a basic distribution of the type we have derived from the analysis of the experimental results of Fage and Johansen the system is no longer stable.

Another point to be noticed is that the assumption that the vortices are circular eddies of constant velocity is by no means necessary in determining the basic flow, but was adopted here by reason of its simplicity. Any type of vortex could have been similarly dealt with, and so long as its area was such that it did not extend for any considerable distance over the centre of the channel the gradient in velocity would not be affected to any material extent. In any case which is at all consistent with the experimental results this gradient will be negative, and will persist of the same magnitude for a great distance down the channel, though ultimately damped out by the viscous action.

Returning to the stability investigation of a vortex street in a bounded fluid, we consider only that case which arises in practice, *i. e.*, the case when the street is confined to the more central portions of the channel. Under these circumstances the effect of the images on the arrangement has been shown by Glauert and Rosenhead to be negligible, and the following discussion will therefore deal only with the effect of the basic velocity in the channel upon the stability of the vortex street.

Take the axis of X down channel and the axis of Y in the plane of the motion at right angles to this. Assume that the basic velocity is steady and is given by

$$u = \mathrm{V}_0 f(y/\mathrm{H}).$$

The vortices are presumed to be moving down-stream in parallel rows situated along the lines $y = \pm h/2$. Then the fluid along these lines will be moving with velocity

$$u = \mathrm{V}_0 f\left(\frac{h}{2\mathrm{H}}\right),$$

due to the basic flow, and the vortices will be travelling down-stream with velocity

$$\mathrm{V}_0 f\left(\frac{h}{2\mathrm{H}}\right) - u_0,$$

where u_0 = velocity due to the mutual interaction of the

vortices, which is dependent upon their individual strength and the dimensions of the street.

If a vortex in the upper row receives a displacement β in the y direction, its velocity due to the general motion in the channel will be

$$u+\delta u = V_0 f\left(\frac{(h/2+\beta)}{H}\right) = V_0 f\left(\frac{h}{2H}\right) + \frac{\beta V_0}{H} f'\left(\frac{h}{2H}\right)$$

to first order in β.

The equations of motion of the displaced system of vortices, as found by Karman *, are :

$$\frac{2\pi a^2}{K}\frac{d\alpha}{dt} = -A\beta - B\alpha' - C\beta',$$

$$\frac{2\pi a^2}{K}\frac{d\beta}{dt} = -A\alpha - C\alpha' + B\beta',$$

where

$$A = \frac{1}{2}\phi(2\pi-\phi) - \frac{\pi^2}{\cosh^2 k\pi},$$

$$B = \text{pure imaginary} \qquad 0<\phi<2\pi,\ k=h/a,$$

$$C = \frac{\pi^2 \cosh k\phi}{\cosh^2 k\pi} - \frac{\pi\phi\cosh k(\pi-\phi)}{\cosh k\pi}.$$

Following the usual method we see that, when a basic velocity distribution is taken into account, to the first of the above equations of motion, a term,

$$-\frac{2\pi a^2}{K}\frac{V}{H} f'\left(\frac{h}{2H}\right)\beta,$$

must be added, due to the basic flow. This is negative, because the velocity producing the vortices is in the opposite direction to $\frac{d\alpha}{dt}$. Thus the equations of motion of the system in a bounded fluid, neglecting the image effects, become

$$\frac{2\pi a^2}{K}\frac{d\alpha}{dt} = -A\beta - B\alpha' - C\beta' - \frac{2\pi a^2}{K}\frac{V}{H} f'\left(\frac{h}{2H}\right)\beta,$$

$$\frac{2\pi a^2}{K}\frac{d\beta}{dt} = -A\alpha - C\alpha' + B\beta'.$$

For convenience, write

$$\theta^2 = \frac{2\pi a^2}{K}\frac{V}{H}, \quad \text{and} \quad f'\left(\frac{h}{2H}\right) = S.$$

* *Loc. cit.*

Hence θ^2 is a positive non-dimensional quantity, and $\frac{VS}{H}$ is the gradient of velocity across the lines $Y = \pm \frac{h}{2}$.

The previous equations can now be written

$$\frac{2\pi a^2}{K}\frac{d\alpha}{dt} = -(A+\theta^2 S)\beta - B\alpha' - C\beta',$$

$$\frac{2\pi a^2}{K}\frac{d\beta}{dt} = -A\alpha - C\alpha' + B\beta'.$$

These have two types of solution :

$$\text{(i.)} \quad \alpha = \alpha', \qquad \beta = -\beta',$$

$$\text{(ii.)} \quad \alpha = -\alpha', \qquad \beta = \beta',$$

and exponentials $e^{\lambda t}$ are involved, the corresponding values of λ being

$$\frac{2\pi a^2}{K}\lambda_1 = -B \pm \sqrt{(A+C)(A-C+\theta^2 S)},$$

$$\frac{2\pi a^2}{K}\lambda_2 = \quad B \pm \sqrt{(A-C)(A+C+\theta^2 S)}.$$

The coefficient B being purely imaginary, it follows that for stability both quantities under the root sign must be negative, *i. e.*,

$$\left.\begin{aligned}(A+C)(A-C+\theta^2 S) &\leq 0,\\ (A-C)(A+C+\theta^2 S) &\leq 0.\end{aligned}\right\} \quad 0 < \phi < 2\pi$$

These are the conditions for stability, and are analogous to Karman's single condition

$$A^2 - C^2 \leq 0, \qquad 0 < \phi < 2\pi.$$

Now, when ϕ is small,

$$A \doteqdot \pi\phi - \frac{\pi^2}{\cosh^2 k\pi},$$

$$C \doteqdot -\pi\phi + \frac{\pi^2}{\cosh^2 k\pi}.$$

Hence the condition

$$(A-C)(A+C+\theta^2 S) < 0$$

becomes

$$-\frac{2\pi^2}{\cosh^2 k\pi}\theta^2 S < 0.$$

But since S, the measure of the basic velocity gradient, is negative, the condition for stability is violated. It appears therefore that when the velocity gradient is negative there is no stable arrangement of the vortex street in the region remote from the walls. It may be remarked, however, that if the vortex street were wide enough, the effect of the images on the motion arising from any displacement of the original system would be, in a sense, contrary to that of the velocity gradient. Thus a possible stable arrangement may exist in which h is only slightly less than H, but this does not correspond to the practical case.

The instability of the vortex street in a channel in which the fluid is in motion past a fixed obstacle is, in fact, borne out by the measurements of Fage and Johansen, who at 5, 10, and 20 diameters behind the obstacle find spacing ratios h/a of 0·248, 0·381, 0·525, indicating a systematic spread of the vortex street.

In the light of the foregoing discussion it appears clear that the theoretical results obtained by Glauert and others on the assumption that the Karman arrangement is maintained stably and unimpaired in a flowing channel do not possess a valid physical basis.

The experiments of Karman and Rubach, on the other hand, were concerned with the motion of a body along a channel in which the fluid was at rest. In these, of course, the calculated arrangement was substantially verified at the particular value of Reynolds's number for their experiments.

XLV. *On the Damping of a Pendulum by Viscous Media (Aniline).* *By* F. E. Hoare, *M.Sc., A.R.C.S.**

Introduction.

In a former paper † the equation

$$\log\frac{a_0}{a_1} = K_1\sqrt{\frac{\eta T}{r^2\rho}} + K_2\cdot\frac{T^2}{xr^{3/2}}\,\frac{a_0-a_1}{\log\dfrac{a_0}{a_1}}$$

was deduced to represent the damping of the oscillation of a simple pendulum when the bob was immersed in water

* Communicated by Prof. F. H. Newman, D.Sc.
† Phil. Mag. ser. 7, viii. p. 899.

where the notation is as previously. The extent to which this equation is theoretically justified is difficult to estimate, but it represents the experimentally observed facts with a fair degree of accuracy, giving mean values for the viscosity η within a few per cent. of the correct value when the constants K_1 and K_2 have been found from the results obtained with one pendulum, and these values then used in conjunction with the results from other pendulums. It was suggested * that the physical meaning of K_1 and K_2 might be found from further experiments, using different liquids, and with that objective in view the following experiments have been made.

Experimental.

The experimental procedure followed was the same as that formerly employed. Three spheres, $1\frac{1}{2}$ in., $1\frac{3}{4}$ in., and 2 in. diameter, suspended by fine wires, were allowed to oscillate in aniline (kindly loaned by Messrs. Baird and Tatlock, London), this liquid being chosen as it has a comparatively high viscosity and can be obtained in a fairly pure condition. Each pendulum was allowed to oscillate first with a short period and then with a long period, the amplitude being observed after a few swings had been made (a_0) and then again after ten complete vibrations (a_1) for each value of the period. The method employed in reading the amplitudes with a telescope having proved very satisfactory in the previous experiments, it was again used in the present work.

Unfortunately, it was impossible to use such large quantities of aniline as of water, and consequently a much smaller containing vessel was used. The dimensions of this were 9 inches deep and 7 inches in diameter, the aniline nearly filling the vessel. These dimensions may be sufficiently small to necessitate a correction for enclosed space such as has been deduced by Stokes †; as, however, the correction of Stokes is obtained from the theory which starts from the assumption that the decay of amplitude is proportional to the velocity, and this assumption has been shown to be erroneous by the previous experiments, it was considered that there would be little justification in employing such a correction.

* *Loc. cit.*

† Stokes, Camb. Phil. Soc. ix. p. 8.

At the conclusion of the experiments the viscosity of the aniline was determined by the flow-tube, method using the Poiseuille formula. The result was in very good agreement with the value generally accepted *, and from this and a determination of the density at 11·3° C. it was concluded that the aniline was sufficiently pure to give results which should agree with the values already mentioned.

Results.

The method of testing the application of the equation is the same as in the previous work. Any two results were selected, actually in this case being the first observed result for the 2 in. sphere when vibrating with a long and short period, and these were used to calculate the values of K_1 and K_2 by substituting the correct values for η and the observed values of a_0 and a_1. Using these values for K_1 and K_2, the value of η for each of the results obtained with the different spheres was computed.

The values of the constants thus obtained are

$$K_1 = 5{\cdot}81,$$

$$K_2 = 6{\cdot}41,$$

the amplitude being measured in cms.

The density as determined at 11·3° C. was 1·02, grs. per c.c., and this value has been used throughout in the calculations.

The following table gives the mean value of the viscosity as determined, using the different spheres :—

Sphere.	T, secs.	Number of Observations.	Temp. ° C.	Mean value for η c.g.s.	True value for η c.g.s.
1½ in.....	2·56	6	14° C.	·0558	·0551
1½ „	3·64	6	10·4° C.	·0604	·0637
1¾ „	2·558	6	12·9° C.	0585	·0575
1¾ „	3·656	6	10·8° C.	·0600	·0627
2 „	2·57	6	12·7° C.	·0624	·0581
2 „	3·644	6	10·2° C.	·0637	·0645

* Kaye and Laby, 'Physical and Chemical Constants,' p. 30.

The values in the last column are obtained by interpolation from the values in Kaye and Laby's book of Constants.

Discussion of Results.

From these results it will be seen that in the case of each sphere the short-period observations give values for the viscosity which are too high, and the long-period observations values which are too low. This systematic variation from the true result can, perhaps, be attributed to three causes. The first and most obvious is some defect in the proposed equation which was not apparent when dealing with water. The second cause may be that aniline is hygroscopic and that during the course of the experiments the viscosity gradually decreased. As all the short-period results were taken first this would account in part for the systematic error, but it would probably be of a smaller magnitude than that indicated. Lastly, there is the neglect of any correction for the enclosed space, and this might be some function of the time of swing.

The values of the constants K_1 and K_2 obtained in the case of water and in the case of aniline do not suggest any simple relation connecting them with other properties of the liquid which might have been expected, and until the mathematical theory is rigorously developed to take into account the term which represents the damping due to the square of the velocity more experimental work will be of little use.

XLVI. *Positive and Negative Photophoresis of Colloidal Particles in Aqueous Solutions. By* Wilfred W. Barkas, *M.Sc.**

IN a previous paper (Phil. Mag. vol. ii. pp. 1019–26, 1926) experiments are described which seem to show the phenomemon of photophoresis in aqueous solutions. If suspensions of copper, silver, gold, or gamboge, set up in a rectangular glass cell (some 10 cm. square and 1 cm. thick) are allowed to settle in the dark for

* Communicated by Prof. A. W. Porter, F.R.S.

several hours, the falling particles (if of sufficient size to settle out) form a horizontal cloud surface some few millimetres below the surface of the liquid. When the cell is illuminated through one of its edges and viewed through the flat faces, it is found after a time that the cloud surface is no longer horizontal, the particles appearing to drift towards the source of light and to heap themselves up on the light side of the cell. The cloud surface takes up a characteristic formation, while the boundary to the cloud in the suspending medium becomes very sharply defined.

The present paper divides itself into two sections: the first deals with further experiments similar to those described in the former paper with modifications of the apparatus, the second with observations made on separate particles in the ultramicroscope.

I. Cloud-drift Experiments.

The glass cell chosen was smaller than before, being about 4 cm. square and 0·8 cm. in thickness. The top of the cell was closed by means of a glass plate, held in place by a tightly-fitting cap of celluloid, enabling the cell to be totally immersed in a thermostat tank. The tank was of plate glass about 20×6 cm. and 16 cm. deep. The cell was placed cross-wise in the tank so that it could be illuminated through only 1 cm. of water, and viewed from one end of the tank. Instead of a lamp heater, a coil of resistance wire (immersed in a thin test-tube full of paraffin oil) was used, and the control and stirrer were designed so as not to obstruct the view of the cell. It was found that the temperature could be kept constant to 0·3° C. in the neighbourhood of 18° to 25° C. The whole tank was placed in a light-tight box about 25 cm. cube made with square openings in its four faces into which could be fitted opaque stops to control the illumination of the cell. The stirrer and control leads entered through a hole in the lid of the box, the stirrer not being connected with the table in any way, so that vibrations of the motor were avoided.

The source of illumination was, as before, a pointolite placed about one metre away, the beam being focussed (after passing through a thick cooling cell) by means of an achromatic lens. This part of the apparatus was mounted

so that it could be easily moved from one side of the tank to the other.

With these precautions it was considered that extraneous disturbances such as temperature changes and vibrations would be eliminated. Under these conditions the former experiments on suspensions of gold, silver, and gamboge were repeated with results identical with those described before.

The following tests were made to determine if the effect was due to convection currents in the liquid.

(A) Removing the cooling cell and concentrating the beam of light into the body of the suspension usually set up true convection currents. These always took up a spiral formation, there being usually more than one centre of convection. The cloud, which was previously horizontal, became churned up and very irregular in optical density. The final condition of the suspension was one of complete mixing, *i. e.* there was no tendency, once convection had occurred, for the cloud to take up the stable and characteristic form described before.

(B) A test was made on a cloud of true solution. The cell was filled with water and a few crystals of potassium permanganate were dropped into it. This was set up in the thermostat and allowed to stand until the permanganate solution had diffused up as a horizontal cloud of decreasing density but of fairly sharp upper boundary. On illuminating the cell in the usual way, no sign of movement of the cloud could be observed after two hours' exposure. On removing the cooling cell and concentrating the beam, convection currents were observed as described in the previous section.

(C) On varying the thickness of the cooling cell, no change in the speed of cloud formation could be observed unless true convection currents occurred.

Further, it should be noticed that the phenomenon was first observed in the case of a suspension set up in a room containing several windows which were illuminated in turn in the course of the day. The cloud always followed the brightest window, though no sunlight fell on the cell itself at any time. It seems unlikely that there could be sufficient temperature gradient across the cell, in this case, to affect the particles.

It would seem therefore, from the results of the above tests, that convection is not the primary cause of the phenomenon.

Intensity of Illumination.

On reducing the intensity of the light on the cell, a point is reached where no photophoresis occurs, even after prolonged exposure. At this stage the photophoretic effect is completely masked by the brownian diffusion of the particles. It is this diffusion which causes the cloud to reassume its former horizontal form after the light has been extinguished.

Colour of Illumination.

No very satisfactory results could be obtained for the drifting of particles under monochromatic illumination, either by the use of filters or by selecting a band of wave-lengths from the spectrum. Presumably the intensity of such a selected beam was not sufficient to overcome the diffusion of the particles. In one instance, however, with a purple gold sol, very slow cloud-drift was obtained with both red and green filters, the direction being negative on Ehrenhaft's convention in each case *. The filters were judged (visually) to be of approximately equal optical density. Thinner filters produced more rapid cloud formation.

Ultra-violet light from a mercury arc was also used. No definite results could be obtained, however, even when the cell was removed from the thermostat tank to avoid absorption by the water. Since photophoresis occurs under X-ray illumination, we may suppose that an insufficient intensity of light was the cause of the null results.

It is hoped to undertake further work in this connexion.

Positive Photophoresis in Liquids.

In the sols so far tried, namely gold, silver, copper, and gamboge, the photophoresis is in each case negative, *i.e.* the motion is towards the source of light. It was found, however, that an oil suspension (prepared by stirring a solution of paraffin oil in alcohol into a large volume of

* *Phys. Zeits.* xviii. pp. 352–368 (1917); *Ann. d. Phys.* no. 10, pp. 81–132 (1918).

water) showed equally marked positive photophoresis, the cloud drifting away from the source of light. This is the only instance so far observed of positive photophoresis in aqueous suspensions. The oil particles being lighter than water, rise upwards from the bottom of the cell and, on illumination, move over to the top corner away from the source of light. Owing to the white colour of the suspension it is not possible to photograph the cloud, but the formation is exactly similar to the case of negative drift reversed, of course, in direction (fig. 1).

II. Microscopic Observations.

In order to observe the drift in separate particles, a modification of the Zsigmondy ultramicroscope was first used (fig. 2). Light from the slit was concentrated through the second lens, in the usual way, and reflected down

Fig. 1.

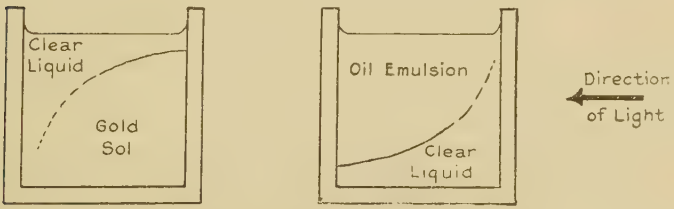

Cloud formation after action of light.

vertically into a low-power condensing objective (O) which brought the light to a focus some 3 cm. distant from the front face. On the front lens was fixed a small silvered right-angled prism which turned the light-beam horizontal. The objective and the prism could be rotated through 180° about a vertical axis, thus sending the beam either right or left as desired. The cell (C) was a one-piece glass trough 1 cm. in length with optical glass ends. This was placed vertically below O and was illuminated by means of the two prisms (P_2 and P_2') placed one on each side of C, as shown in fig. 2. The cell was viewed through the microscope placed with its axis horizontal, the focus of the light being coincident with the axis of the microscope. (The microscope objective is indicated by a dotted circle in the figure.) The prisms P_2 and P_2' were mounted on the stage of the microscope, whose usual adjustments allowed for the necessary centring of the light-beam, while

the cell was mounted on a bracket passing back through the centre of the stage and connected to the condenser mount of the substage. By these means it was possible to change the direction of the light by a simple rotation of the objective " O " through 180°, no re-focussing being necessary. The whole of this portion of the apparatus was heavily lagged with cotton-wool to shield it from external temperature changes.

The eyepiece contained a squared graticule placed so that one set of lines was parallel to the light-beam.

Fig. 2.

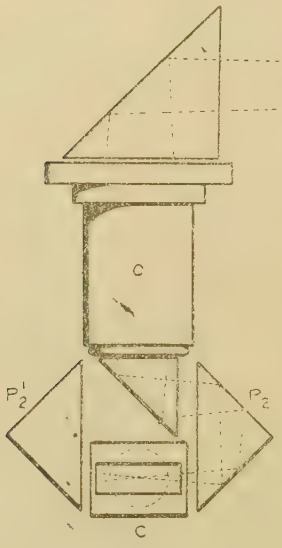

First method of illumination.

The suspensions used were of the same materials as before, but were not identical with the former ones, for the following reasons :—First, the concentrations suitable for viewing in the ultramicroscope were necessarily much lower than those used in section I. As a result the solution was not sufficiently concentrated for the cloud to be seen with the naked eye, and hence no estimate could be made of the distance below the free cloud surface at which the observations were made. Secondly, owing to the somewhat delicate adjustments required for setting up a

solution for viewing, it was not practicable to use a suspension which settled out under gravity. Hence only such suspensions were used as remained indefinitely in suspension, or whose rates of sedimentation were extremely slow. In the case of the large-scale experiments, it was found that no free cloud surface was formed on illuminating a suspension of non-settling particles. This does not mean, however, that no motion of the particles would take place along the path of a restricted beam of light, as an equal and opposite motion would be possible, by diffusion, in the un-illuminated parts of the cell, tending to equalize the distribution throughout the solution. In the microscope the illumination is restricted to a narrow beam in the centre of the cell, so that the motion, if observed, would be due to the action of the light, as the back diffusion would take place outside the field of view.

Owing to the rapid brownian movement of the particles, no general drift can be observed in the microscope, and it becomes necessary to follow a large number of particles and average the results.

The first method adopted was to observe the time taken by any particle to move one square up or down the light-beam. The light was changed in direction after every three or four observations to avoid any tendency to static equilibrium of the cloud under the action of the light.

Preliminary tests on silver particles gave, in general, a larger number going upstream (negative photophoresis) than in the opposite direction, while the average velocity of both groups of particles was very nearly equal. In quantitative measurements the following results may be cited as typical :—

TABLE I.

Sol.	No. of particles moving one square.		Velocity in cm./sec. $\times 10^4$.		Ratio of numbers.	Ratio of velocities.
	+ve.	−ve.	+ve.	−ve.		
Gold	124	148	1·26	1·41	1·19−ve	1·12−ve
Paraffin oil ...	42	39	3·9	3·52	1·07+ve	1·11+ve

In many cases, however, the ratio of the numbers and the velocities were not both of a sign corresponding to

the large-scale experiments, and it soon became apparent that there were several disadvantages in this method of measurement. These were :—(1) The average velocity of the cloud as a whole, apart from the brownian motion, could not be calculated because, unless the time of observation is the same for all particles, the probable distance moved under the molecular bombardment alone will not be the same for all particles. (2) There is no direct means of obtaining a measure of the radius of the particles observed. (3) The time taken for a particle to cross one square in the eyepiece is, in some cases, several minutes, which makes the observation of large numbers of particles very tedious. Larger magnifications could not conveniently be used. Finally (4), owing to the size of the cell required for transverse illumination, the possibility of small convection currents could not be overlooked.

For these reasons the method of observation was changed, and at the same time the apparatus was modified to the use of a Zeiss dark-ground cardioid condenser, the microscope this time being vertical.

The light from the arc was rendered accurately parallel by means of the usual two bench lenses of the ultramicroscope. It issued as a horizontal beam of about 1·5 cm. diameter, and was reflected through a right angle on to the underside of the cardioid (fig. 3), giving the usual dark-ground illumination in a cell (C) about 0·2 mm. deep placed on the microscope stage. The walls of this cell were made of strips of cover-slip mounted on the slide in the form of a square about 1 cm. side. These were smeared with vaseline and the cell filled with the solution. It was sealed by a full-sized cover-slip pressed down lightly from above to remove the excess liquid. The horizontal position of the cell and its extreme thinness assured a minimum of convection currents in the liquid.

Since the cardioid condenser gives a flat cone of illumination, a particle, viewed along the axis of the cone, is equally illuminated on all sides. In order to introduce unidirectional illumination, a circular diaphragm (D) having a single radial slit (S) about 1 mm. wide was placed in the position of the usual iris diaphragm, under the cardioid, on the substage of the microscope. When in position, a small segment only of the annular aperture of the cardoid was illuminated, and, by rotating the stop, the ray could be made to enter the cell from any desired

direction. The substage could be swung out when full illumination was desired.

The ray actually enters the cell at an angle of 40° to the horizontal, but, by racking the microscope, any portion of the ray in the field of view could be brought into focus.

All observations were made at a height of 0·1 mm. above the bottom of the cell, or, more accurately, each observation was begun at this point, though the subsequent movement of the particle necessitated constant focussing. In order to ensure that the apex of the light-cone should be at this point, it was necessary to be able to rack the cardioid slightly without breaking the film of immersion oil between

Fig. 3.

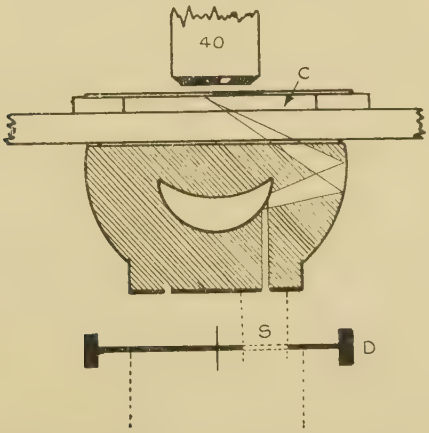

Second method of illumination. Cross-section of cardioid condenser with stop for unidirectional illumination.

it and the slide. As the usual cedar-wood oil becomes very viscous on prolonged exposure, it was replaced in these experiments by santal oil (index of refraction 1·506), which was found to remain mobile indefinitely.

A 30° thermometer was mounted with its bulb as near as possible to the cell, and the whole lagged round with cotton-wool.

In order to facilitate timing, a small square of glass was mounted on the top lens of the eyepiece at 45° to the axis, while the stop-watch was placed some 50 cm. away in such a position that it could be seen as a faint "Pepper's Ghost" superimposed on the image of the

particles. The light falling on the watch could be controlled.

A Zeiss 40 objective and a ×12 eyepiece were used, one side of the eyepiece squares being equivalent to $8{\cdot}33 \times 10^{-4}$ cm., the microscope tube being considerably extended to facilitate viewing.

With this apparatus a particle could be viewed for any desired time. The time chosen throughout the experiments was half a minute. Focussing the microscope to 0·1 mm. above the bottom of the cell, the stop-watch was started at an instant when any particle happened to be under a cross in the eyepiece, and at the end of half a minute its position relative to the cross in question was recorded on squared paper. The direction of the light was reversed after every three or four observations, separate records being taken of the movements of particles under these two directions of illumination. The X axis was taken parallel to the light-beam, the positive direction being that of the light.

From these records the following calculations were made :—

Radius of the Particles.

The radius (a) of a particle moving under molecular bombardment is connected with the average square of the distance moved $\bar{S}^2$ in time t secs. by the equation of Einstein and Smoluchowski :

$$a = \frac{RTt}{3\pi N \eta \bar{S}^2},$$

where η = the viscosity of the suspending medium, T = the absolute temperature, while N and R have their usual significance.

In the case of full illumination, the displacements may be taken parallel to any coordinates. In the case of unidirectional illumination, the displacements at right angles to the light-beam only were taken (Y^2).

Cloud Velocity.

Neglecting for the moment the brownian movement and any possible drifting of the solution as a whole, due to convection currents, we take the displacements parallel to the light-beam, making the sign of the displacement correspond to the direction of the light.

Suppose n_+ particles move, in the positive direction, an average distance x_+, and n_- particles move, in the negative direction, an average distance x_-, then the distance moved by the cloud of particles as a whole will be given by the displacement of an imaginary partition in the cloud which moves such that the average concentration of particles either side of it remains equal. If we take X to be this displacement, we have that

$$n_+(x_+ - X) = n_-(x_- + X).$$

Since X is the distance moved in t secs., the velocity of the cloud, V_c, relative to the light is given by $V_c = X/t$.

(Since the motion perpendicular to the light-beam is supposed to be independent of the light, we need only consider the linear distribution of the particles along the X axis.)

The brownian motion of the particles, being independent of the light, should, on the average, give no displacement of the cloud as a whole, while any convection drift should be eliminated, provided an equal number of observations are made for each direction of the light. No static equilibrium of the cloud is to be expected when the direction of the light is constantly changed. We may, however, calculate the velocity of the cloud, parallel to the coordinate axes, due to accidental convection currents, by use of the above analysis, provided we take the sign of the displacements relative to the cell and not relative to the direction of the light. These results are also entered in Table II. It will be seen that these velocities are in every case very much less than the photophoretic velocity, except in the case of paraffin oil, where it is about one-half.

Force acting on the Particles.

Since the force (F) required to impart a velocity (v) on a particle of radius (a) moving in a fluid of viscosity (η) is given by

$$F = 6\pi\eta a v,$$

we may obtain this force from the calculated values of "a" and V as given above, or directly from the observations of Y and $\overline{X}$ giving

$$F = \frac{2RTX}{NY^2},$$

which is independent of the viscosity of the liquid.

Since, however, the light-beam enters the cell at an angle of 40° to the focal plane of the microscope, the values of the force given above must be multiplied by secant 40° (1·307) to give the force acting along the light-beam necessary to produce the observed velocity in the focal plane.

Pressure acting.

Assuming that the force acts parallel to the light-beam, we may obtain the pressure acting as

$$P = F/\pi a^2.$$

In terms of the actual observations made, this is $P = 6\eta v/a$, or

$$P = \frac{18\pi N\eta^2}{RT} \cdot \frac{\bar{X}}{t} \cdot \frac{\bar{Y}^2}{t}.$$

P being proportional to η^2, any error in the measurement of the temperature will cause a large error in the value of the pressure.

Results.

The results are tabulated in Table II.

Columns 3 and 4 give the number of particles observed and their average velocities in positive and negative directions. The velocities are given in squares per half minute.

Column 5 gives the velocities of the cloud in cm./sec. $\times 10^6$, the sign being relative to the direction of the light.

Columns 6 and 7 give the velocities of the cloud along the X and Y axes respectively in cm./sec. $\times 10^6$ relative to the cell and independent of the direction of the light. These are the convection velocities.

Column 8 gives the mean square of the displacements in half a minute (in terms of the eyepiece scale) perpendicular to the light.

Column 9 shows the average value of the radius of the particles (in cm. $\times 10^5$) calculated from these displacements or by other means.

Columns 10 and 11 give the force (in dynes $\times 10^{11}$) and the pressure respectively.

In the first experiments A, B, and C the method of recording did not permit of obtaining the convection-

TABLE II.

1.	2.	3.		4.		5.	6.	7.	8.	9.	10.	11.
	Number of particles.	x_+.	n_+.	x_-.	n_-.	Photophoretic velocity (cm./sec. $\times 10^6$).	Convection along X axis (cm./sec. $\times 10^6$).	Convection along Y axis (cm./sec. $\times 10^6$).	Mean square of displacement (Y axis).	Mean radius, cm. $\times 10^5$.	Force acting, dynes $\times 10^{11}$.	Pressure, dynes/sq. cm.
(A) Gamboge uncentrifuged.	55	0·459	23	0·566	32	−5·99	—	—	0·35	1·91	−3·22	−·0281
(B) Silver	78	0·631	33	0·674	45	−5·32	—	—	0·498	1·34	−2·09	−·0361
(C) Gold No. 2	60	0·592	25	0·548	35	3·25		—	0·531	1·26	−1·15	−·0232
Ditto	52	0·562	21	0·490	31	−2·90	—	—	0·405	1·69	−1·42	−·0157
(D) Gold No. 1	130	0·358	62	0·418	68	−1·64	0·113 (right)	0·482 (up)	0·336	1·99	−0·917	−·0075
(E) Gamboge centrifuged.	105	0·707	43	0·708	62	−3·56	0·159 (right)	0·213 (down)	0·731	2·68	−2·28	−·0111
Ditto, with full illumination to test size only									0·689	2·82		
Ditto, size given by method of fractional centrifuging										approx. 2·64		
(F) Paraffin oil	84	0·737	51	0·725	33	+4·54	1·89 (left)	2·86 (up)	0·734	2·65	+2·26	+·0141
Ditto, with full illumination to test size only									0·883	2·26		
Ditto (fresh sample).	82	0·715	48	0·742	34	+3·09	0·17 (right)	2·70 (up)	0·782	2·49	+1·75	+·0093
Ditto, with full illumination to test size only									0·855	2·45		

current velocities. This was remedied in the later experiments.

Expt. E.—A centrifuged suspension of gamboge was used and the values of the radius compared. From the centrifuge the radius should be in the neighbourhood of $2{\cdot}64 \times 10^{-5}$ cm.

Expt. F.—Two samples of the same suspension. The results show the positive photophoresis in paraffin oil.

These results all confirm the indications given in the large-scale experiments in section 1. and in the previous paper *, and show that, on the average, migration of the particles does in fact take place under the action of the light. The actual velocities of the cloud appear, however, to be much less than those calculated in the previous paper. On the other hand, the velocity of cloud-drift, in the large-scale experiments calculated from the motion of the upper surface of the cloud, is a maximum value, and must vary from this value near the surface of the cloud down to zero for points near the bottom of the cell.

Comparing these results with those found by Ehrenhaft for photophoresis in gases, we see that in the case of gold and silver the motion in water is opposite to that in air. In a particular case among his results † silver particles of radius $1{\cdot}36 \times 10^{-5}$ cm. are used, and these are sufficiently close to those given in Expt. B above to afford a comparison. Owing to the different viscosities of nitrogen and water, we should not expect the same velocities in the two cases, but for the forces acting we have :—

Silver particles.	Radius.	Force.
In nitrogen (Ehrenhaft)	$1{\cdot}39 \times 10^{-5}$ cm.	$19{\cdot}83 \times 10^{-11}$ dyne.
In water (Barkas).....	$1{\cdot}34 \times 10^{-5}$ cm.	$2{\cdot}09 \times 10^{-11}$ dyne.

Making allowances for the smaller intensity of illumination from the cardioid condenser as compared with that of the true ultramicroscope as used by Ehrenhaft, we may say that the forces involved in the two cases are of the same order of magnitude, though of opposite sign.

* *Loc. cit.*

† *Phys. Zeits.* xviii. p. 353 (1917).

The aim of the present paper, however, is principally to show that both positive and negative photophoresis occur in liquids, and to support the view that the observed motions are not due to convection currents in the suspending liquid as a whole. The number of particles observed in the experiments of section II. is not sufficient to yield very accurate quantitative values of the radius of the particles, but even on this number the *direction* of the cloud-drift is quite definite.

My thanks are due to Professor A. W. Porter, F.R.S., and to Professor E. N. da C. Andrade, D.Sc., for their assistance in connexion with the above work.

Carey Foster Laboratories,
University of London,
University College,
Nov. 1929.

XLVII.—*The Band Spectra of Cadmium and Bismuth.* *By* S. Barratt *and* A. R. Bonar, *Department of Chemistry, University College, London* *.

THE difficulties often encountered in discovering the nature of the molecule responsible for a new band spectrum are well evidenced by the frequent controversies to be found in spectroscopic literature over problems of this type. To the list of spectra of elusive origin must certainly be added the absorption-band spectra which are developed in the vapour of cadmium metal when the specimen is of the usual grade of purity. These bands, which have several times been employed in the calculation of the heat of formation of the cadmium molecule, etc., were first described by Mohler and Moore (J. Opt. Soc. Amer. xv. p. 74. 1927), who distinguished several band groups in the spectrum, and attributed them all (with a reservation in respect of two) to a cadmium molecule of the type Cd_2. In a subsequent paper (J. M. Walter and S. Barratt, Proc. Roy. Soc., A, cxxii. p. 201, 1929) experiments were described which indicated that six of the seven groups were due to the presence of impurities, only Group I. of Mohler and Moore at λ 2212 being a true cadmium

* Communicated by the Authors.

spectrum. This conclusion was reached as the result of two series of observations :—

(1) Specimens of cadmium from different sources show large variations in the relative intensities of the band groups, while it is possible to suppress all the spectra (except Group I.) by adding to the cadmium vapour a trace of an alkali metal, the addition leaving unaffected both Group I. and the atomic absorption. The alkali metal presumably combines in a preferential way with the impurities, yielding compounds which are either non-volatile or possess no absorption in the regions under examination.

(2) The various groups of bands can be individually intensified by adding to the vapour further quantities of certain impurities.

As the result of such experiments Groups III., IV., and V. of Mohler and Moore (lying between λ 3181 and λ 3018) were attributed to a compound of cadmium and chlorine, probably the subchloride CdCl. This conclusion has been amply confirmed in this laboratory by further work, which will shortly be ready for publication, on the cadmium subhalide spectra. Groups VI. and VII. (between λ 3323 and λ 3182) were attributed to the absorption of thallous chloride vapour, present as an impurity in the cadmium. At that time this spectrum was otherwise unknown, but it has since been very fully examined (as the thallous chloride spectrum) by K. Burkow (*Zeitschrift für Physik*, lviii. p. 232, 1929), and we now have ourselves many plates of the spectrum, recorded from pure thallous chloride vapour, showing no trace of cadmium absorption *. It would therefore seem that the origins suggested in the previous paper for Groups III. to VII. are no longer open to serious question.

Group II. of Mohler and Moore (λ 2856–λ 2644) is of greater interest, but we believe that the new facts concerning this spectrum, which are detailed below, fix its origin

* R. K. Waring (Phys. Rev. xxxii. p. 435, 1928) has described this same spectrum as the mercury-thallium spectrum, as he observed it in the absorption spectrum of the vapours of a mercury thallium mixture. Thallium metal, unless specially treated, always contains traces of chlorine, which are quite sufficient to account for this observation. The agreement between his measurements on the bands and those of the authors quoted above is quite satisfactory.

with a reasonable degree of certainty. The origin previously suggested for this spectrum (Walter and Barratt, *loc. cit.*) was the molecule of a cadmium-oxygen compound, not the normal oxide, but possibly one of the type Cd_2O. The experimental evidence for this suggestion was the enhancement of the spectrum caused by the addition of cadmium oxide to the metal in the furnace-tube. It was never found possible, even so, to obtain this band group in the intense development reached by the others (*e. g.*, the CdCl bands) on addition of appropriate impurities. This, it was thought at the time, might indicate instability of the suboxide molecule, but it is now realized that the facts have a far more simple explanation. The same spectrum was ascribed by A. Jablonski (*Bull. Acad. Pol.* p. 163, 1928, and *C. R. Soc. Pol. de Phys.* iii. p. 357, 1928) to the same origin as that which had been assigned to it by Mohler and Moore, namely the Cd_2 molecule, and this conclusion he has recently reaffirmed (*Z. Physik*, lvii. p. 692, 1929). He observed the spectrum both in absorption and in fluorescence. It may also be mentioned that this same spectrum has been described by R. K. Waring (*loc. cit.*) as the spectrum of an indium-cadmium molecule. The conclusion is obviously erroneous, as the spectrum has been obtained by three other workers without the intervention of indium; but the observation is not without interest in view of the results described below. The wave-length comparison in the table leaves no doubt of the identity of Waring's spectrum with that under discussion.

While we had satisfied ourselves, by the experiments described in the previous paper, that this band system was not due to a cadmium molecule, irregularities in the enhancement caused by addition of the oxide to the vapours finally led us to suspect that the hypothesis of a cadmium suboxide molecule was in error. It seemed that the spectrum must be caused by some unsuspected impurity in the cadmium, which was also present, but probably in greater concentration, in the cadmium oxide which we had been using. We made many attempts to produce this spectrum in absorption along the lines suggested by this view, and we finally obtained it from the vapour of a specimen of elementary arsenic in the total absence of cadmium. The same plates, however, also showed the line absorption of bismuth, and, following up

this indication, we were naturally led to examine the behaviour of pure bismuth itself. The vapour of this metal at above 800° C. gave the spectrum in such great intensity that it was evident that its real origin had at last been traced. There was no record whatever of the

Table of Wave-lengths in the Bi_n Spectrum (or "Cd_2" Spectrum).

Mohler & Moore. Cd_2.	Jablonski. Cd_2.	Waring. In-Cd.	(W. & B. Cd+O). B. & B. Bi_n.	Narayan & Rao. Bi_n.
—	—	—	2856	2859·9
—	—	—	2844	2842·9
—	2825	—	2825	2828·2
—	2810	—	2810	2813·5
—	2795	2800·2	2797	2799·8
2781	2781	2787·9	2783	2785·0
2767	2767	2776·3	2769	2772·7
2756	2755	2753·0	2756	2759·6
2745	2745	2741·1	2745	2744·8
2736	2736	2739·7	2732	2732·6
2726	2727	2729·8	2721	2722·0
2709	2708	2712·4	2710	2712·3
2701	2700	2705·5	2699	2701·9
2694	2694	2694·2	2690	2693·2
2680	2678	2684·2	2679	2681·5
2673	2672	2672·1	2673	2670·0
2659	2659	2661·4	2660	—
2653	2654	2652·8	2652	—
—	2646	—	2644	—

sensitive cadmium line λ 3261 on these photographs. We next re-examined all the plates obtained in the earlier experiments which recorded the bands in question, and upon each one was found the bismuth atomic absorption line λ 3067. Further, fortunately the bismuth band spectra have been previously described, so that immediate confirmatory evidence of our conclusion was available. The ultra-violet absorption bands of bismuth, as listed by

Narayan and Rao (Phil. Mag. l. p. 645, 1925), agree quite well with the measurements on this elusive spectrum made by all the authors mentioned above. We have reproduced the individual wave-length estimates in the following table in order that the identity of the spectra may not be in doubt. If the diffuse nature of the bands be taken into consideration, the agreement between the various observers is most satisfactory.

The wave-length lists are almost complete in each case, except that Jablonski has recorded several additional bands on the short wave-length side, which have not otherwise been measured, and therefore do not assist the comparison.

Our experimental conclusion in respect of these bands may be summarized as follows * :—

(1) Conditions can be maintained under which the bands do not appear in dense cadmium vapour.

(2) When the bands are recorded from cadmium vapour so is the bismuth absorption line λ 3067.

(3) The bands are developed at great intensity in the absorption spectra of bismuth vapour when the sensitive cadmium line λ 3261 is absent.

It is only possible to infer that the bands arise from a molecule of bismuth itself or of a bismuth compound. We have examined the behaviour of several specimens of bismuth, and the effects of atmospheres of argon and hydrogen on the spectrum, and also the effect of addition of small quantities of potassium to the absorbing vapours, without detecting any anomaly in the relative intensities of the bands and of the atomic bismuth lines. While the past history of the spectrum inclines one to caution in stating any opinion as to its origin, we believe on the above grounds that it is a true bismuth molecular spectrum. The complexity of the molecule is a more uncertain matter, but having due regard to the very low partial pressures of bismuth at which the bands are observable, it is a reasonable hypothesis that the molecule is Bi_2. There is a second extensive absorption-band system of bismuth. It

* We have thought it unnecessary to give any account of the apparatus used in our experiments, as it remained unchanged from that which has been described in the earlier paper from this laboratory.

is situated in the visible region, and only develops at much higher temperatures than does the system under discussion. These visible bands may possibly be due to a bismuth molecule of greater molecular weight which only appears at higher vapour pressures.

The enhancement of the bands which we found to follow upon additions of cadmium oxide was evidently purely accidental in nature, and was due to the presence of bismuth as impurity in the specimen of cadmium oxide upon which we drew.

The band system, as an inspection of the frequency differences shows, converges towards a short wave-length limit. This convergence limit is given by Jakimski, who has measured the spectrum further in this direction than any of the other observers, as λ 2561. If we assume (1) that the molecule from which the bands originate is Bi_2, and (2) that on dissociation the molecule breaks up into one normal atom and one in the excited state associated with the "raie ultime" of bismuth, λ 3067, then we can calculate in a simple fashion the heat of formation of the molecule. The numerical value so obtained is 0·80 volt, or 18·5 Kg. cals. per gm. mol., which is quite a probable figure for a molecule of this type.

Two of the other spectra discussed in the earlier paper (Walter and Barratt, *loc. cit.*) were assigned to associations of oxygen with zinc and mercury respectively. In view of the present results it would seem not improbable that these spectra also are really due to traces of impurities which have not as yet been recognised. We have continued our attempts to identify them, but so far unsuccessfully, and the spectra would certainly repay further examination. The present investigation will suffice to show that the ultimate conclusions may be quite unexpected ones.

Summary.

(1) A band spectrum hitherto assumed to be that of a cadmium molecule is shown to be due to bismuth.

(2) On certain assumptions as to the nature of the bismuth molecule its heat of formation is estimated at **18·5 Kg. cals.**

XLVIII. *Precision Measurements of X-Ray Reflexion from Crystal Powders.*

To the Editors of the Philosophical Magazine.

GENTLEMEN,—

I AM greatly obliged to Mr. M. Luther Fuller for a letter in the October number of the Philosophical Magazine* where he communicates the result of a new determination of the lattice spacing of cadmium oxide by Pierre van Dyck which agrees closely with the value given by Adamson and myself†, when we proposed cadmium oxide as a standardizing substance for X-ray powder measurements. When determining the lattice constant we investigated whether the difference between our value 4·683 and the result of the previous determinations by Davey and Hoffmann‡ and by Sherrer§ both giving 4·72 could be attributed to impurities. Powders taken with specimens from different sources and with different degree of purity agreed within the limits of error, and it is very gratifying to find that the new determination by van Dyck with extremely pure cadmium oxide prepared from vacuum distilled cadmium gives 4·685, which again agrees with our value within the limits of error. Mr. Fuller mentions that a determination by van Dyck with pure commercial cadmium oxide gave the same value too.

Mr. van Dyck used a standard Davey apparatus with a powder rod, while we used the focussing method described by one of us‖, and the main object of Mr. Luther Fuller's letter is to point to the agreement between the results, in order to show that the methods are equally precise. I fully agree with him in believing that there is no case for claiming the general superiority of one or the other arrangement. On the other hand, the comparison of particular results offers but a limited opportunity for comparing the merits of different methods. In fact, the

* M. Luther Fuller, Phil. Mag. viii. p. 585 (1929).

† J. Duane and J. Adamson, Phil. Mag. vii. p. 507 (1929).

‡ W. P. Davey and E. C. Hoffmann, Phys. Rev. xx. p. [illegible] (1922).

§ P. Scherrer, Zeits. f. Kryst. lvi. p. [illegible] (1921).

‖ J. Duane, Proc. Phys. Soc. Lond. xxxvii. p. 184 (1925).

precision attained will largely depend on the particular experimental conditions, unless an attempt is made to obtain the greatest possible accuracy, which was not done here. The practical purpose of determining whether one or the other arrangement is better suited in any definite case may therefore be served by indicating some points which lead to a certain differentiation.

The features and merits of the simple arrangement possible with a powder rod, giving at one time a record over the greatest angular range and requiring a very small quantity of powder, are well known.

The focussing method, on the other hand, has been developed to meet definite requirements, for which other methods are not so well adapted; namely, the quantitative measurement of intensities and the exact evaluation of angles of deflexion, in particular, in the region of smaller angles. For quantitative intensity measurements it introduces such relations that the evaluation of relative intensities or different reflexions becomes independent of the dimensions and of the absorption coefficient of the particular powder specimen *. For the measurement of angles very sharp symmetric lines can be obtained with wide incident beams for any angle of deflexion, and in particular, by placing the photographic film further away from the powder than the entrance slit of the camera, the distance of the recording film can be increased without too great a loss of intensity. This leads to a reduction of the times of exposure, where the evaluation can be derived from the record of a small angular range; for instance, in determining the lattice constant of cadmium oxide the diameter of the beam falling on the powder was 6 mm., corresponding to an angular width of 2·8°, and the lines measured, viz., 400, 331, 420, 422, 333 for cadmium oxide, and 422, 333, 442, 440, 531, 600, 620 for sodium chloride, were comprised within a range of glancing angles ϑ of 19° for Cu Kα radiation. Again, we can avail ourselves of the focussing condition in order to stress the accuracy of the measurements in the region of small angles of deflexion, the advantage being that the simpler pattern of lines generally found for smaller angles and smaller indices is better adapted for identification than the more complex pattern at

* J. Brentano, Phil. Mag. vi. p. 178 (1928).

larger angles; for instance, in determining the spacing and the rhombohedral angle of carbonates *, the measurements were carried out in an angular range which comprised the first reflexions and did not extend to angles greater than $\theta=47°$. The determination of the rhombohedral angle depends on small changes in the relative position of individual lines, and it would not have been easy to obtain the necessary accuracy for small angles without recurring to focussing. Here the identification of lines at large angles was difficult when several carbonates were present as impurities.

In the second part of his letter Mr. Luther Fuller endorses our proposal of using cadmium oxide as standardizing substance, and says that he had found that cadmium oxide lines were particularly sharp, sharper than the lines from sodium chloride. Our own finding was that the lines from cadmium oxide were slightly, but distinctly, broadened. This diversity may depend on the particular state of the specimens, although in our experiments the broadening has appeared to be a feature of all specimens examined, and Mr. Luther Fuller has certainly experimented with samples from different sources too. It may also depend on the characteristics of the methods we have outlined above: the practical application of the powder-rod method leading to derive a determination from the measurement of a great number of reflexions and to lay less stress on obtaining great sharpness of the individual line; the application of the focussing method giving more prominence to the exact record of each single reflexion.

We have pointed out that the broadening of the cadmium oxide lines may actually appear to be a certain handicap in making exact measurements, and I wish, therefore, to explain that a condition which we desired to be implicity satisfied in selecting a standardizing substance was that it should not only be serviceable as a reference substance for the measurement of angles but also of intensities. This requires that the particles should be so small as to reduce the size of the crystal units sufficiently to make extinction effects negligible, or, at least, that the powder should be sufficiently fine to obtain a uniform average of any residual extinction effect. This restricts the number

* J. Brentano and W. E. Dawson, Phil. Mag. iii. p. 411 (1927); and J. Brentano and J. Adamson, *loc. cit.*

of substances which appear suitable, in particular for substances containing elements of greater atomic weight, where the limit at which primary extinction becomes appreciable can be put at about 100 crystal planes, while much larger units are permissible for crystals constituted of light elements. The limited number of regularly spaced crystal planes reduces the resolving power, and accordingly the sharpness of the lines. It is in this way that cadmium oxide seemed to be best suited among the substances we have investigated with the aim of finding a standardizing substance with great volume absorption and volume scattering.

In the case of sodium chloride, although a very imperfect crystal, extinction effects are by no means negligible, and it has been shown that the ordinary process of grinding will not remove a certain amount of primary extinction *. Considering the relatively small atomic numbers of its constituents, this corresponds to fairly large crystal units consisting on an average of several thousand layers. Accordingly, sodium chloride lines are practically sharp. This was also found to be the case in our experiments.

These points have a certain bearing on the choice of a standardizing substance. A substance of the type of cadmium oxide covers a wide range of requirements, and, apart from the use for intensity measurements, the fact that it is largely constituted of small crystal units giving little extinction enhances the intensity of the reflexions, a point which has also been noted by Mr. Luther Fuller. On the other hand, it must be recognized that, in order to obtain very sharp lines for the most exact angular measurements, a substance with sufficiently large crystal units must be chosen. This involves considerable extinction, and reduction of intensity in particular, with substances consisting of elements with high atomic numbers.

Paris, 31 Dec., 1929. J. Brentano.

* Bragg, James, and Bosanquet, Phil. Mag. xli. p. 309 (1921); xlii. p. 1 (1921); xliv. p. 433 (1922). R. J. Havighurst, Phys. Rev. xxix. p. 882 (1926). J. Brentano, Phil. Mag. iv. p. 620 (1927).

[*The Editors do not hold themselves responsible for the views expressed by their correspondents.*]

Fig. 1. Fig. 2. Fig. 3. Fig. 4. Fig. 5.

1.—30 % CO + 70 % Air. Initial pressure 1 atmosphere. Fan at rest

2.—20 % H_2 + 10 % O_2 + 70 % N_2. " " "

3.—20 % H_2 + 10 % O_2 + 70 % Ar. " " "

4.—26 % CO + 30 % O_2 + 44 % CO_2. " " Fan running at 1500 r.p.m.

5. 26 % CO + 30 % O_2 + 44 % N_2. " " " "

Speed of film 1 revolution per second in each case.

Fig. 6. Fig. 7. Fig. 8. Fig. 9.

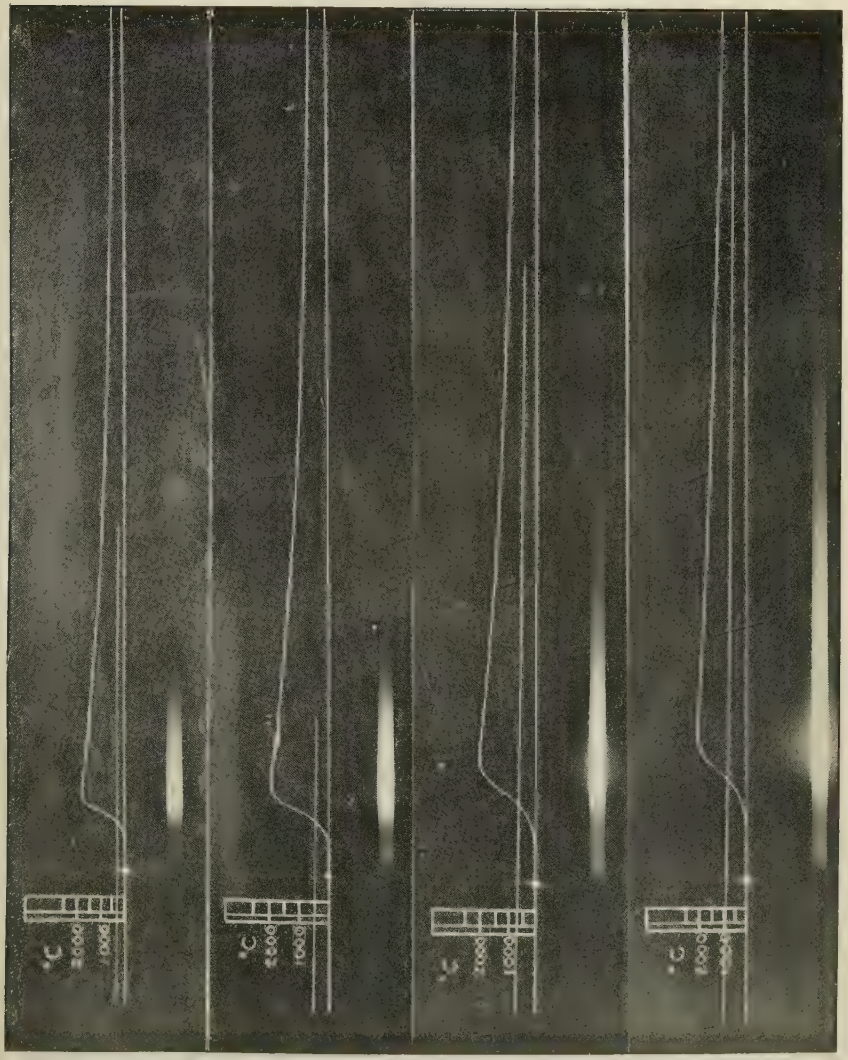

6. 28 % CO+72 % Air. Initial pressure $\frac{3}{4}$ atmosphere. Fan at rest.
7. " " " 1 " "
8. " " " 2 atmospheres. "
9. " " " 3 " "

Speed of film 1 revolution per second in each case.

Fig. 11. Fig. 12. Fig. 13. Fig. 14. Fig. 15.

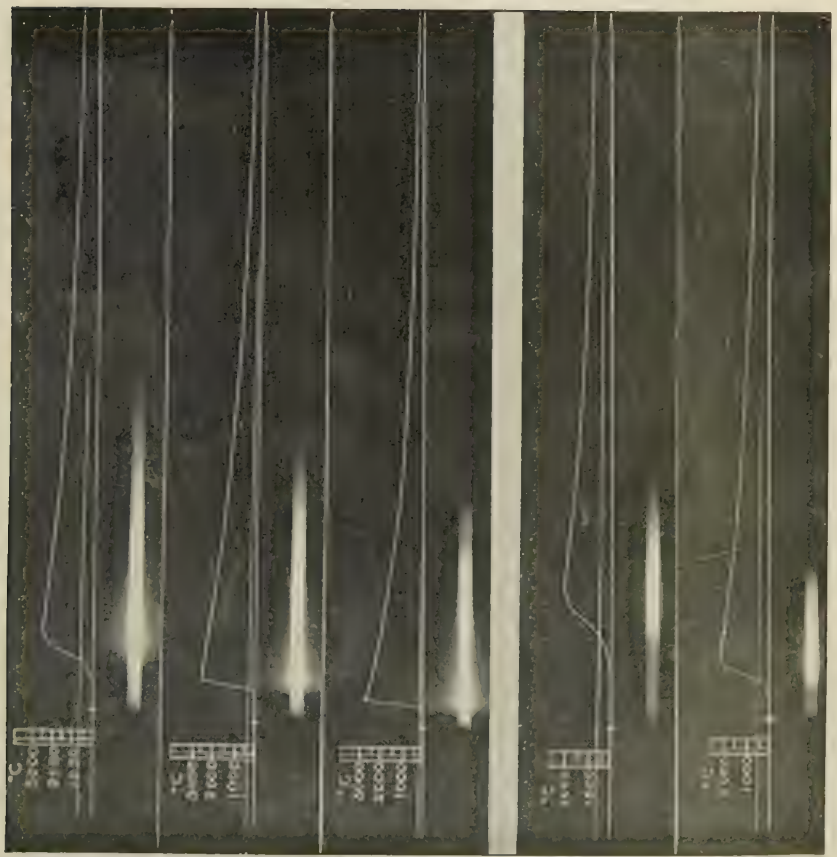

11.—50 % CO + 25 % O_2 + 25 % CO_2. Initial pressure 1 atmosphere. Fan at rest.
12.— „ „ „ „ „ Fan running at 1500 r.p.m.
13.— „ „ „ „ „ 2800 „
14.—35 % CO + 65 % Air (partially dried). „ „ Fan at rest.
15.— „ „ (saturated with water-vapour at 15° C. „

Speed of film 1 revolution per second in each case.

Fig. 16.

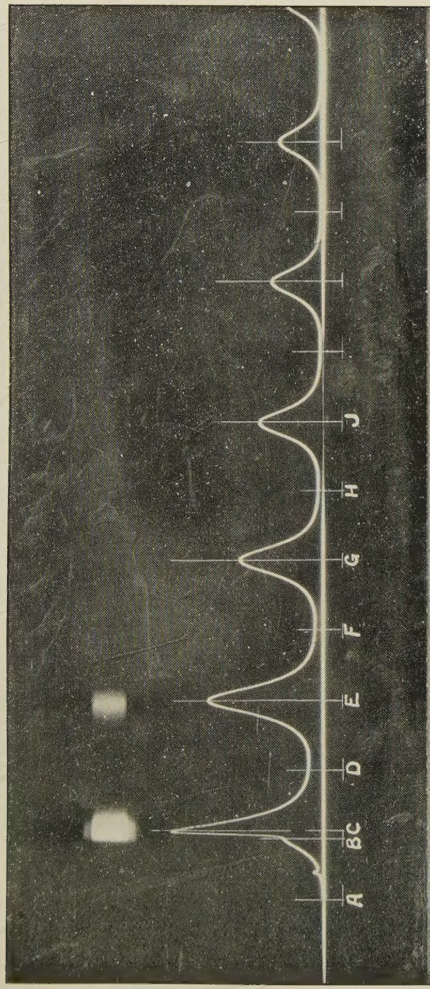

Fig. 17.

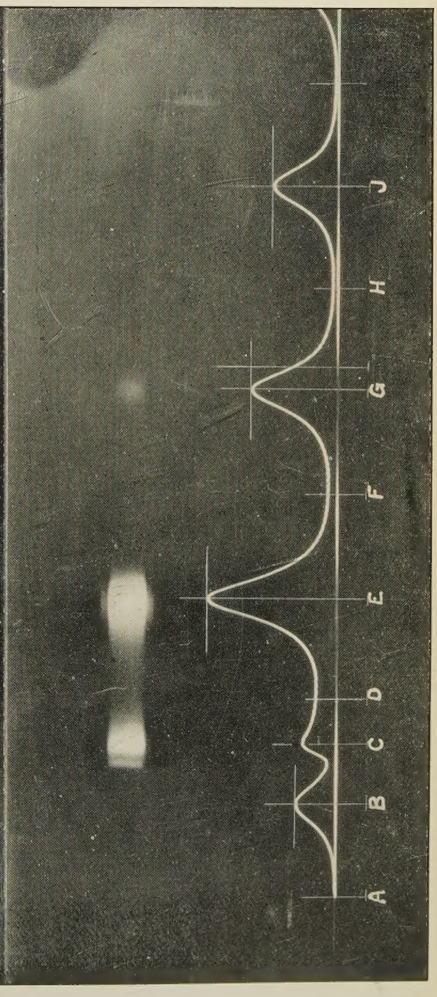

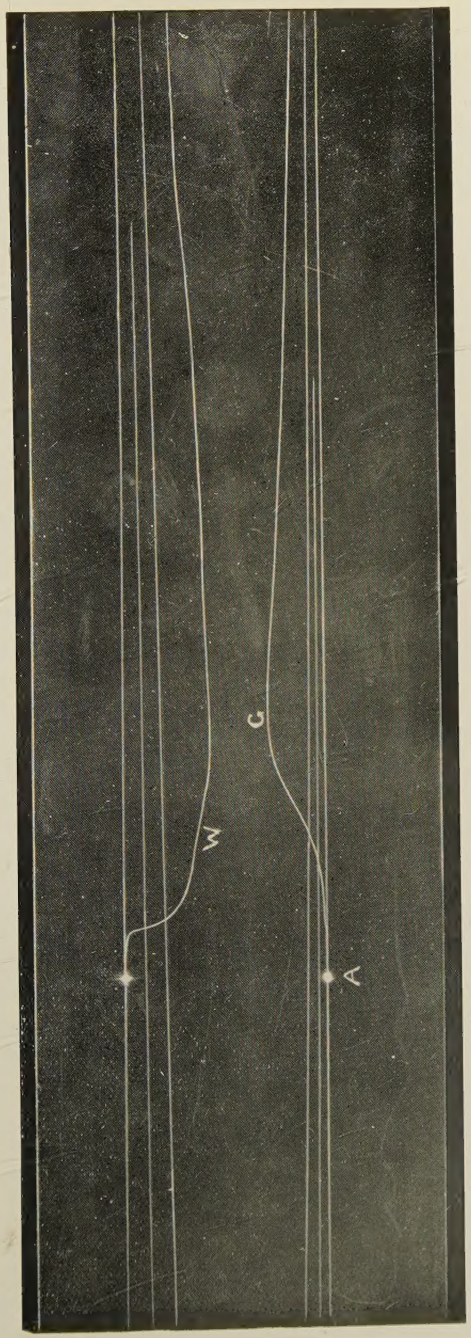

Fig. 2.